

**STRUCTURAL HEALTH MONITORING AND ITS APPLICATION  
TO A BRIDGE WITH  
SPRAYED FIBRE REINFORCED POLYMER REPAIR**

by

**TZU-YIN TIFFANY LIN**

B.A.Sc., The University of British Columbia, 2001

A THESIS SUBMITTED IN PARTIAL FULFILLMENT OF THE REQUIREMENTS  
FOR THE DEGREE OF

**MASTER OF APPLIED SCIENCE**

in

THE FACULTY OF GRADUATE STUDIES

**(Civil Engineering)**

THE UNIVERSITY OF BRITISH COLUMBIA

April 2007

© Tzu-Yin Tiffany Lin, 2007

## ABSTRACT

Structural Health Monitoring (SHM) is an emerging field in Civil Engineering, which implements the advances in various “high technologies” into developing a diagnostic system for monitoring the integrity of civil structures. With the increasing concern with infrastructure crisis, the demand for SHM has grown significantly over the past decade in response to the urgent needs for better damage detection and monitoring tools. SHM makes remote control, real-time, and continuous monitoring on civil structures possible, which is extremely beneficial, especially in the study for innovative materials/designs and on the prevention for catastrophic failure events. SHM on important civil structures is foreseen to become common practice in the near future, and therefore this thesis is devoted to the study of SHM process, and focusing its application on concrete bridges.

The study of the SHM process is done through twofold: extensive literature research and an actual application to a fully instrumented short-span concrete bridge. The literature research includes three main themes: 1.) an introduction on SHM, focusing on the current state of our bridge inventory and the needs; 2.) a study on the global condition assessment methods for bridges, discussed through the four subsystems of SHM: *Static Field Testing*, *Dynamic Field Testing*, *Periodic Monitoring*, and *Continuous Monitoring*, as well as common practice for bridge inspection/evaluation currently and their problems; 3.) an exploration on the components of SHM process, presented according to *Operational Evaluation*, *Data Acquisition*, *Data Communication*, *Data Management*, and *Diagnostics*.

The actual application of SHM involved with a shear deficient bridge, called Safe Bridge, being repaired by an innovative technique, the *sprayed FRP*, invented by Dr. N. Banthia of UBC. Safe Bridge project is the testing bed for both the long-term performance study of the *sprayed FRP* reinforcement and the SHM process. Two field tests on Safe Bridge performed in 2003 and 2005 are covered in this thesis. Static load and rolling load were applied under certain loading positions and data were gathered from both strain gauges and long-gauge fibre optic sensors. An IP-built-in data acquisition system was also tested for the possibility of remote control on Safe Bridge in the future. Data analysis steps are presented and data comparisons were made to evaluate the condition and field performance of the *sprayed FRP*. Results showed that the sprayed layer was in similar condition as when they were just applied in 2002, and occurrence of delaminations is unlikely.



# TABLE OF CONTENTS

<b>ABSTRACT.....</b>	<b>ii</b>
<b>TABLE OF CONTENTS.....</b>	<b>iii</b>
<b>LIST OF TABLES.....</b>	<b>vii</b>
<b>LIST OF FIGURES .....</b>	<b>viii</b>
<b>ACKNOWLEDGEMENTS .....</b>	<b>xiii</b>
<b>CHAPTER 1 INTRODUCTION.....</b>	<b>1</b>
1.1 CURRENT ISSUES AND NEEDS.....	1
1.2 STRUCTURAL HEALTH MONITORING (SHM).....	7
1.3 THE SAFE BRIDGE PROJECT.....	11
1.4 THESIS OBJECTIVE AND SCOPE.....	12
<b>CHAPTER 2 LITERATURE REVIEW - STRUCTURAL HEALTH MONITORING .....</b>	<b>14</b>
2.1 INTRODUCTION .....	15
2.2 GLOBAL CONDITION ASSESSMENT METHODS FOR BRIDGES .....	19
2.2.1 Visual Inspection.....	20
2.2.1.1 Signs of Deterioration .....	20
2.2.1.2 Rating Systems.....	22
2.2.1.3 Reliability of Visual Inspection.....	23
2.2.2 Field Testing .....	26
2.2.2.1 Load-Carrying Capacity Rating for Bridges .....	27
2.2.2.2 Static Field Testing.....	28
2.2.2.2.1 Types of Static Field Testing .....	31
2.2.2.3 Dynamic Field Testing .....	34
2.2.2.3.1 Types of Dynamic Field Testing.....	37
2.2.3 Long Term Monitoring .....	40
2.2.3.1 Periodic Monitoring .....	43
2.2.3.2 Continuous Monitoring .....	44
2.3 COMPONENTS OF STRUCTURAL HEALTH MONITORING PROCESS .....	47

2.3.1 Operational Evaluation .....	47
2.3.2 Data Acquisition .....	48
2.3.2.1 Sensors .....	50
2.3.2.1.1 Common Traditional Sensors.....	51
2.3.2.1.1.1 Strain Gauges .....	52
2.3.2.1.1.2 Linear Variable Differential Transducers (LVDTs).....	58
2.3.2.1.1.3 Accelerometers.....	59
2.3.2.1.1.4 Temperature Sensors.....	60
2.3.2.1.2 Advanced Fibre Optic Sensors.....	60
2.3.2.1.2.1 Optical Fibre and Fibre Optic Sensor Technology.....	62
2.3.2.1.2.2 Common FOS Types for Bridge Applications.....	66
2.3.2.2 Data Acquisition System.....	70
2.3.2.2.1 Signal Conditioners.....	71
2.3.2.2.2 Data Acquisition Boards .....	73
2.3.2.2.3 Data Acquisition Program.....	75
2.3.3 Data Communication .....	76
2.3.3.1 Wired Transmission .....	77
2.3.3.2 Wireless Transmission .....	78
2.3.4 Data Management .....	79
2.3.4.1 Data Processing.....	80
2.3.4.2 Data Storage and Retrieval.....	81
2.3.5 Diagnostics.....	81
<b>CHAPTER 3 BACKGROUND INFORMATION FOR SAFE BRIDGE PROJECT .....</b>	<b>83</b>
3.1 PRECAST CONCRETE CHANNEL BEAM BRIDGE.....	83
3.1.1 Major Problems.....	84
3.1.2 Potential Retrofit Method - FRP .....	87
3.2 SAFE BRIDGE .....	89
3.2.1 Bridge Description .....	90
3.2.2 Bridge Problems.....	94
<b>CHAPTER 4 FIRST FIELD TESTING (2003).....</b>	<b>99</b>
4.1 SENSOR LOCATIONS.....	100
4.2 TRUCK INFORMATION .....	101

4.3	LOADING TYPES AND POSITIONS .....	102
4.3.1	Static Load Positions.....	102
4.3.2	Rolling Load Positions.....	104
4.4	DATA PROCESSING AND TESTING RESULTS .....	105
4.4.1	For Static Load Testing.....	106
4.4.2	Rolling Load Testing .....	109
4.5	TESTING RESULT COMPARISONS .....	112
4.5.1	Static Load Test Results.....	114
4.5.1.1	After_Repair 2002 vs. Strain_Reading 2003.....	115
4.5.1.2	Before_Repair 2001 vs. Strain_Reading 2003 .....	122
4.5.2	Rolling Load Test Results.....	126
4.5.2.1	After_Repair 2002 vs. Strain_Reading 2003.....	128
4.5.2.2	Before_Repair 2002 vs. Strain_Reading 2003 .....	133
4.6	DATA COMPARISONS BETWEEN DIFFERENT DAQ SYSTEMS .....	138
4.6.1	Static Load Testing Results.....	139
4.6.2	Rolling Load Testing Results.....	142
<b>CHAPTER 5</b>	<b>SECOND FIELD TESTING (2005).....</b>	<b>145</b>
5.1	SENSOR LOCATIONS.....	145
5.2	TESTING VEHICLE.....	148
5.3	LOADING POSITIONS.....	149
5.4	DATA PROCESSING .....	152
5.4.1	Conversion: Displacement to Average Strains .....	153
5.4.2	Temperature and Load Effect Adjustment.....	155
5.4.3	Data Conversion: Maximum Strain vs. Average Strain.....	157
5.5	TESTING RESULTS AND COMPARISONS .....	159
5.5.1	FOS_2005 Reading vs. Initial FOS Reading .....	161
5.5.2	FT Sensor Readings vs. Strain Gauge Readings.....	162
<b>CHAPTER 6</b>	<b>STRUCTURAL HEALTH MONITORING ON SAFE BRIDGE.....</b>	<b>164</b>
6.1	OPERATIONAL EVALUATION AND SET-UP DESIGN .....	164
6.1.1	Set-Up for Strain_Reading 2003.....	166
6.1.2	Set-Up for FOS_2005 .....	167
6.2	DATA ACQUISITION.....	169

6.2.1 Sensors .....	169
6.2.1.1 Strain Gauge .....	170
6.2.1.2 Long-Gauge Fibre Optic Sensor.....	173
6.2.2 Data Acquisition Systems .....	174
6.2.2.1 Traditional DAQ Systems .....	174
6.2.2.2 Web-Based DAQ System .....	176
6.2.2.3 FOS Interrogator .....	181
6.3 DATA COMMUNICATION .....	184
6.3.1 For Strain Gauge Readings .....	184
6.3.2 For Fiber Optic FT Sensor Readings .....	187
6.4 DATA MANAGEMENT .....	189
6.4.1 Data Processing.....	189
6.4.2 Data Storage and Retrieval .....	190
6.5 DIAGNOSTICS .....	190
 <b>CHAPTER 7 CONCLUSIONS AND RECOMMENDATIONS FOR FUTURE WORKS.....</b>	<b>192</b>
7.1 CONCLUSIONS .....	193
7.2 RECOMMENDATIONS FOR FUTURE WORK .....	197
7.3 REFERENCES.....	200
 <b>APPENDICES.....</b>	<b>216</b>
APPENDIX I - STANDARD DRAWINGS OF PCCB GIRDER BRIDGES .....	216
APPENDIX II - SUMMARY TABLE: EXISTING PCCB BRIDGES IN VANCOUVER ISLAND, BC .....	223
APPENDIX III - CONDITION INSPECTION REPORTS FOR SAFE BRIDGE .....	225
APPENDIX IV - TIME-STRAIN HISTORY OF THE 6 STATIC LOAD POSITIONS – <i>I/O Tech DAQBook</i> .....	230
APPENDIX V - TIME-STRAIN HISTORY OF THE 6 STATIC LOAD POSITIONS – <i>WebDAQ/100</i> .....	234
APPENDIX VI - TIME-STRAIN HISTORY OF THE 3 ROLLING LOAD POSITIONS – <i>WebDAQ/100</i> .....	238
APPENDIX VII - WEIGHT SCALE TICKET OF THE 2005 FIELD TESTING TRUCK .....	241
APPENDIX VIII - SPECIFICATIONS OF THE LONG-GAUGE FT SENSORS .....	243
APPENDIX IX - SPECIFICATIONS OF <i>WebDAQ/100</i> .....	245
APPENDIX X - SPECIFICATIONS OF THE FTI-3300 SYSTEM.....	250

## LIST OF TABLES

Table 1-1	Examples of Disasters with Significant Losses in the Past Decade .....	4
Table 2-1	Measurements that can not be obtained by Visual Inspection .....	25
Table 2-2	Four Levels of Structural Health Monitoring Systems Based on Sensing Approach .....	46
Table 4-1	Summary of Static Strains under Six Loading Positions – Field Test 2003 .....	109
Table 4-2	Largest Strain Readings Induced by the Three Rolling Load Positions – Field Test 2003.....	112
Table 4-3	Maximum Strains under Six Static Load Positions - Field Test 2002 .....	116
Table 4-4	Static Strains under Six Loading Positions with Load Factor Applied – Field Test 2003.....	116
Table 4-5	Static Strains under Six Loading Positions – <i>Before_Repair 2001</i> (Load Factor Applied) .....	122
Table 6-1	The Magnitude and Location of the Largest Strain for the Six Static Loading Positions.....	191

## LIST OF FIGURES

Figure 1-1	Infrastructure Growth Profile in Canada and the Estimated Remaining Life .....	2
Figure 1-2	Age of Infrastructure in Canada and Its Used Life Expectancy .....	3
Figure 1-3	Growth of Deferred Maintenance and Infrastructure Backlog with Time in Canada .....	5
Figure 1-4	Fields usually Involved in a SHM System .....	9
Figure 1-5	Six Subsets of a Structural Health Monitoring System .....	10
Figure 1-6	Four Subsystems of a Structural Health Monitoring System .....	10
Figure 2-1	The Collapse of Silver Bridge Spanning West Virginia and Ohio, U.S. ....	16
Figure 2-2	Number of Total and Deficient Bridges according to Year Built, by Dec. 2005 .....	17
Figure 2-3	Number of Failed Bridges with Respect to Year and Phase of Failure Occurrences.....	18
Figure 2-4	Signs of Concrete Deterioration: (a) Efflorescence; (b) Leaching.....	21
Figure 2-5	Signs of Concrete Deterioration : (a) Honeycombing; (b) Exudation.....	21
Figure 2-6	Bridge Condition Rating Categories for NBI Database .....	22
Figure 2-7	Bridge Appraisal Rating Categories for NBI Database .....	23
Figure 2-8	Types of Rating Vehicles for Bridge Field Testing in U.S. ....	28
Figure 2-9	Photos of the Failure of <i>de la Concorde Blvd.</i> in Montreal on Sept. 30, 2006 .....	30
Figure 2-10	Hypothetical Load Deflection Response of Bridge .....	33
Figure 2-11	Examples of Forced Excitation Methods.....	36
Figure 2-12	Example of An <i>Averaged Normalized Power Spectral Density</i> Plot.....	39
Figure 2-13	The “Time Scale” for Bridge Monitoring in Terms Magnitude in Frequency.....	41
Figure 2-14	Components of a Typical Foil Strain Gauge.....	53
Figure 2-15	The Linear Variable Differential Transformer: a. Photo of an LVDT under Bridge.....	58
Figure 2-16	Distribution of Fibre Optic Sensor Types According to Measurands and Technology ...	61
Figure 2-17	Basic Structure of Optical Fibre .....	63
Figure 2-18	Types of Mode Propagation in Optical Fiber .....	64
Figure 2-19	Attenuation vs. Wavelength for LASERs in Fiber Optic Use .....	65
Figure 2-20	Operation Mechanism of the Fiber Bragg Grating Sensor .....	67
Figure 2-21	Two Types of Fabry-Perot Gauge (schematic): (a) Self-Compensated in Temperature; (b) Non-Compensated in Temperature .....	68
Figure 2-22	Photonic Circuit for Measuring Long Gauge Strain .....	69
Figure 2-23	Basic Components of a Computer-Based Data Acquisition System .....	70
Figure 2-24	[a] Effect of Low Sampling Rate: Aliasing; [b] Effects of Increasing Sampling Rate....	74

Figure 2-25 Example of An Analog Wave to be Digitized with 3-bit Resolution .....	75
Figure 2-26 A Radio-grade Flexible Coaxial Cable .....	78
Figure 3-1 Behavior of a Cracked Beam .....	86
Figure 3-2 The Spray Equipment and Process of <i>Sprayed FRP</i> .....	88
Figure 3-3 Photos of Safe Bridge: (a) Side View; (b) Road View .....	90
Figure 3-4 Photos of Logging Trucks passing through Safe Bridge .....	91
Figure 3-5 Plan and Section of Safe Bridge .....	92
Figure 3-6 Detailed Dimension of Channel Beam Cross Section.....	93
Figure 3-7 Reinforcement Details and Dimensions of Channel Beam Cross Section.....	93
Figure 3-8 Stirrup Spacing of Safe Bridge's Channel Beam Girders .....	94
Figure 3-9 Locations of Inadequate Cover .....	95
Figure 3-10 Photos of Safe Bridge Showing Deteriorating Conditions (Sept. 2001).....	96
Figure 3-11 Applying Mortar to Cover the Steel Rebar .....	97
Figure 3-12 Locations of the GFRP Reinforcement.....	97
Figure 3-13 Sprayed GFRP Reinforcement: [a] GFRP Spry in Process; [b] the Finished Surfaces ...	98
Figure 3-14 GFRP Wrap Reinforcement: [a] Wrap GFRP in Process; [b] the GFRP sheets.....	98
Figure 4-1 Photos Under Safe Bridge and the LVDT Set-Up for Before_Repair_2001 .....	99
Figure 4-2 Strain Gauge Locations on Safe Bridge .....	100
Figure 4-3 Testing Truck for <i>Strain_Reading 2003</i> : [a] Photo; [b] Truck Dimensions .....	101
Figure 4-4 Six Loading Positions for the Static Load Testing.....	103
Figure 4-5 Photo of Safe Bridge with Red Mark at Center-line: 2003 Field Test.....	103
Figure 4-6 Transverse Truck Positions for Static Loading Test.....	104
Figure 4-7 The Three Loading Positions for the Rolling Load Tests .....	105
Figure 4-8 Strain-Time History of 2003 Static Load Testing Under Load Position 2 – Original ...	106
Figure 4-9 Time-Strain History of 2003 Static Load Testing Under Position 2 – After Zeroing....	107
Figure 4-10 Plot of Six Strain Values Due to Static Truck Load at Position 2 .....	108
Figure 4-11 Plot of 2003 Field Test Results - Rolling Load Position I (60Hz Data) .....	110
Figure 4-12 Plot of 2003 Field Test Results - Rolling Load Position I (15 Hz Data) .....	110
Figure 4-13 of 2003 Field Test Results - Rolling Load Position II (15 Hz Data) .....	111
Figure 4-14 of 2003 Field Test Results - Rolling Load Position III (15 Hz Data).....	111
Figure 4-15 Summary of 2003 Static Load Testing Results (with load factor applied).....	114
Figure 4-16 Time-Strain History for Static Load Position 4 - 2002 Field Testing.....	117

Figure 4-17 Time-Strain History for Static Load Position 6 - 2002 Field Testing.....	117
Figure 4-18 Comparison between 2002 and 2003 Field Test Results - Load Position 1 & 2 .....	119
Figure 4-19 Comparisons between 2002 and 2003 Field Test Results - Load Position 3 & 4 .....	120
Figure 4-20 Comparisons between 2002 and 2003 Field Test Results - Load Position 5 & 6 .....	121
Figure 4-21 Comparison between 2001 and 2003 Field Test (Static Load) - Load Position 1 & 2 ..	123
Figure 4-22 Comparison between 2001 and 2003 Field Test (Static Load) - Load Position 3 & 4 ..	124
Figure 4-23 Comparison between 2001 and 2003 Field Test (Static Load) - Load Position 5 & 6 ..	125
Figure 4-24 Example of Rolling Load Time-Strain Curve Pattern – 2003 Roll I .....	127
Figure 4-25 Comparisons between 2002 and 2003 Rolling Load Test - Position I.....	129
Figure 4-26 Comparisons between 2002 and 2003 Rolling Load Test - Position II .....	130
Figure 4-27 Comparisons between 2002 and 2003 Rolling Load Test - Position III.....	132
Figure 4-28 Comparisons between 2001 and 2003 Rolling Load Test - Position I.....	134
Figure 4-29 Comparisons between 2001 and 2003 Rolling Load Test - Position II .....	136
Figure 4-30 Comparisons between 2001 and 2003 Rolling Load Test - Position III .....	137
Figure 4-31 <i>I/O TechDaqBook</i> Data vs. <i>WebDAQ/100</i> Data: 2003 Field Test Static Position 1 .....	140
Figure 4-32 <i>I/O TechDaqBook</i> Data vs. <i>WebDAQ/100</i> Data: 2003 Field Test Static Position 4 .....	141
Figure 4-33 <i>I/O TechDaqBook</i> vs. <i>WebDAQ/100</i> : 2003 Field Test – Rolling Load Position II .....	143
Figure 5-1 Photos of the 5 m-Long Gauge FOS Locations: (a) Girder 2 & 6; (b) Girder 10.....	146
Figure 5-2 Locations of the Long Gauge FOS on Safe Bridge .....	147
Figure 5-3 The Standard Three-Axle 28 ton Truck used for Field Test 2005 .....	148
Figure 5-4 Planned Truck Loading Positions for <i>FOS_2005</i> .....	149
Figure 5-5 Truck Loading Position 1, 2, and 3 for <i>FOS_2005</i> .....	149
Figure 5-6 (a) Mark-ups along the Concrete Curb; (b) Draw <i>Quarter</i> - and <i>Center</i> - Reference Lines; (c) Position of the Tandem-axle to the Reference Line .....	150
Figure 5-7 Actual Truck Loading Positions for Field Test 2005.....	151
Figure 5-8 A Segment of Raw Data from <i>FOS_2005</i> .....	152
Figure 5-9 Time-Displacement Graph for FT Sensor #560.....	154
Figure 5-10 The Reference Lines Used to Match the Mid-span Line .....	156
Figure 5-11 Beam Model for Safe Bridge Loading Cases.....	158
Figure 5-12 Microstrains for Sensor#554 under 9 Loading Positions: <i>FOS_2005</i> .....	159
Figure 5-13 Plot of FT Sensor#560 under 9 Loading Positions: <i>FOS_2005</i> .....	160
Figure 5-14 Plot of FT Sensor#562 under 9 Loading Positions: <i>FOS_2005</i> .....	160



Figure 5-15 Plot of FT Sensor#560 under Six Loading Positions in <i>After_Repair 2002</i> .....	161
Figure 5-16 Locations of both Strain Gauges and FOSs .....	162
Figure 6-1 Schematic Drawing of System Set-Ups for Field Test 2003 .....	166
Figure 6-2 Field Test 2003 Site Photos: [a] Data Acquisition Equipments on the Trunk of a Van [b] Position of the Van to Safe Bridge (red circle).....	167
Figure 6-3 Schematic Drawing of System Set-Ups for Field Test 2005 .....	168
Figure 6-4 Field Test 2005 Site Photos: [a] Equipments Set Up on the Back of a Truck; [b] Surge Protection Equipment for FTI-300 .....	169
Figure 6-5 Safe Bridge Site Photos (2002): [a] Installation of Strain Gauge on Steel Rebar; [b] Spot Welding of Strain Gauge .....	171
Figure 6-6 Safe Bridge Site Photos (2002): [a] Strain Gauge with 3-wire Bondable Terminals; [b] Shielded Cable for Strain Gauge ...	172
Figure 6-7 Safe Bridge Site Photos (2002): [a] Strain Gauge with Mastic Foil Coating Protection;[b] Strain Gauge Covered with Patching Material.....	172
Figure 6-8 Field Test 2005 Site Photos: [a] FT-Sensor on Girder 6 with Storage Box Open; [b] FT-Sensor Covered with Protection Epoxy.....	174
Figure 6-9 Field Test 2003 Site Photos: [a] Data Acquisition Systems for Strain Gauge Readings [b] The I/O Tech DaqBook .....	175
Figure 6-10 Field Test 2003: Example of A Screen Shot of <i>DaqView</i> .....	175
Figure 6-11 Field Test 2003: Web Site for <i>WebDAQ/100</i> - Home Page.....	178
Figure 6-12 Field Test 2003: Web Site for <i>WebDAQ/100</i> – Acquisition Setup Page .....	178
Figure 6-13 Field Test 2003: Web Site for <i>WebDAQ/100</i> – Report Page .....	179
Figure 6-14 Field Test 2003: [a] Integrated System with <i>WebDAQ/100</i> & Wireless Communication; [b] Location of DAQ system with <i>WebDAQ/100</i> and the Operator .....	180
Figure 6-15 Field Test 2003: Connectors of Wires and Connecting to <i>WebDAQ/100</i> .....	180
Figure 6-16 Field Test 2003: <i>WebDAQ/100</i> Screen Shots: [a] Hyperlink: “Download Data”; [b] Hyperlink: “View Graph”.....	181
Figure 6-17 Field Test 2003: <i>WebDAQ/100</i> Screen Shots: [a] Acquisition Setup Page; [b] Sampling Rate Set-up .....	181
Figure 6-18 Field Test 2005: DAQ System Setup - FTI-3300 and Laptop .....	182
Figure 6-19 Field Test 2005: Screen Shots of FOX-Ware for FTI-3300 (Channel 1~6) .....	183
Figure 6-20 Safe Bridge Site Photos: Conduits for Strain Gauge Wires.....	184

Figure 6-21	Conduits for SG Wires and Storage Boxes on the East Abutment .....	185
Figure 6-22	Six SG Wire Cables Taken Out from Storage Box to Connect to Signal Conditioner..	185
Figure 6-23	Field Test 2003 Site Photos: Connect Sensor Cables with Signal Conditioner Cable...	185
Figure 6-24	Field Test 2003 Site Photos:	
	Wire Connections to Signal Conditioner and DAQ Board .....	186
Figure 6-25	Field Test 2003 Site Photos: Wiring between Signal Conditioner and <i>WebDAQ/100</i> ..	186
Figure 6-26	Field Test 2005 Site Photos: [a] FT-Sensors Taken Out from Junction Box;	
	[b] Connector of FT Sensor and Sensor Number .....	187
Figure 6-27	Field Test 2005 Site Photos:	
	Fiber Optic Extension Cables to FT-Sensor and FTI-3300.....	187
Figure 6-28	Field Test 2005 Site Photos: FT-Sensor Head; Cleaning the Optical; FO Connection .	188
Figure 6-29	Field Test 2005 Site Photos: [a] Connecting Optical Fiber to FTI-3300	[b]
	Cleaning Optical Head with Laboratory-grade Ethanol.....	188
Figure 6-30	Maximum Static Strain Comparisons between Three Field Tests .....	191

## ACKNOWLEDGEMENTS

I would like to extend my sincere gratitude to all who have involved in this research project, and who have helped me directly or indirectly to make this thesis writing possible; this includes people that are not mentioned in particular below.

First and foremost I would like to extend my heartfelt appreciation to my supervisor Dr. Nemkumar Banthia for his invaluable understanding, patient, and guidance. Without his trust, encouragement, and support, this thesis work would not be possible. I want to thank him giving me the opportunity to work on a topic that is new in the field and being confident with me. I also enjoyed the flexible and pressure-free teaching style and working environment.

Recognition is also due to the organizations and agencies who have contributed to this research project, in particular the Network of centres of excellence ISIS Canada and Dr. Mufti, the president and the second reader of my thesis, and the Ministry of Transportation (MoT) and Highways of British Columbia. In particular I would like to thank Ian Sturrock for providing me valuable information and references from the MoT; Dr. R.C. Tennyson's help in technical questions; and Evangeline Rivera who came all the way from Manitoba to make the 2005 field test successful.

I also would like to acknowledge the outstanding performance and significant help from the technical staffs and my colleagues, especially to Scott Jackson and John Wong, who were the key people for equipment set-up and made the field testing possible. Also appreciated are the encouragement and help from my colleagues.

Last but not least, I really want to thank my family (mom, dad, brothers Tony and Pat) and Jack's family (Mr. and Mrs. Wu, and Patty) for their care, and support over the years; especially to my parents and Jack, for their endless love, encouragement, and help; without them, the thesis would never be able to completed. Thank you very much for being there for me all the way; I will always be there for all of you.

---

## ***Chapter 1***

### **First Field Testing (2003)**

---

Safety and reliability of civil structures are a major concern and responsibility of civil engineers. In response to the current needs for better damage detection and monitoring tools, a new discipline in civil engineering has emerged: Structural Health Monitoring (SHM). SHM on important infrastructure and structures is foreseen to become common practice in the near future, and for civil engineers today, it is important to gain sufficient understanding of this new field. This thesis is devoted to the study of SHM process, and its application to a shear-deficient bridge, called Safe Bridge, which was strengthened by an innovative repair method.

The purpose of this introductory chapter is to present readers with some background information about SHM in general, and introduce the research undertaken by the author. The first section will introduce the present day context for this thesis: the political, economic, and technical issues which have impacted the civil engineering industry, and how they have contributed to the present need for SHM. The second section will provide a basic introduction to SHM, providing discussions of the constraints faced before, the benefits of SHM, and definitions and terminologies often associated with SHM. Regarding the Safe Bridge project, it has been an on-going project under the auspices of ISIS Canada. As such, the third section will briefly introduce ISIS Canada and provide a summary of previous work that has been performed on Safe Bridge. The final section of this chapter will introduce the objectives of this research, and present an outline of the thesis.

#### **1.1 Current Issues and Needs**

*Infrastructure Crisis* has been one of the biggest issues in the civil engineering field for the last two decades. The term never got much attention until the 90s, when the *Infrastructure Deficit Hypothesis* was massively propagated during the presidency elections in the U.S. [1,2,3]. The general public started to be aware of the issue, and in the late 90s, *Infrastructure Crisis* had become an international concern and a global worry [4,5,6,7,8]. *Infrastructure Deficit Hypothesis* basically states that a decline in the public capital formation (i.e. infrastructure) will lower the private sector productivity,

and therefore lower a nation's real income and weaken the international competitiveness [3]. The U.S. Federal Reserve Board has concluded that the failure of civil infrastructure systems to perform at their expected level can reduce 1% of the national gross domestic product (GDP) [9]. Despite the correctness of the hypothesis, the state of infrastructure is indeed alarming in many countries, and the financial burden is huge. According to American Society of Civil Engineers (ASCE), infrastructure in the U.S. received an overall grade of D (Poor) in their *2005 Infrastructure Report Card*; the report also estimated that \$1.6 trillion would be needed in the next five years to alleviate potential problems with their civil infrastructure [10]. In Canada, the deficit for its municipal infrastructure, which represents 70% of the country's total infrastructure, was estimated to be \$60 billion in 2004, and expected to grow at \$2 billion per year [11,12]. To solve the infrastructure deficit problem, civil engineers play an important role in the technical side to provide solutions and assist in better infrastructure management.

From a civil engineering point of view, the two major factors that lead to today's infrastructure problems are "deterioration of aging systems" and "decades of deferred maintenance work" [13,14]. For U.S. and Canada (as well as most of the developed countries), the "construction boom" started in the 50<sup>th</sup> and peaked in the 60<sup>th</sup> and 70<sup>th</sup>, so the majority of the infrastructure today are more than 40 years old (see Figure 1-1) [14,15].

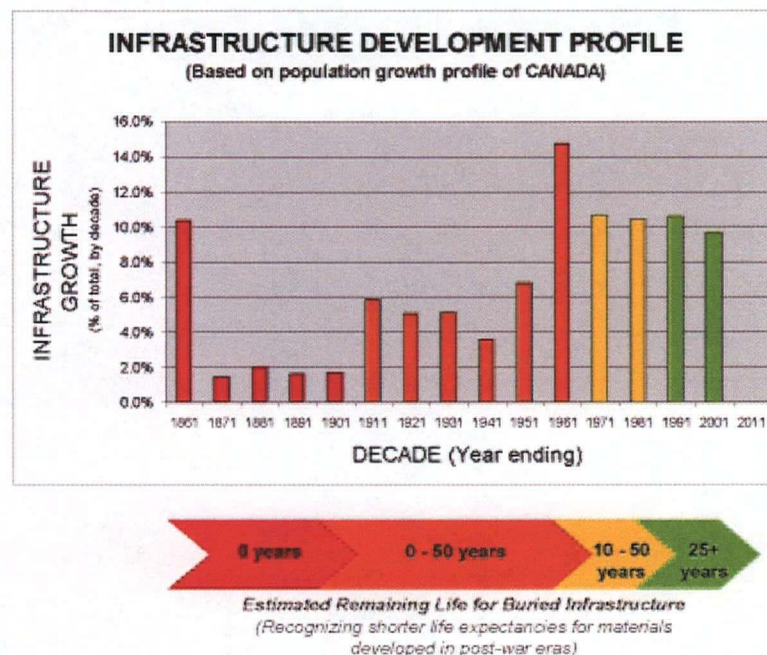


Figure 1-1 Infrastructure Growth Profile in Canada and the Estimated Remaining Life  
Source: [16] (Courtesy R.V. Anderson Associates Limited)



Using Canada as an example, according to Statistic Canada (1994), 37-years is a reasonable number to be used as the average service life for existing infrastructure [17]. By year 2004, about 60% of our infrastructure was at least 40 years old (see Figure 1-2) [11]. All materials deteriorate with time, and the deteriorating rate is further increased by factors such as severe weather, overload, fatigue, pollutions/chemicals, and structural settlement [18]. For countries like Canada, which has extreme weather conditions in a year, and de-icing salts are used tremendously in most parts of the country, life expectancy of the infrastructure can be adversely affected.

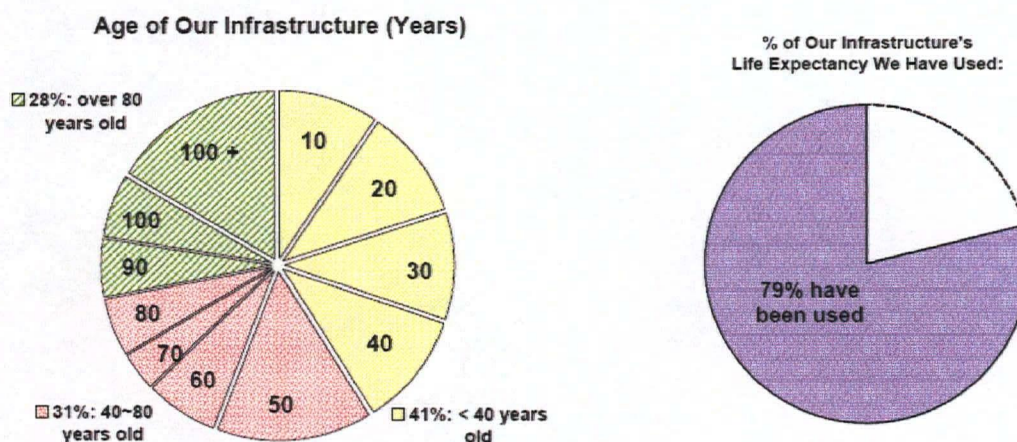


Figure 1-2 Age of Infrastructure in Canada and Its Used Life Expectancy  
Source: [11]

Moreover, design codes and regulations have been modified significantly over the years, and many old structures no longer meet the current standards [19]. For example, structural dynamics was in an undeveloped state before the 60th, and therefore, provisions for areas like seismic design and bridge aerodynamic in earlier codes were very minimum and significantly inadequate [20]. As a result, structures built before the modern design guidelines of the 80th have a much higher vulnerability to be damaged or collapse when subjected to extreme events like earthquakes [21,22].

In fact, the concern on the safety and reliability of structures and infrastructure has further risen in recent years after several catastrophic disasters happened one after another all over the world (see Table 1-1). Serious damage and destruction on structures and infrastructure happened during these events and resulted in tremendous financial loss, social and psychological impact, and worst of all, significant casualties and deaths. These painful lessons remind us that hazards do occur, whether they are natural or man-caused, and we do not have control over them. Scientists have warned that the climate today is in rapid change then ever, and governments will need to deal with increasingly



volatile natural hazards in the future [23]. The impacts of hazards can be significantly reduced if we are properly prepared.

Table 1-1 Examples of Disasters with Significant Losses in the Past Decade [24-38].

Time	Location	Comments
<b>Earthquake [24,25,26,27,28]:</b>		
Jan. 16, 1995	Japan, Kobe	Worst earthquake in Japan since 1923; over 5,500 deaths and 26,000 injured; economic loss at ~200 billion USD.
Aug. 17, 1999	Turkey	Over 17,000 deaths, primarily caused by collapse of nearly 76,000 structures; damage estimate at 3~ 6.5 billion USD.
Sep. 20, 1999	Taiwan	Over 10,000 injured/deaths; over 38000 structural collapse; Damage estimate at 14 billion USD.
Jan. 26, 2001	Gujarat, India	Over 20,000 people were killed, ~167,000 injured; Damage estimate at 2.1 billion USD.
Dec. 26, 2004	Sumatra, Indian Ocean	Induced Tsunami; affected more than 10 countries directly, and over 283000 people were killed.
<b>Hurricane / Tornadoes [29,30,31,32]:</b>		
May 3, 1999	Oklahoma City, OK	36 lives were lost, 775 injured, and with a total cost of over 1.2 billion in damage.
August, 2004	Hurricane Charley; USA	Estimate of over \$14 billion in damage/costs; More than 34 lives lost.
Sept. 05, 2005	Hurricane Katrina; USA	Estimated more than 1000 lives were lost. damage estimate hits \$125 billion
<b>Floods [33,34,35]:</b>		
December 19, 1999	Caracas, Venezuela	More than 20,000 lives were lost. Estimate of over \$2 billion in damage/costs.
November 10, 2001	Algiers, Algeria	More than 600 lives were lost, and lead to local protests. Estimate of over \$300 million in damage/costs.
July 23 – Aug. 16, 2005	Maharashtra, India	More than 987 lives were lost, and lead to local protests. Estimate of over \$3.5 billion in damage/costs.
<b>Man-Caused [36,37,38]:</b>		
Sept. 11, 2001	Terrorist Attacks New York, USA	Official counts record 2,986 deaths in total. Estimate of over \$30 billion in damage/costs.
Aug. 14-15, 2003	Power Blackout USA and Canada	Estimate of over \$6 billion damage/costs.

Deferred maintenance is another major reason for today's infrastructure problems. People used to think that civil structures are maintenance-free fixtures, and minimum or no maintenance actions were applied on infrastructure in earlier days [39]. However, the reality is, once deterioration sets in, it continues to compound exponentially. If the maintenance is not completed in year one, the costs of maintenance or repair will grow exponentially in subsequent years [23,40,41] (Figure 1-3). The detrimental effects of deferred maintenance have already shown by the huge "infrastructure gap", or infrastructure under funding, that many countries are facing today. In Canada, infrastructure gap was



estimated to be between \$50 billion to \$125 billion in 2004, which was 6-10 times the level of all annual government infrastructure budget combined [42]. In a world where financial reality can not keep up the pace with the growing demand of maintaining deteriorating structures, it is crucial that those who are responsible for making maintenance decisions make the best possible use of the limited financial resources. Maintenance and repair funds should be applied first to those with the steepest degradation curves, that is, those in the most critical damage condition (line b in Figure 1-3). Current practice of structural assessments relies heavily on visual inspection methods, which are highly speculative, expensive, and inefficient [43]. Also, components to be inspected are often difficult or dangerous to access for inspectors. It is clear that the need for better damage detection and structural capacity assessment methods for aging structures is strong.

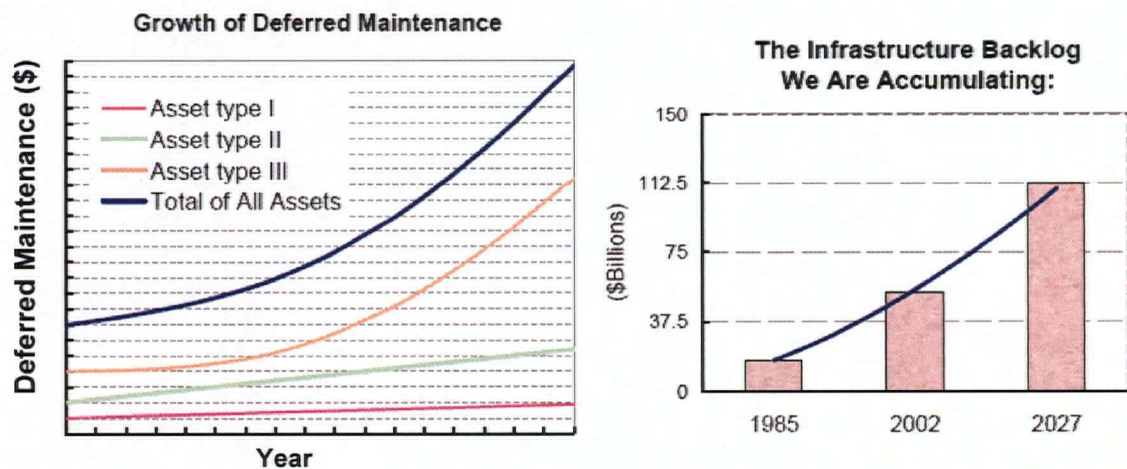


Figure 1-3 Growth of Deferred Maintenance and Infrastructure Backlog with Time in Canada  
Sources: (L) [17]; (R) [11]

As for new constructions, there is a need to explore new technologies. Innovative materials, procedures, and/or designs help enhance long-term durability, increase the expected service life, and therefore eliminate the escalating growth in infrastructure backlog. Problems uncovered from old structures should help us avoid them in new constructions; otherwise, problems we face today will keep coming back, and we will never get out of the vicious circle. For example, corrosion of steel reinforcements and components has been one of the most common and costly problems for civil structures since the 80s, and it still is today [44,45,46]. Improving the durability of steel is certainly one approach, but a further step is to search for a substitute that does not corrode.



Fiber Reinforced Polymers (FRPs), which have been used in fields like automotive and aerospace for decades, have been proven to be a very promising material for civil engineering applications [47,48]. However, in North America, the construction industry is still conservative in the use of FRP over traditional construction materials. In fact, innovations in civil engineering will never gain widespread usage until it is standardized in regulations and codes. Design codes can never be developed without enough understanding and confidence in the long-term field performance of the new technology [49]. If the field performance of the structure with innovative elements can be monitored continuously, the study and evaluation of the new technology can be sped up significantly.

The conservative attitude that the industry holds toward “changes” is another problem associated with the civil engineering field, which is reflected clearly by its *lag time*. *Lag time* means “the difference in time between a new idea’s conception and its acceptance by the industry” [50]. The lag time for the computer industry is about one year, for the aerospace industry is about two years, but for the construction industry, it is about fifty years! In fact, Construction and Education are the two industries that have the longest lag time [49]. This explains why civil engineering is often referred to as a “sun-set industry” today. Sure there are good reasons for civil engineers to be conservative, considering the unbearable consequences a structural failure could lead to. However, we are in the *Information Era* now, an era in which information and technology are doubling every eighteen months (according to Moore’s Law) [ 51 ], and interdisciplinary information exchange and collaboration is the fastest way for different fields to move to the next level. With the exploding advancement in the high-tech fields such as sensing, communication, internet, and computers, civil engineers today definitely should make use of the available technologies to shorten the “lag time” of the construction industry, and to create a better and safer living environment.

In response to the needs and current trends, Structural Health Monitoring (SHM) emerged as a new discipline for civil engineering in the mid 90<sup>th</sup> and has grown significantly over the past few years. SHM makes real-time, continuous monitoring and remote control on civil structures possible, which not only gathers valuable information on structural integrity, response, and capacity, but also is able to prevent catastrophic failures and assist in better infrastructure maintenance and management strategies. How does SHM respond to the needs? *“The immediacy and sensitivity of SHM can allow for short-term verification of innovative designs, early detection of problems, avoidance of catastrophic failures, effective allocation of resources, and reduced service disruptions and maintenance costs”*---ISIS Canada [49].

## 1.2 Structural Health Monitoring (SHM)

SHM usually involves the implementation of advanced sensing and communication systems in to the structures, so that the integrity and the true field responses can be monitored and obtained remotely; similar to people monitoring their health conditions with specialized equipments, this might be how the term *Structural Health Monitoring* evolved [49,52].

SHM has been used in aerospace, aeronautical, and mechanical industries for a long time, but field application of such system in civil structures posed significant technical challenges, even in the mid-90s [53,54,55]. Civil structures are usually much larger in size and relatively distributed and spatial, and the components to be monitored are often embedded or difficult to be accessed [39]. Also, civil structures are not mass production produced like machines; each of the structure is unique in functionality, and is exposed to different environmental conditions. Sensors and electrical devices to be used have to be able to sustain all environmental effects such as temperature change and humidity. In addition to the technical constraints, many other practical issues like economic consideration, placement of the wiring systems, public safety, accessibility, and vandalism, all made the already intricate process more challenging. Nonetheless, benefits of continuous monitoring and remote control on civil structures are countless, for example: [49,53,56,57,58]

- Measurement data can be used to detect damage that is not visible;
- Post-disaster damage assessment can be performed much faster and accurate;
- Down time and service disruptions can be avoided or minimized;
- Human resources and maintenance costs can be significantly reduced;
- Real, instant structural responses under unexpected extreme events can be captured, and the collected information can increase understanding of true structural behavior, and therefore improve future design codes and regulations.

The list is certainly not comprehensive. Besides being a damage detection tool, SHM for civil engineering application can also be used to determine the strength of the structure. The potential and benefits of SHM for civil engineering usage is unlimited. Therefore, since the mid-90<sup>th</sup>, when technologies started to become available, SHM quickly became the subject of major international research, and has grown rapidly especially in the past few years. Thanks to the exploding advancements in technologies, technical constraint is no longer the major obstacle, and it is predicted that SHM will be commonplace in the near future to provide check-ups and maintenance services for critical infrastructure and structures [49,59,60].

Being a damage detection tool, the first step is to define what “damage” is, and when is the structure considered to be “damaged”; this is actually not as intuitive as it first seems, since all materials contain defect at the microstructural level [53]. For civil engineering application, *damage* can be roughly defined as “changes to the material and/or geometric properties of the structure, including changes to the boundary conditions and system connectivity, which adversely affect the current or future performance of the structure [61].” Implicit in this definition, a common way is to assume an initial state of the structure to represent the “undamaged” state, and then compare the data gathered from later states of the structure to the initial baseline. In terms of the “damage detection capability”, a SHM system can have six different levels (Rytter, 1998) [54]:

- Level 1: *detect* the existence of damage;
- Level 2: *detect* and *locate* the damage;
- Level 3: *detect*, *locate*, and *quantify* the damage (i.e. *severity* of damage);
- Level 4: estimate the remaining service life (*prognosis*);
- Level 5: *self- diagnostics*;
- Level 6: *self-healing*;

The level increases with degrees of complexity, with Level 6 being the most “intelligent” system. Currently, to the best of our knowledge, we are not aware of any real civil applications of SHM that reaches Level 5; the technology is just not there yet. In fact, depending on the definition of SHM, most of the civil SHM applications fall under level 1. Definition of SHM can take many forms, and it usually includes, and is overlapped with, *Non-Destructive Testing* (NDT), which involves the examination of the structure at a more localized level [53]. As the name implies, all assessment methods that remain non-intrusive can be counted as NDT, including visual, impact echo, ultrasonic, thermograph, X-ray, electro-magnetic, eddy current, and radiographic techniques [62,63,64]. NDT is usually carried out off-line; it is very helpful in determining the exact location and the extent of the damage, but “priori knowledge” of the existence and approximate location of the damage is required. Civil engineers usually refer to SHM as the “Global Health Monitoring” method and NDT as the “Local Health Monitoring” method [52,65]. Both global and local health monitoring are necessary to reach a level 3 damage detection capability. As for Level 4, the SHM system must be able to run continuously for a long enough period of time (e.g. a year) to gather the type of information that is needed for the estimation of the remaining service life. For clarity and simplicity reasons, NDT will not be covered in this report, and only the “global health monitoring” aspect of SHM will be discussed.

Clearly, SHM is an intricate and sophisticated process, and requires networking of professionals from different fields. SHM systems usually require expertise from the five fields shown in Figure 1-4 [66]. Civil engineer is the major player in *Smart Structure & Materials* and *Structural Behavior & Analysis*. As for *Sensors & Actuators* and *Remote Monitoring & Communication*, planning and execution is performed by experts from relevant fields such as electrical and mechanical engineering. For *Intelligent Processing & Data Management*, depending on the complexity and requirement of the project, the work can be handled directly by civil engineers using a common spreadsheet program, or may need advanced software and experts from the computer science/engineering and programming fields (e.g. if *PR*, *pattern recognition*, is required).

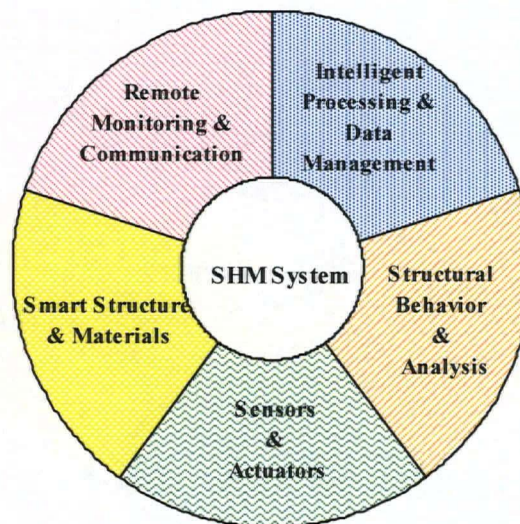


Figure 1-4 Fields usually Involved in a SHM System [66]

High-technology fields do play an important role in SHM; nonetheless, as pointed out by [67], “*whether infrastructure system problems may be addressed without the leadership of civil (and environmental) engineers is a valid question.*” Civil engineers are the only ones that have the actual experience with various stages of construction and structural failures. In order to design an effective and optimal SHM system to deal with structural problems and infrastructure issues, civil engineers are to take the leadership of the multidisciplinary team. To be a good leader, it is important for the civil engineers to have sufficient knowledge and understanding of all the different fields involved in a SHM system, for the sake of effective communication and efficiency.

There are different ways to approach the study of SHM process. The Los Alamos National Laboratory (LANL) in U.S. defines SHM in the context of the *Statistical Pattern Recognition*

*Paradigm*, which can be described as a four-part process: (1) Operational Evaluation, (2) Data Acquisition, Fusion, and Cleansing, (3) Feature Extraction and Information Condensation, and (4) Statistical Model Development for Feature Discrimination [61,68]. The Canadian Network of Centers of Excellence on Intelligent Sensing for Innovative Structures (ISIS Canada) defines SHM based on the objectives and the physical systems required to achieve the objectives, and categorizes SHM into six subsets and four subsystems (Figure 1-5 and Figure 1-6) [49].

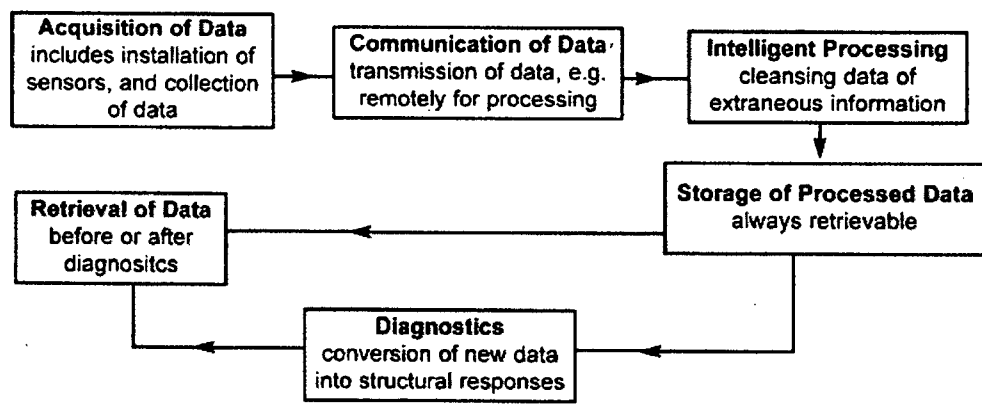


Figure 1-5 Six Subsets of a Structural Health Monitoring System [49]  
(Courtesy - ISIS Canada)

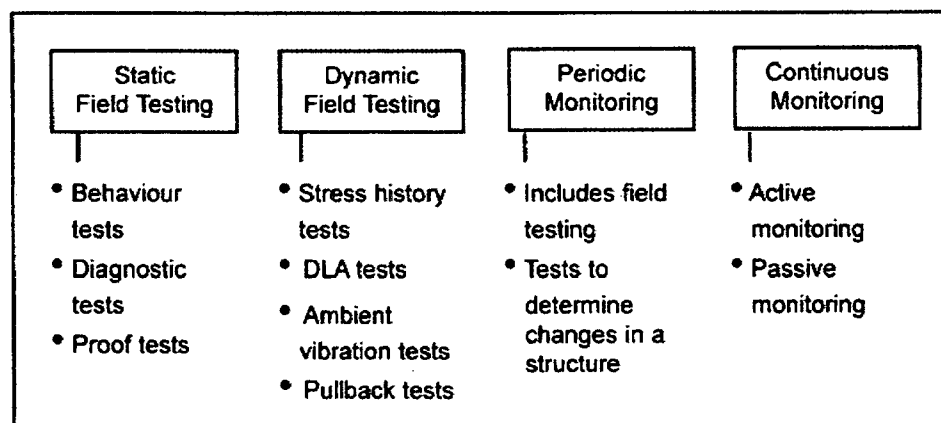


Figure 1-6 Four Subsystems of a Structural Health Monitoring System [49]  
(Courtesy - ISIS Canada)

This categorization method proposed by ISIS Canada is clear and easy-to-follow for civil engineers without much exposure to SHM; combining with the definition from LANL make the picture of SHM process even more complete. Therefore, the two will be combined and adopted in this thesis report to construct the sections and chapters for the study of the SHM process.

### 1.3 The Safe Bridge Project

As mentioned in Chapter 1.1, the deteriorating infrastructure problem is a global crisis, and Canada is not an exception. Canadian Government already recognized the danger of relying on traditional construction and maintenance practices, and the urge to use advance technology to reduce the maintenance costs and increase the life of civil engineering structures. Therefore, in 1995, ISIS Canada (Intelligent Sensing for Innovative Structures) was established by the federally funded Networks of Centers of Excellence (NCE) program to “*advance civil engineering to a world leadership position, through the development and application of fiber reinforced polymers (FRPs) and integrated intelligent fiber optic sensor (FOS) technologies, for the benefit of Canadians through innovative and intelligent infrastructure [69].*” Besides the creation of four design manuals related to FOS, SHM and FRPs by 2001, ISIS Canada further developed the new discipline, *Civionics*, which integrates Civil Engineering and Electrophotonics, and created the *Civionics Specifications* in 2004 [48,49,70,71,72]. With outstanding achievements and contributions, ISIS Canada is presently in its second funding cycle (1<sup>st</sup> cycle was from 1995 to 2002) and has four themes for its current research program; it will receive another \$12.8 million in funding for year 2006 to 2009. The network currently encompasses 13 universities, 25 Project Leaders, 276 researchers, and 36 multidisciplinary demonstration projects across Canada [69].

Dr. Nemkumar Banthia of University of British Columbia (UBC), being one of the Project Leader and the Director of Theme 2 research program, “Materials Science and Innovative Structures,” is the inventor of an innovative repair and strengthening technique called *Sprayed FRP*. *Sprayed FRP* consists of using a spray gun to spray polymer and short, randomly distributed fibers concurrently on the surface that is to be repaired [73]. The sprayed FRP demonstrated very promising laboratory results, and the ministry was very interested in its field performance, with a possibility of adopting it for future infrastructure repairs [74]. Under the auspices of ISIS Canada and the Ministry of Transportation of British Columbia, the new technique was applied to a short-span, shear-deficient concrete bridge called Safe Bridge, located in Vancouver Island, B.C.. The Safe Bridge project also became Project T3.3.18 under ISIS Canada in year 2001, and Project 1.3.8 for the second funding cycle, commenced April 1<sup>st</sup>, 2002 [75].

Safe Bridge is the first field application of the Sprayed FRP technique in the world. The project not only investigates the long-term, field performance of the Sprayed FRP, but also is treated as the testing ground for SHM process [76,77]. Both strain gauges and FOSs were installed on Safe Bridge

to make it a “smart bridge.” The ultimate purpose of the instrumentation is to get an understanding of the long-term behavior of the new strengthening material, and the composite behavior with concrete under real field condition. The measurements shall increase the experience and confidence in using the new material. The scale and instrumentation of the project is relatively simple compared to many other SHM applications. Nonetheless, this project serves as an excellent example of how SHM can assist in the study of new technology for civil engineering, and is an easy-to-follow case study for those who do not have any background knowledge of SHM. Safe Bridge project is also the first SHM study case for the Material group of Civil Engineering in UBC. Being one of the leading universities in the research of FRPs and specialized concrete in Canada, SHM will greatly benefit the group in the study and investigation of innovative construction materials.

Safe Bridge was repaired with the FRP spray in Sept. 2001. Strain gauges were embedded on the steel rebar before the spray was applied; FOSs were installed on the sprayed FRP coating after the repair process. Truck load testing was performed both before and after the repair. Besides the strain gauges, LVDTs were also used during the two initial loading tests to measure the mid-span deflections. The LVDTs were temporarily set up, and removed right away after the load testing. No data was gathered from the FOSs during these initial tests. The testing results showed significant improvement in the bending capacity of the girders as both the strains and deflections were reduced by 13~28% [78]. More information about the tests performed on Safe Bridge in year 2001 and 2002 can be found in “*Strengthening of Safe Bridge, Duncan, British Columbia: Use of Hybrid Fiber Reinforced Mortar and Sprayed Glass Fiber Reinforced Polymer*” and “*Experimental And Finite Element Analysis of A Damaged Reinforced Concrete Bridge Strengthened with Sprayed Glass Fiber reinforced Polymers*” [75,79].

Later, two more field tests were performed on Safe Bridge, and SHM components were tested during these two tests; these two field tests are the focus of this thesis. This thesis will compare the results from the later two field tests to the earlier test results as well to show the effectiveness of the new repair method.

#### **1.4 Thesis Objective and Scope**

The objectives of this thesis work are two folds. One is to continue to study and investigate the field performance of the sprayed FRP technique. The potential of sprayed FRP is huge, and the investigation of its long term field performance is a must in order to translate the technique from the

laboratory to the real market. Besides being a reinforcement to increase the strength and toughness (energy absorbing ability) of the repaired component, the spray itself can also act as protective coating to enhance the long-term durability of the repaired structure. Also, the spray technique is handy and convenient to apply on any shape or surface, and is estimated to save significantly in cost when compared to traditional steel jacketing or normal FRP jacketing [80]. Fatigue behavior of the sprayed FRP under field condition is a critical aspect that needs to be explored. SHM can be very beneficial in this regard as the required information may be collected by continuous monitoring. Therefore, even though fatigue life prediction of Safe Bridge is not covered in this thesis, it is the ultimate goal behind the application of SHM to Safe Bridge.

The second objective is to get hands-on experience with the SHM process itself. Learning a multidisciplinary topic is not an easy task, and the fastest way is to learn it from actual experiences. Even though there are many papers on SHM today, most of these writings are targeting only at a particular aspect of SHM, or is written for one particular field application. Besides Design Manual No.2 created by ISIS Canada, there is not much publication that is written for the purpose of documenting the complete process of SHM to civil engineers who is interested in this new field [49]. This thesis is written not only as a report on the Safe Bridge project, but also as an introductory reference on SHM for civil engineers. The intention of the thesis is not to present a comprehensive literature research for SHM (in fact, it is impossible to do so because the field is growing everyday), but rather, is to help learners of the new field to expedite in the learning process and to avoid common mistakes they could make in their first SHM application.

With these two objectives in mind, the thesis report is organized into 7 chapters. Chapter 2 is the literature review of SHM, focusing on concrete bridge applications; it starts with an introduction on current state of bridge inventory in North America and the particular needs, and then moves into the discussion of current practice for bridge global condition assessment methods; the final section is devoted to the study of various components of SHM process. Chapter 3 provides background information on the Safe Bridge project, including literature research on relevant topics and specific information on the Safe Bridge itself. Chapters 4 and 5 will present detail information about the two field tests performed in 2003 and 2005 respectively, including their testing procedures, the testing results and data processing steps performed, and concluded with the comparisons between different field testing results. Chapter 6 describes Safe Bridge Project from an SHM perspective, and the subsections will follow the same title and orders as the subsections in Chapter 2, to show how each SHM component is applied in a real case. Finally, Chapter 7 gives conclusions of this thesis work and recommendations for future work.



---

## *Chapter 2*

### Literature Review - Structural Health Monitoring on Bridges

---

Within all civil infrastructures, bridge is the dominant research area for SHM application, as the number of deficient bridges is huge, and better assessment methods are in urgent need [65]. Current practice relies heavily on visual inspection (VI), which is subjective, slow, and dangerous for inspectors, and most of all, limited in providing reliable assessment results. Field load testing, a subsystem of SHM, has proven to be a much better assessment method, but the traditional way of practice still holds many drawbacks, such as time-consuming, costly, and always require service disruption of roadway. SHM on bridges, which makes remote control and long-term monitoring possible, is a much safer and effective way for bridge condition assessment. Data with different time frame can be collected and for more usages. With a basic understanding in current bridge assessment methods and the major components of SHM process, the two can be integrated better and the benefits from new technology can be truly utilized.

This chapter contains three major themes: 1. the current state of our bridge inventory and the needs; 2. current practice for existing bridge inspection and evaluation and the four subsystems of SHM (include field testing and long-term monitoring); 3. the major components of a SHM system. The first theme also includes a brief discussion on the history and evolution of the bridge inspection regulations in U.S., and why “bridge” is a demanding field for SHM. As for the second theme, it is important to know how bridges are evaluated today and what the four subsystems of SHM are, in order to understand how SHM technology can be utilized for bridge maintenance and management. With an understanding of the potential roles SHM can play in bridge assessment and management, the next step is to study SHM components in detail, to gain more knowledge about the new discipline. For the ease of studying, SHM process is divided into five components, adopted from the definitions developed by ISIS Canada and LANL, as mentioned in chapter 1.2. Again, for a multidisciplinary field like SHM, it is impossible to cover all components explicitly. The aim is to give readers a general idea about SHM.

## 2.1 Introduction

Bridges play a critical role within the transportation network to support a nation's economy and mobility; however, the condition of our bridge inventory today is alarming. In U.S., approximately 4 billion vehicles are crossing bridges per day, but out of every four bridges, there is one considered to be "deficient" [65,81]. The number of deficient bridges is the most commonly used measure to evaluate the condition of a nation's bridges in North America [82]. In this section, the data from the U.S. National Bridge Inventory (NBI), will be used to demonstrate and represent the current state of bridge inventory in North America [82], because Canada is using similar evaluation systems as the U.S., but does not have as comprehensive source of information for bridge inventory on the national level as the NBI records [82].

The definition of "deficient bridge" is established by the U.S. Department of Transportation Federal Highway Administration (FHWA), and the evaluation is based on the data collected according to the National Bridge Inspection Standards (NBIS) and recorded in the National Bridge Inventory (NBI) [82]. The NBIS, together with the Special Bridge Replacement Program (has been renamed to HBRRP, Highway Bridge Replacement and Rehabilitation Program), are the first major programs established in the national-level for bridge inspection and safety evaluation [82]. NBIS requires periodic inspections to identify bridge conditions, maintenance needs and safety problems; it also requires all states to maintain written inspection reports about current inventory of all bridges [83]. According to the regulation, all bridges in excess of 6.1 meters on public roads have to be inspected, in general, every two years [82]. The HBRRP is responsible for providing federal funds to states for bridge replacement and rehabilitation [83]. To be eligible for HBRRP, a bridge must be classified as "deficient" in NBI first [84].

According to NBIS, there are two types of deficient bridges: *structurally deficient* or *functionally obsolete* [81]. *Structurally deficient* bridges are the ones contain deteriorated structural components and often show reductions in load-carrying capacity. Therefore, structurally deficient bridges usually need immediate rehabilitation; if not, restrictions on weight/speed/volume of traffic must be applied for these bridges to remain open [85,86]. *Functionally obsolete* bridges are not necessarily unsafe structurally, but due to their older design features (such as its clearance, deck geometry, alignment, etc.), they may not be able to accommodate current traffic, or, they do not meet current standards [85,86]. Again, load restrictions may be required. It is estimated that there are over 100,000 posted bridges currently exist in U.S., and another 50,000 bridges should be load posted [87].

Based on the latest NBI record, within the total 594,616 bridges in U.S., there are 75,871 (12.8%) structurally deficient and 80,306 (13.5%) functionally obsolete bridges by the end of year 2005 [88]. Inadequate load capacity (i.e. low load rating) is the most significant factor contributing to structural deficiency [89]. As structural deficiencies are considered more critical in terms of safety, for a bridge that is both structurally deficient and functionally obsolete, it is counted as structurally deficient [81]. So far, within the 75,871 structurally deficient bridges, nearly half of them also have some type of functional obsolescence [81]. The bridges suffer from both deficiencies should be the ones with the steepest degradation curves (as shown in Figure 1.3). If the data is correct, currently there are more than 37,000 bridges in U.S. need immediate repair, reinforcement, or replacement.

A long existing problem with bridge inventory management is, legislations and researches are often “passive” – they established and conducted in response to catastrophic events. Bridges play such an important role in people’s daily life, but national-level legislations for bridge inspection and maintenance had never been established, until the end of year 1967, when a disastrous bridge collapse happened (see Figure 2-1) [83]. Thirty-seven vehicles fell into water when the Silver Bridge collapsed, and resulted in 46 deaths [84]. In response to the tragic event, the two landmark legislations (NBIS and SBRP) were finally developed and enacted on Dec. 31, 1970. Over the past 36 years, the legislations have been modified and tailored, but the “price” for the fine-tuning was high. For example: the failure of the I-95 Mianus River Bridge in 1983, which killed 6 people, triggered the research for corrosion and fatigue behavior of steel connections; two scour-induced bridge failures in 1987 and 1989 led to additional guidance for scour assessment and requirement for underwater inspection; the collapse of the Cypress Viaduct on 1989 due to the Loma Prieta Earthquake killed 42 people, and raised the awareness of the need for bridge seismic retrofit [82,83,90].

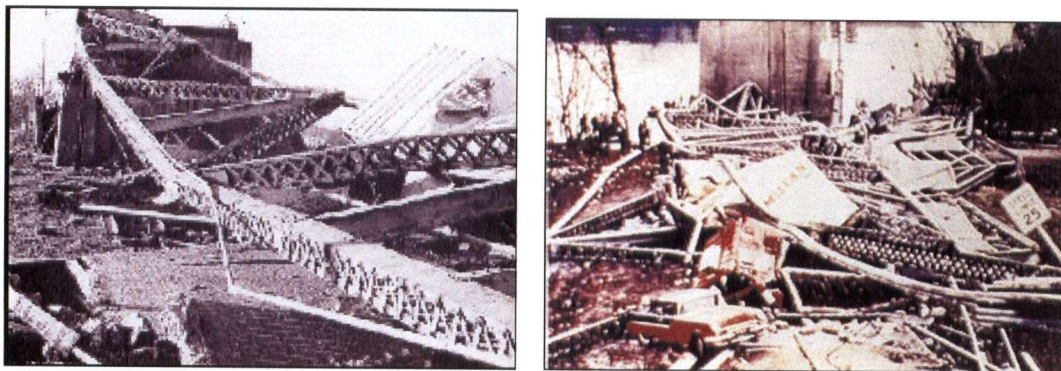


Figure 2-1 The Collapse of Silver Bridge Spanning West Virginia and Ohio, U.S.

Source: <http://www.fhwa.dot.gov/infrastructure/rw93.htm> (left);  
<http://www.tfhr.gov/pubrds/jan00/nde.htm> (right)

The routine of a tragic event → death and casualties → financial and social impact → extensive media coverage and public anger → congressional inquiry → investigation and researches → additional legislations, has replayed again and again over the years [90]. For some of the incidents, the failure bridge had just passed its regular routine inspection; there were also cases that “*problems were foreseen and warned by alert engineers, but potential solutions were delayed due to either excessive costs imposed by existing technology or the reluctance to adopt new technology [90]*”. Clearly, passive inspection should be turned into active monitoring; new technologies for repair and maintenance are in urgent need, and they should be supported and utilized.

The number of deficient bridges actually has declined steadily since 1994, from 32.5% to today’s 26.3%, mainly from the *structural deficient* group [81]. Possible reasons could include the increase awareness of infrastructure crisis and the emergence of SHM technology. Nonetheless, it is estimated that \$7.3 billion is required annually just to stop the backlog from increasing, and \$9.4 billion per year is needed for the next 20 years to eliminate all bridge deficiencies [10]. In fact, the problems with deteriorating bridges will continue for another two decades, as over 60% of the bridge inventory was built between 1955~1990 (see Figure 2-2).

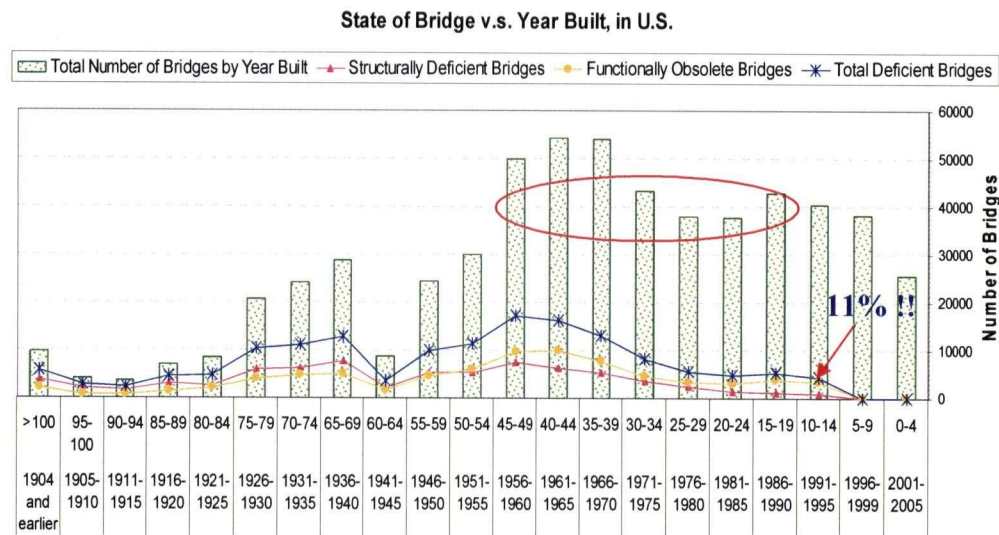


Figure 2-2 Number of Total and Deficient Bridges according to Year Built, by Dec. 2005  
Source: <http://www.fhwa.dot.gov/bridge/defbr05.xls>

The majority of the deficient bridges today were built during the construction boom from 1955 to 1970. Nonetheless, after the construction boom, there were still significant numbers of bridges constructed during 1975~1995, as shown in Figure 2-2. Even though most bridges are designed for a



50+ years design life, certain components, like the deck, typically require major repair/replacement every 15 to 20 years [91]. The more scary fact is, there are already 11% of the “young bridges” (the 10~15-year-old group) being classified as deficient bridges today (Figure 2-2) [88]. These data point out two things: first, “new” bridges can be deficient too, and both new and old bridges need regular “health check”; second, the “health check” method for bridges has to be efficient and reliability, so that the limited financial resources can be spent effectively. Consequence of inaccurate assessment results is not only waste in unnecessary spending, the worst is to miss the real problematic bridges and harm public safety.

The performances of bridge management programs really rely on the data input. No matter how elaborate and sophisticated the analysis and algorithms employed, the final recommended decisions can not be any better than the data upon which they are based [88]. Since the 90s, technologies in many fields of engineering have advanced significantly, but bridge performance has not improved accordingly. Within the period of 1989-2000, in U.S. alone, there were still over 500 bridge failures happened (Figure 2-3) [92]. With all the sophisticated technology employed in bridge design and construction today, the examination and maintenance of bridges still depend mainly on visual inspection [43]. Clearly, from the data, visual inspection is not doing the job well. Also from Figure 2-3, within all the failure cases, more than three-fourth were unknown for its failure type or failure stage. There is not doubt that our bridge management system still needs lots of improvement.

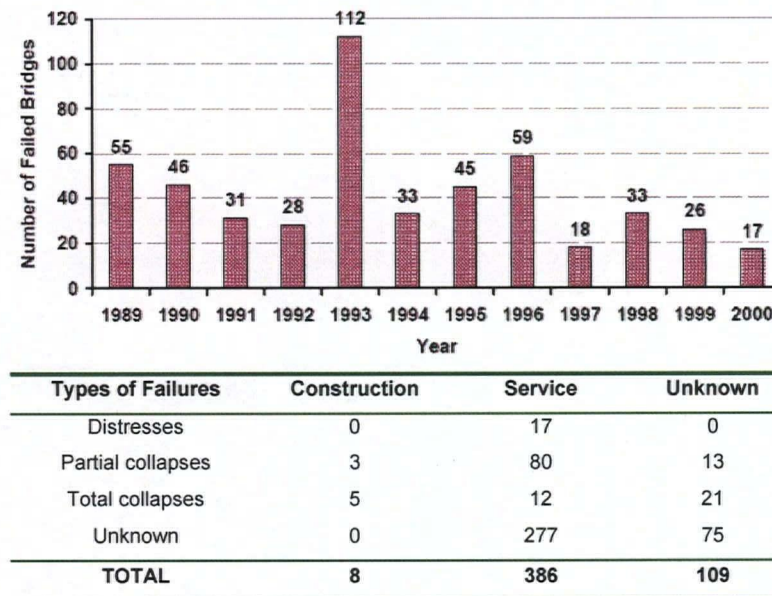


Figure 2-3 Number of Failed Bridges with Respect to Year and Phase of Failure Occurrences  
Source: [92]

SHM, the technology that makes “smart bridge” possible, is available today. This technology can provide the quantitative and objective information necessary to move beyond our current bridge management system. With reliable and timely data and information, bridge assessment can be done more efficiently and accurately, and catastrophic failures can be prevented. With the growth and maturing of SHM technology, it should be gradually adopted into the bridge management system. Therefore, it is important to have basic knowledge on how bridges are evaluated today in order to understand how SHM can be integrated with current practice. The next section is devoted to the literature research for common global condition assessment methods for bridges. Rather than applying to all types of bridges, the discussion will focus mainly on short-to-medium span, reinforced concrete bridges. Not only that Safe Bridge falls under this category, concrete is the dominant construction material for existing bridge inventory, and most bridges that need rehabilitation/replacement are short-span bridges [82,93].

## 2.2 Global Condition Assessment Methods for Bridges

The primary reason of bridge inspection is to assure public safety and confidence; the second function is to provide data, as also required by regulations, for bridge evaluation and bridge management programs [83]. Two types of criteria are widely used in assessing the safety of existing bridges: the *general condition* and the *load-carrying capacity* of the bridge [94]. These criteria are used routinely to determine if a bridge can remain open for public usage with/without special restrictions. In many countries, the two criteria are “quantified” for acceptable levels in codes, for the ease of evaluation and as part of the bridge management system. In U.S., the *Condition Rating* for bridges is based on visual inspection only; the *load-carrying capacity*, evaluated by *Load Rating*, normally is calculated analytically, also according to visual inspection results. When the analytical results are in doubt, *field testing* is performed to verify the true field responses of the tested bridge. Canada follows a similar system for bridge inspection and evaluation, as indicated in Section 14 of the Canadian Highway Bridge Design Code [95].

The “global condition assessment methods” here refers to the assessment practices normally carried out for most bridges, the *condition rating* and the *field testing*. As mentioned in Ch 1.2, field testing (including *static field testing* and *dynamic field testing*) can be viewed as two of the subsystems of SHM; the other two subsystems are related to long-term monitoring (*periodic monitoring* and

*continuous monitoring*). Basic understanding about the four subsystems help one to see the benefits of SHM from different aspects, and how SHM can be engaged with current practice. Again, there are also many other nondestructive assessment methods available today for detecting specific bridge problems, but this section is not intended to cover them. *Visual inspection, field testing, and long-term monitoring* are the focus of this section.

## **2.2.1 Visual Inspection**

Visual Inspection (VI) refers to all unaided inspection/evaluation techniques that use the five senses with only very basic tools, such as flashlights, measuring tape, sounding hammers, etc. [96]. Current practice usually involves with visual observation and simple physical inspection methods like hammer sounding or chain dragging [52]. Hammer and chain are “sounding method” tools used to detect debonds, delaminations, and voids; hammers are used more on structural components beneath the deck area, and dragging chains are used for inspecting the deck surface area [83]. Inspectors try to distinguish defected area by listening to the sounds reflected from tapping or striking the concrete surface. Therefore, the accuracy of this type of method relies heavily on the inspector’s experiences and personal judgement, and the process is time-consuming and impractical for large areas. It often takes four or five professionals a full week just to inspect a single average-size bridge [97]. Furthermore, visual inspection is not only expensive, subjective and slow, it can be dangerous for inspectors.

### **2.2.1.1 Signs of Deterioration**

For concrete bridges, inspectors usually look for cracks and spallings, as they are the most predictable indications for future deterioration [83]. Besides cracks and spalls, some other common signs of concrete deterioration include efflorescence, leaching (Figure 2-4), honeycombing, and exudation (Figure 2-5).

Efflorescence is a white deposit on concrete caused by crystallization of calcium chloride brought to the surface by moisture in the concrete. If a concrete surface show evidence of efflorescence, there might be increasing porosity and leaching problem which could lead to serious disintegration of concrete (concrete deteriorated into small fragments or particles) [83] (Figure 2-4). Efflorescence is also a common problem for bridges in Canada because of the extensive use of de-icing salt.



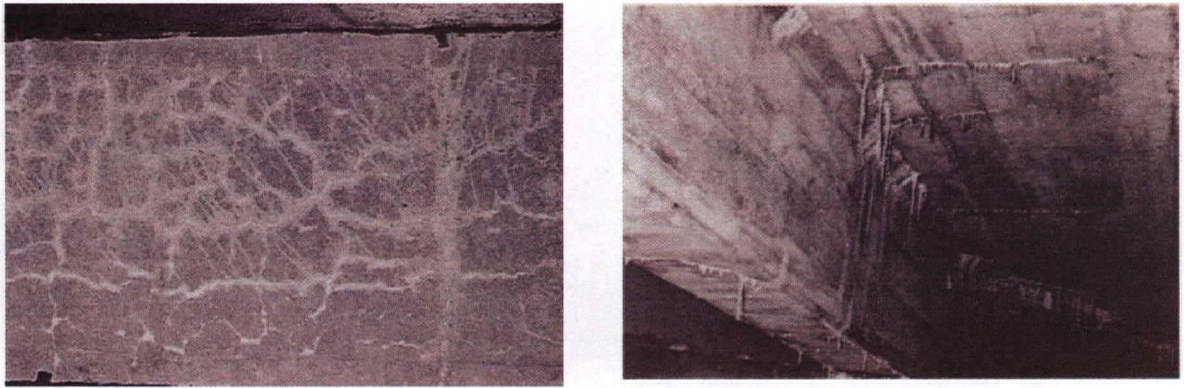


Figure 2-4 Signs of Concrete Deterioration: (a) Efflorescence; (b) Leaching  
Source: [83] (Courtesy- S.H. Park)



Figure 2-5 Signs of Concrete Deterioration : (a) Honeycombing; (b) Exudation  
Source: L: [98](Courtesy - Syracuse University); R:[83]

Honeycombing is the formation of small holes or voids caused by insufficient fill in between the spaces of coarse aggregate particles [83]. Honeycombing is more common appear on vertical components (e.g. columns, walls), and is usually caused by segregation of concrete during construction. Exudation is a liquid or viscous gel-like material discharged through pore, crack, or opening in the surface of concrete [99].

Since the bridge will be rated based on the inspector's field report, inspector should describe the type, size, direction, location and appearance of any unusual signs clearly, and the possible causes and extent of deterioration should be noted. In addition, it is important for bridge inspectors to have knowledge and understanding on bridge materials, as the behaviour of a bridge under load is very much influenced by the properties of the materials.



### 2.2.1.2 Rating Systems

According to AASHTO's *Manual for Condition Evaluation of Bridges (1994)*, there are five types of bridge inspections: *Initial Inspection*, *Routine Inspection*, *In-Depth Inspection*, *Damage Inspection*, and *Special Inspection* [100]. *Routine Inspection* is most commonly performed, followed by the *In-Depth Inspection* [101]. *Routine Inspection* is typically completed using only VI techniques, and the results are used to update the *Condition Rating* and *Appraisal Rating* for the inspected bridge[84].

*Condition Ratings* are the primary criteria used to classify bridge deficiencies, and the NBI database contains ratings on three primary components of a bridge: the deck, superstructure, and substructure. The rating is assigned based upon a 0~9 scale to the three components (see Figure 2-6), and a rating of 4 (poor) or less will put the bridge under the "deficient" category [84]. 80% of all structurally deficient bridges have condition rating deficiencies in their three primary components; the remaining 20% of structural deficiencies are classified based on inadequate structural appraisal ratings.

Rating	Condition Category	Description
9	Excellent	
8	Very Good	
7	Good	No problems noted.
6	Satisfactory	Some minor problems.
5	Fair	All primary structural elements are sound but may have minor section loss, cracking, spalling, or scour.
4	Poor	Advanced section loss, deterioration, spalling, or scour.
3	Serious	Loss of section, deterioration, spalling, or scour have seriously affected the primary structural components. Local failures are possible. Fatigue cracks in steel or shear cracks in concrete may be present.
2	Critical	Advanced deterioration of primary structural elements. Fatigue cracks in steel or shear cracks in concrete may be present or scour may be removed substructure support. Unless closely monitored, it may be necessary to close the bridge until corrective action is taken.
1	Imminent Failure	Major deterioration or section loss present in critical structural components, or obvious loss present in critical structural components, or obvious vertical or horizontal movement affecting structural stability. Bridge is closed to traffic, but corrective action may put back in light service.
0	Failed	Out of service; beyond corrective action.

Figure 2-6 Bridge Condition Rating Categories for NBI Database [84]

*Appraisal Ratings* are essentially a comparison between the existing conditions of the bridge to the current design standards, and assigned to each bridge for *Waterway Adequacy*, *Structural Evaluation (Load Carrying Capacity)*, *Approach alignment*, *Deck Geometry*, and *Under-clearances*. Similarly, a 0 to 9 scale is given and the bridge is classified as deficient when the appraisal rating is 3 or less [82] (see Figure 2-7).

Rating	Description
N	Not applicable.
9	Superior to present desirable criteria.
8	Equal to present desirable criteria.
7	Better than present minimum criteria.
6	Equal to present minimum criteria.
5	Somewhat better than minimum adequacy to tolerate being left in place as is.
4	Meets minimum tolerable limits to be left in place as is.
3	Basically intolerable requiring a high priority of corrective action.
2	Basically intolerable requiring a high priority of replacement.
1	This value of rating code is not used.
0	Bridge closed.

Figure 2-7 Bridge Appraisal Rating Categories for NBI Database  
Source: [82]

### 2.2.1.3 Reliability of Visual Inspection

There is no doubt that the accuracy and reliability of the inspection results are critical to the allocation of the limited financial resources, but clearly, these rating methods are subjective and non-quantitative. Since the implementation of the NBIS in 1971, a complete study of the reliability of VI had never been undertaken. In light of these, the FHWA started a comprehensive study to examine the reliability of VI for highway bridges in 1998 [43]. The study consisted of a review of existing literature on the topic, a survey of bridge inspection agencies, and a series of performance trials involving bridge inspectors from 49 State Department of Transportation; the study also discuss

factors that may affect the inspector and inspection results [96]. After more than three years of investigation and study, the process and results are fully documented in a two-volume final report entitled *Reliability of Visual Inspection for Highway Bridges* [96]. Only some of the major findings are summarized in the following; interested readers are encouraged to read the original reports for more information.

The result of the investigation has shown that the methods used and data collected in Routine Inspections can vary considerably from State to State. During the performance trials, on average, four or five different Condition Rating values were assigned to the bridges' three primary components [96]. It was discovered that Condition Ratings are generally not assigned through a systematic approach, and it was predicted that 95% of the Condition Ratings from different inspectors will be distributed over five contiguous Condition Ratings (centered about the average). It was concluded that the 0-9 scale is not refined enough to allow for reliable Routine Inspection results. Concerns about the reliability of the Appraisal Ratings were high too. For example, the structural appraisal rating is based upon the Inventory rating of the bridges (truck load testing). According to the data, there is significant number of bridges with substandard load capacity, but for almost 40% of these "weak bridges", the method used to calculate their load capacity could not be reported. Again, this raises questions about the reliability of the appraisal ratings to classify deficient bridges [84].

Even for In-Depth Inspection, which *"is generally completed at longer intervals than Routine Inspections and may include the use of more advance NDE techniques"* and therefore supposed to *"identify deficiencies not normally detected during Routine Inspection"*, it was found that the results rarely reveal deficiencies beyond those that could be noted during a Routine Inspection. The main reason should be that In-Depth Inspection is still performed based mainly on visual inspections. The primary data used to evaluate the in-depth inspections were the inspectors' field notes, which summarize specific deficiencies identified in the bridge. From the reliability study, it was found that the frequency with which field notes are taken varies considerably. In fact, most of the inspectors did not make notes of the types of defects (like weld cracks) that were designed to identify during the investigation [43]. This shows that despite the problems with the rating system, the "inspector" is also a main reason for inconsistent/inaccurate field inspection results. Another example, many inspectors did not indicate the presence of important structural aspects of the bridge, such as support conditions and fracture/fatigue-critical members. There was significant variability between how long inspectors anticipate they need to complete an inspection and the actually time spent. Finally, it was found that professional engineers are typically not present on site for bridge inspection [96].

Visual inspection is highly variable, subjective and inherently unable to detect invisible deterioration, damage or distress [97]. There are many types of damage and deterioration that are beyond the capabilities of visual inspection to be detected. Some of the measurement and detection needs currently not met by our standard practice of visual inspections are summarized in Table 2.1 [102]. Deteriorations that do not manifest visible symptom(s) are not detected or quantified. Some deteriorations, when becomes visible, are already in severe condition (e.g. corrosion of reinforcement in concrete) [88].

Table 2-1 Measurements that can not be obtained by Visual Inspection [102]

Damage	Detection	Operation	Service
<ul style="list-style-type: none"> <li>• Impact</li> <li>• Overload</li> <li>• Scour</li> <li>• Seismic</li> <li>• Fatigue</li> <li>• Settlement</li> <li>• Movement</li> </ul>	<ul style="list-style-type: none"> <li>• Corrosion</li> <li>• Fatigue</li> <li>• Water absorption</li> <li>• Prestress Force Loss</li> <li>• Unintended Behavior</li> </ul>	<ul style="list-style-type: none"> <li>• Traffic counts</li> <li>• Weight of trucks</li> <li>• Maximum stress</li> <li>• Stress cycles</li> <li>• Deflection</li> <li>• Displacement</li> </ul>	<ul style="list-style-type: none"> <li>• Congestion</li> <li>• Accidents</li> <li>• Reduced traffic capacity</li> <li>• Performance measures</li> </ul>

A bridge management program relies so heavily on visual inspection can be very problematic. Based on the number of failure bridges over the past twenty years, the non-quantitative and gross nature of the NBI data has proven to be inadequate for effective bridge management. The NBI is also severely limited in providing adequate measures of bridge performances for quality improvement and asset management initiatives. As pointed out by Jim Cooper, the former director of Bridge Technology at the FHWA, *“Owners, and in particular, their “traditional” bridge engineers, continue to rely on visual inspection to determine bridge viability. THAT MUST CHANGE. With so many bridges deemed structurally deficient and limited funding, determining which bridges need immediate rehabilitation or replacement should not be left to a simple visual inspection- and yet that is the common practice”* [103]. With so many problems associated with visual inspection, instrumented monitoring is expected to complement inspection methods, to provide an objective measure of the state-of-health of existing bridge inventory, and to alert officials to bridge deterioration or failure.

### 2.2.2 Field Testing

Filed testing here refers to the practice of applying standard truck loads statically or dynamically to the bridge. As stated in the "Canadian Highway Bridge Design Code", "*bridges may be considered for load testing if the Engineer deems that the analytical evaluation does not accurately assess the actual behaviour of the bridge, or there is otherwise a need to establish the actual behaviour of the bridge or its components*" [95]. The field testing is often performed to verify the load-carrying capacity calculated based on the visual inspection results. It is already recognized that true picture of the behaviour of a bridge is not available until it is in-service, and currently, engineers rely a lot on modeling techniques to predict a bridge's field responses. Field testing is also required for "unconventional" cases that the regular analytical formula do not apply; for example, when new material or new repair technique has been used.

As mentioned earlier, there are a significant number of posted bridges existing today, and the predominant factor leading to structural deficiency is a low load rating [89]. While the load restriction is meant to ensure the safety of the traveling public, at the same time it also brings significant inconvenience and financial cost to many, due to the fact that people need to detour around the posted bridge. In addition, the posted bridges are likely the ones in priority to receive the costly repair/replacement funding [87]. Therefore, it is important that the load-carrying capacity of the posted bridge is accurately estimated.

Current rating practices are based on the procedures outlined in the "*Manual for Maintenance Inspection of Bridges*" and the "*Guideline Specification for Strength Evaluation of Existing Steel and Concrete Bridge*" in U.S. [83,104]. The conservative assumptions made during the rating analysis process inherently lead to a bridge evaluation that frequently underestimates the actual bridge capacity [105]. Field testing provides accurate values for many of the assumed properties, and the subsequent evaluation of the bridge better represents the actual capacity [105]. It has been found that most bridges have inherent reserves of strength that can not be detected with simple visual assessment. Field testing can investigate these reserves and allow a more realistic assessment of the bridge [52].

It is important to have a basic understanding on how the load carrying capacity is evaluated analytically currently, in order to recognize the need for field testing. Therefore, a brief discussion on

current practice for load ratings will first be provided before the introduction of the two types of field testing: the static field testing and the dynamic field testing.

### 2.2.2.1 Load-Carrying Capacity Rating for Bridges

Currently in U.S., the bridge load-carrying capacity is evaluated with respect to structural strength [83]. The "AASHTO Manual for Condition Evaluation of Bridges" provides the basis for *Allowable Stress Method* and *Load Factor Method*, while the "Guideline Specification for Strength Evaluation of Existing Steel and Concrete Bridge (1989)" uses the *Load Resistance Factor Rating*. The following shows the basic rating equations for each of the method [83]:

**I. Allowable Stress (AS) Method:**

$$C = D + RF (L) (1 + I)$$

$C$  = capacity

$D$  = dead load effect

$L$  = live load effect

$I$  = impact factor for live loads

**II. Load Factor (LF) Method:**

$$C = 1.3D + A2 RF (L) (1 + I)$$

$RF$  = rating factor for the live load carry capacity

$A2$  = load factors

$\phi$  = resistance factor

**III. Load Resistance Factor (LRFD) Method:**

$$\phi R_n = \gamma_D D + (RF) \gamma_L (L + I)$$

$\gamma_D$  = dead load factor

$\gamma_L$  = live load factor

Highway bridges are rated at two levels, the *Inventory Rating* and the *Operating Rating*. The *Inventory Rating* defines the load level at which a bridge can be safely used during its whole life time (for indefinite time); whereas the *Operating Rating* gives the absolute maximum permissible load level for a bridge [83]. No load greater than the *Operating Rating* should be permitted to cross the bridge.

The general standard rating vehicles used for bridge field testing in U.S. are (Figure 2-8):

- H 20 (20 tons)
- HS 20 loading (36 tons)
- Type 3 (25 tons)
- Type 3-S2 (36 tons)
- Type 3-3 (40 tons)

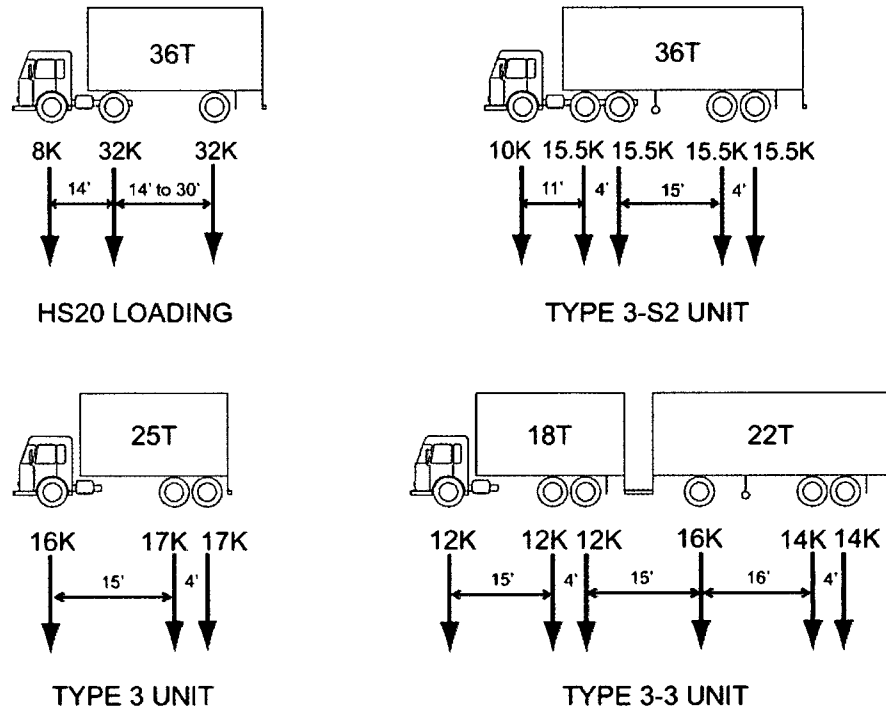


Figure 2-8 Types of Rating Vehicles for Bridge Field Testing in U.S.  
Source: [4]

Which type of rating truck to be used mainly depends on the size and type of the bridge, and the traffic volume. Most of the highway bridges today are designed for HS 20 loading in the States. For field testing on short span, rural bridges, like Safe Bridge, Type 3 unit is usually used. These vehicles can be used for both static and dynamic field testing.

### 2.2.2.2 Static Field Testing

Static Field Testing here refers to the common practice of placing known truck load at strategic locations on the bridge, and bridge responses are collected through sensing and data acquisition systems. Static field-testing for bridges has a long history of been in practice. In the early 90s, bridge field testing was performed with uniformly distributed load, which simulated the actual traffic, and the induced deflections were measured manually [49]. The early practice was very time- and labour- consuming, and the health of the bridge was only based on its flexure stiffness [49]. Gradually, with the advances in technology and the increasing capacity of testing equipments, more accurate measurements can be performed. Nonetheless, most field tests are still performed as special

projects by university scholars and research groups. Main reasons include the fact that field testing is still relatively expensive and time-consuming (compared to visual assessments), and most of all, service disruption of the roadway is required.

The Ontario Ministry of Transportation (Bakht and Jaeger) in Canada, the Florida Department of Transportation (DoT) (El Shahawy and Garcia) and the New York DoT (Fu et al.) in U.S. are a few authorities in North America that have extensive experiences with field testing to rate their bridges [87]. Over 250 bridges have been load tested in Ontario, and the results showed that, in most cases, the actual load-carrying capacity is higher than the value calculated by analytical models and load rating methods [49]. There were also many cases that the data collected were totally out of surprise, and it was tempting to reason the cause as instrument malfunction [49]. However, most of the time, the unexpected readings were really from unexpected bridge behaviors. Some common factors attribute to the “surprising bridge behaviors” include unintended continuity, two-way slab action, end/bearing restraints, composite/non-composite action, and flexural participation from the curbs/railings [49,106]. Some interesting examples of unexpected testing results can be found in [49,107].

The worst-case scenario is to have a bridge’s actual load-carrying capacity be lower than expected. The consequence of overlooking a problematic bridge can be serious; the tragic highway-overpass-failure just happened recently in Montreal, Canada is one example. On Sept. 30, 2006 noon, the three eastbound lanes plus the pedestrian sidewalk of the de la Concorde Blvd. overpass suddenly collapsed and crumbled onto Highway 19 beneath it [108] (Figure 2-9). Two vehicles were crushed completely and all five passengers in the vehicles were killed immediately [108]. An hour before the collapse, a piece of concrete measuring 38 cm by 18 cm was reported fallen off from the structure [109]. A patroller was sent to inspect the overpass immediately to conduct visual and auditory inspections [109]. At the time, the inspector judged that there was no need to close the roadway. According to the Transportation Quebec, patrollers are trained to evaluate, but they are not required to have engineering background. This incident showed clearly the problems with current practice of bridge assessment.

The fallen overpass was built in 1970, and it was designed for a lifespan of 70 years [108]. According to the local regulation, similar structures are inspected yearly, and they receive in-depth inspections every three years. This particular overpass just passed its regular inspection in May 2005 [109]. After the incident, another overpass built at the same time by the same company was closed



immediately for inspection. About 20 more similar traffic structures were inspected again over the next 48 hours [109]. All these are the consequences of one bridge failure.



Figure 2-9 Photos of the Failure of *de la Concorde Blvd. Overpass* in Montreal on Sept. 30, 2006  
*Source: [109] (Courtesy Ryan Remiorz)*

The cause of the incident was believed to be debonding between the rebar and concrete, resulting from corrosion of the steel reinforcements [110]. As can be observed from the photos, the failure surfaces were quite “clean”, as if they were cut through by a knife, and steel rebar could be seen sticking out of the failure surface. It is possible that, after debonding happened and the composite action lost, the section of roadway was unable to support its own weight [110]. Failure in concrete is always catastrophic. Deterioration in the bridge could be not observable, therefore visual inspection could not pick up the problem and the tragedy happened.

As mentioned in Ch 1, Static Field Testing can be viewed as a subsystem of SHM. The equipments used for all four subsystems are similar in the way that some kinds of sensing and data acquisition systems are always involved. Nonetheless, static field testing can be said as the “simplest” one to be conducted, because its time-frame is relatively short and the required instrumentation is usually the least sophisticated. Therefore, it is the most-often performed type of field testing. In addition, for the purpose of identifying actual load-carrying capacity of a bridge, data from Static Field Testing is usually sufficient to give satisfying results.

More about the sensing and communication systems will be given in Section 2.3 when talking about the components of SHM system in detail. The following will give an introduction of the three types of static field testing.

#### **2.2.2.2.1 Types of Static Field Tests**

The three types of static field tests commonly performed are *Behaviour Tests*, *Diagnostic Tests*, and *Proof Tests* ; all three use known truck load as the static testing load [49]. These methods are different in terms of their purposes, the level of load applied, and/or the manner in which the experimental findings are used to arrive at a load rating [106]. The *Behaviour* and *Diagnostic* tests are actually similar, only differ in their testing purpose, and some people use the two terms interchangeably.

The *Behaviour* and *Diagnostic* tests are performed more often than the *Proof test*. The main reason is that *Proof Test* is “risky” – it could cause permanent damage to the tested bridge; therefore, *Proof Test* should only be conducted by qualified professionals [49]. Also, a *Proof test* always takes longer time than the other two types of static field tests, and usually requires closing of all the traffic lanes on the bridge until the completion of the testing [106]. Here, the definition of the three types of static field testing are based on ISIS Canada’s Design Manual No. 2 [49].

##### ***Behaviour tests***

Usually, the static field testing are performed to “*study the mechanics of bridge behaviour*” or “*to verify certain methods of analysis*”. It is customary to refer the field test as *Behaviour Test* when the testing purpose is to verify a certain method of analysis. In a behaviour test, the bridge is always loaded below its elastic load limit (i.e. the maximum service load legally permitted), and the data

collected are usually strain and/or deflection measurements according to different loading positions of the truck. In most cases, the loading positions are chosen to create maximum strain/deflection effects. Behaviour testing results are mostly used to calibrate the analytical model created to represent the existing condition of the bridges. It is important to notice that behaviour test does not provide the maximum capacity of the bridge directly [111]. The significance of verifying the analytical model is not just beneficial to the tested bridge, the model to obtain the actual response and condition of that particular bridge, it is also beneficial for the study and evaluation of bridges with similar design and age, and for new bridges using similar design [49].

### ***Diagnostic tests***

When the major purpose of a static field-testing is to study the interaction between different components of a bridge, the test is referred to as the Diagnostic Test. Similar to the Behaviour Test, during a *Diagnostic test*, the bridge is loaded within its elastic load limit (see Figure 2-10), and strain and/or deflection measurements are taken at strategic locations. The effects of interaction between different components of a bridge can be beneficial or detrimental to the bridge performance, and it is not always easy to be identified. The load-carrying capacity of a particular component of the bridge may decide the overall load carry capacity, and it is especially important to find the source of distress to a particular component when the interaction give negative effects. In many cases, the source of distress can be eliminated by simple remedial measures [49]; therefore expensive and unnecessary retrofitting/replacement can be avoided. If the interaction effect is found to be positive, the advantage can be utilized and load carry capacity maybe further enhanced.

### ***Proof tests***

*Proof Test* is quite different from the previous two types, especially in the magnitude of the load applies; it is performed to directly detect the safe load-carrying capacity of the tested bridge. During the testing, loads are applied in increment to the bridge (label 1 to 5 in Figure 2-10) until a target *proof load* is reached and/or non-linear behaviour is observed [106]. *Proof Load* is defined as “*the maximum load of a given configuration that the bridge has withstood without suffering any damage* [49]”. Therefore, one most important step in Proof Testing is to decide the minimum value of proof load. , which is actually not an easy task. According to the Ontario Highway Bridge Design Code (OHBDC, 1992) and the Canadian Highway Bridge Design Code (CHBDC, 2000), for a bridge to be classified as structurally-adequate, the proof load should be “*of such magnitude as to induce at least the same maximum load effects as those induced by factored design live loads including the dynamic*



*load allowance (DLA)*” [49]. Even though when compared to the behaviour/diagnostic testing, proof testing uses a much higher load, if based on the OHBDC and CHBDC criteria, the magnitude of proof load should still be “safe”, that is, not to cause permanent damage. So far, for all the proof tests conducted in Ontario, there has not been any cases that leave permanent strains in the bridge.

Proof Test was not performed on Safe Bridge; therefore it is only briefly introduced here. More discussion on the comparison between proof loads and legal loads, as well as the scale-down factor that should be applied on proof loads for deficient bridges can be found in [49].

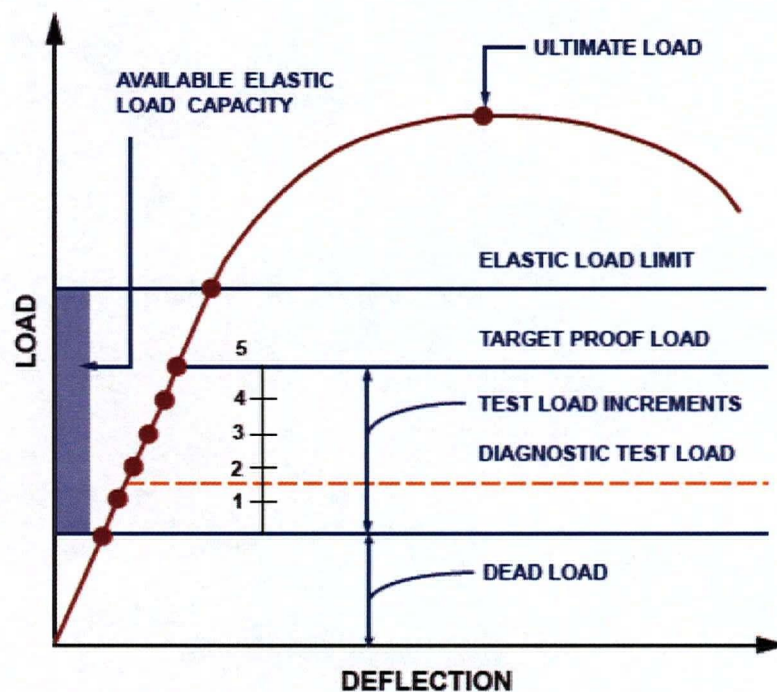


Figure 2-10 Hypothetical Load Deflection Response of Bridge

Source: [112]

For all three types of static field testing, the measurements can be used to adjust or refine the load rating of the bridge. How to incorporate the field measurements into the capacity rating is not within the scope of this thesis. Nonetheless, interested readers can obtain relevant information from papers written by researchers like Goble et al. (2000), Cai and Shahawy (2001), and Barker (2001) [106].

### 2.2.2.3 Dynamic Field Testing

Dynamic Field Testing is the second subsystem of SHM. The use of vibration monitoring for structural integrity assessment is effective and already well established in the mechanical and aerospace industries. The basic principle is based on the fact that dynamic response is a sensitive indicator of the physical integrity of any structure [113]. The first civil engineering application of vibration monitoring was probably in the field of pile integrity testing [113]. Records of dynamic field testing on bridges can be found as early as in the 20s in Europe, but these early testing could not provide much information, due to equipment/device constraints and insufficient knowledge about structural dynamics [49,114]. With the growth in technology, SHM techniques based on changes in dynamic characteristics have become a popular topic among researchers for the past two decades [52]. Almost all SHM projects mentioned in LANL's "*A Review of Structural Health Monitoring Literature: 1996-2001*" are based on the dynamic/vibration characteristics of structure [115].

As mentioned earlier, occurrence of damage in a structure will reduce structural rigidity (stiffness) and leads to changes in its dynamic properties. Dynamic characteristics include system parameters (mass, stiffness, and damping) and modal parameters (natural frequencies, mode shapes, and modal damping values) [20]. These parameters characterized the condition of the structure, and they can be measured from dynamic tests. Therefore, results from dynamic tests conducted at different time can be compared to identify changes in structural conditions [113]. However, in terms of detecting load-carrying capacity, dynamic testing on its own may not be effective, especially when the relationship between the "stiffness" and "strength" of the bridge is not linear [116]. For example, localized steel rebar corrosion inside a bridge's specific component may have little effect on the over-all stiffness, but may have large impact on the strength and therefore reduces the load-carrying capacity significantly [116].

Two problems have been discovered with vibration-based SHM techniques: (1) insensitivity to localized damage; (2) significant influences from environmental effects [52]. Vibration characteristics are global properties of a structure; when the damage is substantial, dynamic-characteristic-monitoring can work well in detecting the existence of damage [49, 52]. However, for localized damage or damage at incipient stage, the results are not as successful [52]. As for environmental effects, temperature changes, moisture and other environmental factors can also induce changes in dynamic characteristics. It has been found in many research works that, when damage is small, the noises from environmental effects can be greater than the effects due to real damage, and

give misleading results [52]. For example, Rizkalla, Bemokrane, and Tadros found that traffic-induced loads have a negligible effect on the bridge girder strains in comparison to the thermally induced loads, and it is necessary to measure temperatures as well because thermal effects on the measured strains are dominant [117]. An ongoing research area for current SHM study is focusing on solving these problems with innovative sensors/signal processing systems and sophisticated mathematical techniques and control theories [49, 52].

Common reasons for bridge dynamic testing include seismic assessment, studies of the aerodynamic responses, correlation of numerical models with measured data, bridge condition monitoring, and studies related to the development of dynamic impact factors for design of the bridges [114]. During dynamic field testing, the most common practice is to run a truck with known axle configuration at different speeds and over a prescribed “bump” on the bridge to create dynamic excitation. This method has been used since the 20s, and is still in use today [49]. The most commonly used sensor type for dynamic field testing is the accelerometers, and the dynamic loads used to excite the bridge can be generated either by *forced excitation methods* or *ambient excitation methods* [114].

*Forced excitation methods* include the use of shakers, actuators, step relaxation, and any methods of measured impact (see Figure 2-11) [115]. Dynamic testing with forced excitation is often referred to as *Measured-Input Test* because the input force is known. In most cases, the input-force is well characterized; therefore, identification techniques for determining the bridge’s modal characteristics (i.e. mode shapes, resonant frequency, modal-damping ratio) can be well established [114]. Another advantage of *forced excitation test* over *ambient force test* is that, the input force can be controlled. Therefore, one can make the input force strong enough to dominate over noise disturbance, and minimize the errors due to noises at the testing point [115]. In addition, forced excitation is usually a local excitation targeting a specific structural region/component, so the environmental and operation effects can be mitigated. However, forced excitation is only suitable for small bridges because of its localized excitation effect; it is not practical for large-scale bridges. It is also important to choose the “right” locations to input the forces to obtain the interested modes [113]. Finally, this type of testing relies on the vibrator control unit completely; if the unit is suddenly broken or not working properly, the whole test has to be called off [113]. Examples of SHM projects based on forced excitation methods are provided in [114, 115].

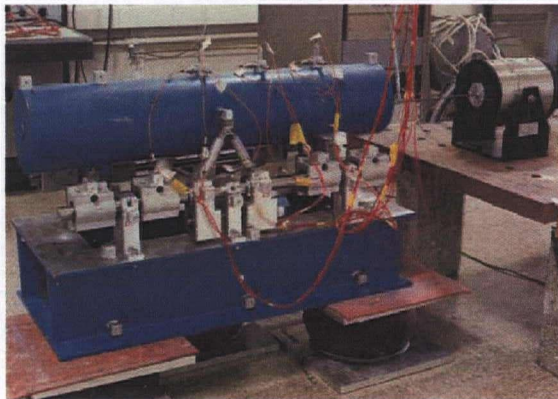




(a) Mechanical Eccentric Mass Shaker



(b) Hydraulic Shaker



(c) Electro-dynamic Shaker



(d) Step-relaxation (applied to a wind turbine)

Figure 2-11 Examples of Forced Excitation Methods

Source: [115] (Courtesy: Los Alamos National Laboratory)

*Ambient excitation* is defined as the excitation experienced by a structure under its normal operating conditions [114,115]. For bridges, its ambient excitations can include the traffic, wind, wave/current, and earthquake. Besides the seismic excitation, most of the input forces are not, or can not be, measured/recorded during the test [115]. From bridge monitoring point of view, ambient excitation seems to be a better source of loading than forced excitation, because bridges are constantly exposed to different loads in the operating environment, and the structural responses to the ambient excitation are the actual “*in-situ* responses” of the bridge. In addition, bridge size is not limited for ambient excitation. Especially when traffic disruption is not allowed, ambient excitation testing becomes the only valid choice [114].

### 2.2.2.3.1 Types of Dynamic Field Testing

According to ISIS Canada, dynamic field testing for bridges can be categorized into four types: *Stress History Tests*, *DLA Tests*, *Ambient Vibration Tests*, and *Pull-Back Tests* [49]. Dynamic field testing was not performed on Safe Bridge, but they play important roles in SHM field; therefore the section is included but the four types of dynamic field testing will only be briefly introduced. More information about the four types can be found in the ISIS Canada Design Manual #2 [49].

#### ***Stress History Tests***

The purpose of Stress History Test is to find the distribution of stress range in fatigue-prone components on the bridge [49]. The data is collected continuously for a short period of time under the bridge's normal operating condition. The early practice used sensors with pre-assigned range of strain, and the counter attached with the sensing system is recording the number of strain value that falls into its assigned strain range [49]. Therefore, at the end of the testing period, a histogram showing different strain ranges induced in the instrumented component was obtained. The problem with this method was that the collected data was difficult to be interpreted. Nonetheless, SHM technology today can store large amounts of data and intelligent data processing is available. With continuous monitoring, the frequency distribution of different stress ranges can be easily obtained and the bridge's fatigue life can be established.

#### ***DLA Tests***

DLA stands for *dynamic load allowance*. The *DLA Factor*, or *Impact Factor*, is an amplification factor commonly used in bridge code provisions for design to account for the dynamic effects from traffic. Besides the given formulation, some design codes allow engineers to determinate the DLA factor themselves through dynamic testing; this is one common reason for people to perform dynamic field testing. DLA test is also done by running specific test vehicles through the bridge.

The determination of a bridge's dynamic amplification factor is actually difficult. It has found that many factors can influence the testing results, such as the testing vehicle type and vehicle weight, and the vehicle positions with respect to the reference point [49]. Even when the bridge and the testing vehicle are the same, the values of dynamic amplification factors still varies significantly, as can be observed from different technical literature reports [49]. Currently, for design purpose, a single value of amplification factor is used in many code provisions to represent the maximum dynamic responses. As concluded in the ISIS Canada Design Manual #2 [49], "*it is not a practical*



*proposition to determine a representative value of the DLA for a given bridge by dynamic testing.”* Nonetheless, dynamic testing is still a useful research tool in formulating more reliable specifications for DLA.

### ***Ambient Vibration Tests***

As mentioned earlier, ambient vibration tests for bridge means measuring the bridge responses directly under its normal operational condition, and no controlled external force is applied. Accelerometers with a frequency range from 0.025 to 800 Hz are usually used to cover the frequency ranges of interest [118]. The number and locations of the sensors, and the length of measurement period, need to be arranged carefully to ensure that all the modes of interest will be properly recorded; these decisions should be done by people with good knowledge in dynamic testing and the tested bridge [119].

Ambient Vibration Test is also referred to as the *modal test* when the testing purpose is to obtain modal characteristics of the bridge [49]. The first step in obtaining the modal properties from ambient vibration measurement is the determination of all possible natural frequencies of the modes participating in the vibration of the bridge [119]. Testing measurements can be plotted directly as accelerations vs. time, and the function for the plot can be written as:

$$f(t) = A_1 \sin 2\pi f_1 t + A_2 \sin 2\pi f_2 t + A_3 \sin 2\pi f_3 t + \dots$$

where  $A_1$ ,  $A_2$ ,  $A_3$ , etc. are the modal amplitudes or modal ratios, and  $f_1$ ,  $f_2$ ,  $f_3$ , etc. are the various natural frequencies of the bridge [49]. The values of modal amplitudes can further transfer to power spectral density (PSD). A spectral densities normalization and averaging function, denoted as the averaged normalized power spectral density (ANPSD), can be obtained from the PSD to identify the most probable natural frequencies [119]. Figure 2-12 is an example of ANPSD plot indicating various peak frequencies in the transverse, vertical and torsional directions. Most of the peak values should correspond to the natural frequencies of the tested bridge, but one should also be aware of the possibilities that, the frequency of a dominant exciting force, like a heavy truck, is included [49]. Additional analysis and checking with the transfer function, coherence, and phase between pairs of records, should be performed to confirm the testing results [119]. In addition, a “real natural frequency value” may be in the vicinity of a peak value shown on the ASPSD plot, due to the effects of averaging multiple records and presence of damping [119]. The FE model of the bridge can then be calibrated with the actual natural frequencies and mode shapes. In order to obtain the natural

frequencies correctly, dynamic field testing should be repeated until their ANPSD plots show repeatable results [49]. With advanced technology today, the ANPSD plots can be obtained easily with specialized computer programs.

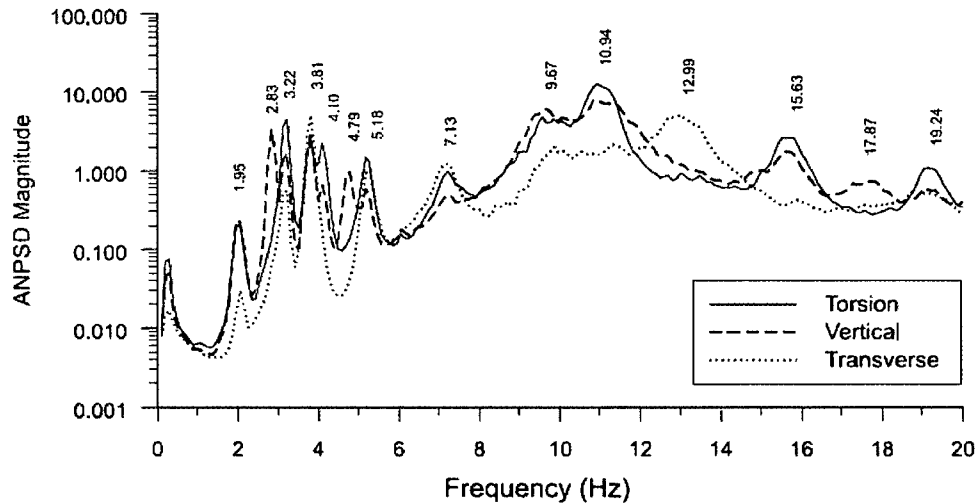


Figure 2-12 Example of An *Averaged Normalized Power Spectral Density* Plot  
Source: [119] (Courtesy – C.E. Ventura)

### ***Pull-Back Tests***

A Pull-Back Test is performed when the lateral vibration characteristics of the bridge is of interest [49]. Traffic loads usually do not induced much lateral excitation to the bridge, and therefore it is difficult to detect the lateral vibration behavior of the bridge with ambient vibration tests. A Pull-Back test is usually performed by pulling the bridge with a thick cable in the lateral direction and anchored on the other end, and then releasing the cable suddenly [49]. Measurements from accelerometers are collected from the moment the cable is released and let the bridge vibrate freely. The process of data analysis is similar to that of ambient vibration test. Since the bridge vibrates freely, damping characteristics of the bridge in the lateral direction can also be obtained. Important factors to be considered for pull-back test are the magnitude of the lateral test force, and the quick-release mechanism to be employed.

### 2.2.3 Long Term Monitoring

The benefits of long term monitoring have been recognized for a long time, but due to practical difficulties and technical constraints (as discussed before), truly continuous monitoring could not be realized in earlier days. Historically, bridge monitoring programs were implemented for the study of the load-structure-response relationships and the calibration of assumptions for modeling [65]. In North America, the earliest documented systematic bridge monitoring exercise was conducted on the Golden Gate and Bay Bridge in San Francisco in 1937, and the objectives were to study the dynamic behavior and possible consequences of earthquake [65,120]. Most of the earlier monitoring were focused on important long-span bridges, or “high-profile” bridges with special design. In addition to the concern on the field performance of the bridge itself, the projects were also seen as opportunities to implement and study SHM systems.

In recent years, applications on conventional short-span bridges started to gain popularity; these applications are, as described in [65], “*less glamour but possibly ultimately more beneficial developments of SHM*”. For small bridges, their global responses are more sensitive to defects, and visual inspections are less frequently applied, so SHM systems can and will make a real contribution [65]. In addition, SHM systems for small-scale bridges usually contain less technical challenges and constraints when compared to large bridges, and therefore it is possible to make commercially available SHM products that are applicable to most common types of short-span bridges; this will greatly reduce the cost for installing SHM system, the major concerns for bridge owners, and truly utilize SHM technology.

“Long-term monitoring” covers the last two subsystems of SHM: “periodic monitoring” and “continuous monitoring”; and they are the major research themes for today’s SHM discipline. When the term “SHM” is used, many people actually mean “long-term monitoring”. Therefore, the importance and difficulties for long-term monitoring are similar to the ones mentioned earlier for SHM technology and they will not be repeated again here. The issues and techniques of all possible long-term monitoring methods are too vast to be covered completely; some popular investigating topics for long-term monitoring include *the overall monitoring strategy, installation procedures, systems architecture, temperature compensation, durability, compatibility with other materials, sensor standardization, data analysis, and cost-benefit analysis*. Many issues are case-specific. This thesis can only briefly touch some of the general issues for long-term monitoring projects. The components of SHM systems will be discussed in more detail in later sections, so issues related to

different aspects of SHM will be presented accordingly. The rest of the section will discuss the different applications of long-term monitoring on bridges, based on their “time-scale”, and issues relating to sensors, one of the biggest concerns for all long-term monitoring projects.

Long-term monitoring can be used in bridge applications for a wide range of purposes that involve different time and spatial scales. Based on the sampling rate for monitoring, the time scale for bridge applications can cover up to 16 orders of magnitude in frequency, as shown in Figure 2-13 [97]. The ultimate time scale is the service life of the bridge, which is at least 50-years for old bridges, and can be up to two hundred years for “especially important” bridges. Current Canadian Highway Bridge Design Code requires 75 years to be the service life for new bridges [121]. Continuous monitoring on a bridge from its construction stage until the end of its service life is the most “complete” level for bridge monitoring, but it rarely is required and performed. One situation where continuous monitoring may be necessary is when the purpose of the monitoring is to obtain true field responses of the bridge under unexpected hazards like natural disaster or serious vehicle collision, or to provide warnings. The occurrence of these rare events known in advance, so continuous monitoring is required; unless the data acquisition system has special triggering set-ups.

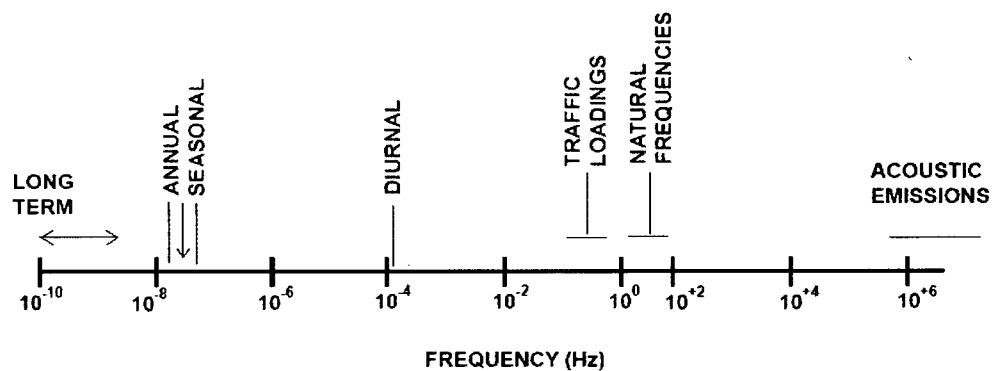


Figure 2-13 The “Time Scale” for Bridge Monitoring in Terms Magnitude in Frequency  
Source: [97]

Next to life-time-monitoring is with the “year” scale. Monitoring on the scale of years to decades are mainly for the study of deterioration processes, such as corrosion of rebar, alkali-aggregate reactions of concrete, and fatigue of steel [97]. If the deterioration process is slow and warning signs will be available, or the deterioration process will not lead to catastrophic failure of the bridge, the monitoring can be periodic instead of continuous.

The next level of time scale is less than a year, from seasonal to diurnal. These scales are closely associated with climatic variables; seasonal monitoring is especially important when the monitored variables are influenced by seasonal changes; this is common because many measurements are sensitive to temperature. Conversely, changes in the natural frequency with temperature can also be used to diagnose deterioration, such as the sticking of bearings [97]. Other seasonal changes that can affect monitoring results include wind, tidal, and human activities. Similarly, for diurnal time-scale, temperature and tidal varies. Traffic loading is another important factor that may show different pattern in a seasonal, monthly, weekly, or even daily scale. Information such as traffic volumes, size, number and weight of trucks the bridge carry, etc. are important for true life cycle cost analysis and performance based specification [84].

With the possibility that long term monitoring may need to cover “16-orders of magnitude in frequency”, one major issue follows is the performance and robustness of the sensors, which may be required to perform reliably for the lifetime of the bridge. Many traditional sensors used heavily for conventional bridge field testing are not suitable for long-term monitoring. For example, the conventional strain gauges are susceptible to electromagnetic and radio interference, dependence on signal amplitude, and have tendency to drift over time [122]; all these limit their usefulness in long-term monitoring applications. The monitoring results will not be meaningful if the data are problematic themselves.

Another concern is sensor malfunctioning. A fault in the sensor network will have undesirable consequences whether or not the integrity of the bridge is compromised [53]. One solutions is to have redundancy of sensors to assure the functioning of the system even in situation of data loss from some sensors, so that proper assessment of the monitoring results can still be achieved [123]. There are also suggestions to have the sensors be monitored themselves – either by self-monitoring or to monitor each other. These indeed are potential solutions for sensor failures, which is highly likely to happen for conventional sensors performing long-term monitoring [53]. However, these solutions also take away the major advantage of traditional sensors – their lower costs. Therefore, seeking new types of sensors that is suitable for long-term monitoring becomes the trend.

Many advanced sensing technologies are implemented for long-term monitoring; FOS is the most popular for “internal sensing” and GPS has a great potential for “external sensing” for global performance monitoring [65,123]; in addition, when the scale of the structure is large and a significant number of sensors are required, wireless sensors may become a “must”. Since FOS is



used in Safe Bridge project, the discussion for advanced sensors will focus on FOS only; GPS technology and wireless sensors will not be covered in this thesis. Nonetheless, it is important for SHM engineers to be aware of the existence of different sensing technologies, so that the optimal SHM system can be developed. [124,125,126] are some references for wireless sensing for SHM applications; [123,127] show applications of GPS technology combined with FOSs for bridge monitoring.

Fibre optic sensor (FOSs) is one major research area for SHM technology today. The phenomena that can be monitored by FOS arrays range over many orders of magnitude, and it has many unique characteristics, such as corrosion-resistant and immunity to EMI/RFI, make it suitable for long-term monitoring applications [70,97]. In addition, FOS is easy to install and stay fastened in position better than traditional wire gauges, and it can act as both the data collector and data transmitter. More information about FOS will be provided in later sections. It is important to notice that FOS will play an integral role in SHM system, especially for long term monitoring applications.

The issues and considerations mentioned in this section are applicable to both Periodic Monitoring and Continuous Monitoring. In the following, these last two subsystems of SHM will be briefly introduced for some of their specific features.

#### **2.2.3.1 Periodic Monitoring**

The common purpose of periodic monitoring is to determine changes in structure (e.g. movement of piers) or to trace long-term performance of certain component(s) of the bridge (e.g. cracking on deck or a repairing layer) through intermittent measurements over a period. Periodic monitoring is the third subsystem of SHM, and actually most of the SHM on bridge falls under this category, because it can include the two field testing subsystems discussed earlier, and the fourth subsystem, “continuous monitoring”, is seldom necessary.

When the static field testing is performed on a bridge repeatedly from time to time, the bridge can be viewed as under “periodic monitoring” as well; this is currently the most commonly performed type of periodic monitoring. For conventional static field testing, traditional sensors can be used and a temporary monitoring system can be mobilized for the testing at any time; these instruments are cheap compare to the more advanced systems for long-term monitoring. Also, new parameters can

be added or removed from the system as needed during each testing; this “flexibility” is another advantage of this type of periodic monitoring. Lastly, there is potential for improvement: when new instruments or testing methods are developed, they can be deployed for better testing results. Nonetheless, because the data acquisition systems (sometimes also the sensors) are not permanently installed, significant works for cabling, transport of all equipments, and skilled personnel for set-up and data collecting are required every time the field testing is performed; this “repeating portion” of field testing actually occupy significant time and cost. Most of all, this type of periodic monitoring can easily lead to inconsistency, because any changes in instruments, measurements, testing methods, or even testing vehicle, more or less affect the testing results.

Static field testing has relatively short testing period, and that is the main reason why instrumentations can stay “simple”. With the increase in monitoring time, issues like the stability and robustness of instruments become important. As mentioned earlier, the time scale for periodic monitoring can vary from as short as couple of hours, to as long as decades, depending on the application and the type of bridge being monitored. Therefore, sensors permanently installed in the bridge are preferred. Actually, when the time scale is up to the “year” level, the requirements on instruments and data management become similar to the level for continuous monitoring.

Periodic monitoring has been successfully applied in many bridges around the world, and it works well in most studies related to bridges; its biggest limitation is on the study for extreme event responses. Typical measurements for periodic monitoring include strains, displacements/rotations, accelerations, and temperature. Please refer to ISIS Canada Design Manual No. 2 for examples of periodic monitoring on crack growth monitoring and repair tracking, and through static field testing, ambient vibrations, and testing under moving traffic load [49].

### **2.2.3.2 Continuous Monitoring**

Continuous monitoring is the fourth subsystem of SHM, which can provide the most comprehensive data about the bridge’s health and performance, but also requires the most sophisticated planning and instrumentations. Continuous monitoring goes beyond the capability of the other three subsystems of SHM; it not only able to obtain true bridge responses under unexpected extreme events, but also can provide monitoring during the construction period. Examples of applications related to construction period include the monitoring of shrinkage strains produced in concrete during the initial hardening

process, or tracking the prestress forces applied to steel strains for precast concrete components [97,128]. The advantages from continuous monitoring are endless, but at the same time, the challenges need to be deal with for a successful continuous monitoring system is enormous.

Besides the issues relating to the robustness of sensors and equipments, as mentioned earlier, remote control and wireless data transfer are usually accompanied with continuous monitoring system, and therefore power supply is also an issue. In addition, equal, if not more, challenges come from the processing, management, and storage of the tremendous amount of data coming from continuous monitoring. More information related to data management will be given in later sections. The rest of this section will be devoted to the discussion on “*passive monitoring*” vs. “*active monitoring*”, an important decision to make during planning, especially for long term monitoring projects.

“*Passive*” or “*Active*” monitoring depends on if *passive sensing* or *active sensing* system is used. *Passive sensing* means the monitored bridge is subjected to unknown external excitation, and the response of the bridge is passively recorded [115]. The passive system is powered only for interrogation of the sensor array and downloading the data [129]. Passive, peak deflection sensors have proven to provide adequate information for routine structural monitoring; for example, static field testing applies on a bridge periodically for the measurement of its peak deflection under the truck load is of this kind. Passive sensors are usually worked as baseline sensors in most SHM system, and the advantage is that they require minimum maintenance [129].

In active sensing mode, a controlled internal excitation (known input) is applied to the bridge by the built-in actuators and sensors, and the corresponding structural responses due to the internal excitation are measured at the same time; therefore real-time structural response histories can be obtained with active sensors [115]. Active sensing system requires real-time power and data acquisition systems with sufficient storage capacity to handle the significant volume of data [129]. Because the response signals of a structure are often affected by operational and environmental variations of the structure, the employment of a known excitation force makes the subsequent signal processing and system identification much easier [115]. The main advantage for active system is the ability to provide complete picture of structural behavior, including responses to extreme events. Nonetheless, active systems are more expensive to install and operate because maintenance is required. Also, if power is lost during extreme events, the active system is no longer working and the data of interest cannot be obtained [129].

Because each of the sensing approach has its own strengths, a “hybrid system”, or “semi-active sensor” that combine both active and passive sensors become popular. Flexibility, relatively low-maintenance cost, and long-term design life (system life estimated at 10 to 20 years) make the hybrid system ideal to satisfy most bridge monitoring needs [129].

When combining active/passive sensing with remote/manual control, four types of SHM systems can be identified. Thompson and others [129] summarized the four types of SHM system in the table below (see Table 2-2). As can be seen from the table, the first two levels of systems are sufficient for the two field testing subsystems of SHM. For periodic monitoring, depending on the project and the length of testing/monitoring time, either one is possible. However, for continuous monitoring, both active and passive sensing will be required.

Table 2-2 Four Levels of Structural Health Monitoring Systems Based on Sensing Approach [129]

<b>System Identification</b>	<b>Components</b>	<b>Description</b>	<b>Applications</b>
<b>Passive Manual</b>	Passive sensor array. Hard-wired junction box Hand-held detector or pc	System is manually interrogated as necessary. Lowest cost, maintenance-free.	Low level of concern. Quantitative data supplement inspection.
<b>Passive Remote</b>	Passive sensor array. Hard-wired junction box Cellular telephone Solar panels/battery bank	System remotely interrogated at programmed intervals. Data automatically transferred to central receiving station (San Diego, CA). Programmed to respond and call in at specified strain levels. Internet data display.	Routine infrastructure monitoring. Ideal for post-earthquake assessment monitoring. Remote programming possible.
<b>Passive Active</b>	Passive/active sensor array. Hard-wired junction box Cellular telephone Conventional power with solar panel back-up Wireless interface option.	System remotely interrogated at programmed intervals. Active sensors operated in semi-active mode. Data automatically transferred to central receiving station (San Diego, CA). Programmed to respond and call in at specified strain levels. Internet data display	Routine infrastructure monitoring. Increased information about present conditions. Remote programming possible.
<b>Active Passive</b>	Active sensor array. Passive back-up system. Hard-wired junction box Cellular telephone Conventional power with solar panel back-up Wireless interface option.	System operates continuously. Central station data transfer at programmed intervals. Programmed to respond and call in a specified strain levels. Internet data display. Highest cost system (capital plus maintenance).	Highest level of concern. Beyond routine monitoring applications. Time history of loading and structural response possible. Remote programming possible.

## **2.3 Components of Structural Health Monitoring Process**

As mentioned in Chapter 1.2, the definitions of SHM given by ISIS Canada (Fig. 1-6) and LANL are combined to construct the sections for the study of SHM system. Therefore, this section will contain five sub-sections: *Operational Evaluation*, *Data Acquisition*, *Data Communication*, *Data Management*, and *Diagnostics*. Each of these components for SHM can be a thesis topic itself, and it is impossible to cover them in details. The five components will be briefly introduced here, and readers are encouraged to read at least the two above sources [49,115] to get a more complete picture about SHM. One should also note that, even though the five components seems like five steps in order for the construction of a SHM system, there is actually no clear “boundaries” between them; all the five components are closely linked and associated with each other. Therefore, many issues and considerations may be applicable to more than one of the component.

### **2.3.1 Operational Evaluation**

Ideally, it would be nice to turn all existing bridges into “smart bridges”, and to install SHM systems to all new bridges, so that all bridges’ health conditions can be checked regularly and conveniently. However, it is not yet possible today, and it is not practical from the cost-benefit perspective. In the real world, “cost” is always one major concern for owners. Typically, adding a relatively comprehensive monitoring system to a new structure will add about 1% of the total construction cost [130]. This percentage includes the system hardware and installation fee, but does not cover the cost associated with data analysis. Nonetheless, one cannot judge the “value” of a SHM system simply by a monetary number. Owners should consider the pros and cons from the life-cycle cost perspective. In addition, if a catastrophic failure is prevented and therefore death is avoided, any spending on the SHM system is worthwhile.

There are four groups of bridges that in particular should utilize SHM technology [97,131]:

1. existing bridges that contain severe deterioration;
2. “important bridges” that form critical links in the transportation network and will bring significant impacts to the society if damaged;
3. bridges that are likely/possible to encounter extreme events, such as earthquake, hurricane, or terrorist attack;
4. bridges contain “unconventional features”, such as new materials or innovative design, and little is known about the new feature.



In the LANL Report, *Operational Evaluation* is the first step of the four-step process of the *statistical pattern recognition paradigm* [115]. The four questions to be answered in this stage are:

1. What are the life-safety and/or economic justification for performing the SHM?
2. How is damage defined for the system and, for multiple damage possibilities, which case are of the most concern?
3. What are the conditions, both operational and environmental, under which the system to be monitored functions?
4. What are the limitations on acquiring data in the operational environment?

Depending on the scope and complexity of different project, the “importance” of the four issues may weight differently; nonetheless, all these are important aspects that should be considered thoroughly in preparing a meaningful and successful SHM system. It is important to set limits on what will be monitored and how will the monitoring be done. Operational evaluation begins to tailor the monitoring process to unique aspects of the structure, and tries to take advantage of the unique features of the damage that is to be detected [132].

### **2.3.2 Data Acquisition**

As shown in Figure 1-6, “Acquisition of Data” is the first subset of the actual implantation of a SHM system, and it consists of two major elements: sensors and data acquisition systems (include both hardware and software). Sensors measure and detect the defined physical changes from the structure; data acquisition systems transfer the data from sensors and convert them to digital signals so that the computer can “read”.

Following up with the considerations and decisions made in Operational Evaluation, the main issues to be deal with for Data Acquisition include [115]:

- Excitation mechanism
- What parameters / quantities to be measured
- Number and types of sensors (include considerations for resolution, bandwidth, etc.)
- Locations of the sensors
- Data acquisition system to be used
- Power supply
- Set-up plan for all instruments (site-based)

The decisions are made based on the purpose for the SHM system, the considerations made during the Operational Evaluation stage, the availability of utilities, the tender specifications, and the specific “condition”/ characteristics of the site. Security and protection of the instruments should also be considered if the sensors and DAQ system(s) will be permanently located on the site. Of course, economic consideration always plays a major role. For long-term monitoring project, it has been found that cable-based sensing system have high installation costs and leave wires vulnerable to ambient signal noise interferences. A report from the California DoT stated that it costs over \$300,000 US per toll bridge to install a measurement system comprised of 60 to 90 accelerometers; to protect the wires from the bridge’s harsh environment, a wire conduit require a cost of \$10 US per linear foot [133].

The number and location of sensors is critical for “correct” monitoring results. Most long-term global health monitoring projects have been based on vibration-based damage detection methods; even just 30 years ago, it was common to use less than five accelerometers to perform the monitoring, due to the high cost of sensors [52]. With so little accelerometers involved, in most case only the fundamental mode could be obtained. Today, the prices for conventional sensors are so affordable that some long-span bridges use over hundred of sensors. The problems come with the massive number of sensors is another issue; but it is important to use enough sensors to generate meaningful results. In particular, when conventional sensors are used for long-term monitoring purpose, extra number of sensors should be used as back-ups [53]. As for the location of sensors, when the bridge is small and in simple structural form, the locations of sensors may be decided by experienced structural engineers directly. However, most bridges do not work like a simple beam; for better monitoring results and effective sensor placement, a detailed structural analysis using advanced technique, such as finite element modeling, should be performed in prior to verify the optimal sensor locations [97,115].

A popular ongoing research area for data acquisition is to “distribute the computational load” among different elements within the whole data acquisition network [134]. A problem with long-term monitoring is that a tremendous amount of data are being collected but not analyzed because processing all the data would be too costly [52]. One way to deal with this problem is to improve the sensors and DAQ systems so that they can perform certain level of data processing before the data are sent to the computer(s). In this case, the amount of data that need to be transmitted and processed can be reduced significantly. Smart, distributed systems with local digitization and decision nodes will be solve many difficulties we are facing today [134].

Both sensors and data acquisition systems need power, which can be an issue for bridges located at remote sites and no AC source near by. In general, issues related to the design of power supply include [135]:

- Power generation: the source of energy; i.e. external powered or self-powered
- Power transmission: the path of energy; e.g. capacity of wires
- Power storage: the location of energy; e.g. capacity of batteries
- Power consumption: energy-consumption and power efficiency, low power technology

Power supply is especially an issue for remote continuous monitoring. Self-powered sensors are often required to be used, so power generation mechanism and power storage are main issues to be considered. Most wireless sensors are powered by batteries, and if the batteries are charged by solar power, then the need to be close to an AC source is solved [52]. For a distributed sensors network, power transmission and power storage are of major concern [135].

Works at this stage determine the success of obtaining structural responses, and require expertise from many different fields. For long term monitoring projects, many steps in *data acquisition* is a one-time job, so it is worth to spend time for careful planning and field works. The design manual “*Civionics Specifications*” by ISIS Canada [72] provides detailed specifications for three types of FOSs that are popular for bridge monitoring, and the support equipment and systems commonly used for data acquisition set-ups. It is a good reference for civil engineers who do not have much field experiences with instrumentation for bridge testing/monitoring. In the following, “sensors” and “data acquisition systems” will be discussed separately, focusing on the units commonly used and the relevant technical terms. Since FOS is a relatively advanced field, an introduction on optical fibre and its technology will also be provided. It is important for the civil engineers to have basic knowledge on these to communicate with people from different fields to optimize the SHM system.

### 2.3.2.1 Sensors

Sensors are the first essential component in a monitoring system and are essential for the accuracy and reliability of the measurement. The type of sensors can be classified according to the quantity (variable) it measures; some common quantities for bridge monitoring are:

- Mechanical Quantities : strains, displacement, acceleration, rotation, distortion, weight, force/torque

- Thermal Quantities: temperature
- Chemical Quantities: moisture (humidity), pH value
- Electro-/Optical Quantities: voltage, light, frequency phase, visual/images

The choice of the sensors depends on if the “attributes” of the sensor(s) match the requirements of the application. Major “attributes” that can be used as the criteria for the selection and evaluation of sensors include: dimension of variables, size, operating range, accessibility, sensitivity (the minimum change the sensor can recognize), data format (continuous or discrete; analog or digital), active or passive sensing, physical contact, operating principle, and its “intelligence” (such as capability for on-board data processing and decision-making) [136].

There are almost unlimited number of possible sensing and measurement technologies that can be developed for highway bridge applications; with more new types of sensors, improved SHM systems also become feasible. Some examples of “new sensors” for specific usage include the LIDAR (Light or Laser Imaging Detection and Ranging) to capture 3D position of objects; infrared thermography to detect debonding; MEMS (micro-electromechanical system) for accelerometers and other applications; shearography to detect out-of-plane displacements caused by delaminations; and several systems for corrosion, such as the nuclear magnetic resonance (NMR) capsules to detect chloride ions, the *Galvashield XP* to reduce localized ring anode corrosion of reinforcing steel [52].

These sensors typically targeting one specific type of damage, and are more suitable for “local monitoring”. Here the discussion will be focus on the sensors typically used to monitor the “global health condition” of bridges. Both the conventional types of sensors and the popular FOSs for SHM will be briefly introduced because the conventional sensors are still used massively for bridge field testing; also, they could be used for the studying and testing of new types of sensors. Many projects study the field performance of FOSs, and both the FOSs and conventional electric resistance strain gauges are installed to verify the results [123].

#### **2.3.2.1.1 Common Traditional Sensors**

The most commonly measured quantities for static field testing are strain and deflection (displacement); for dynamic field testing is the acceleration [115,137]. In addition, temperature is an important measurement as well to quantify the environmental effect. Therefore, the most commonly

used sensors for bridge field testing are strain gauges, linear variable differential transducers (LVDTs), accelerometers, and temperature sensors. These sensors have been in use for a long time in many different industries; their technology is pretty much matured and there are many commercially available products on market; therefore, the biggest advantage of using conventional sensors is their relatively low cost. There are also more choices for the support systems (like the compatible DAQ systems), and easy to find skilled personnel who are familiar with the sensors.

These four common conventional sensors will be briefly introduced in the following. Since strain gauges are used in Safe Bridge project, it will be discussed in greater detail than the other three types of sensors. Note that the Design Manual No. 2 by ISIS Canada [49] has a very good summary section about these four conventional sensors as well, especially on the introduction of strain gauge. The manual provides elaborate explanation on the parameters for selecting foil strain gauges, as well as the attachment techniques and the methods for environmental and mechanical protection. In addition, potential source of errors and noise control considerations are discussed in great detail. Foil strain gauge remains the most widely used sensor for bridge testing/monitoring applications; it is installed in almost all instrumented bridges. The information can be provided here is very limited; civil engineers are encouraged to at least read the ISIS Canada reference if they will be involved in a SHM project that utilizes strain gauges.

#### **2.3.2.1.1.1 Strain Gauges**

“Strain” is a very useful physical quantity for structural integrity analysis and monitoring; high strain level gives warning to potential problems: it could be an indication of fatigue or yielding in the material, or occurrence of de-bonding. Strain values can be used to compute a structure’s load, moment, and stress; it can also be used for frequency analysis. With special design and placement, an array of strain gauges can further be used as transducers for torque, load, pressure, and acceleration [126]. No wonder strain gauge is the most widely used sensor type for bridge applications.

There are many different types of strain gauges available on market; for civil engineering applications, the most familiar to researchers are the *foil strain gauges* and the *vibrating wire strain gauges* [138]. The discussion will focus on the foil strain gauge because it is used the most often for strain measurements; as for the vibrating wire strain gauges, the discussion will focus on its advantages and disadvantages to the foil strain gauges in terms of for bridge monitoring applications.

*Foil strain gauges*, also known as the *electrical resistance strain gauges*, are the most commonly used and least expensive type of strain gauge [49,139]; the ones installed in Safe Bridge are also of this kind. The basic mechanism for foil strain gauge is that, the resistance of an electrically conductive material changes with its dimensional changes when the material is deformed elastically. When the material stretches, it becomes longer and narrower, which increases the resistance; the change in resistance is then converted to an absolute voltage by a Wheatstone bridge [139]. The result value is linearly proportional to strain by a constant. This constant is the *gauge factor*.

There are thousands of foil strain gauges available with different characteristics for different usages and applications; selecting an appropriate one is the first step. The major issues to be considered for selecting the strain gauges for bridge testing/monitoring are [49,140]:

- Suitability for the operating and environmental conditions
- Accuracy and stability of measurements
- Magnitude, type, and duration of the measurement
- Ease for installation

Cost is usually not a major concern for the selection because the cost of sensor itself is relatively low; by choosing a more expensive gauge that has features for faster installation will probably save more from the installation cost [49].

The general components of a typical foil strain gauge are shown in Figure 2-14. The important parameters for the choice of foil strain gauges are as follows [49, 140]: *Gauge Length*, *Grid Width*, *Gauge Materials*, and the *Gauge Resistance*.

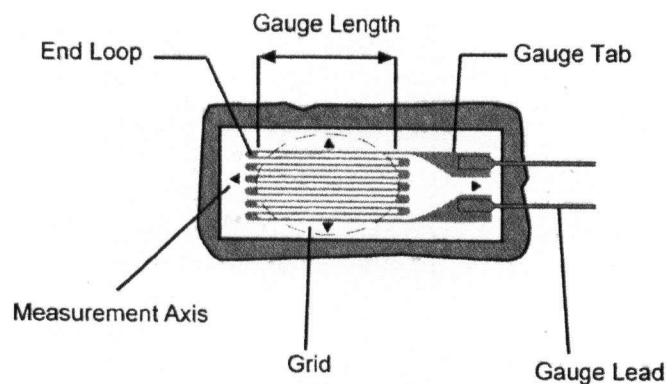


Figure 2-14 Components of a Typical Foil Strain Gauge  
Source: [49] (Courtesy – ISIS Canada)



**Gauge Length** is the strain-sensitive length of the strain gauge (see Figure 2-14). The gauge length can vary from 0.2 mm to 100 mm; for common application, a gauge length between 3 mm to 6 mm is recommended for the ease of installation, availability, and lower cost. Nonetheless, for special cases, such as when a highly localized strain is to be measured or very little space is available for mounting the gauge, and accuracy is not critical, then a shorter strain gauge should be used. For example, when the strain gradient near or on a small size fillet, hole, or notch is of interest. On the other hand, when the object to be measured has non-homogeneous material properties, or when heat dissipation is an issue, a longer gauge should be used. For example, when the gauge is to be attached on concrete surface, the gauge length should be long enough to cover several aggregates; usually at least 5 times the size of the largest aggregate in the concrete should be used.

**Grid Width** is determined by the number of “loops” on the gauge. Usually wider grids are preferred because they provide better heat dissipation and stability. For non-homogeneous materials like concrete, wider gauge can provide better results because the strain is averaged over wider area. However, when strain gradient changes significantly perpendicular to the gauge and the strain is measured over a short length, a narrow grid strain gauge would be preferred.

**Gauge Material** is the principal factor that controls a strain gauge’s operating characteristics. A strain gauge typically contains of three parts: the *wire* (the sensing alloy), the backing (the carrier), and the *adhesives*. The material of the *wire* is the most important. Thermal output, zero-stability, fatigue life, and sensitivity to strain are the criteria for choosing the wire material. Constantan alloy is the most widely used type, probably because it has the best “overall properties”, such as adequately high strain sensitivity, good fatigue life, relatively high elongation capacity, and self-temperature-compensated. It is also the least expensive type. Constantan wire is suitable for applications measuring static/quasi-static strains and plastic deformation, and applications under normal operating conditions (e.g. will not encounter extreme temperature). When the application is for a long period of time, a nickel-chromium wire is preferred because it offers much better zero stability. Both the constantan and nickel-chromium have a gauge factor around 2.0. For applications that need high signal-noise ratio, that measure dynamic strains and/or cyclic loadings, the isoelastic alloy is preferred, because it has superior fatigue life and higher gauge factor (around 3.2).

The carrier is for the protection and ease of handle for the wire. The carrier is usually made of dielectric material which provide good insulation between the wire and the specimen; the most common backing material is polyimide. When one wants to minimize the error induced by the backing, epoxy should be used; but epoxy backings are brittle and require skilled workmanship for installation. There are also weldable strain gauges which use metal carriers. Weldable gauges are preferred when bonding conditions are not ideal, but in exchange accuracy sacrifices a little. If the strain gauge is to be placed inside the concrete, the embedment strain gauge, which consists of a long foil gauge (~100 mm) embedded in a polymer concrete block, is preferred. As mentioned earlier, the long length is to avoid localized strain effects from aggregate discontinuities; the polymer concrete block is to protect the strain gauge from mechanical damage during construction and environmental attacks.

Adhesives are used to secure the strain gauges to the measuring component. Cyanoacrylate cement only need short curing time (like 10 minutes), so it is good for cases when the gauges need to be used soon as possible; but it is not suitable for applications that will last for longer time (like a few months). If higher bond strength is required and higher strains at failure will be encountered, epoxy should be used; but the curing process is more trouble and takes a long time; high temperature (120°C) is required to be applied for several hours to complete the polymerization. There are also special cements for high-temperature (ceramic cement) or dry environment (cellulose nitrate cement). A gauge having a shifting glue interface is highly unsuitable for long-term monitoring due to drifting problems [49].

**Gauge Resistance** of a strain gauge is commonly produced to be 350 ohms or 120 ohms. The electrical resistance is directly related to the sensitivity. For a given wire material, the higher the resistance, the higher the sensitivity; therefore, normally a higher resistance is preferred. High resistance also results in lower volumes of heat when same voltage is applied. Heat generation is an issue for low-heat-conductivity materials such as composites because increase in temperature affects the strain readings. In addition, higher gauge resistance also decrease the “lead wire effects” (explain later) and improves the signal-to-noise ratio of the measurement. Nonetheless, if fatigue loading is an issue, the lower 120 ohms resistance should be used; the lower resistance wire is larger in diameter and therefore better fatigue resistant. Also, the 120 ohms gauges are usually cheaper than the 350 ohms strain gauges.

For bridge field applications, a major task with the use of foil strain gauges is to provide proper environmental and mechanical protections; the gauges should always be covered with a suitable coating right after the installation [49]. It has found that moisture is the most common cause for gauge failure in field applications; moisture causes grid corrosion and leads to inaccurate measurement and zero-drift [49]. When the strain gauges are close to water surface, such as underneath bridge girders that span over a river with short clearance, extra care should be taken. Different protecting materials are available from strain gauge suppliers for different situations. For example, a layer of Nitrile rubber coating is adequate when the gauge will not subject to rain and snow; double layers of the rubber coating with aluminum foil in between can provide better protection for more severe conditions; Teflon can be used if electrical conductivity is an issue; Epoxy provides good protection against chemical attacks, but they absorb moisture and therefore not suitable for long-term monitoring in humid area [49].

Major sources of errors for foil strain gauge measurement include the lead wire effects, the sensitivity to the transverse strain, and most of all, the temperature effect [49]. Foil strain gauges generally wired to the readout unit; the lead wires can cause two types of errors: one is related to the temperature change induced by the resistance changes in the lead wires; the other error is known as “lead wire desensitization”, which happens when the lead wire resistance is significant in comparison to that of the gauge itself [49]. Depending on the bridge circuit configurations (quarter-, half- or full-), the two types of errors may or may not be an issue; but lead wire desensitization must be corrected for the half-bridge configurations [49]. Correction procedures can be found in standard textbooks.

As for the transverse strain effect, it is an issue when the transverse strain is relatively large when compared to its longitudinal strain. The gauge factor (GF) is defined as the ratio of the rate of resistance variation caused by uni-axial stress applied along the gauge axis; therefore, a strain gauge actually has two gauge factors: one is aligned to and the other is perpendicular to the strain field [49]. The GF given by manufactures is the one aligned to the strain field, and it is theoretically correct only when the gauge is attached to a material with a Poisson ratio equal to that of the material used for gauge calibration [49].

Temperature effect to foil strain gauges is the biggest source of error for its measurement of static strain; and this is in addition to the error from temperature effect of the lead wires [49]. Two causes add up the effects: (1) it is the nature of the gauge’s electrical resistance to be sensitive to temperature changes; (2) the difference between the thermal expansion coefficient of the gauge and the substrate

material that the gauge is attached on; the effects from both are generally referred to as the “thermal output” of the foil strain gauge [49]. In order to obtain the true mechanical strain, the thermal output must be deducted from the strain measurement. One should also be aware that thermal output is not exactly proportional to the temperature change [49]. One solution is to use a “dummy gauge” to adjust for the temperature effect; however, it is difficult to create the condition that the dummy gauge is unstrained but it is experiencing identical environment condition as the active gauges, especially for field applications [49]. Therefore, for field applications, the temperature-compensated gauges are preferred to be used; these gauges have small thermal output within a certain range of temperature change, and *Constantan* and *Karma* are the two most commonly used alloy having self-temperature-compensation properties [141]. Usually manufactures will provide thermal output graphs for their strain gauges, which should be used to adjust the strain readings. Formula for the temperature-effect-corrections, include the calculation for change in gauge factor, can be found in [49] and many other strain gauge related references.

Since the signal produced by foil strain gauge is usually low-level and can be easily interfered by many other sources, noise control is very important for foil strain gauges, especially for bridge field applications, where the lead wires between sensors and readout unit are relatively long comparing to laboratory set-ups, and all sorts of environmental attacks usually exist. Electrostatic and Magnetic noises are most common for foil strain gauges. The two most common methods for noise control are: (1) amplify the signals with signal conditioners; (2) provide shielding and pay attention to the wiring to minimize environmental noises [49]. The noise level is really project- and site- specific. When planning the SHM system set-up, the “characteristics” of the site should be investigated and experienced technicians should be consulted for best wiring design and noise control. Besides the ISIS Design Manual No.2, reference [142] provides a good summary for noise control in strain measurement and with more references provided; reference [143] contains all the links for the instrumentation and measurements for strain gauges.

As for the Vibrating Wire (VW) strain gages, they are encased in sealed steel tube and are larger in size (usually over 100 mm in length) than the foil strain gauges. VW strain gauges can be embedded in concrete or attached to the surface of components [49]. Its biggest advantage over foil strain gauges is that it does not drift over time, therefore it can be used for long term monitoring projects. However, although more stable over the long term, VW strain gauges can not sample fast enough to characterize live load effects adequately, limiting its usage for many bridge applications [49].

### 2.3.2.1.1.2 Linear Variable Differential Transducers (LVDTs)

LVDT is a well established sensor design that has been in use for many decades for the measurement of displacement and within closed loops for the control of positioning [144]. The basic components of a LVDT consists of a cylindrical array of a primary and secondary windings with a separate cylindrical core which passes through the center (see Figure 2-15 [b]). The primary windings are energized with a constant amplitude AC (alternate current), usually with frequency in the range of 1 to 10 kHz; this produces an alternating magnetic field in the centre of the transducer and induces a signal into the secondary windings [145]. Movement of the core causes change in signals; as the windings are wound in a certain precise manner, the magnitude of the output voltage is linearly proportional to the distance moved by the core (up to its limit of travel). The phase of the voltage indicates the direction of the displacement [75]. The key specification for choosing LVDT is its range of measurement. Accuracy is measured as a percentage of the full scale of measurement. Outputs for LVDTs can be analog voltage/current, digital, or even parallel/serial computer output [146].

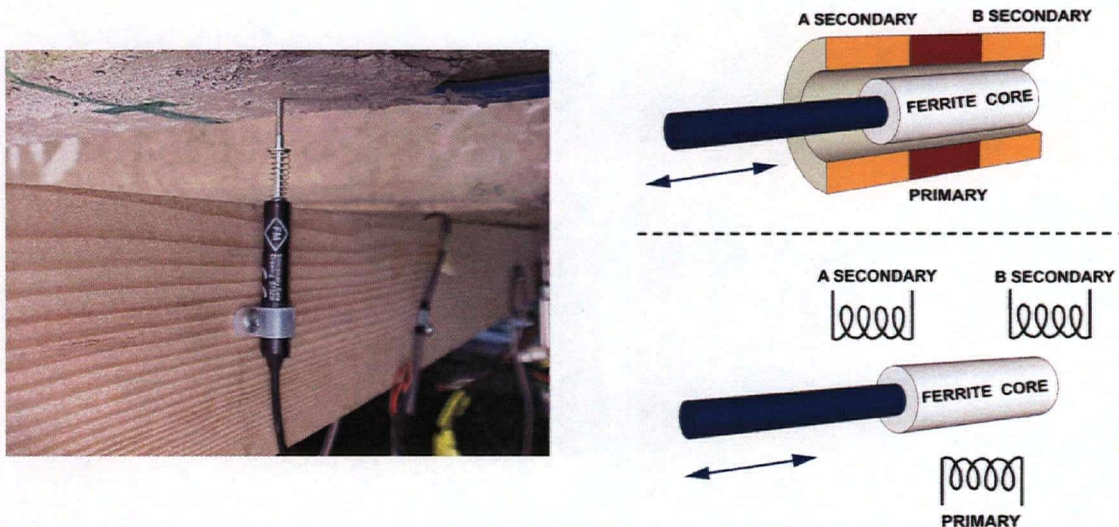


Figure 2-15 The Linear Variable Differential Transformer: a. Photo of an LVDT under Bridge; b. Basic Structure of LVDT [145]

The distinct advantage of LVDT is that, since the sliding core does not make physical contact with other components of the assembly, there is no friction generated and the LVDT can be completely sealed against the environment, making the LVDT a highly reliable and long last device [144,145]. However, LVDT has a fundamental problem of needing a physical reference; if reference movements can not be prevented, the measurements will be affected [127]. The set-up for LVDT for long term monitoring is especially difficult for bridges span over waterways, which actually consists 80% of all

bridges in U.S. [84]. Therefore, for deflection measurement, new technologies have been developed for more precise and convenient method, such as laser measurement and the GPS systems [88].

#### **2.3.2.1.1.3 Accelerometers**

Accelerometer, which measures accelerations caused by forced excitation, impact or ambient vibrations, is the most commonly used sensor to gather structure's dynamic characteristics [137]. As mentioned earlier, conventionally, a major effort for SHM research focused on damage detection methods using acceleration signals, and therefore the accelerometers became one popular sensor for many SHM projects.

Accelerometers can be installed on a structure easily and the signals are immediately available; there are also a wide range of specifications available for different applications, including the relatively harsh field environment [127]. These characteristics of accelerometers add up its popularity for bridge monitoring applications. Similar to the foil strain gauges, the accelerometers are also vulnerable to electromagnetic and radio interference; nonetheless, they can still be used for long-term monitoring because they do not depend on signal amplitude, and do not drift over time [138].

Important parameters to be considered when choosing accelerometers include: range of acceleration (measured in "g's"), frequency range, transverse sensitivity (the sensitivity to motion in the non-active direction), mounting errors, temperature and acoustic noise sensitivity, and mass [147,148]. The specification sheets of an accelerometer typically will provide information on most of these parameters; the damping coefficient, and a scale factor that relates the output to an acceleration input are often provided as well [149].

For civil engineering applications, either *piezoelectric accelerometers* or *spring-mass accelerometers* are normally used [49]. The spring-mass accelerometer is the "simplest" type of accelerometer which measures mass motion by attaching a spring mass to the wiper arm of a potentiometer; the mass position is conveyed as a change in resistance [150]. The spring-mass accelerometers are only suitable for *steady-state* acceleration or *low-frequency* vibration measurements because its own natural frequency is generally less than 30 Hz [150].

As for the piezoelectric accelerometers, a piezoelectric crystal (often quartz or ceramic) is spring-loaded with a test mass in contact with the crystal; the crystal produces electric charges when a force

is exerted by the mass under some acceleration [148]. The voltage is then converted into accelerations. The crystal has high impedance itself, so a high-input impedance, low-noise detector is required. The output levels are usually in the milli-volt ranges [150]. Although piezoelectric accelerometers have relatively low sensitivity compared to other types of accelerometers, they can measure the highest acceleration range (up to 100,000 g's) [151]. Its own natural frequency is very high (may exceed 5000 Hz), make it suitable for vibration and shock measurements [150].

#### **2.3.2.1.1.4 Temperature Sensors**

Common conventional temperature sensors for civil engineering applications include resistance temperature device (RTD) and the vibrating wire (VW) temperature sensors [49]. RTD operates based on the fact that the electrical resistance of a material changes with change in temperature. There are two types of RTDs: metallic sensors and thermistors [49]. Common materials used for the metallic sensors include nickel, copper, and platinum; platinum is by far the most popular because of its wide temperature range, accuracy, and stability [152]. Thermistors are based on resistance change in a ceramic semiconductor. The operation range of the thermistors is smaller than that of the metallic counterpart, but thermistors usually provide higher accuracy [49]. RTDs serve as the standard sensors for temperature measurements due to their excellent repeatability and stability [152]. However, their biggest problem is that, the current for operating them more or less creates certain amount of heat, which affects the accuracy of the temperature readings [49].

The VW temperature sensors have a similar mechanism as the VW strain gauges: a change in temperature causes a change in the frequency signal output from the sensor; the readout unit processes the signal and converts it to a voltage proportional to the temperature [49]. The VW temperature sensor is encased in a cylinder and has no physical contact with the surrounding. Therefore, the advantage of using VW temperature sensor is that the effect of the strains on the temperature readings is not a concern [49].

#### **2.3.2.1.2 Advanced Fibre Optic Sensors**

The study of fibre optic sensors (FOSs) started about 30 years ago [153]. Since then, various ideas and techniques have been proposed and developed for various measurands and applications. Nonetheless, FOSs have only recently become widely available. Strain and temperature are the most widely studied measurands, and the fibre grating sensor represents the most widely researched



technology for fibre optic sensors (see Figure 2-16) [154]. Besides military usage, the existing market of fibre optic sensors is dominated by a few specific segments, and SHM field is one of the top three [153]. This is not surprising. As mentioned earlier, many traditional sensors are not suitable for long term/ remote monitoring purposes; therefore, demands in advanced sensors like FOSs are growing with the development of SHM technology. The following are some major advantages of FOSs over the conventional sensors [70,154,155]:

- Immunity to electromagnetic and radio frequency interference (EMI/RFI)
- Long-term stability
- Distributed sensing and multiplexing capabilities
- Low creep with little disturbance to the structure
- Electrical passivity (sensors do not conduct electricity)
- Corrosion-resistant
- Light weight and small size
- Can work as both sensor and a data conduit, and with large bandwidth
- Relatively safe in flammable environments
- Response that is not restricted to intensity-based systems
- Flexibility for surface mounting or embedment in the structure
- Embeddable in FRP construction products during manufacture

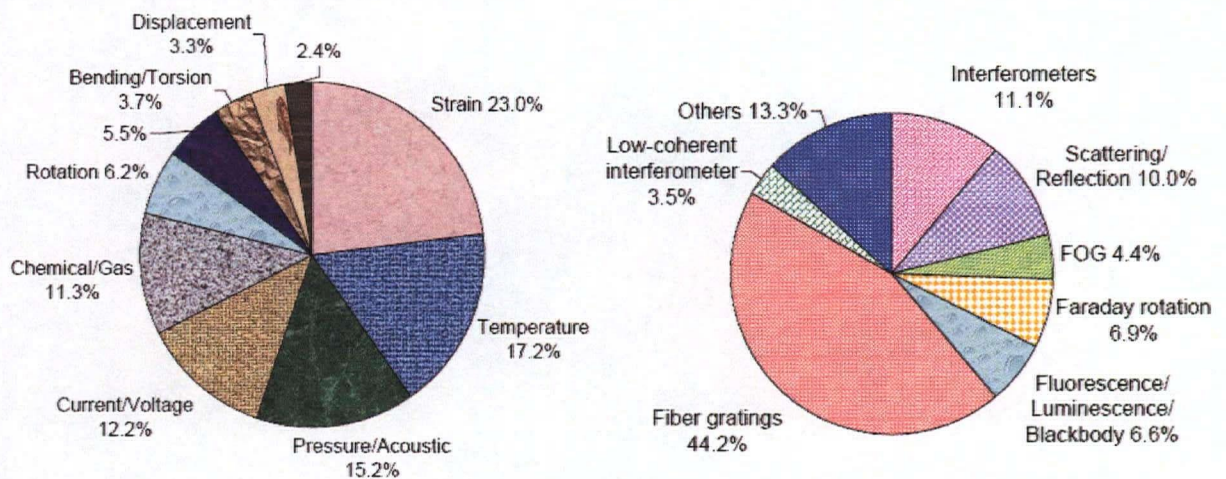


Figure 2-16 Distribution of Fibre Optic Sensor Types According to Measurands and Technology  
Source: [154]

For bridge monitoring, the two most important characteristics for sensor choice is high resolution (for high-speed traffic) and long-term durability and stability (for environmental effects), and FOSs show

superior performances than the conventional sensors on both. FOSs are used mostly to measure strains in bridge projects; in fact, the technology has been grown to the point that they are considered as the ideal substitute to the traditional strain gauges [156]. Especially for the monitoring of composite wrap rehabilitation, traffic flows (weigh-in-motion measurements), environmental loads and extreme temperatures, FOSs can provide better measurement methodologies that were not previously available [70,97]. For both new and rehabilitation construction, FOSs can be easily bonded/embedded to the structure to provide complete strain histories including strains from concrete curing, construction loads, in-situ service loads, to strains due to creep and temperature changes [70]. This information is especially important in verifying the design assumptions for new design/materials and understanding its long-term in-situ behavior. The weigh-in-motion data can be used to estimate the probability of the maximum load rating of the bridge being exceeded, or to predict the remaining service life based on the fatigue cycles observed [97].

With its superior performance under extreme temperature, FOSs for temperature measurement is also of high interest. As mentioned earlier, long-term strain measurements always need to be adjusted for temperature effects; temperature FOSs can also be utilized in monitoring the concrete curing process, the freeze-and-thaw cycle, and the prediction of ice formation, which could not be done easily with conventional temperature sensors [97]. In addition, since corrosion is one of the most common problems among existing bridges, many research works also focus on chemical sensing with FOSs. Detection of chloride ion concentration, concrete conductivity, and the variation in pH can be utilized in the monitoring of corrosion conditions of the steel rebar inside reinforced concrete [102].

The significance of FOSs to the growth of SHM is clear. It is important for today's civil engineers to have basic understanding about the FO technology and be aware of what are available. The following will first introduce what optical fibre is and how it is applied to sensing technology, and then summarize the three common types of FOSs that are available on market and suitable for civil engineering applications.

#### **2.3.2.1.2.1 Optical Fibre and Fibre Optic Sensor Technology**

An optical fibre is a fine cylindrical dielectric waveguide that transmits signals in the form of light; the signals can be computer data or coded voice communication [157,158]. The basic structure of a single optical fibre include three parts [70,159,160]:



- Core – the center of the fibre, where the light travels
- Cladding –surrounding of core, confines the light in the core by its refractive index differential
- Buffer Coatings – plastic coating used to protect the fibre from damage and moisture

The core and the cladding is made of glass or plastic, and the buffer coating is usually made of acrylate or polyimide material. The softening temperatures associated with an acrylate coating is around 100 °C and for polyimide is around 400 to 500 °C [70].

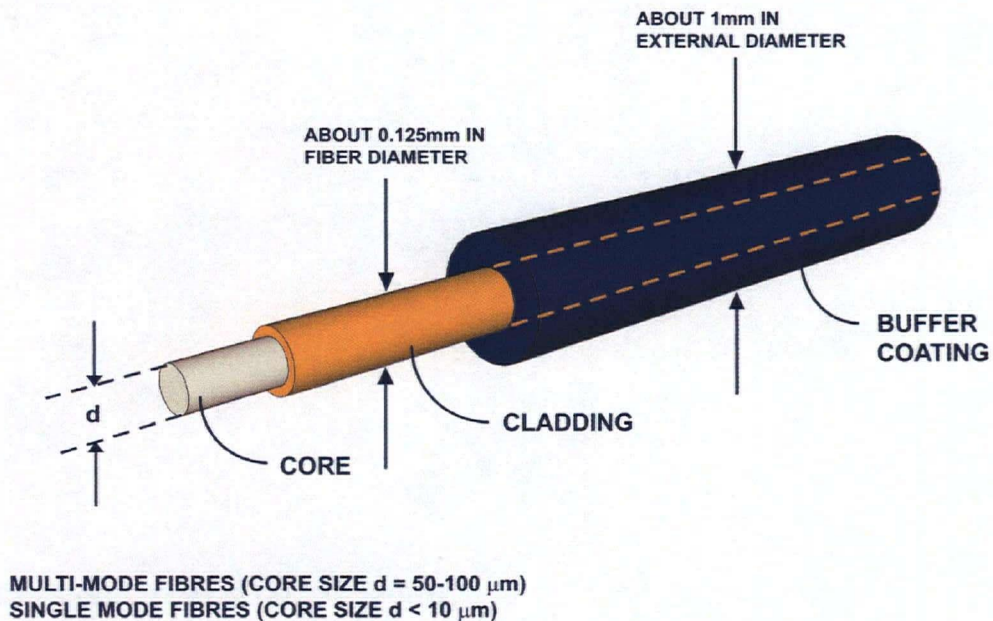


Figure 2-17 Basic Structure of Optical Fibre  
Source: [49,161]

There are two types of optical fibers: *single-mode fibers* and *multi-mode fibers* [162]. A mode is a defined path in which the light travels, and it depends on the geometry, the index profile of the fiber, and the wavelength of the light [159]. The single-mode fibre has a relatively narrow core diameter (about 9 microns) which is close to the wavelength of the light [160]. With such a narrow diameter, light can only travel straight through the fibre in one mode; therefore, it is called a *single-mode* fibre.

Multi-mode fibers have the core diameter much greater than the wavelength of light ( $\sim 1$  micron), typically in the range from 50 to 100 microns [70]. Since the core is wide, lights can come into the fibre at different angles, and propagate down the fibre based on the principle of *Total Internal Reflection* (TIR). TIR is directly related to the fact that the refractive index of the cladding is less than the refractive index of the core, so the light is confined inside the cladding [159].

When the refractive index of the core and the cladding stay constant all along the fibre, it is referred to as a *step index fiber*, because the refractive index “steps up” as the light moves from the cladding to the core. A problem with the multi-mode, step-index fiber is the occurrence of *Modal Dispersion*, which is caused by the fact that different modes of light arrive at the end of the fiber (i.e. to the receiver) at different time (see Figure 2-18). This is because different modes of light make different number of reflections along their travel, so their actual traveling lengths are slightly different. Therefore, when the traveling distance (i.e. fiber length) of the light signals gets long, the differences become significant, and there will be distortion on the signals when they arrive at the end of the fiber.

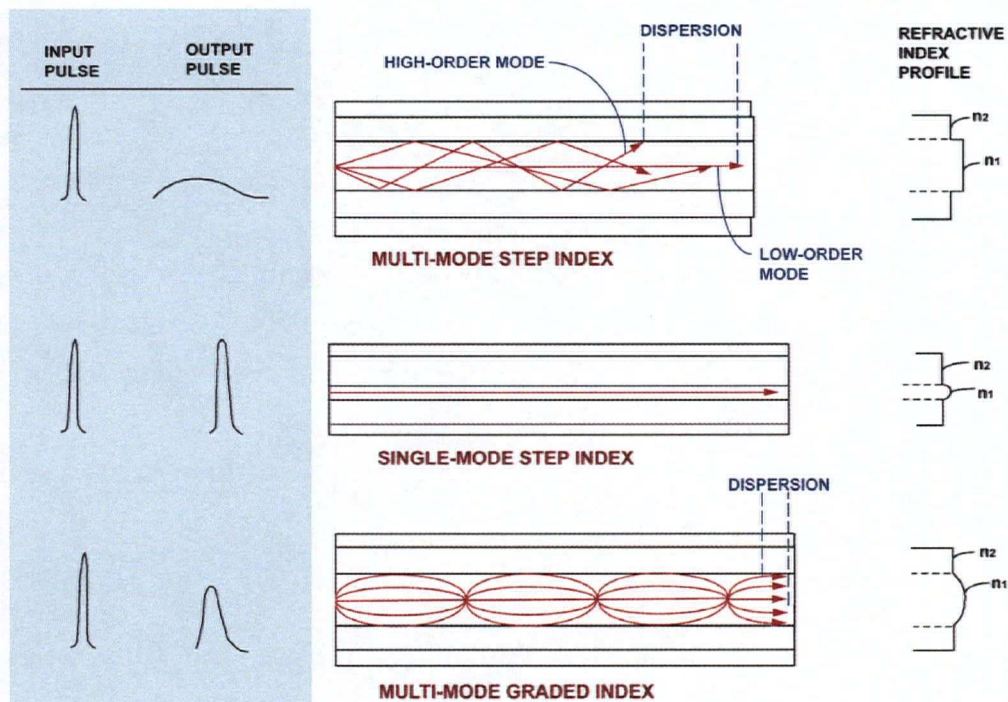


Figure 2-18 Types of Mode Propagation in Optical Fiber  
Source: [163]

One way to decrease modal dispersion is to “grade” the refractive index of the core; make the refractive index decreases with increasing radial distance from the fiber axis [158]. This type of fiber is called a *Graded Index fiber*. The refractive index affects the speed the light travels. Because of the varying in refractive index across the diameter of the core, the light rays will travel in sinusoidal paths and at different speed, which make more of the modes arrive at the end of the fiber at the same time [157,158] (see Figure 2-18). The graded-index fiber can support transmission speed up to 500 MHz over distances up to 1 km, whereas the step-index fibre only supports about 10 MHz over the same distance [164].



Comparing the two modes of fibers, single-mode fibers have the advantages of larger bandwidth, low *attenuation* (signal loss), and lower cost [70]. The bandwidth determines the amount of information that can be carried. Single-mode fibers have bandwidth at around 100 GHz-km, whereas the highest multi-mode fibers bandwidth is about 1 GHz-km [70]; obviously the single-mode fibre has much better information-carrying capacity. **Attenuation** means the intensity of light decreases as it moves along the fiber. Attenuation measurement is in *decibels* (dB), a logarithmic unit that indicates the ratio of output power to input power; each optical fiber has its own attenuation value that is usually shown in *decibels per kilometers* (dB/km). The three main reasons for attenuation are: (1) atomic absorption of light photons; (2) scattering of light by flaws and impurities; (3) reflection by splices and connectors [158]. In general, single-mode fibers have smaller attenuation than multi-mode fibers. Due to these reasons, single-mode fibers are used for high speed transmission over long distance, and multi-mode fibers are mostly used for short-distance transmission, such as LANs. The relationship between the attenuation and wavelength is shown in Figure 2-19; it is clear from the graph that attenuation is at its minima when wavelengths are about to 1300nm and 1550nm [165].

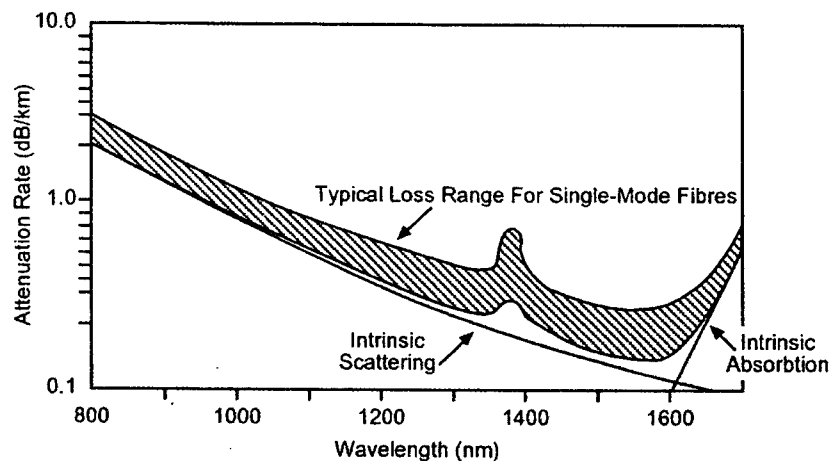


Figure 2-19 Attenuation vs. Wavelength for LASERs in Fiber Optic Use  
Source: [70] (Courtesy – ISIS Canada)

For fiber optic sensors to operate, light sources are required to power the fiber and to transmit the data. There are two main light sources used for FOSs: the light Emitting Diodes (LED's) and the Laser Diodes (LD's) [70]. LED's are broadband and low power (range 1 ~ 10 mW); they are also sensitive to temperature, and the output power can change about 0.5% per °C [70]. On the other hand, LD's have very narrow bandwidth, ranging from 5~30 nm, depending on the laser chip design; its output power also depends on the applied current, but generally much larger than LED's (range from 2, 3 mW to Watts) [70]. Typical commercial LD's have wavelengths at 850nm, 1300 nm,

1550nm, which coincide with the three “troughs” section (where attenuation is lower) on Figure 2-19. LD’s are generally reliable at room temperature, but high temperature still reduce their service life [70].

The cost for LD’s is much higher than LED’s, therefore normally LED’s are preferred to be used as the light source. Due to the small size of the core for single-mode fibers, it is more difficult to couple the light source and a narrow beam is required, which means the LD’s may need to be used instead of LED’s. Generally speaking, the light source for single-mode fibers is usually more expensive than the one for multi-mode fiber. Therefore, although the single-mode fiber are cheaper in unit cost in the fiber itself, multi-mode has the advantage of low connection and system costs that may lead to lower overall cost [159].

For strain measurement, the FOS attached on or embedded in the structural component expands or contracts due to the mechanical and temperature strains on the component. Therefore, the light sent through the fiber to the sensor is modulated by the strain effect. The FOS reflects back an optical signal to an analytical device which translates the reflected light into numerical measurements of the change in sensor length, and therefore strain is obtained [70]. The different techniques used to read the different types of information from the light wave, as well as the way the light wave is modified, result form the different types of FO sensors available. In the following, the common techniques of FOSs available on market today will be introduced.

#### **2.3.2.1.2.2 Common FOS Types for Bridge Applications**

For civil engineering applications, the three most commonly used type of FOSs are the Fibre Bragg Grating (FBG), the Fabry-Perot (FP) sensor, and the Long Gauge Fibre Optic Sensors. The FBG and FP sensors are the “point” type sensors with gauge lengths usually less than 1 cm (similar to the size of conventional strain gauges) and they measure local strain changes at specific locations [166].

On the other hand, the Long Gauge FOSs can have gauge lengths ranging from a few meters to several kilometers. There are two types of Long Gauge FOSs: one is the “integrated” type that uses a conventional telecom optical fibers to measure the path displacement between two points; the other is the “distributed” type based on the Brillouin scattering principle, which takes readings at various positions along the optical fiber over very long distances. The discussion for Long Gauge FOS here will focus on the “integrated” type only because it is the type used on Safe Bridge.



The ISIS Canada Design Manual No. 1 "Installation, Use and Repair of Fibre Optic Sensors" provides very thorough coverage about these sensors [70]; Design Manual 6 "Civionics Specifications" [72] also gives proper handling and instrumentation procedures, as well as the data acquisition systems (the "interrogators") to be used, for all the three types of FOSs.

As mentioned earlier, the Fiber Bragg Gratings (FBG) is the most widely used FOS type. FBG can measure both strain and temperature. FBG is fabricated by creating a modulation in the refractive index of the glass fiber over a local region using UV radiation; the length of the region is the gauge length of FBG [156]. The grating reflects the incoming broadband light in a very narrow spectrum centered about the Bragg wavelength, and the remainder of the spectrum is transmitted (see Figure 2-20). In short, FBG measures strain according to the change in wavelength due to straining of the grating [138, 167]. Light source for FBG can be either the LED's or the LD's.

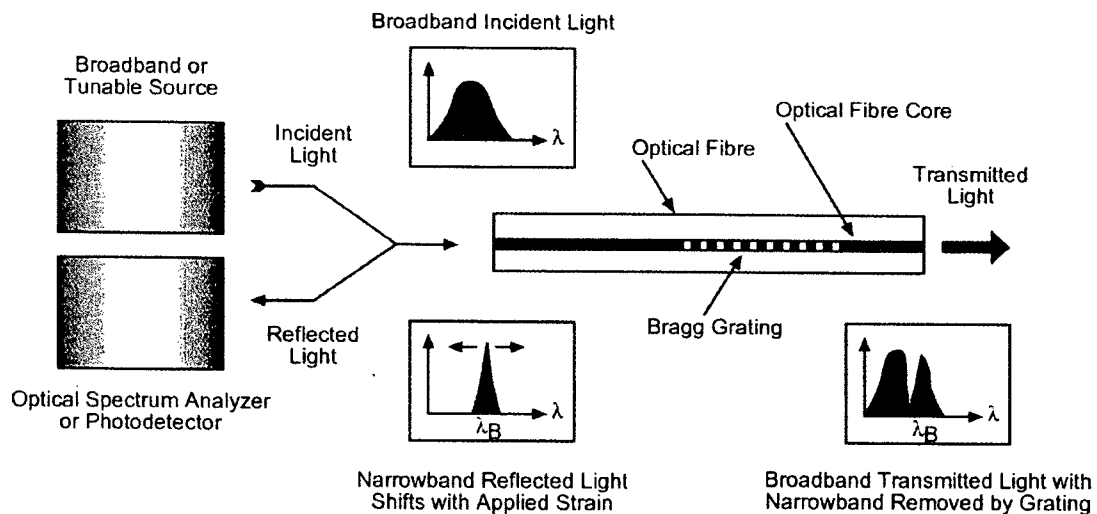


Figure 2-20 Operation Mechanism of the Fiber Bragg Grating Sensor

Source: [70] (Courtesy – ISIS Canada)

The major advantage of FBG is its ability to be multiplexed on a single fiber optic cable, which allows as many as 100 sensors to be calibrated and form a system together [168]. This provides a monitoring system with much higher spatial resolution and therefore able to obtain more valuable information (e.g. higher number of vibration modes) than the conventional systems consisting of several individual sensors [97,168]. Also, the FBG sensors can easily be connected to standard fibre optic telecom cable for data transmission [70]. In addition, the Bragg grating system operates by sensing the wavelength shift, but not the amplitude, of the light reflected back from the grating. This

parameter is absolute and will not be affected by losses in the connecting fibers and couplers, or recalibration and re-initialization of the system; therefore the system is more reliable and repeatable than other types of FOS that use other measurement technique, such as interferometry [70,97].

The Fabry-Perot sensors operate based on the interferometric measurement of a change in gap (cavity length) with a white light broadband source [156]; the gap is between two cleaved optical fiber ends contained in a glass capillary tube and usually range between 9 and 26 microns [70] (see Figure 2-21). The change in gap length is directly related to the strain it experienced. The FP sensor is designed around a FP Interferometer and usually consists of two multi-mode fibers [70]. The FP interferometer can be used to measure strain, force/load, temperature, pressure, and displacement. By using the multi-mode fibers, the FP sensor is easier to splice and connected, and loses less light signals when subjected to bending [70]. Unique attributes of FP sensors include the isolation of the sensor from the incoming optical fibre, and built-in thermal compensation capability. The FP shares most of the advantages of the FBG except the multiplexing function.

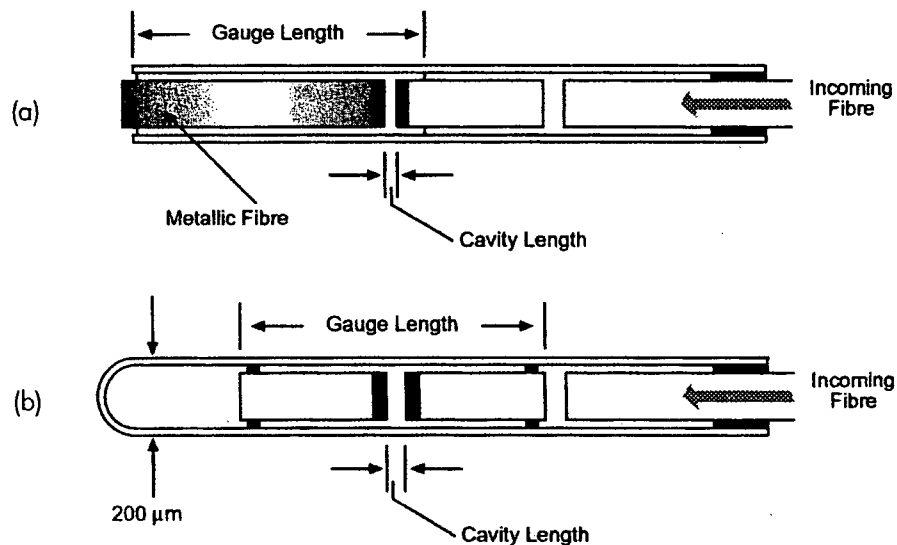


Figure 2-21 Two Types of Fabry-Perot Gauge (schematic): (a) Self-Compensated in Temperature;  
(b) Non-Compensated in Temperature  
Source: [70] (Courtesy – ISIS Canada)

Both FBG and FP sensors have been applied to many bridge structures across Canada to measure local strain distributions and have proven to be a better point sensor than the conventional strain gauges for field applications [49]. Nonetheless, if the objective is to monitor the general integrity and global behavior of the bridge, a point strain measurement is not suitable; a sensor with longer gauge should be used to provide an overall average measurements.

The “integrated” type of Long Gauge (LG) FOS measures the displacement change between two points on/in the structure. LG FOS is made of conventional telecom optical fiber with arbitrary length having two mirrors formed at the two ends of the fiber [70]. The gauge length is the distance between the two points. The gauge length can be a few centimeters to hundreds of meters [156]. In short, the LG integrated sensor system operates based on the principle of low coherence interferometry using a short coherence length source, a LED [70] (see Figure 2-22). The light from the LED first splits into two, travels two different path lengths, and then are recombined at a photodetector. The coherence length of the LED is about 10 micrometers; if the difference in the two path lengths is less than that, they will start to interfere each other after they are recombined. The interference pattern is monitored by the photodetector. The peak of the interference pattern occurs when the two light paths are exactly the same. The measured value is the precise total displacement over the gauge length [70].

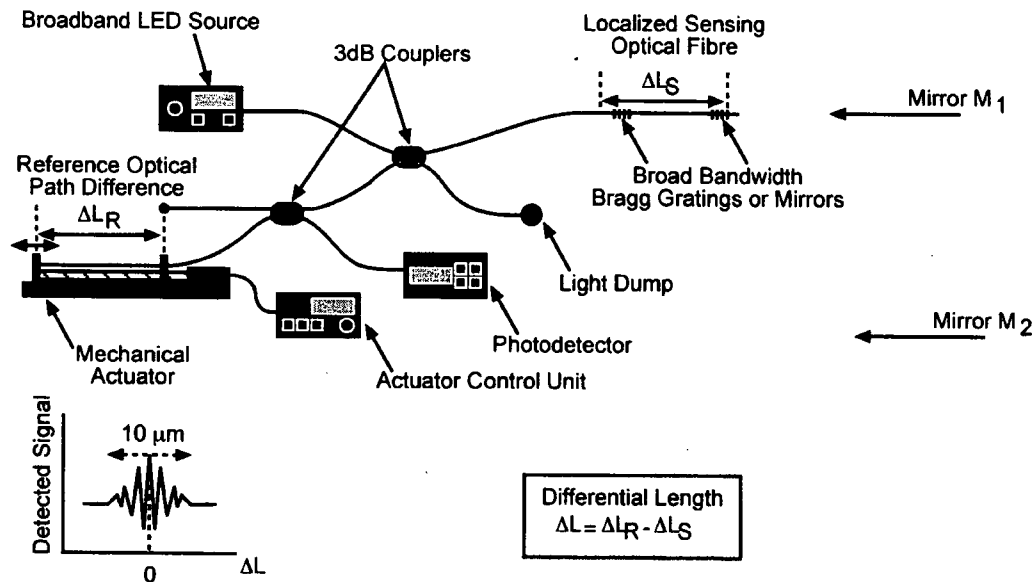


Figure 2-22 Photonic Circuit for Measuring Long Gauge Strain  
Source: [70] (Courtesy – ISIS Canada)

When the global behavior is of interest, the LG FOS is most suitable than the point-type sensors properties because it is not affected much by local stress concentrations. “Flexibility” is also an advantage of LG FOS; it can be used in many different configurations, and both attached on or embedded in concrete [156,169]. LG FOS is particularly suited to monitor crack growth [169] and permanent long-term static deformation for both thermal or mechanical loadings. Finally, LG FOS has better heat dissipation ability due to their longer gauge length.

### 2.3.2.2 Data Acquisition System

The main function of the data acquisition system (DAQ) is to collect, digitize, and sometimes including process signal inputs from sensor(s) [170]. The most “simple form” of DAQ system involves with a readout unit that receives the data from the sensors directly and convert them into engineering values as output. The operator can read the output directly and record the data manually; this type of DAQ system is cheap and easy to set-up, but obviously it only works for cases that the amount of data generated is small, and when the testing period is short [49]. Other common types of DAQ system include data loggers, networked systems, and PC (computer)-based systems [171]. Most of the bridge testing/monitoring projects so far use the computer-based DAQ system; therefore, the discussion here will focus on the PC-based DAQ systems.

The three basic components for computer-based DAQ systems are signal conditioners, data acquisition boards, and a computer, as shown in Figure 2-23 [49]. These three components will be discussed separately in the up-coming sections.

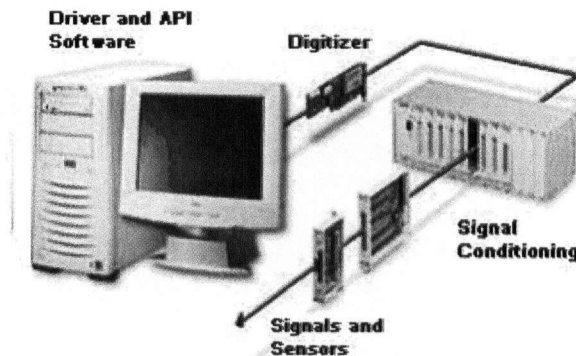


Figure 2-23 Basic Components of a Computer-Based Data Acquisition System  
Source: [172] (courtesy - National Instruments Corporation)

The common device specifications to be considered when looking for a data acquisition system are *number of analog input channels, digital I/O channels, sampling frequency, resolution, and accuracy (Range and Gain)* [173]; these parameters are usually controlled by the data acquisition board, so their meanings will be explained under the *Data Acquisition Boards* section later. In particular, the sampling rate to be used must match the “time scale” (as discussed in Section 2.2.3) of interest. For

example, frequencies used in modal analysis can be up to 40 Hz, which means for a single sensor, the DAQ system should read the data at a minimum of 80 Hz [174]. When many sensors are correlated, the phase information will also be required and an even higher sampling rate should be used [97].

For conventional field testing, one or two experienced technicians familiar with the DAQ system is usually sufficient to complete the task successfully. Nonetheless, when the time scale becomes long and the number of sensors becomes big, especially when different types of sensors are used and networked, the design and set-up of the DAQ system(s) can become very complex. Specialists from relevant fields should definitely be consulted from the design stage. For permanent systems, the issues related to installation, maintenance, and security should be addressed. For example, fans and heat sinks on the back of the data acquisition units shall not be blocked. The ruggedness and long-term stability of the DAQ system itself will also be a concern. Again, economic considerations will play a major role in making decisions about the type and extent of the DAQ system(s) to be used.

For a civil engineer in the SHM team, it is important to gain basic knowledge about DAQ systems and be able to understand the technical terms commonly used by technicians or on the device specifications. The following sections will introduce the three basic components of DAQ system briefly. References [172] and [49] provide a more thorough introduction on DAQ systems that readers can refer to if more information is needed. Even more technical details can be easily found in references like the Handbook of Mechatronics [113].

#### **2.3.2.2.1 Signal Conditioners**

Signal conditioner, as the name implies, “condition” the signals from sensors; they are almost always needed because many sensors and transducers require signal conditioning before a computer-based DAQ system can effectively and accurately acquire the signals [175]. The function requirements are closely related to the type(s) and numbers of sensor(s) it need to “serve”, and the environment of the testing site. The important functions of signal conditioners are given and briefly explained in the following [49,172,175,176]:

- **Amplification:** often the signals from sensors are very small in magnitude, so they need to be amplified to the level better match with the maximum input range of the data acquisition board for the highest possible accuracy, and to increase the resolution and sensitivity of the measurement.

A good practice is to place the signal conditioner as close to the sensors as possible, to boost the signal level before it is affected by environmental noise (increase the signal-to-noise ratio).

- **Attenuation:** is the opposite of *Amplification*. The voltage(s) from the sensor(s) exceed the input range of the data acquisition board, and therefore the amplitude of the input signal needed to be diminished.
- **Isolation:** prevent the problem of “ground loop”, which is caused by improper grounding of the system and can affect the measurement or even damage the system. Isolation can also block high-voltage surges and reject high common-mode voltage, which protects the DAQ unit, the computer, and the operator.
- **Bridge completion:** sensors such as strain gauges and resistive temperature sensors require additional resistors to work with them to complete the Wheatstone bridge circuit; signal conditioners can work as the resistor(s).
- **Multiplexing:** is necessary for high-channel-count applications (when many sensors are used). The analog-to-digital converter (ADC) is usually the most expensive component in a DAQ system. Multiplexing enables several analog signals (from several sensors) to be processed by a single ADC, which is a cost-effective way to expand the signal count of the system.
- **Simultaneous sampling:** for application like vibration measurement, simultaneous sampling is required; that is, to measure two or more signals at the same instant time. Similar to multiplexing, signal conditioner can provide simultaneous sampling solution to avoid significant costs in purchasing many digitizers for each channel.
- **Sensor excitation:** many sensors require external excitations to work; for example, strain gauges and resistive temperature sensors require DC voltage/current input and LVDT and vibrating wire gauge require AC current for their operation. Signal conditioners can generate the input signals for these sensors.

Other important criteria to consider with signal conditioning include the packaging (modular versus integrated), durability, I/O count, advanced features, and cost [172]. Signal conditioners assist sensors to operate properly, maximize the accuracy of the data acquisition, and improve safety.



#### 2.3.2.2.2 Data Acquisition Boards

After signal conditioning, the signals are still in analog form, which cannot be “read” by the computers; therefore, a “digitizer”, or data acquisition board, is required, so that the computer will be able to interpret the data. DAQ board can be a “plug-in” board if it is installed inside a computer, or a “stand-alone” hardware that requires its own power supply and connected to a computer through a special cable [49]. There are also products available that combine the functions of signal conditioning and DAQ board into one unit.

The important parameters to be considered for the choice of DAQ board are given and explained in the following. These parameters are usually given in the device specification from manufactures [49,172,176,177].

- **Number of Analog Input Channels:**

The number of signals (usually mean the number of sensors) that can be simultaneously connected to the DAQ board. The number of channels available is halved when the connection is made *differential-ended* than *single-ended*. Single-ended connection means one of the two leads from the sensor is connected to an input channel of DAQ board, and the other lead is connected to the common ground. This mode of connection utilize the most of input channels available, but should only be used when: (1) input signals are high-level ( $\geq 1$  Volt); (2) all input signals can share a common ground reference; (3) noise from surrounding will not be significant (e.g. lead wire between sensor and DAQ board is less than 4.5m).

When these three criteria are not met, the connection should be made *differential-ended*, which means the two leads from the sensor are connected to two input channels of the DAQ board, and that is why the number of sensors can be connected is halved. The differential-ended connection reduces noise errors because the common-mode noise picked up by both leads is canceled out. Therefore, a good practice is, try to always use differential-ended connection when enough input channels are available.

- **Sampling Frequency:**

The number of analog-to-digital conversions the DAQ board runs in a second (unit in Hz); that is, the number of readings to computer in a second. The sampling frequency has to be high enough to represent the input signal correctly. When the sampling rate is too slow, the measured result can represent a completely different signal, and leads to false data measurement; this is referred

to as an “aliasing error”; see Figure 2-24. On the other hand, using an unnecessarily high sampling rate will increase the burden of data processing and storage, and lead to waste in time and money. For dynamic testing, the sampling rate must be greater than twice the frequency measured for accurate results, according to the *Nyquist Theory* [178].

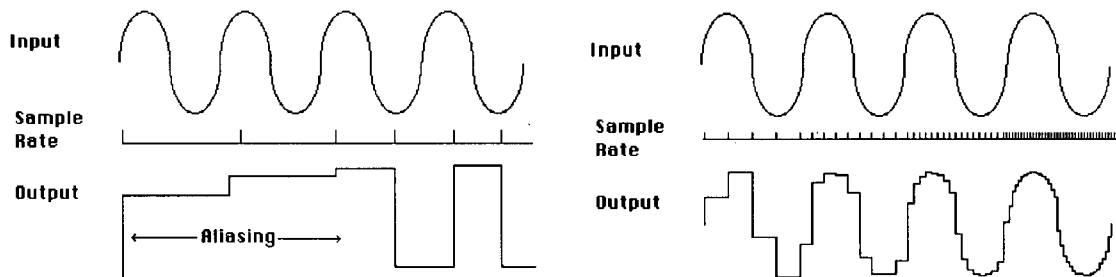


Figure 2-24 [a] Effect of Low Sampling Rate: Aliasing; [b] Effects of Increasing Sampling Rate  
 Source: [178] (courtesy – Peter Elsea)

Another important issue relate to sampling rate is the effect of “multi-channel scanning”. When many channels are active at the same time (“parallel channels”), most DAQ board reads the multi-channel inputs by multiplexing – a single analog-to-digital converter (ADC) performs the conversion of signals by switching between channels. Sampling all the channels in a row by multiplexing is called “scanning”. Since only one ADC is sampling all the channels, the effective sampling rate of each individual channel is reduced in proportion to the number of channels being sampled. Therefore, if the desired frequency is 50 Hz and 6 parallel channels are used, then the sampling rate to be used on the DAQ board should be 300 Hz, but not 50 Hz.

- **Resolution:**

The resolution of the DAQ board determines the sensitivity and precision of the converted signal. Resolution is measured in “bit”. “ $n$  bit” resolution means the signal voltage range is divided into “2 to the power of  $n$ ” equal divisions. Theoretically, one half the division is the smallest voltage change that the DAQ board can detect. Therefore, the higher the resolution, the more divisions the voltage range is broken into, and the smaller the detectable voltage change. For example, an ADC with 3-bit resolution divides the analog signal range into 8 equal divisions, and each division is represented by a binary code between 000 to 111 (see Figure 2-25). If the range of signal is 10 Volt, then the smallest detectable voltage change is 0.625 Volt ( $10 \div 8 \div 2 = 0.625$ ). Similarly, 5-bit resolution means 32 divisions ( $2^5 = 32$ ) representing by 32 sets of binary code between 00000 and 11111 combination.

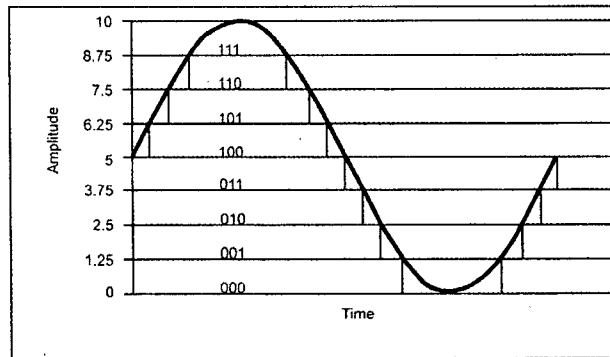


Figure 2-25 Example of An Analog Wave to be Digitized with 3-bit Resolution  
Source: [49] (courtesy – ISIS Canada)

- **Range:**

The “Range” of a DAQ board means the maximum and minimum voltage level it can read. Since the DAQ board divides the whole range into equal divisions according to its resolution, the smaller the range means the higher the accuracy. Nonetheless, a DAQ board with small range may also means fewer types of sensors are compatible.

- **Gain:**

The “Gain” is an amplification factor for signals. When the input analog signal is too low in voltage, “Gain” is used to amplify the signal before it is converted to a digital signal, therefore increase the accuracy of the conversion. Nonetheless, one should be aware not to select a Gain that over amplified the signal to make the signal greater than the DAQ board’s range.

### 2.3.2.2.3 Data Acquisition Program

For a computer-based DAQ system, the DAQ program is an essential component because it provides the interface for the user to control the whole DAQ system, and to set-up the system to work in a desired way that is suitable for the particular application. Many DAQ hardwares come with software programs on market. Most of these software programs hide the low-level, complicated programming section and provide user-friendly, graphical interface for users [49]. Nonetheless, the users also get to modify the content by writing their own program. One should be aware of the programming language(s) the system read.

### 2.3.3 Data Communication

*Data communication* includes the transfer of data from the sensors to the DAQ systems, and from the DAQ systems to the computer(s) for data processing and storage; *data communication* works closely with *data acquisition* to complete the gathering of structure responses. Signals are either in analog or digital form. The conventional practice for bridge instrumentation is to run cable wires between the sensors and a centralized DAQ system [115,125]. With the increase in the demand and complexity of new SHM systems, the traditional wiring systems became impractical and problematic, especially for long-term monitoring applications. Addressing the problems, remote control monitoring, which provides one-time installation of the whole DAQ system, and wireless communication of data, which avoids cumbersome cabling, become the popular solutions for long-term monitoring projects [134]. Major design parameters for data communication include the type of transmission (e.g. wired or wireless), transmission bandwidth (frequency, Hz), transmission rate (bits per seconds), and transmission standards (e.g. interface standards). Depending on the size and requirements of the SHM system, both wired and wireless technologies may need to be combined to develop an optical solution.

In addition, with the increased popularity in using fibre optic sensors for SHM, optical fibers themselves also become a common media to transfer data between the FOSs and the DAQ system. Major advantages of the optical fiber cables over copper wires are: higher information carrying capacity (less energy loss and higher bandwidth), lighter in size and weight (easy to handle), better security and stability (immune to many interferences), and less electrical power consumption (save power cost) [158]. On the other hand, the disadvantages are their higher unit price and the need for special care and skilled personnel. Additional training is required for people to handle optical fibre cables properly on site. For example, to join optical fibers will require expensive precision splicing and measurement equipment; fibre optic cable shall not be coiled to a radius less than the minimum bend radius as stipulated by the manufacturer [726].

Again, ISIS Canada Design Manual No. 6 [72] provides detailed specifications for many components related to the *communication* of SHM system, such as the cables, the conduits, the junction boxes, the cable termination, and even the control rooms. Issues that should be aware of during the installation of these components are also discussed. Civil engineers lacking field testing and instrumentation experiences are strongly recommended to read this manual for their first SHM project. The design manual is condensed and clear, so the information provided inside will not be repeated here. In the

following, the wired and wireless communication technology commonly used for bridge testing and monitoring will only be briefly introduced. *Data Communication* is itself a broad and sophisticated field; if the communication system will become highly complicated due to project needs, experts from the field should be consulted and be in charge of the design and installation of the communication systems. Nonetheless, it is the civil engineer's responsibility to gain basic knowledge about *Data Communication* to be able to understand the design and be able to incorporate this subset to the other components of the overall SHM system.

### **2.3.3.1 Wired Transmission**

For most bridge field testing, wire pairs/cables are used to connect the sensors and DAQ system. Wire pairs and wire cables, in which the signal travels in the form of electrical current, are susceptible to ambient electrical and electromagnetic interferences; and the longer the wire, the worse the noise effects [134]. Longer runs of wire cables are also more likely to be damaged in field environment. The potential type and sources of noise, and the length restriction of wiring (from DAQ system) are two major factors to be considered during the design stage for the communication system. Most of all, the cost for cabling is often an issue because it is a time- and labor- consuming process; the installation and maintenance fee are often high. Based on past experiences, the installation time of a wiring measurement system for large-scale bridges can consume over 75% of the total testing time; the labor cost for installation can be over 25% of the total system cost [125]. In order to protect the wires from the bridge's harsh environment, wire conduits are required to be installed, and the cost is about \$10 per linear foot; the cost for conduit only can add up dramatically when the bridge is long, the number of sensors is big, and the DAQ system can not be placed close by [133].

As for the data transfer between DAQ system and computer(s), when the equipment components are within short distance, either transmission wires are used directly, or a Local Area Network (LAN) connected by Ethernet cables is created [115,138]. Ethernet cables are often made of coaxial cables or special grades of twisted pair wires. Coaxial cables are like an "improved version" of the conventional copper wires. Please refer to Figure 2-26: a coaxial cable usually consists of a copper wire ("D") surrounded by an insulating spacer ("C"), and then a cylindrical conducting sheath (copper mesh, "B"), and finally an outer insulating layer ("A") [179]. Therefore, coaxial cables are much less susceptible to electrical and electromagnetic interference, which is the major advantage over conventional wires.

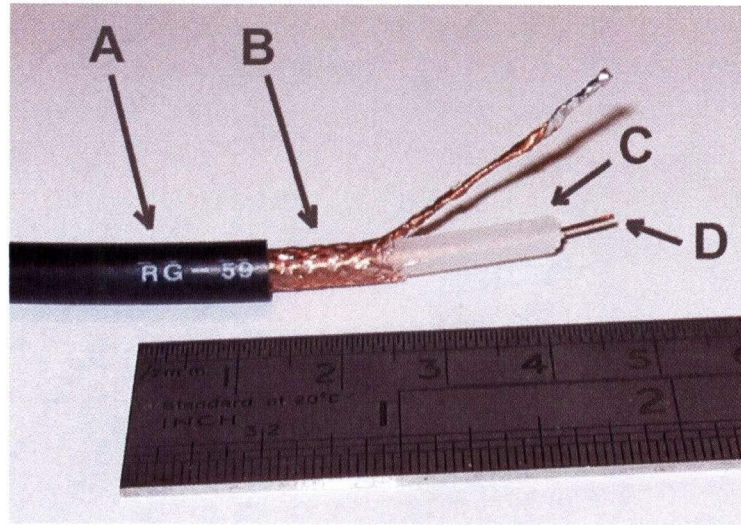


Figure 2-26 A Radio-grade Flexible Coaxial Cable

Source: [179] (courtesy – Heron)

Coaxial cables are usually used to carry high-frequency or broadband signal, so it is commonly used for Ethernet LAN; they are relatively inexpensive today, widely available, and can transfer data reasonably fast [138]. Today's Ethernet cables can easily transfer data from 10 to 100 megabits per second (Mbps); the newer Gigabit Ethernet can transfer data up to 1000 Mbps [180]. However, there is lengths limit for Ethernet cables. Repeaters are required for longer lengths usage [115]. Also, all stations on the Ethernet LAN have an equal chance of sending data and cannot reserve priority [181]. These two factors make the Ethernet LAN still is impractical to be used for real-time bridge SHM.

### 2.3.3.2 Wireless Transmission

The North American shipments of wireless products for monitoring and control was estimated to grow at a compound annual growth rate of over 47% from 2001 to 2006 [182]. As mentioned earlier, the challenges and high costs of wire management for SHM systems have made wireless sensors become a popular research area. There are several different types of wireless sensors designed for bridge monitoring purpose available on market already, but it is not within the scope of this thesis to introduce them. Only two aspects about wireless sensors will be briefly made. First, wireless sensors still hold some disadvantages over conventional sensors. The biggest disadvantage is that, they have limited communication distance [52]. Also, wireless sensors are usually larger in size and higher at cost [138]. Most wireless sensors are powered by batteries, and if the batteries utilize solar power, the requirement for the sensors to be close to an AC source can be eliminated [138]. Nonetheless,

many wireless sensors are “wireless” only in terms of the data transfer between the sensor and the DAQ system; their applications still require wires for power supply [52]. The life of the batteries is a concern for long-term monitoring as well. Second, current research trends for wireless sensors include: (1) to make the sensor “really wireless” utilizing either the Bluetooth or IEEE 802.11b wireless protocols [182]; (2) making the wireless sensor programmable to perform some limited data processing; for example, the design of the wireless sensing unit has been extended to include microcontrollers that embody computational power for data interrogation [134]. In fact, not just the wireless sensor, a present focus of SHM research is to distribute the computational load among all the components in the data acquisition network [55,134].

As for the wireless data transfer between the DAQ system and the PC, either the GSM/GPRS Cellular network, Infrared Frequency (IF), or Radio Frequency (RF) can be used [115]. Depends on project need, the transmission speed, which can vary from 1 Mbps to 54 Mbps for RF systems, and up to 622 Mbps for IF systems, may be of concern [138]. An emerging technology for short-distance communication within a LAN is to use the Bluetooth technology, but the distance is limited to only around 10 meters, and interference is a concern [138]. In addition, recently, more and more DAQ systems have IP built-in, so the data received can be directly controlled and viewed through Internet. The two main issues to be aware of with the use of wireless communication is interference and security.

### **2.3.4 Data Management**

The Data Management here include two major components of SHM system, *Data Processing* and *Data Storage & Retrieval*. Without proper data processing, no matter how much how fancy and robust the sensing systems are and how much data have been collected, either nothing is told or wrong thing is told. As for the storage and retrieval of data, the tasks can be tricky for continuous monitoring projects. Like what a professor said, “it’s more about what we do with the data” [103]. Good management with the data is what keeps the value of SHM lasting. The exact tasks for *Data Management* are different for different projects; it is difficult to cover all of them, and they are not within the scope of this thesis. In the following, the two subsets of *Data Management* will be discussed generally.



#### 2.3.4.1 Data Processing

This subset is closely related to various forms of information technology (IT) such as database management, signal processing, data mining, expert system and heuristics. Data processing include two major steps: *Data Cleansing* and *Data Normalization*.

*Data cleansing* is the process of selectively choosing data to be accepted or to be rejected for the feature selection process [115]. Under field environment, there are always “unavoidable” and/or “unidentified” signals come with the desired signals. Unidentified signals can be caused by various reasons (wire effect, interference from power pole, etc.) and they are usually considered as white noise [135]. Techniques to be used for data cleansing include filtering and re-sampling set-ups. Data cleansing is usually based on the knowledge of the individuals directly involved with the data acquisition [115], and the “cleansing process” can be as simple as manually deleting/ignoring the suspicious part of the data, or based on advanced programming and automatic sampling programs.

Data cleansing deals with the “unidentified signals”, and *Data normalization* deals with the “unavoidable signals”. *Data normalization* refers to the process of separating the environmental and operation variations from the measurement of interest (deterioration or degradation) to enhance the sensitivity of the features to damage [65]. Variability can be caused by different environmental (e.g. season) and testing conditions (e.g. loading positions), changes in the data reduction/analysis process, or unit-to-unit inconsistencies (e.g. instrument set-up). Most of the time, not all sources of variability can be eliminated; one should try to minimize the extent and to make appropriate measurements to quantify the variations.

There are two common ways to normalize the data. One is to normalize the measured responses by the measured inputs. When environmental or operating-condition variability is an issue, “*the need can arise to normalize the data in some temporal fashion to facilitate the comparison of data measured at similar times of an environmental or operational cycle* [115]”. The other method is to normalize the data by measuring the varying environmental or operational parameters directly. For example, extra measurement on the temperature is of this kind.

Besides these two general steps, specific data processing procedures are required for special cases. For example, for continuous monitoring, the amount of data is so significant that “*data compression*” should be performed. A novel signal processing technology using wavelet theory is for this purpose

[135]. When multiple types of sensors are used, “*data fusion*” is required to correlate all the inputs to enhance the fidelity of the damaged detection process [115]. Common examples of data fusion include the extraction of mode shapes from sensor arrays and the averaging for spectral quantities to remove noise from the measurements [115].

#### **2.3.4.2 Data Storage and Retrieval**

The “data” here refers to the “processed” data as discussed above. The storage of data first may seem straight forward and nothing to talk about. Nonetheless, proper storage is actually an important part for a successful SHM process and bridge management, especially for periodic monitoring, where testing results from different times need to be retrieved from time to time by different people for comparison. Therefore, not only that the medium used for storage should last and remain retrievable for many years, the data file itself should be “self-explanatory” in terms of clear format for different people to read [49].

The amount of data is closely related to the number of sensors deployed and the frequency and length of time for the testing/monitoring. For most static field testing, the amount of data is not so significant that both the raw data and the interpreted results can be saved together. However, for dynamic field testing, the amount of data is usually very voluminous; situations for long term monitoring can be even worse. For these cases, one may need to consider only store the processed data, which has the disadvantage that data can not be re-interpret in the future [49]. For data storage, the most important decision to make is what to be kept and what to be abandon, which is also govern by the importance of data and the confidence of the interpretation [49]. In addition, if the data analysis method is pretty “subjective”, it is better to keep the raw data so that in the future when different personnel is involved with data analysis and comparison, the file can be re-interpret.

#### **2.3.5 Diagnostics**

The final component is *Diagnostics* – the interpretation of the processed data, also viewed by many as the most important component in the SHM system. The interpretation results are really what the whole thing is for, which answer the question(s) that initiate the need and the start of SHM system. SHM aims to investigate the structural integrity by relating the structural properties to the changes in the static and/or dynamic responses [135]. The actual implementation of this portion of the SHM

process will be application specific, so this section can only briefly discuss this topic. It is often involved with the conversion of abstract parameters into quantities that directly relate to the responses/properties of the structure [49]. Works for *Diagnostics* can be as simple as direct comparison between two sets of data or plots, or implementing algorithms to process the data for damage detection.

*Diagnostics* is also referred to as the “*Feature Extraction*” stage of SHM, which has received the most attention in SHM technical literature [115]. The fundamental damage detection method is based on fitting some model to the measured system response data. Differences between measured data and model prediction are used to adjust the model. The adjusted model is then compared to the original model to determine the possible location and level of damage. These methods depend on the accuracy of the analytical model [52]. An alternative method is to identify features that directly compare the sensor waveforms or spectra of these waveforms. The most common methods of feature extraction comes from correlating observations of measured quantities with the first-hand observations of the degrading system [115].

Many global health monitoring methods focus on using the dynamic properties of structure, for example, detecting the shifts in resonant frequency or changes in mode shapes [52]. Some other methods include the *Matrix Update Method*, *Statistical Pattern Recognition Approach*, and *Artificial Neural Networks* [52]. The Los Alamos National Laboratory Report [115] also presents many examples of different feature extraction methods, and provides discussions on *Statistical Discrimination* development for *supervised* and *unsupervised* learning. Algorithms for vibration-based damage detection is itself a sophisticated field and introduction on all these methods are not within the scope of this thesis; nonetheless, it is a good thing for people interested in SHM to know that many techniques exist to perform damage detection for various kind of bridge problems.

---

## Chapter 3


### Background Information for Safe Bridge Project

---

Besides being the testing bed for the study of SHM process, Safe Bridge is also the first testing site for the new repair technique, *Sprayed FRP*, and this thesis covers two follow-up field tests on Safe Bridge. Therefore, in addition to the brief introduction on Safe Bridge project in chapter 1.3, this chapter is devoted to provide more background knowledge related to Safe Bridge, including literature research on *precast concrete channel beam bridge*, details on the site, material properties, and structural components of Safe Bridge, and inspection results and problems discovered from Safe Bridge before the repair.

#### 3.1 Precast Concrete Channel Beam Bridge

The three basic forms for bridges are the *beam*, the *arch* and the *suspension* [83,183,184]. Within the three forms, *beam bridge* is by far the most widely used type, because it is the least expensive, simple in structure, convenient to fabricate and erect, and with less construction time [183,185]. The only disadvantage about beam bridges is its limitation in span length. Therefore, almost all short-span bridges are *beam* type and made with reinforced concrete [185].

As the name implies, *precast concrete channel beam bridge* (PCCB bridge) is the type of beam bridge composed of simply-supported, multi-adjacent precast channel beams. During the 50s and 60s, PCCB were commonly used to construct short span, county/rural bridges in North America, especially when girder depth is limited [83,186,187]. The precast channel beam has an inverted channel shape in cross section (like “”), and is normally made of normal or light weight concrete [188]. When placing several channel beams side-by-side and connect them longitudinally with shear connectors, the horizontal section forms the deck area, and the two vertical “legs” act like shallow beams with the primary flexural reinforcement on the bottom of the “legs” [105,188]. The deck surface is generally overlaid with asphalt wearing surface or concrete [105,189].

PCCB bridges constructed prior to the 70s usually had a design life of 50 years [187,190]. In U.S., PCCB bridges that are over 50 years old have been identified in 14 states; for examples, about 600 PCCB bridges in Iowa and 400 in Arkansas are reaching their design life and still remain in use today [189,191]. In Canada, the province Alberta alone has approximately 1200 existing PCCB bridges (PCCB is called "Type G stringers" in Alberta) [192]. Some states in U.S. still use PCCB (with improved design) to construct their short-span rural bridges today.

Regarding the geometric properties and design load, older PCCB used in U.S. had a span length ranging from 19 to 36 feet, with 19-feet to be the most commonly used; H15 loading (15 ton truck) was the design standard and there was no provision for shear reinforcement [189,193]. Today, bridges should be designed for minimum HS 20 truck load according to the AASHTO Specification [194]. Early PCCB bridges constructed in Canada were designed for HS 20 truck (~320 kN) but with minimum shear reinforcement; span lengths varied from 6.1m to 11.6m, with 6.7 m (22 feet) and 8.5 m (28 feet) to be the most common types [188,192]. Today, according to Canadian Highway Bridge Design Code, CL-625 Truck (625kN) is the standard design load and service life of a new bridge should be 75 years.

The number of girders to be used depended on the width of each channel beam and the requirement on the roadway width. Canadian channel beams are typically 912 mm wide and 407 mm (1'-4") deep, therefore ten channel beams are usually used to construct a two-lane bridge with a pedestrian side-walk [188]. Please see Appendix I for geometric and reinforcement details of a typical 22' and 28' PCCBs, according to BC Ministry of Transportation (MoT) standards (year of drawing is 1956), and a 20' Type G stringer from MoT of Alberta MoT (year 1957). In U.S., some states used a wider type of channel beam (1105 mm) so that only seven girders were needed for a two-lane roadway [195].

### **3.1.1 Major Problems**

Concerns on PCCB bridges started in the late 90s, as many of them showed signs of serious deterioration [105]. The most common form of deterioration exhibited on PCCB bridges are spalling of the concrete cover and corrosion of the primary flexure reinforcements and stirrups on the bottom side of the two "legs" [105,191]. The spall of concrete cover was initiated by the corrosion of the steel reinforcement, which was mainly caused by insufficient cover thickness; concrete cover in old

bridges are usually insufficient when compared to current standard [83]. Minimum concrete cover required by older AASHTO code during the 50s was one inch, whereas today's standard requires a minimum of two inch [196]. After the spall of concrete cover, corrosion process in steel rebar further speed up, and eventually lead to lose of section.

An additional source of concern about PCCB is its inadequate shear capacity. As can be observed from the technical drawings in Appendix I, PCCB built before the 70s has minimum shear reinforcement. Some PCCB used in U.S. were even fabricated with no shear reinforcement at all [191]. Shear failure of RC beams is catastrophic and does not give enough warning ahead; therefore, PCCBs without sufficient shear capacity need to be reinforced immediately.

Besides the two major problems mentioned above, some PCCBs also showed signs of concrete degradation and lose of sections [186]. For PCCB bridges, inspectors should pay attention especially to the following area/signs [83]:

- Shear cracks near the support
- Flexure cracks at the tension zone (for both the "legs" and the deck area)
- Bearing – if spalling or crushed concrete on sight
- Leakage at the seam between the adjacent beams – could be indicator of a broken shear key
- Area exposed to drainage – e.g. at the ends of the beams and around the scuppers
- Tie rods or strands – check for tightness and corrosion

Cracks with efflorescence or rust stains are indicators of insufficient reinforcement cover and corrosion of reinforcing steel. If signs of leakage do present between beams, live load testing should be performed, and inspectors should observe if differential beam deflections happen. When two adjacent beams deflect differently under same loading condition, it is highly possible that the shear key connecting the two beams is broken [83]. As for area exposed to drainage, that is the place most likely to have concrete contamination and/or concrete spall to occur [83].

Due to the severe signs of deterioration, many PCCB bridges are rated as deficient bridges and need to be load posted in order to remain open [105,193]. While the traffic volume for most PCCB bridges is relatively small, many of them are used by heavy vehicles such as logging trucks. These heavy vehicles may need to use longer haul routes to avoid a posted bridge, result in waste in time and money. Therefore, many field and laboratory tests were carried out to verify the effects of the

deteriorations to the safety and performance of PCCB bridges [105,186,192,197,198]. Fortunately, for most of the tested PCCB or PCCB bridges, the measured strains and deflections were well within acceptable level. However, for PCCB loaded to failure, the dominant failure mode was indeed the catastrophic shear failure [187]. The findings can be explained by the “catenary effect” and “tied arch action” of RC beams (see Figure 3-1) [83].

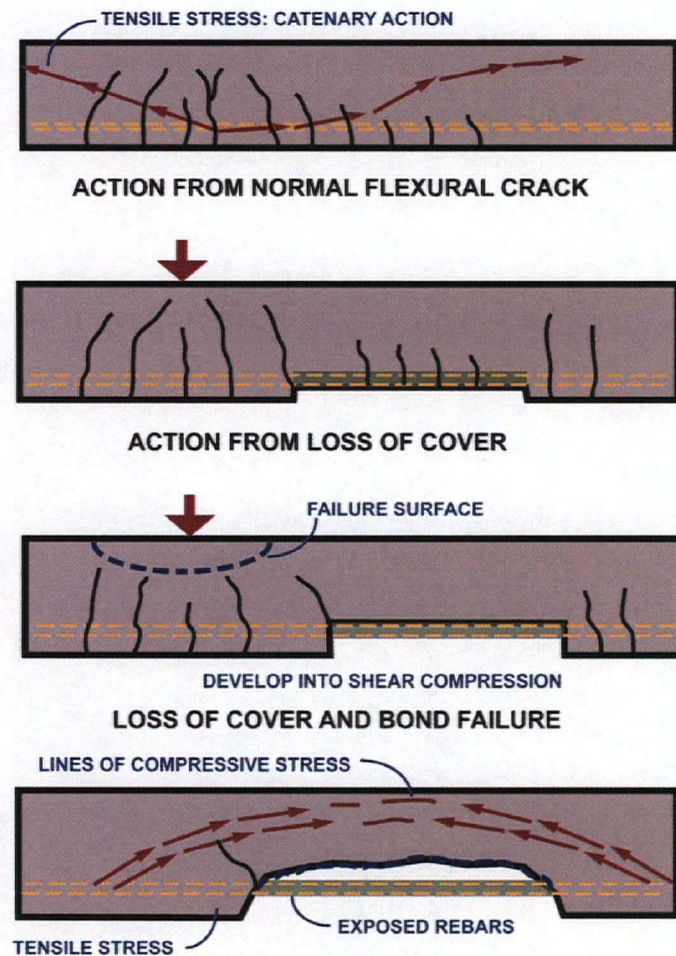


Figure 3-1 Behavior of a Cracked Beam  
Source: [83]

For cracked RC beams, loss of concrete cover does not necessarily mean loss of the flexural strength, as long as the bond between the steel rebar and concrete still work on the other side. When debonding between steel rebar and concrete happens, redistribution of stresses will not be able to occur, and tensile stress will increase in the bond loss region. Stress concentration at the inner re-entrant corner of the rebar exposure area accumulates and eventually leads to large spall of concrete and loss



of concrete on both sides of the tension reinforcement, and this is when the strength of the beam is reduced (due to lost of composite action). The large spalls at the bottom of the beam result in catenary effects (i.e. hanging wires between two supports), which make the spalled concrete beam act like a tied arch, as shown in Figure 3-1. As a result, the end of the anchorage of the beam actually reduces the cracks in the beam and carrying loads for which the beam was originally designed. However, the failure mode will be the sudden shear compression failure in concrete [83]. According to studies from University of Alberta, 3 to 5 mm wide diagonal shear cracks can be observed right before failure [199]. If there were cross section loss of stirrups at bends (due to corrosion), the crack widths could be reduced quite substantially and not much sign given before the sudden failure [199].

Even though flexural strength is within safety level, shear deficiency is indeed a problem and the catastrophic shear failure is not allowed [105]. With the significant amount of deteriorating PCCB bridges existing today, it is not possible to replace all of them; therefore, there has been emphasis on seeking effective retrofit methods to deal with this problem [188].

### **3.1.2 Potential Retrofit Method - FRP**

An effective strengthening technique for concrete bridges is involved with the use of fiber-reinforced polymer (FRP) [47]. Strengthening of concrete members with externally bonded FRP sheets/plates has been developed well over the past fifteen years; it is commercially available today and can be implemented easily in the field [71]. The drivers for this technology are several, the major ones perhaps are the installation flexibility and significant improvement in mechanical properties [200]. FRP strengthening system is an ideal solution for the PCCB bridge problem, because it not only improves the beam performance in terms of shear and flexure, the FRP layer also acts as protector for the bottom reinforcing steel, which solves the problem with insufficient concrete cover. Literature research on FRP and its strengthening techniques are not within the scope of this thesis and will not be covered. A significant number of studies have been done on FRP reinforced concrete bridges, [193,201,202,203,204] are some examples; interested readers can find related studies easily.

Major issues with FRP products are their higher cost and concerns with delamination [197]. FRP material is more expensive when compared to their steel plate counterpart. However, the higher cost of FRP can be compensated by savings in labors because the light weight of FRP makes installation process much faster and easier than steel jacketing [205]. Delamination is indeed a problem with

FRP plates/laminates due to their low peel resistance [205]. Catastrophic debonding of FRP can be minimized with careful surface preparation; however, when applied area is large, significant surface preparation work will be a time consuming process and add up labors and costs. In addition, because FRP laminates carry fibres all in one direction, they are very strong in the direction of the fibre alignment but significantly weaker in the perpendicular direction, and they give high brittleness and poor fracture toughness [205]. In view of these, Dr. N. Banthia in University of British Columbia, Canada, took a further step in the FRP technology and developed the novel reinforcing technique – sprayed FRP coating.

The innovation of *sprayed FRP* was inspired from shotcreting, the process of projecting concrete or mortar at high speed pneumatically onto a surface [206]. As mentioned in section 1.3, sprayed FRP consists of the use of a spray gun to shoot polymer and glass fibres concurrently. Resin/catalyst mixture from the lower nozzle of the spray gun and chopped fibers from the top-mounted chopper unit are sprayed at high speed simultaneously to the repaired surface (Figure 3-2) [207]. The two streams combine and form a two dimensional random distribution layer of fibres encapsulated by a fully catalyzed resin. This process allows the operator to build up the FRP reinforcing layer to whatever thickness is preferred. The length of the fibre is also adjustable from 8 to 60 mm [205]. After spraying, a ribbed aluminum roller is used to force out any entrapped air voids and to work the material into a consistent thickness.

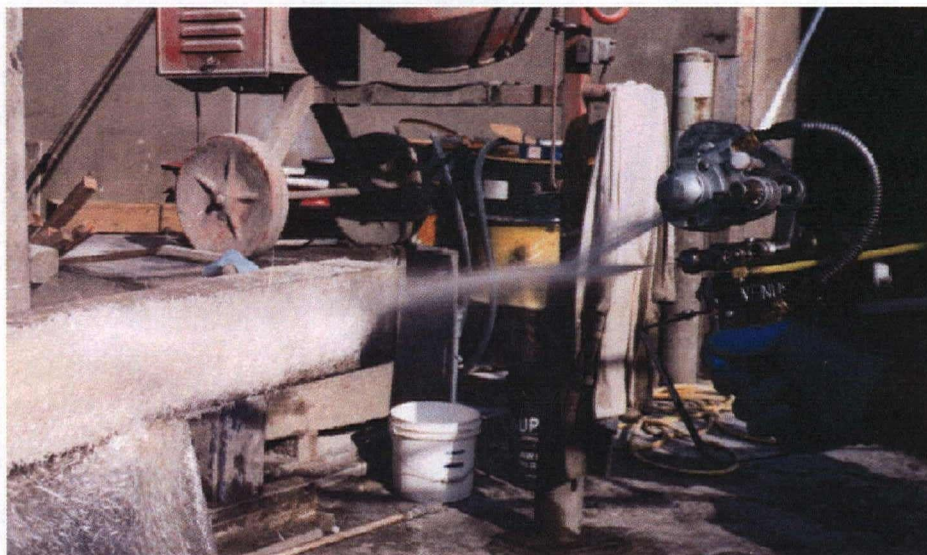


Figure 3-2 The Spray Equipment and Process of *Sprayed FRP*  
Source: [205]

Since the copped fibres are randomly distributed on the applied surface, the Sprayed FRP layer is two-dimensionally isotropic with identical mechanical properties in any direction in the plane of placement. Even though the ultimate strength is lower than the traditional unidirectional continuous FRP laminates in their fibre alignment direction, sprayed FRP is less brittle and gives higher fracture toughness [205]. One does not need to worry about the direction for application, and the sprayed FRP requires much less surface preparation when compared to the traditional FRP laminates. Therefore, with compatible reinforcing results, sprayed FRP can save significantly in terms of labor and application time. The advantages of sprayed FRP make it an ideal candidate for reinforcing the old PCCB bridges, because the deteriorating PCCB bridges do not need significant increase in flexure strength. Sprayed FRP can provide enough shear reinforcement and act as rebar protectors; at the same time, installation time and cost required surpass the traditional FRP plate/laminate techniques. Therefore, it is worthwhile to investigate further the field performance of this potential repair technique.

Sprayed FRP itself is not the focus of this thesis, so only a brief introduction is provided here. Nonetheless, the material and its application technique are important parts of the Safe Bridge project, and readers are encouraged to explore more about them. More information can be found in the references used in this section, and the thesis work "*Rehabilitation of Reinforced Concrete Beams with Sprayed Glass Fiber Reinforced Polymers*" by Andrew J. Boyd, which compared the new sprayed GFRP and the commercially available continuous fiber wrap system [197]. According to this study, both materials improved structural performance of the tested beams, but the sprayed GFRP out-perform the traditional FRP wrap in all the following categories: ultimate load carrying ability, energy absorption, and strain-hardening ability. Some recent studies and testing further demonstrate the outstanding performance of sprayed GFRP for aggressive environmental protection and for seismic, blast, and impact strengthening [205,208,209].

Next section will give specific information about Safe Bridge, the first bridge in the world retrofitted by the innovative sprayed GFRP repair method.

### **3.2 Safe Bridge**

Constructed in 1955, Safe Bridge is one of the seventeen PCCB bridges still remain in use in Vancouver Island, B.C., Canada today (see list in Appendix II) [210]. Since the late 90s, serious



deteriorations were found in many of the PCCB bridges during their routine field inspection; apparently, all these degrading PCCB bridges need to be repaired or replaced sooner or later. With limited financial resources, repair is the much preferred option for deteriorating bridges, and therefore the BC Ministry of Transportation was very interested in the innovative sprayed FRP repair technique. Safe Bridge, being one of the shortest PCCB bridge and in serious deteriorating condition, was chosen to be the testing site for the new repair method.

### 3.2.1 Bridge Description

Safe Bridge locates around the Cowichan Lake area in Youbou, a town near Duncan, B.C., Canada. The bridge spans over a small creek that flows into Cowichan Lake and contains two-lane traffic with a pedestrian sidewalk (Figure 3-3). The clearance under the bridge is about 1.2 m at the upstream end and 2.1 m at the downstream end [76].



Figure 3-3 Photos of Safe Bridge: (a) Side View; (b) Road View

The single-span bridge does not serve a significant amount of traffic volume, but because it is on a logging route, Safe Bridge has to carry heavy logging trucks like the ones shown in Figure 3-4. Therefore Safe Bridge needs to have a sound structural integrity for the extreme high load, and failure of Safe Bridge could affect local logging industry adversely.





Figure 3-4 Photos of Logging Trucks passing through Safe Bridge

Safe Bridge consists of ten precast concrete channel beams. Each of the PCCB is 26 feet long ( $\sim 7.9$  m) and approximately 3 feet wide ( $\sim 0.91$  m). Span length is 8.2 m on road surface and 7.6 meter from face to face of abutment (Figure 3-5 Plan View; roadway crown not shown). Total width of Safe Bridge is about 9.1 m, including a 1.5 m wide pedestrian sidewalk and two-lane traffic roadway. 10 inch wide concrete curbs are used to separate the roadway and the pedestrian sidewalk and on the two side of the bridge. According to the BC MoT standard drawing from the 60s (Appendix II), the exterior girders (Girder 1 and 10 shown in Figure 3-5 Section) should have a different cross section configuration than the regular “ $\pi$ ” shape; the concrete curb is precast together with the channel beam (Figure 3-5). In Figure 3-5, the ten channel beams are shown in red dashed lines; approximately two girders are used for the sidewalk and four girders are used for each of the traffic lane.



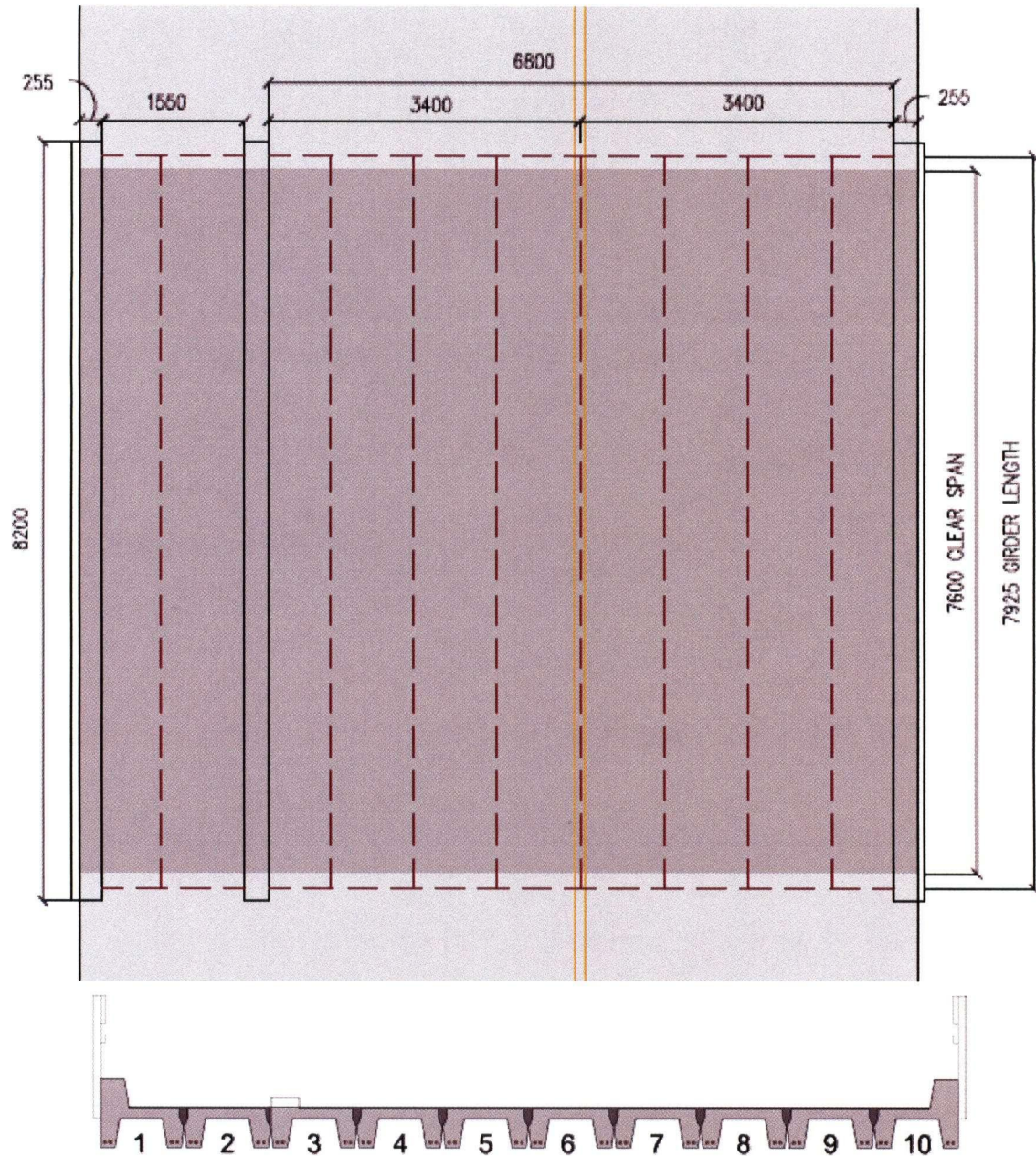


Figure 3-5 Plan and Section of Safe Bridge

The PCCBs were cast from normal concrete with lightweight aggregates; compressive strength is about 35 MPa, and density is approximately  $18.8 \text{ kN/m}^3$  [188,207]. For steel reinforcements, the major flexure reinforcement is #9 rebar (imperial size; about 25 mm diameter) and all other reinforcements are #3 rebar (10 mm; see Figure 3-7); tensile strengths of the steel rebar range from 304-408 MPa [188].



The longitudinal reinforcement ratio is only about 1.3% for Safe Bridge, whereas current standard requires a minimum of 3% [188,211]. The #10 longitudinal rebar used in Safe Bridge have an unusual square cross section, and there are small bumps on the surface of the rebar at approximately 50.8mm spacing to increase the interlocking effect with concrete [78]. The channel beams are joined together by a shear key within the top 178 mm of the beams (see Figure 3-6 and Figure 3-7), and the channel sections are covered with a layer of asphalt to create the road surface [79].

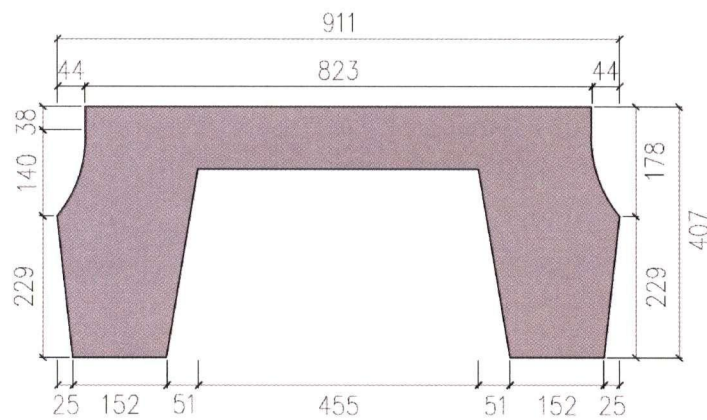


Figure 3-6 Detailed Dimension of Channel Beam Cross Section

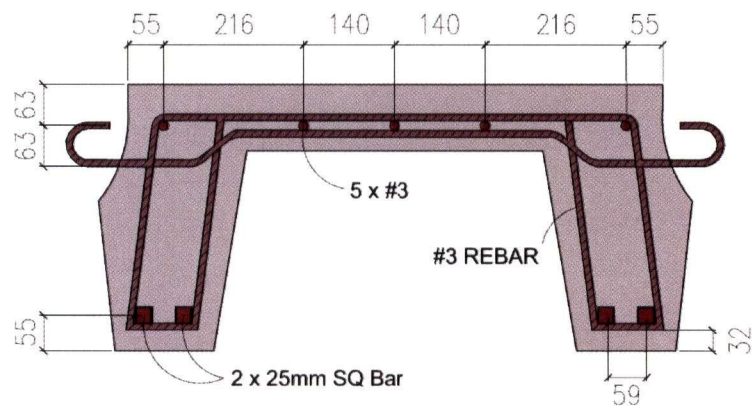


Figure 3-7 Reinforcement Details and Dimensions of Channel Beam Cross Section

For shear reinforcement, according to the field inspection record, the stirrup spacing varies from a minimum of 270 mm at the ends of the beam to a maximum of 1505 mm in the center portion of the beam, see Figure 3-8 [212]. When compared to today's standards, the shear reinforcement is insufficient [213].

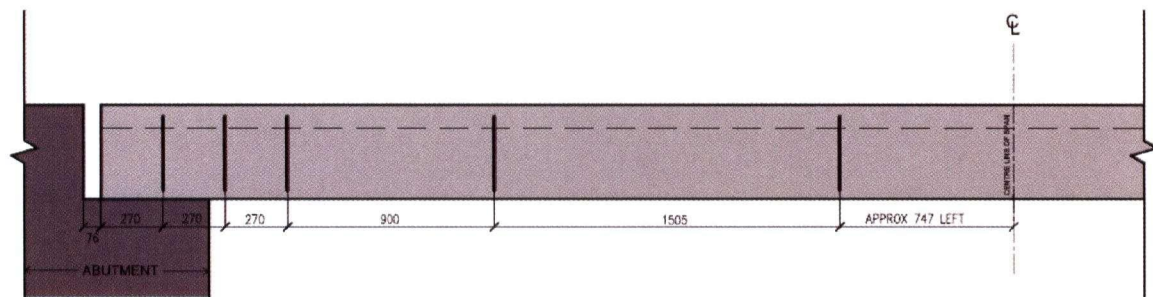


Figure 3-8 Stirrup Spacing of Safe Bridge's Channel Beam Girders

### 3.2.2 Bridge Problems

The last visual inspection performed on Safe Bridge before the repair was done on the summer of 2001; a copy of the Condition Inspection Report dated July 30<sup>th</sup> 2001 is attached in Appendix III as reference (with another Condition Report dated May 26, 2005, three and a half years after the repair) [214]. Detailed visual inspection and geometric measurements were performed, and significant signs of deterioration were observed mainly on the bottom side of Safe Bridge. According to Mike Penner's notes, no significant deflection was observed on Safe Bridge when it is under heavy load. However, *"concrete cover over stirrups was minimal on the inside face of the channel beam and the base of each leg; spalling was frequent at these locations. Conversely, concrete cover was 25 mm or more on the outside face of each leg and not a single area of spalling was observed. Based on the observation, it appears that the deterioration of these stringers is a direct result of the lack of cover to stirrups at the locations mentioned [214] (see Figure 3-9)."* According to Mike Penner's field note, concrete cover on inside of the channel and leg bases are from no cover at all (reinforcement exposed) to the most of only 10 mm. Today, concrete cover for bridges usually require for a minimum of 2 inch (~50mm). Fortunately, no section loss was noted on the exposed square rebar, and no corrosion or cracking on outside legs of the channel girders.

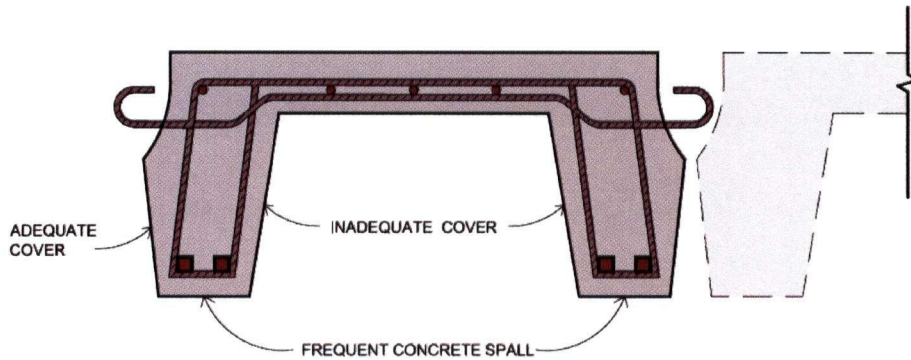


Figure 3-9 Locations of Inadequate Cover

The threshold for initiation of corrosion is when chloride ion concentration exceeds 1.2 lb/cy or 0.2% cement weight [83]. Main sources of chloride ion are deicing salts and marine environment. Contributing factors to corrosion include: shallow cover, high permeability caused by high water cement ratio, insufficient consolidation and insufficient curing, and surface cracks which allow water to reach the steel surface. As steel corrodes, it expands about 7 to 10 times of original volume and causes tremendous expansion force which results in concrete above steel to crack. As corrosion continues, spalling eventually occurs [83]. Therefore corrosion problems of bridges are very common in Canada, since de-icing salts are used tremendously and constantly in most part of the country.

Before the repair, several photos were taken under Safe Bridge, and Mike Penner's observations can be clearly seen from the photos (see Figure 3-10). From photo (a), one of the girders had the bottom side of its mid-span severely spalled, and both of the shear stirrups and the square flexural rebar were exposed in air. Photo (b) is the example of inadequate cover on the inside face of the channel beam and the corner of the leg. The bumps on the surface of the square rebar and the rust stain on concrete can be clearly seen in this photo; and again, stirrups are spaced far apart. Photo (c) was taken at the support area of the abutment; concrete was severely spalled and both stirrup and longitudinal reinforcements were exposed. Shear spacing at the support is much closer compared to the middle section, but 270 mm is still much wider than current practice. Overall, there were four channel legs with severe spalling over a length of approximately two meters [215].



Clearly Safe Bridge was in serious deteriorating condition, and shear deficiency needed immediate repair. Therefore, Safe Bridge became the ideal testing bed for the study of SHM process and the *sprayed FRP* technique.

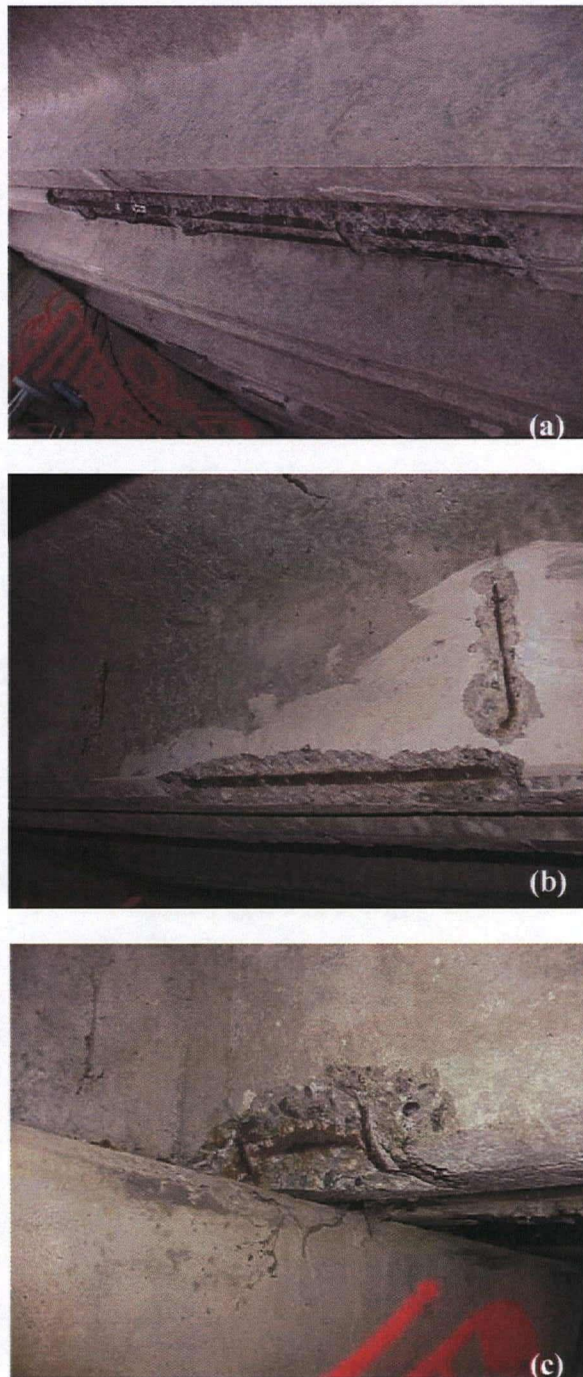


Figure 3-10 Photos of Safe Bridge Showing Deteriorating Conditions (Sept. 2001)

Before applying the sprayed GFRP, the girders needed to be reformed first, especially for area with severe spalling and cracking (see Figure 3-11); a high-performance fiber reinforced cementitious matrix were used, which mixed with both carbon and polypropylene fibers. More about the thin repair and reform of the girder can be found in [79].



Figure 3-11 Applying Mortar to Cover the Steel Rebar

The areas of the girder where the GFRP reinforcement were applied is shown in Figure 3-12. Note that the *spray*- technique was applied on only the two girders under the pedestrian walk; the rest of the girders were reinforced with GFRP wrap. The material properties for both are exactly the same, only the applying technique is different. Some photos related to the GFRP spray and the GFRP wrap are shown in Figure 3-13 and Figure 3-14.

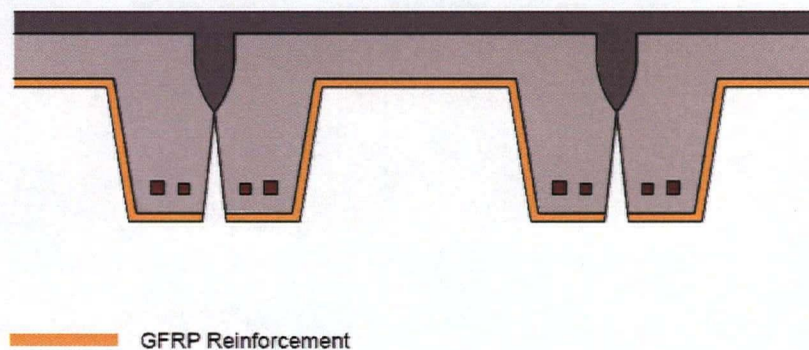


Figure 3-12 Locations of the GFRP Reinforcement



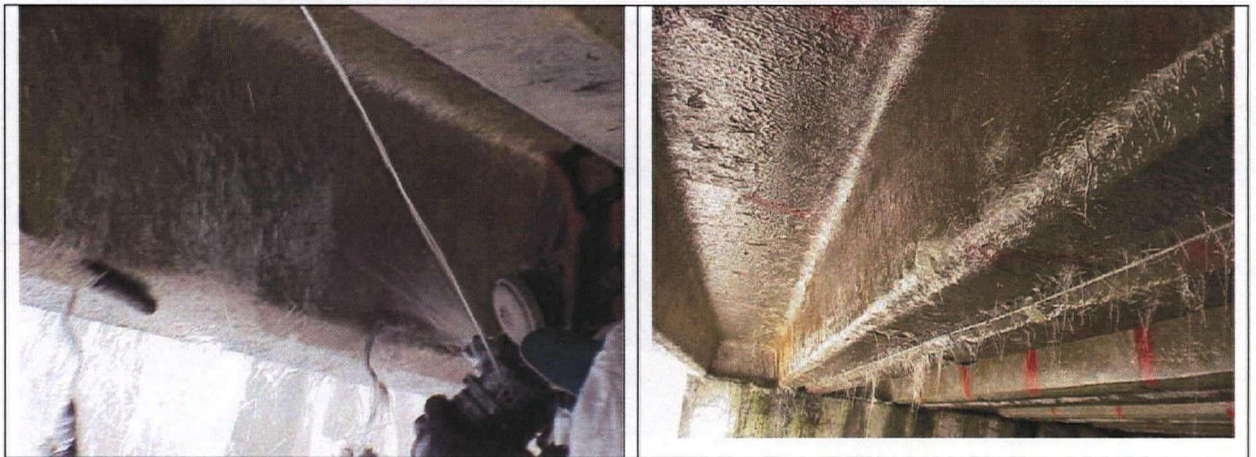


Figure 3-13 Sprayed GFRP Reinforcement: [a] GFRP Spry in Process; [b] the Finished Surfaces

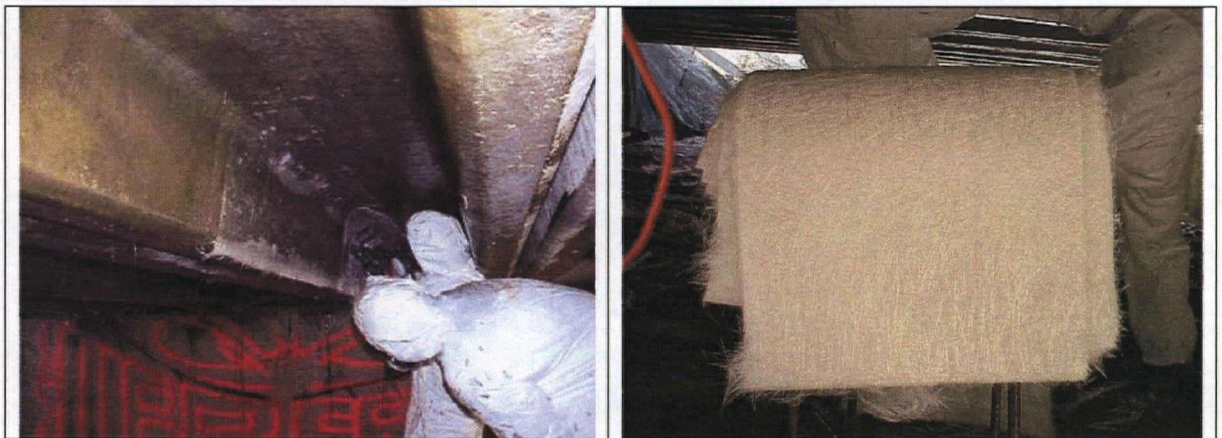


Figure 3-14 GFRP Wrap Reinforcement: [a] Wrap GFRP in Process; [b] the GFRP sheets



---

## Chapter 4

### First Field Testing (2003)

---

The first field testing covered in this thesis was performed on October 15, 2003, twenty months after the 2002 testing; this testing is hereby referred to as “*Strain\_Reading 2003*”, and the two previous testing are referred to as “*Before\_Repair 2001*” and “*After\_Repair 2002*”. The two objectives for the 2003 field testing were:

1. Perform *Static Load* and *Rolling Load* tests in a similar manner as the previous two field tests and by comparing the testing results to evaluate *Sprayed FRP*’s field performance.
2. Test out a new type of data acquisition (DAQ) system for the study of the SHM process; the new DAQ system has an IP built-in and a software program that allow users to monitor and gather data through internet access.

Testing procedures and loading conditions were kept the same as the 2001 and 2002 testing except that LVDTs were not used this time. The major reason was that set-up for LVDT is cumbersome, time-consuming, and not necessary. Since Safe Bridge spans over a creek, water surface needed to be covered and wood frame supports needed to be constructed (Figure 4-1).

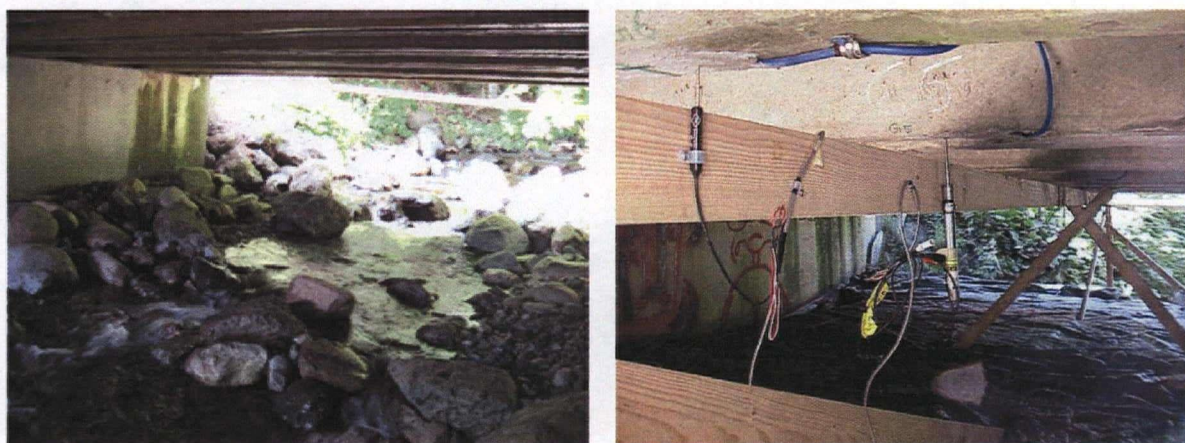


Figure 4-1 Photos Under Safe Bridge and the LVDT Set-Up for Before\_Repair\_2001

With the two objectives for this time's testing, strain measurements would be sufficient to check the field performance of sprayed FRP; data of mid-span deflections do not give much addition information. After considering the gains and loss, it was decided not to use LVDTs this time. In addition, from SHM point of view, LVDT is not an ideal sensor type for long term monitoring, especially when the bridge spans over waterway. Performing the testing without LVDTs would not affect the study of SHM process.

This chapter will provide information about the strain gauge locations, and the loading truck and loading positions used for *Strain\_Reading 2003*, as well as the data processing procedures and testing results. The data gathered from both DAQ systems (the traditional one and the advanced IP built-in one) will be compared to verify the suitability of the new DAQ system for remote control purpose. Specific information about the strain gauges and the two DAQ systems will be given in Chapter 6, when discussing Safe Bridge project from SHM point of view.

#### 4.1 Sensor Locations

During the 2003 field testing, data were collected using the strain gauges only. These strain gauges were installed on the major reinforcements in certain girders of Safe Bridge, and they measure point strains. Since they are only sensitive to localized changes, to place them at the "right" locations become extremely important. As mentioned in Chapter 2, usually the "right locations" are places where maximum strains occur. For example, for a simply supported, single-span beam, the maximum possible bending moment under the worst loading condition will occur at mid-span. For Safe Bridge, six strain gauges were used, and they were attached on the mid-span of the flexure rebar in the "leg" of the channel-beam. More discussion on the number of sensors to use and the locations of the strain gauges will be given later in Chapter 6. This section will simply give the locations of the strain gauges. The exact locations of the six strain gauges on Safe Bridge are shown in figure below. For the ease of discussion, the girders are numbered from 1 to 10, and the strain gauges are numbered from 1 to 6, as shown in Figure 4-2.

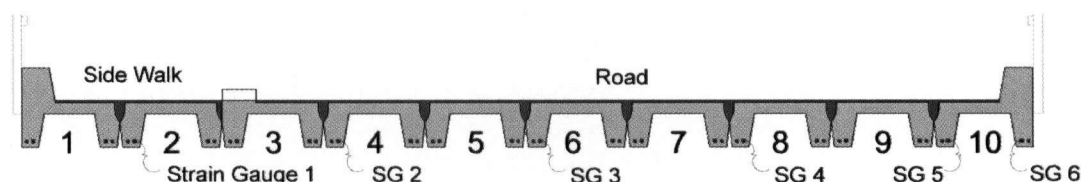


Figure 4-2 Stain Gauge Locations on Safe Bridge



## 4.2 Truck Information

The testing vehicle used for Safe Bridge is the standard 28-tons fully-loaded dump truck (see photo in Figure 4-3 [a]), the Level 3 CL3-W Truck according to the Canadian Highway Bridge Design Code and BC Ministry of Transportation [213]; it is similar to the Type 3 Unit used in U.S. shown in Figure 2-8. The loading truck is weighted first in scale station before the field testing, so that the exact axle loads and total weight of the vehicle is available. The exact load distribution of the front and rear axle is an important piece information if certain analysis, such as a detailed stress check, is required later. For a standard 28 ton dump truck commonly used in BC, Canada, approximately 1/3 of the weight goes to the front axle and 2/3 of the weight goes to the double rear axles.

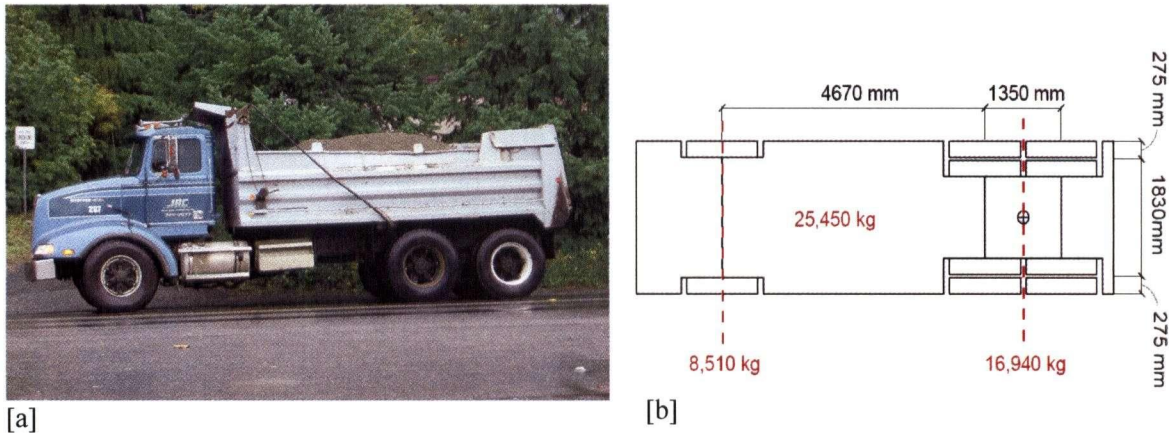


Figure 4-3 Testing Truck for *Strain\_Reading 2003*: [a] Photo; [b] Truck Dimensions

Detailed dimensions and axle loads of the testing truck for *Strain\_Reading 2003* is given in Figure 4-3 [b]. For structural analysis modeling, this truck load can be represented by three concentrated loads (point loads) with 4.67 meters between the front and first-rear axle, and the two rear axles 1.35 meters apart. The total distance of the three axles is about 6 m, which covers pretty much the total 7.6 meters span of Safe Bridge, and therefore there is not point to use a larger (longer) testing truck. The wheel distance on the transverse direction of the rear axles is measured from the center of the tandem-axles, and it is about 1.8 meters. This distance is important when one needs to analyze the load distribution between girders transversely. The exact total weight of the 2003 testing truck was 25,450 kg (~28.1 ton or 250 kN) with the front axle weighted around 8,510 kg and the total rear axles weighted around 16,940 kg.

### 4.3 Loading Types and Positions

Two types of load testing were performed, the *Static Load Testing* and the *Rolling Load Testing*. The *Static Load Testing* involved with placing the truck as a stationary load at strategic locations on the bridge and collect the strain readings induced by that loading position. Based on the classification of the type of static field testing given in Ch 2, the one performed on Safe Bridge was more like the "Diagnostic Test", because the Safe Bridge field test was performed to see if delaminations occurs between the concrete and the reinforcing GFRP layer, which matches the definition for Diagnostic Test - "diagnose the effects of component interaction."

As for the *Rolling Load* test, the truck was moving at a speed less than 10 km/hr crossing the bridge; strain readings were collected starting before the truck entered the bridge and stopped after the truck completely left the bridge. Even though the truck was not stationary, the testing was not considered as a dynamic field testing, because the truck was still moving at a relatively slow speed, and not much dynamic effects were induced. The *Rolling Load* testing is considered as a quasi-static load testing. Nonetheless, for the rolling load testing, a higher sampling rate was used to obtain the strain response to time more accurately. The following section will give the loading positions used for both the *static* and *rolling load* tests during the 2003 field testing and the reasons behind them.

#### 4.3.1 Static Load Positions

As mentioned earlier, Safe Bridge is single-span and simply supported, and the loading truck can be seen as three point loads with the rear two closely spaced. Therefore, across the span, the maximum moment will occur when one of the rear axle loads is placed at mid-span. Accordingly, it was decided to have two loading positions on the longitudinal direction: have the rear two axles placed successively at the mid-span (see Figure 4-4).

In the transverse direction, three positions are possible to create worst loading conditions over the girders: the center, and the two extreme eccentric sides. Therefore, it was decided to take three transverse positions: the center, and two mirror images of eccentric positions on the two sides of the road. For the two eccentric positions, the truck driver was told to drive the truck as close to the concrete curb as possible. With two longitudinal positions and three transverse positions, there were total six loading positions for the static load test (Figure 4-4). The six-static-load-positions were used for all three field testing conducted on Safe Bridge in 2001, 2002, and 2003.

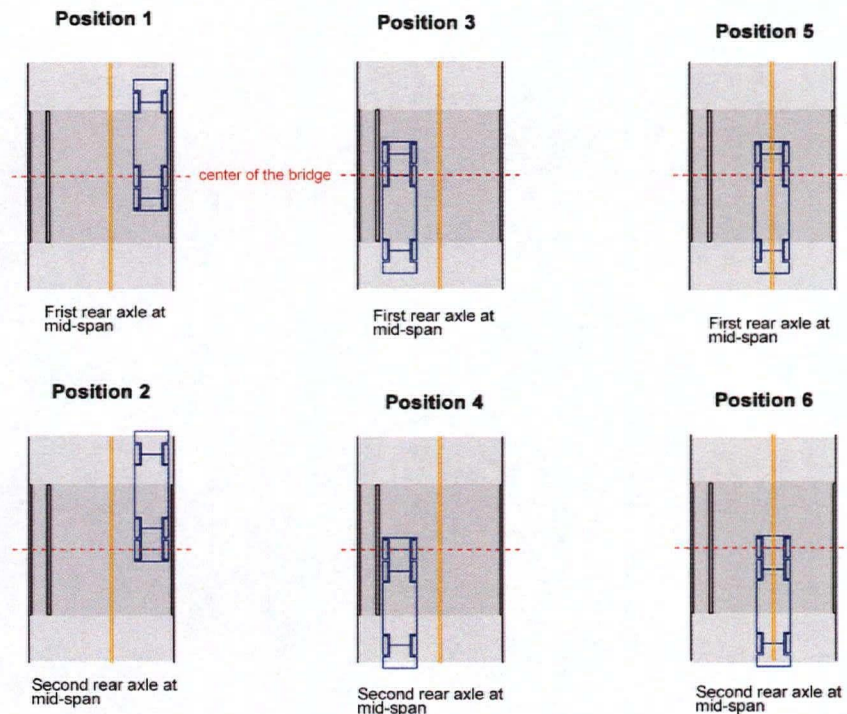


Figure 4-4 Six Loading Positions for the Static Load Testing

The truck was moving in extremely low speed ( $< 1$  km/hr) during the static load testing to minimize the dynamic effects on the strain readings. Center line of the span was drawn by red chalk to make sure the truck would stop at the “right” positions. The truck braked for at least 40 seconds when it was on the desired loading positions, to make sure the time was long enough to obtain true static readings. The sampling rate used was 10 Hz (10 readings per second) for both DAQ systems.

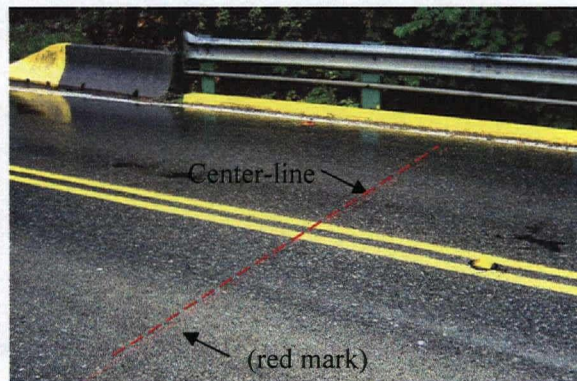


Figure 4-5 Photo of Safe Bridge with Red Mark at Center-line: 2003 Field Test



When corresponding the truck load position to the girders, the truck is right above girder 8 to 10 for Position 1 & 2 (the “extreme right”), above girder 3 to 5 for Position 3 & 4 (the “extreme left”), and above girder 6 and 7 for Position 5 & 6, as shown in Figure 4-6. Therefore, if all girders and their connecting conditions are “equally healthy”, Strain Gauge#5 is most likely to give the largest strain reading under Position 1 & 2; Strain Gauge#2 to give the largest strains for Position 3 & 4; and Strain Gauge#3 to experienced the highest strain for Position 5 & 6. Since Girder 1 & 2 are used as side walk, strain readings from Strain Gauge#1 is expected to be relatively small most of the time.

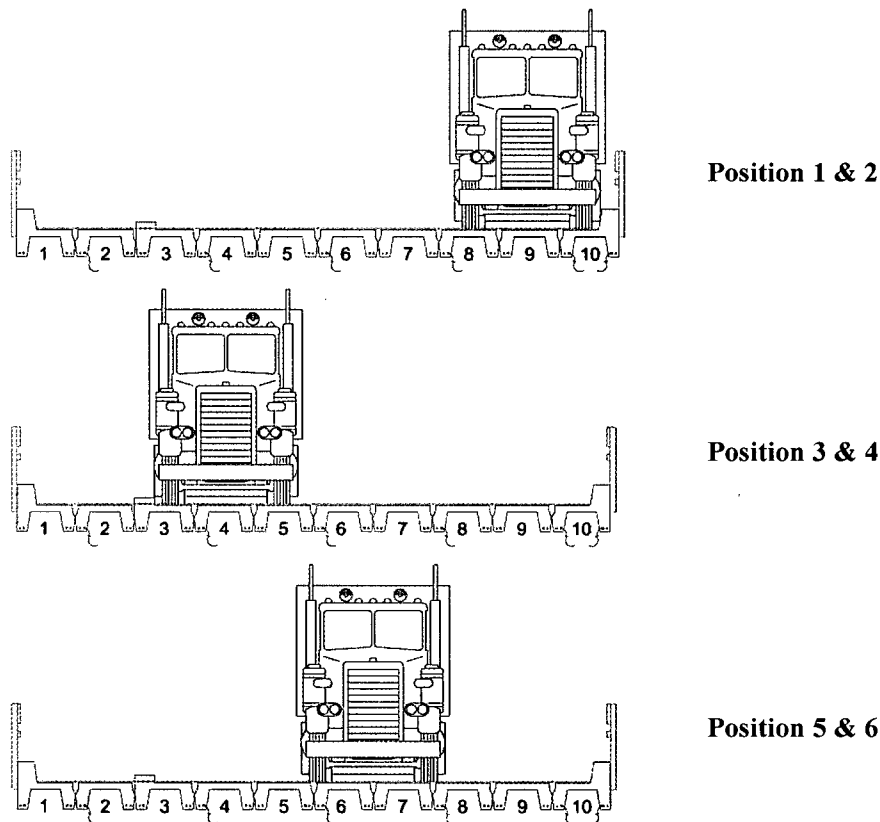


Figure 4-6 Transverse Truck Positions for Static Loading Test

#### 4.3.2 Rolling Load Positions

The purpose of the *Rolling Load* test was to observe the bridge girder response to moving loads. Nonetheless, the traditional strain gauge and DAQ system do have limitations in high frequency readings; also, since the purpose of this time’s testing was not to obtain dynamic characteristics of the bridge, it was decided to perform quasi-static load testing instead of true dynamic load testing.

Because the truck was not stationary, the sampling rate needed to be increased to catch the bridge response more accurately. Therefore, the sampling rate was increased from 10 Hz to 60 Hz (60 readings/sec) for the *Rolling Load* tests. Regarding the loading positions, again, all possible worst case conditions should be considered. Similar to the *static load testing*, the *rolling load testing* adopted the three transverse loading positions: extreme right (“Roll 1”), extreme left (“Roll 2”), and center (“Roll 3”) (see Figure 4-7).

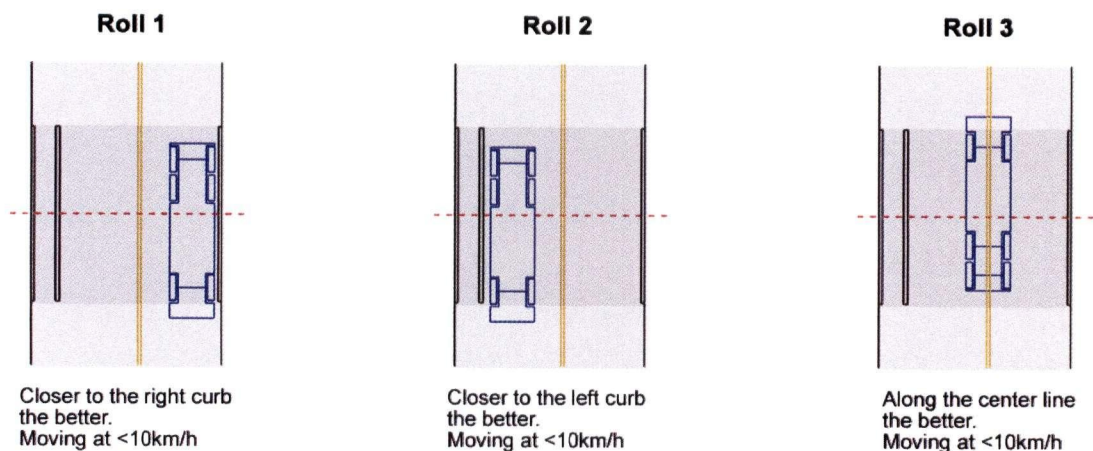


Figure 4-7 The Three Loading Positions for the Rolling Load Tests

#### 4.4 Data Processing and Testing Results

The testing results provided in this section are based on the data gathered from the “traditional DAQ system”, called *I/O Tech DaqBook*, which is similar to the system used during the previous two load testing, *Before\_Repair 2001* and *After\_Repair 2002*. These results will be compared with the 2001 and 2002 testing results in Section 4.5. As for the new DAQ system *WebDAQ/100*, it was the first time for the team to use it for bridge field testing, and the purpose for using *WebDAQ/100* was to test out its on-line and remote control functions, at the same time gaining experiences with the new equipment. Therefore, the results from *WebDAQ/100* will be compared with the results from *I/O Tech DaqBook* during this time’s testing for verification, but will not be used to compare with the previous two field tests. *WebDAQ/100* results and comparisons will be given in section 4.6.

#### 4.4.1 For Static Load Testing

This section presents the procedures taken to obtain the maximum strain values for the six strain gauges under the six static load positions. The data from load position 2 will be used as example to demonstrate the data processing steps. Since the DAQ system actually records voltage from the strain gauges, the first step was to convert the raw data from  $\mu\text{V}$  ( $10^{-6}$  Volt) to  $\mu\epsilon$  (microstrain). The conversion is done by multiplying the raw data to the Gauge Factor (in  $\mu\epsilon/\text{V}$ ), which is a specific value depends on the strain gauge used. After the conversion, the data for load position 2 was plotted directly and shown in Figure 4-8.

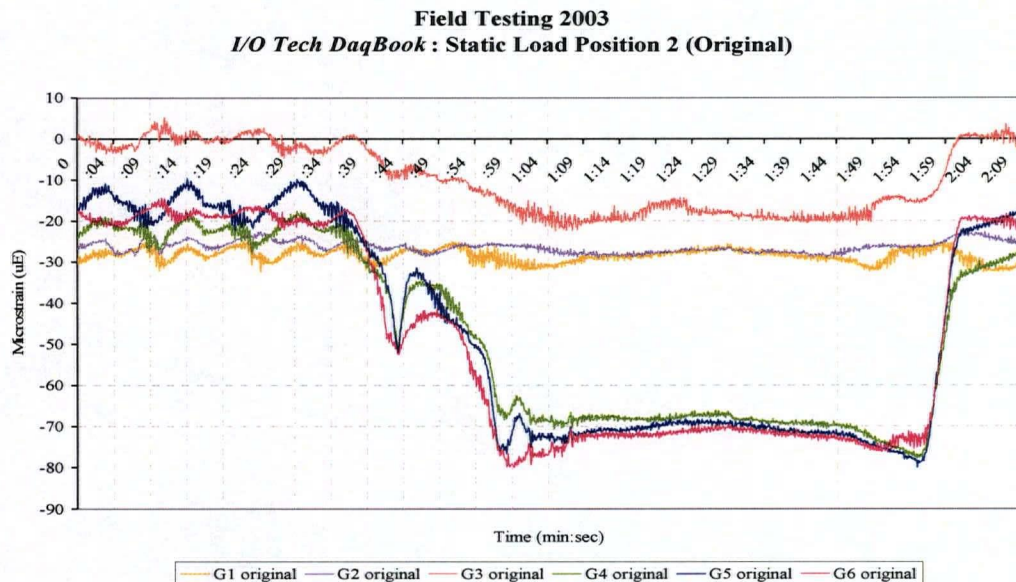


Figure 4-8 Strain-Time History of 2003 Static Load Testing Under Load Position 2 – Original

As can be seen from Figure 4-8, the reference point for each strain gauge was different, and they were not “zeroed”; therefore, the next step is to perform base line correction. This is done by subtracting all data to an “initial value”, which represents the condition when there is no load on the bridge. Since the readings flocculated, the initial value can not be simply taken as the very first reading. Therefore an average value is used. The initial value was obtained by averaging 5 seconds of data (50 readings) from the period around 10 seconds before the truck entering the bridge. In the case of Static Load Position 2, the initial value was taken by averaging the data from time :19 to :24 sec.



The next step is to determine the strain value that represents the mid-span strain induced by the static truck load. Again, use Static Load Position 2 as an example. From observing the plot (see Figure 4-9), one can tell that the truck entered the bridge at time around :36 sec on plot, and *Peak 1* was induced when the front axle crossing the mid-span line; *Peak 2* was induced when the second rear axle just arrived at the mid-span mark and the truck braked. The truck braked for almost a minute; and at time 1:55, one can observe the third peak, which should be the time when the truck started to move again. After time 2:05, the truck left the bridge completely and the strain readings were back to initial values.

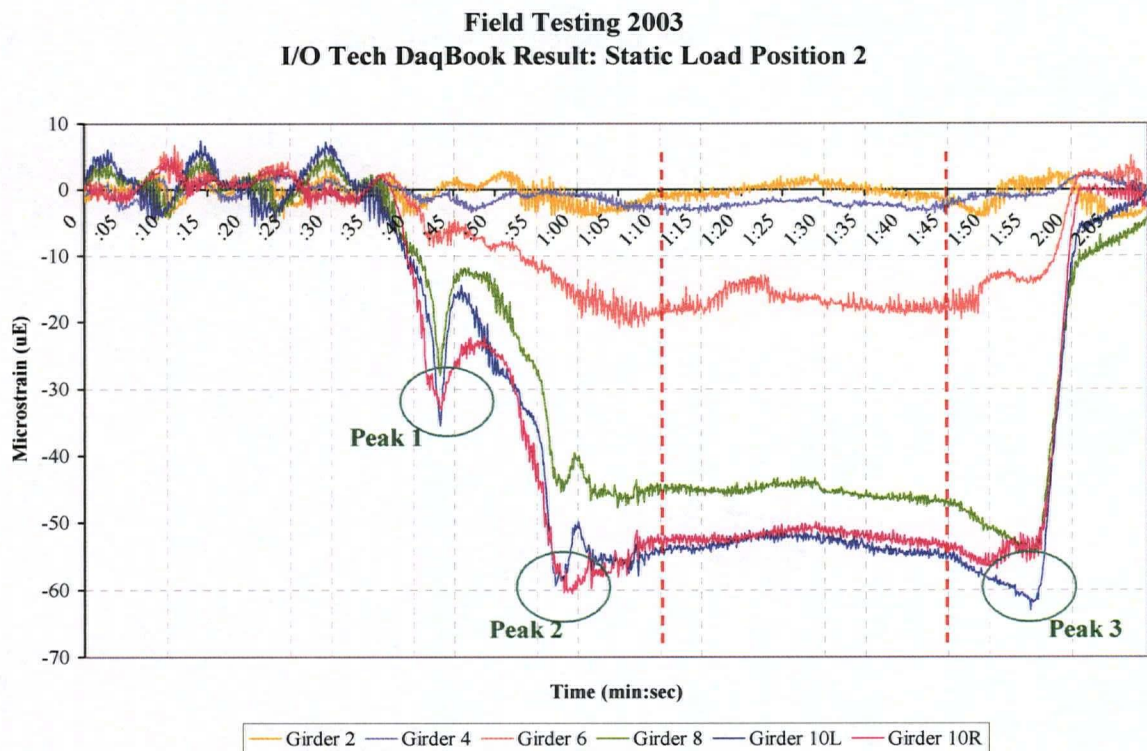


Figure 4-9 Time-Strain History of 2003 Static Load Testing Under Position 2 – After Zeroing

Theoretically, the strain reading should be a constant value during the period when the truck was stopped at Load Position 2 (between *Peak 2* & *Peak 3*); however, clearly from the plot, the readings fluctuated quite a bit. The two peaks (*Peak 2* and *Peak 3*) must have been due to the extra forces from braking and restarting of the truck; therefore data close to the two peaks should be excluded. In this case, the strain due to the static truck load was calculated by averaging all the readings between

the time period 1:10~1:45, when the effects from braking had gradually ceased. Nonetheless, although in much smaller magnitude, the data still fluctuated during this time; this is not surprising because the truck was not turned off completely, so there was effect from the engine vibration. The readings are also sensitive to other noise and environment effects. The results calculated for all six strain gauges under Static Load Position 2 are plotted together and shown in Figure 4-10.

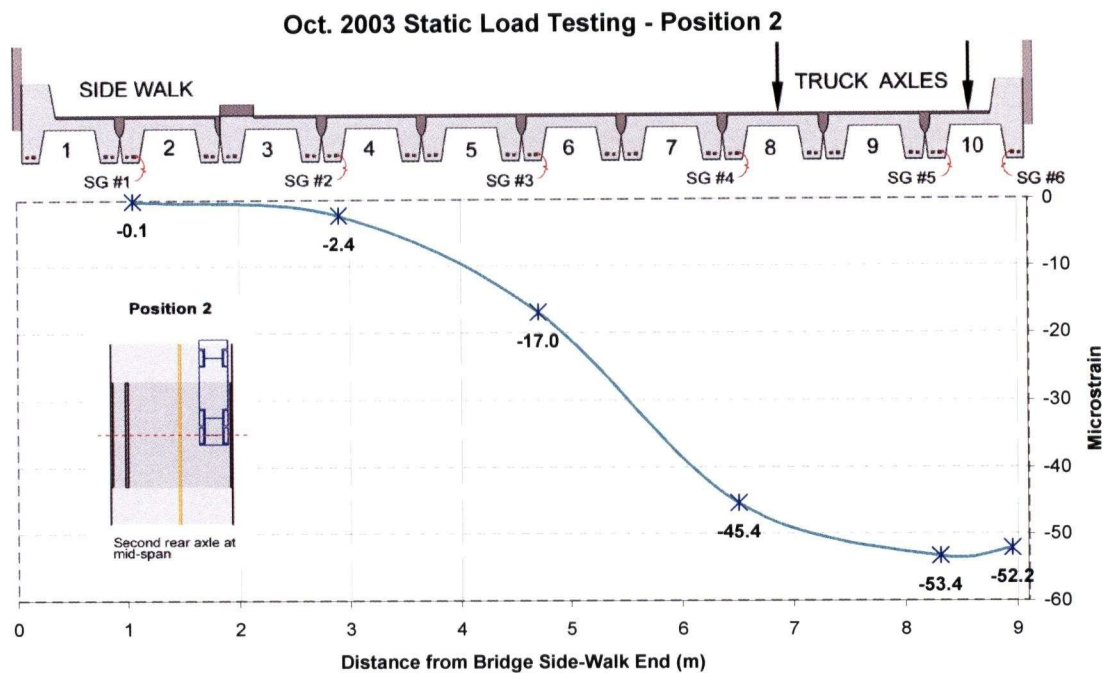

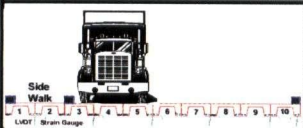
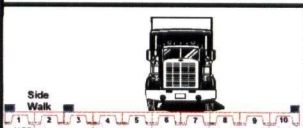

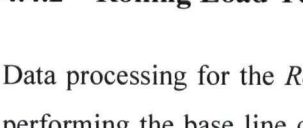
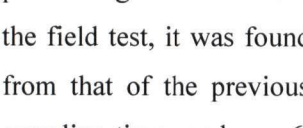


Figure 4-10 Plot of Six Strain Values Due to Static Truck Load at Position 2

Similar processing procedures were applied to all six sets of data from the six loading positions, and the results are summarized in Table 4-1. Since each strain value is the average of many readings, the standard deviation is also calculated. Standard deviation measures how widely values are dispersed from the mean, and therefore the smaller the standard deviation, the better the mean is representing the group of data. All six zeroed Time-Strain History plots are attached in Appendix IV. From the plots, except Position 1 & 2, one can see Position 3 & 4, and Position 5 & 6 have very similar Time-Strain history curves, which was as expected.



Table 4-1 Summary of Static Strains under Six Loading Positions - Field Test 2003

2003 Static Load Testing Results							
*Truck Weight = 25,450 kg Strain Gauge (SG) Locations		Girder 2	Girder 4	Girder 6	Girder 8	Girder 10L	Girder 10R
Truck Position	Load Position	SG #1	SG #2	SG #3	SG #4	SG #5	SG #6
	Position 1	-0.5	-2.5	-15.4	-50.4	-62.9	-55.3
	std. dev.	1.4	0.6	1.4	3.7	4.1	1.4
	Position 2	-0.1	-2.4	-17.0	-45.4	-53.4	-52.2
	std. dev.	0.9	0.5	1.4	0.9	1.0	0.8
	Position 3	-16.8	-65.4	-47.8	-11.0	-0.6	-2.6
	std. dev.	1.5	1.4	1.8	1.8	2.3	1.9
	Position 4	-16.5	-67.0	-50.4	-11.8	-1.6	-1.7
	std. dev.	1.6	1.8	2.4	1.8	2.4	1.7
	Position 5	-2.6	-19.5	-72.0	-58.7	-14.9	-8.3
	std. dev.	1.5	1.1	1.6	2.6	1.8	1.3
	Position 6	-2.9	-20.5	-71.9	-55.6	-15.5	-8.4
	std. dev.	1.4	0.9	1.8	2.9	2.0	1.5

#### 4.4.2 Rolling Load Testing

Data processing for the *Rolling Load* test results were supposed to be quite straight forward – after performing the base line correction, the Time-Strain curves can be plotted directly. However, after the field test, it was found that the sampling rate used for the 2003 Rolling Load test was different from that of the previous two field tests. During the 2001 and 2002 *Rolling Load testing*, the sampling time used was 60 msec (0.06 sec), or 16.67 data/sec = 16.67 Hz; the 2003 testing used 60 Hz. In order to compare the time-strain plots from all three field testing directly, similar sampling rate, if not identical, should be used. Therefore, one extra step is required – converting the 60 Hz data into 16.67 Hz. It is only possible to convert data from higher-frequency into lower-frequency, but not vice versa.

Similar to the *Static* testing results, the first thing to do with the raw data was to calculate the initial values and to perform base-line corrections. Rolling Load Position 1 (hereby referred to as “Roll I”) will be used as example here. Figure 4-11 shows the zeroed time-strain plot based on the original 60Hz data. The sampling rate was high enough to catch reading lags (examples indicated by red circles on the figure), as can be observed from Figure 4-11; these were not seen on the *Static testing* plots. As for converting the sampling rate, every four readings in the original 60 Hz data were averaged to give one “representing reading”. Therefore, after the averaging process, there are 15 “representing readings” in a second, so the sampling rate of the new set of data becomes 15 Hz,

which is much closer to the desired 16.67 Hz. The Time-Strain history for Roll I after averaging is shown in Figure 4-12. Clearly from the plot, fluctuations on the 15Hz-plot is much less, and the effect of the reading lag is much reduced.

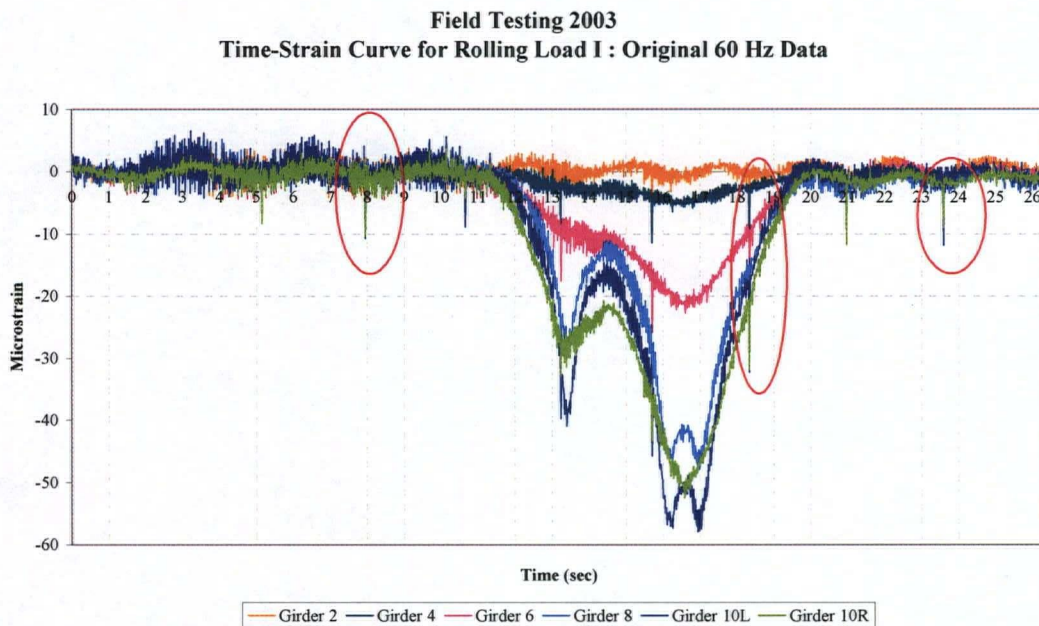


Figure 4-11 Plot of 2003 Field Test Results - Rolling Load Position I (60Hz Data)

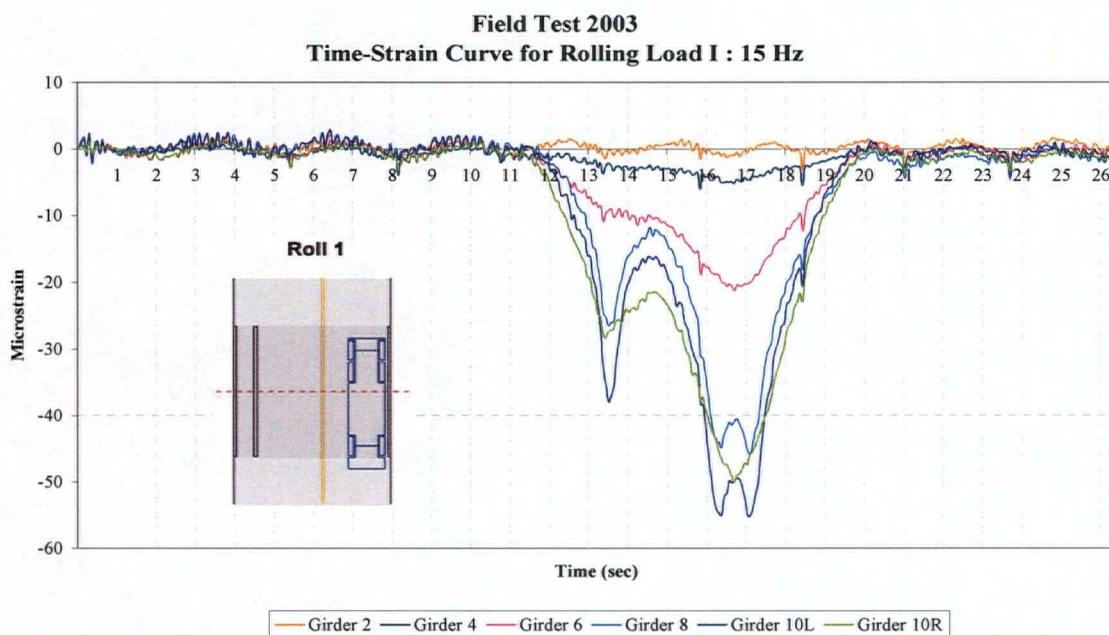


Figure 4-12 Plot of 2003 Field Test Results - Rolling Load Position I (15 Hz Data)



This “averaging” step was applied to all data from the three loading positions for rolling load, and the plots for Roll II and Roll III are shown below as Figure 4-13 and Figure 4-14.

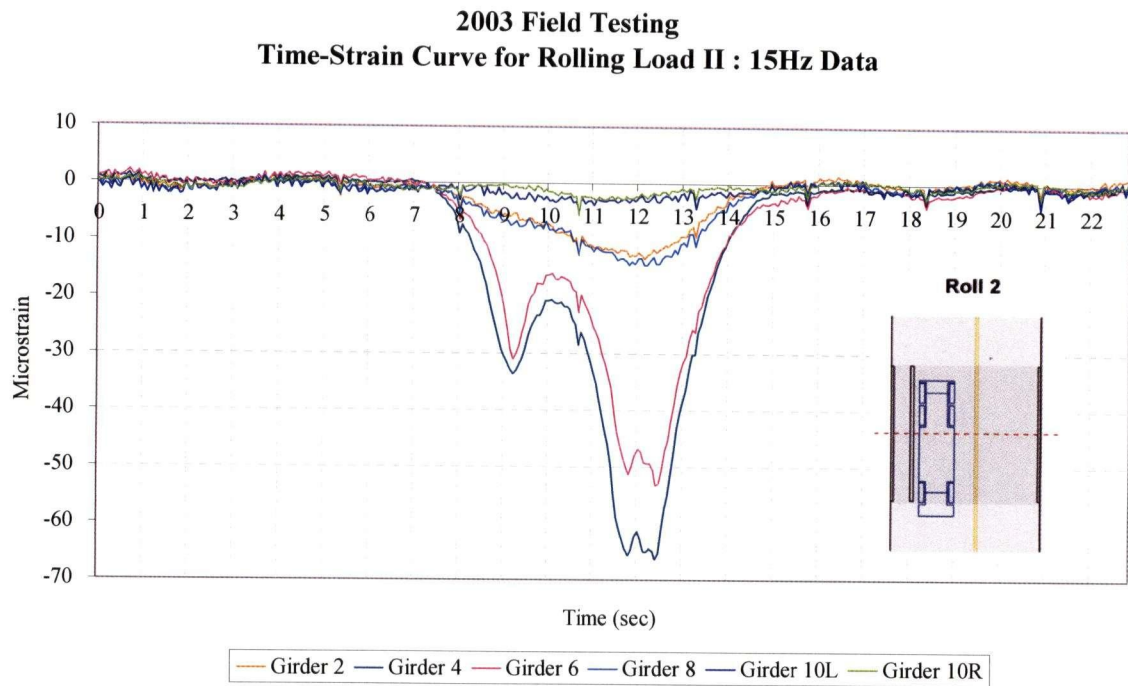


Figure 4-13 of 2003 Field Test Results - Rolling Load Position II (15 Hz Data)

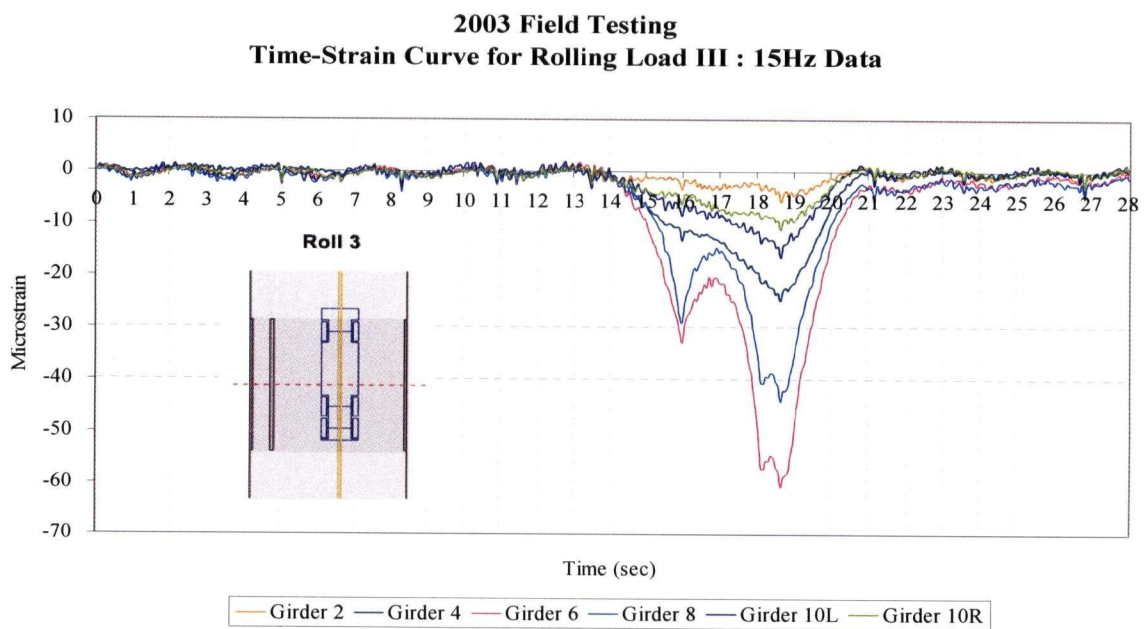


Figure 4-14 of 2003 Field Test Results - Rolling Load Position III (15 Hz Data)

From observing the three rolling load plots (Figure 4-12~14), one can obtain the approximate vehicle speed. It took around 8 seconds for Roll I, and 7 seconds for Roll II and III, for the truck to pass through the bridge, which is equivalent to about 6 km/hr for Roll I, and 7 km/hr for Roll II and III. Speed of the truck does have effects on the strain readings. Under “smooth road condition”, one can expect that the higher the vehicle speed, the lower the strain readings. Nonetheless, if the road condition is bumpy, the higher the speed will induce higher dynamic effect, therefore result in higher strains.

Table 4-2 is the summary of the “worst strains” obtained from the six strain gauges. The numbers are based on the 15 Hz data, and obvious reading lags were ignored. Since the data contain noises, the largest number within the data may not be the maximum strain caused purely by the truck load; this is especially true when the strain readings are small. Therefore, when comparing Table 4-2 to the static results (Table 4-1), only the strain readings from the worst two girders are used here (the bolded numbers in Table 4-2). The worst strain readings for each rolling position are marked in red. Most of the worst readings from the rolling load results are smaller or close to the static load results. Since the asphalt road surface is relatively smooth, moving load indeed give less strain effects than the equivalent static load. Nonetheless, one thing does match between the two tables: the “order of strain gauges giving larger strains”. In terms of loading positions, Roll I is “equivalent to” Static Position 1&2, Roll II to Static Position 3&4, and Roll III to Static Position 5&6. Using Roll III as example: for both Roll III and Static 5&6, the worst (largest) strain value was given by Strain Gauge #3 (SG#3) in Girder 6, followed by SG#4, SG#2, SG#5, SG#6, and SG#1 had the smallest worst strain reading. Therefore the test results should be quite reliable.

Table 4-2 Largest Strain Readings Induced by the Three Rolling Load Positions – Field Test 2003

	<i>Girder 2</i>	<i>Girder 4</i>	<i>Girder 6</i>	<i>Girder 8</i>	<i>Girder 10L</i>	<i>Girder 10R</i>
<b>Load Positions</b>	<b>SG #1</b>	<b>SG #2</b>	<b>SG #3</b>	<b>SG #4</b>	<b>SG #5</b>	<b>SG #6</b>
<b>Roll Test I</b>	- 1.2	-4.6	-20.4	<b>-45.4</b>	<b>-55.1</b>	<b>-50.1</b>
<b>Roll Test II</b>	-12.6	<b>-65.3</b>	<b>-52.9</b>	-14.4	-5.3	-5.7
<b>Roll Test III</b>	-6.0	-24.9	<b>-57.6</b>	<b>-41.2</b>	-16.6	-11.3

#### 4.5 Testing Result Comparisons

In this section, the 2003 field testing results will be compared with the testing results from the 2001 (before repair) and the 2002 (after repair) field tests, to see how well the *sprayed FRP* performs over the years in field condition. As mentioned in Ch 1, data analysis and comparison of the 2001 and

2002 testing had been performed by Nandakumar [79] and Mortazavi [78]. However, one issue concerns the author is, should the results from Nandakumar and Mortazavi be used directly to compare with the 2003 results. A comparison between two things is meaningful only when there is only one variable between the two things. In another word, apples have to be compared with apples; apples can not be compared with oranges. The “variable” between the three field testing is the “time” they took place, so all other elements that could effect the testing results should be kept as similar as possible, or modifications should be made to account for the effects. Based on this argument, the author would like to make sure similar data processing procedures had been performed on the 2001 and 2002 data. Since the author could not confirm the process with the original two authors in person, she decided to obtain the original raw data from 2001 and 2002 field tests and re-analyze them in the same way. Unfortunately, the original data for the 2001 Static Load testing could not be obtained. Therefore, the 2001 Static Load testing results presented in [79] (by Nandakumar) will be used.

Besides the analysis procedures, truck weight is another important factor that affects testing results: the heavier the testing vehicle, the larger the strains. The weight of the 2003 testing truck was 25,450 kg; the 2002 testing truck was 24,940 kg; weight for the 2001 testing truck could not be found. Nonetheless, for the 2001 testing results shown in [78], a load factor had been applied. Therefore, all the data will be adjusted to correspond to the 2002 truck, 24,490 kg. Since the weight used was way below the elastic load limit of the bridge, the relationship between the weight and the strain is still within the elastic range, and they are linear proportional to each other. Therefore, a load factor of  $0.98 (= 24,940 / 25,450)$  will be applied to the 2003 testing results.

Regarding the temperature effect, nothing had been done to the data for temperature adjustment. This is because for the static and rolling load testing, the time duration is relatively short, and therefore it was assumed that the change in temperature during this short period of time would not give significant influence to the strain readings. Nonetheless, the 2001 testing was conducted on September, the 2002 testing was on February, and the 2003 testing was on October. The author was not involved in the previous two testing, so the weather conditions during those two testing were unknown. As for the 2003 testing, it was conducted on a raining day and the “internal temperature” (the strain gauges’ temperature) was around 13 °C. The temperature and humidity more or less affect the strain readings. Even though temperature adjustment was considered unnecessary, this factor should still be kept in mind when comparing the data from all three years.



In the following, for both the static and rolling load tests, first the 2003 data will be compared to the 2002 data, so see if there were significant change in the repaired girders' "health condition" after twenty months in operating environment. Then the 2003 data will be compared with the 2001 data, when the bridge had not been repaired with *sprayed FRP*, to see how effective the repair method is.

#### 4.5.1 Static Load Test Results

Before performing the comparisons, the analyzed results from each testing should be "checked" individually first; this helps the engineers to pick up "surprising" analyzing results. The unexpected results could be correct, or it could be due to careless mistakes made during the data processing stage, or it could be due to malfunctions of the sensing system. If the analyzed result contains error itself in the first place, the comparisons made based on it become meaningless. This checking step helps to avoid time/resource wasting and to increase confidence with the testing results.

After applying the 0.98 load factor to all values, the 2003 static load testing results from all six loading positions are plotted together and shown in Figure 4-15.

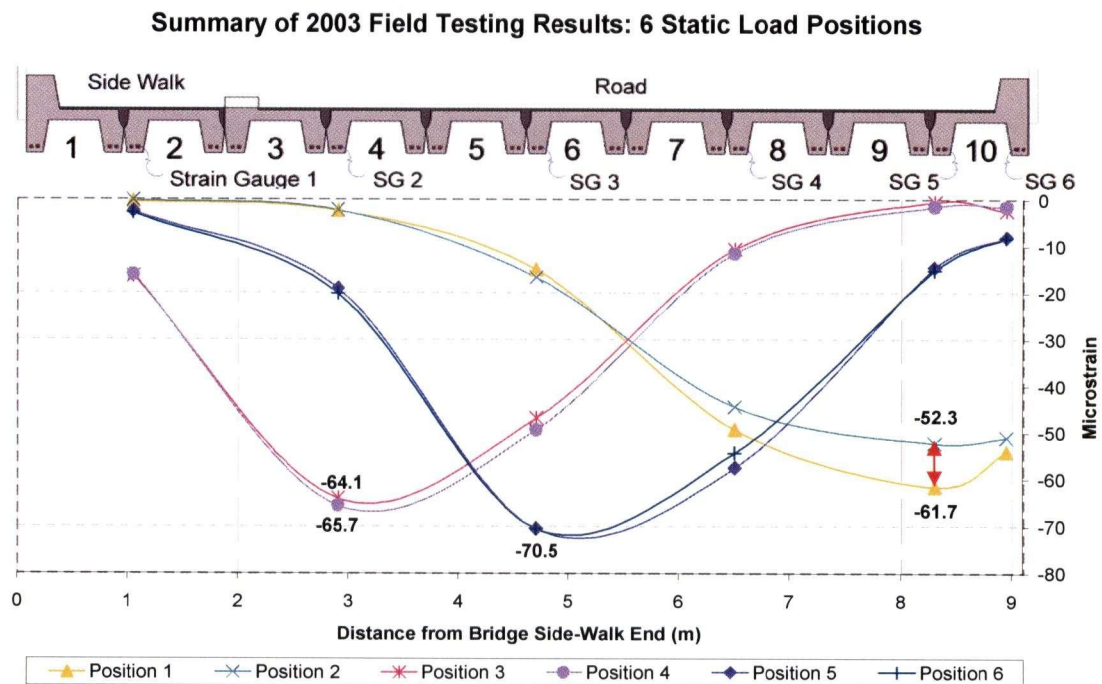


Figure 4-15 Summary of 2003 Static Load Testing Results (with load factor applied)

The strain readings are expected to be similar between Position 1 & 2, Position 3 & 4, and Position 5 & 6, because the two rear axles are very close to each other, so their loading positions are similar. From Figure 4-15, Position 3&4 and Position 5&6 indeed have almost identical strain curves. The only two corresponding readings that have relatively larger difference are from Strain Gauge #5 (SG5) under Position 1 (strain = 61.7) and 2 (strain = 52.3). Nonetheless, SG5 of Position 1 also has an unusual large standard deviation value equal to 4.1 (please refer to Table 4-1), which means the measured data were in the range of  $61.7 \pm 4.1 \mu\epsilon$ . "4.1" is actually the highest standard deviation value in Table 4-1; most of the standard deviations are less than  $2 \mu\epsilon$  (see Table 4-1). Since the two highest standard deviations were both from Position 1 (from SG 4 and SG5), it seems like the sensors were experiencing higher noises during the time when the truck was on Position 1. Therefore, the larger difference between SG5 of Position 1 and 2 could be due to noise effect. The strain at Girder 10L(SG#5) due to load position 1 could be a value lower than  $61.7 \mu\epsilon$ .

Regarding the locations of largest strain, all three "load position pairs" had their largest strain occurred at the same place (both occurred at SG#5 in Girder 10 L for Position 1 & 2; both at SG#2 in Girder 4 for Position 3 & 4; and both at SG#3 in Girder 6 for Position 5 & 6); this result matches what was expected. The largest strain under each loading position is marked in red in Table 4-1.

The 2003 Static Load Testing results are now ready to be compared with the previous two field tests.

#### **4.5.1.1 After\_Repair 2002 vs. Strain\_Reading 2003**

As mentioned earlier, 2002 data was re-analyzed for consistency, and the result is summarized in Table 4-3 below. For the ease of comparison, the 2003 summary table, with the 0.98 load factored applied, is shown on the same page as Table 4-4. According to [78], during the 2002 field testing, SG#2 in Girder 4 was malfunctioned, and therefore data for SG#2 was unavailable. The maximum strain values obtained from each loading position are marked in red; since SG#2 data, which are expected to give the largest strain when under Position 3 & 4, are not available, one cannot guarantee the worst strain locations. Also note that Position 1 and 2 for the 2002 testing did not have their largest strain occurring at the same location, and neither of them is from the expected SG#5.

When comparing Table 4-3 to the results analyzed by Nandakumar [79], the values are actually quite close; the differences are all less than  $2 \mu\epsilon$ , except the five numbers filled with shading in Table 4-3.

Table 4-3 Maximum Strains under Six Static Load Positions - Field Test 2002







2002 Static Load Testing Results							
Strain Gauge Locations		Girder 2	Girder 4	Girder 6	Girder 8	Girder 10L	Girder 10R
Truck Position	Load Position	SG #1	SG #2	SG #3	SG #4	SG #5	SG #6
	Position 1	-1.0	n/a	-14.9	-53.2	-53.1	-50.5
	std. dev.	1.7		1.1	2.0	1.8	1.3
	Position 2	-0.6	n/a	-13.1	-43.9	-50.0	-54.1
	std. dev.	2.0		1.2	3.1	3.7	3.0
	Position 3	-13.1	n/a	-42.0	-10.5	-1.6	-1.5
	std. dev.	1.6		1.0	1.6	1.1	1.1
	Position 4	-11.9	n/a	-42.5	-8.9	-1.6	-1.1
	std. dev.	1.5		1.1	1.6	1.2	1.1
	Position 5	-2.6	n/a	-70.6	-57.4	-12.5	-7.4
	std. dev.	1.6		1.3	1.3	1.2	1.1
	Position 6	-2.0	n/a	-65.1	-51.7	-10.9	-5.9
	std. dev.	1.6		1.3	1.3	1.2	1.1

Table 4-4 Static Strains under Six Loading Positions with Load Factor Applied - Field Test 2003

2003 Static Load Testing Results (load factor applied)							
Strain Gauge Locations		Girder 2	Girder 4	Girder 6	Girder 8	Girder 10L	Girder 10R
Truck Position	Load Position	SG #1	SG #2	SG #3	SG #4	SG #5	SG #6
	Position 1	-0.5	-2.5	-15.1	-49.3	-61.7	-54.2
	std. dev.	1.4	0.6	1.4	3.6	4.0	1.4
	Position 2	-0.1	-2.3	-16.6	-44.5	-52.3	-51.1
	std. dev.	0.9	0.5	1.4	0.9	1.0	0.8
	Position 3	-16.4	-64.1	-46.9	-10.7	-0.6	-2.5
	std. dev.	1.5	1.3	1.7	1.7	2.2	1.8
	Position 4	-16.2	-65.7	-49.4	-11.5	-1.5	-1.6
	std. dev.	1.5	1.7	2.3	1.8	2.4	1.6
	Position 5	-2.5	-19.1	-70.5	-57.5	-14.6	-8.1
	std. dev.	1.5	1.1	1.5	2.5	1.8	1.3
	Position 6	-2.9	-20.1	-70.5	-54.4	-15.1	-8.2
	std. dev.	1.4	0.9	1.8	2.8	1.9	1.4

During the re-analyzing, problems were found with the data of *Position 4* and *Position 6*. For *Position 4*, the measuring period for the time before and after the truck crossing the bridge seem got cut-off (see Figure 4-16). For *Position 6*, the plot is having similar problem as *Position 4*, but also seem to contain extra data (see Figure 4-17). Therefore, when calculating the initial values for these



two sets, and to decide the period representing the static load on position, assumptions needed to be made. This could be one reason why the five numbers shaded in Table 4-3 are having greater differences, because different people may make different assumptions to process the data, which affects the analyzing results significantly.

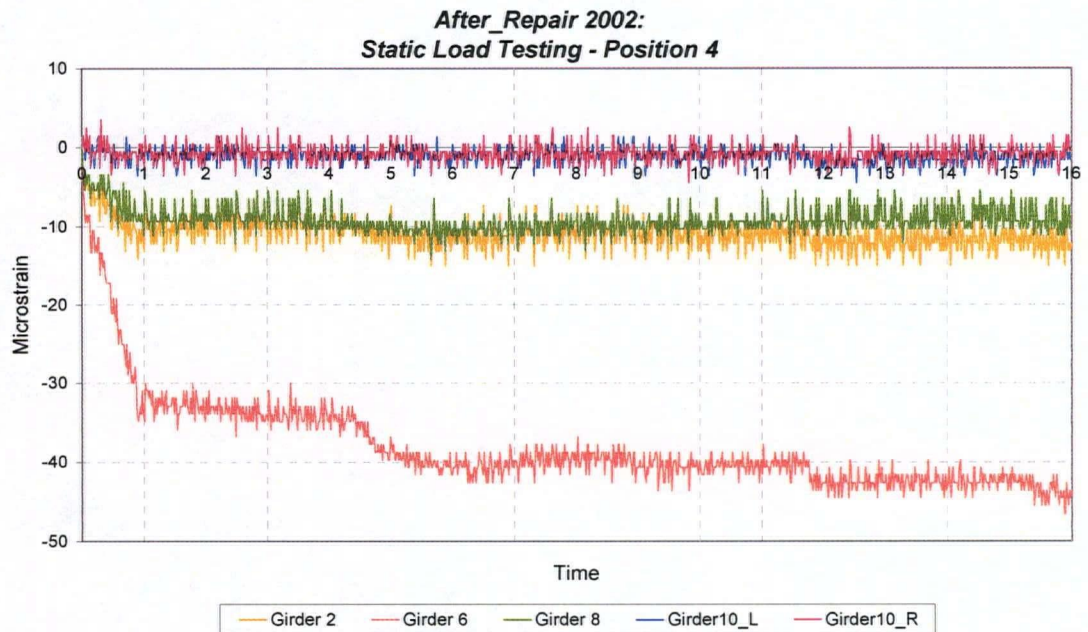


Figure 4-16 Time-Strain History for Static Load Position 4 - 2002 Field Testing

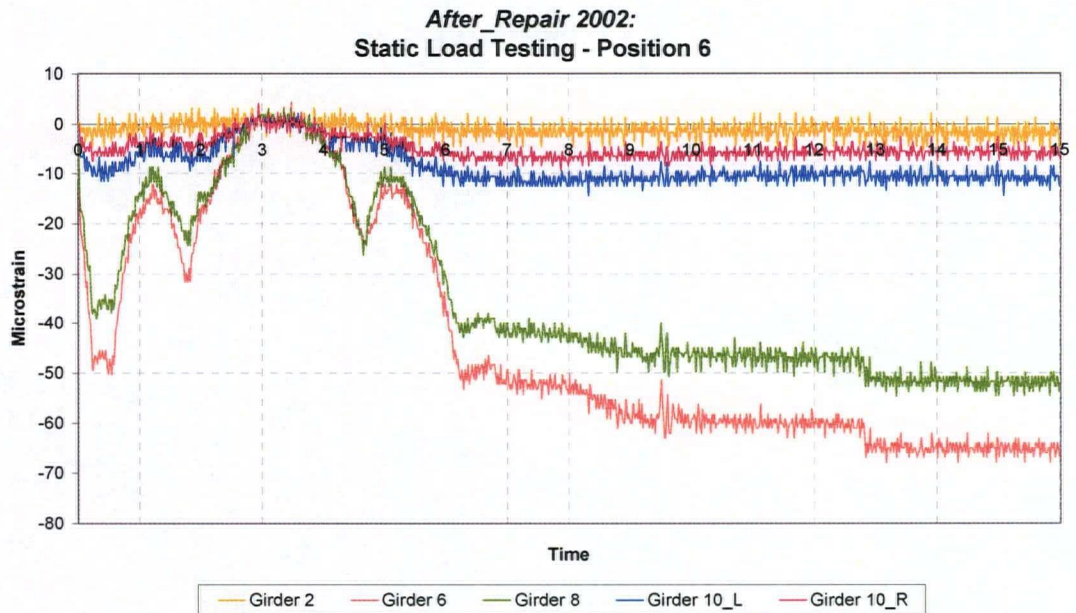


Figure 4-17 Time-Strain History for Static Load Position 6 - 2002 Field Testing

In the following, the comparisons between *Strain\_Reading 2003* and *After\_Repair 2002* will be done by plotting their static strain values on the same graph. For clarity, each plot will contain only the two loading positions that create similar effects on the bridge, so there will be three plots in total for the static strain comparisons (Figure 4-18 to Figure 4-20).

Even though all values from the six strain gauges are plotted on graph, the focus (comparison) will only be on the two girders affected by the truck load the most, because the worst loading condition is what we really care about. In addition, for the smaller strain values, they may be dominated by the noise effect rather than the truck load, so the comparisons between them (strains from the less critical girders) are less representative. Also noted that the six strain values (five for 2002 data) are connected together mainly for the ease of comparison and to give a more clear sense on the effect of the truck positions to the bridge transversely; the curve is not necessarily representing the actual strain values across each girder.

The ideal condition is to see the 2003 static strains stay at the same values as their 2002 counterparts; this means the conditions of the girders stay the same after 20 months. Also, theoretically speaking, the 2003 values can not be smaller than the corresponding 2002 values (assume the 2002 measurements were "correct") because the nature of the materials (creep, fatigue) and the damage from the environment; girder conditions can not be "improving" over time by itself. Nonetheless, there are too many variables and factors that can affect the testing result, and microstrain is a very small unit and therefore is sensitive to many effects; therefore, with rational judgment, certain range of minor difference can be ignored, and the girder will still be considered "no change".

For Position 1 and 2, the critical girders are girder 8 and 10, and SG#5 is expected to give the highest strain readings, assuming all girders are in similar "health condition". However, as can be seen from Figure 4-18, the 2002 results were not quite as expected: SG#4 gave the highest strain under Position 1, but when under Position 2, SG#6 became the highest. Nonetheless, the standard deviations for these three critical strains (SG#4, 5, 6) were also the higher ones within the table (see Table 4-3); especially for Load Position 2, all three standard deviations are above 3  $\mu\epsilon$ . The higher the standard deviations means the greater the data fluctuated, and the less representative the mean values. This unexpected result also contributes to the situation that, for SG#4 under Position 1, the 2002 strain is actually greater than the 2003 value (by 4  $\mu\epsilon$ ). Nonetheless, the standard deviations for the Position 1 values are relatively large ( $\pm 2.0$  and 3.6; see Table 4-3 and Table 4-4), so a 4  $\mu\epsilon$  difference is considered "unchanged". As for Position 2, the strains from SG#4 for both testing are about the same.



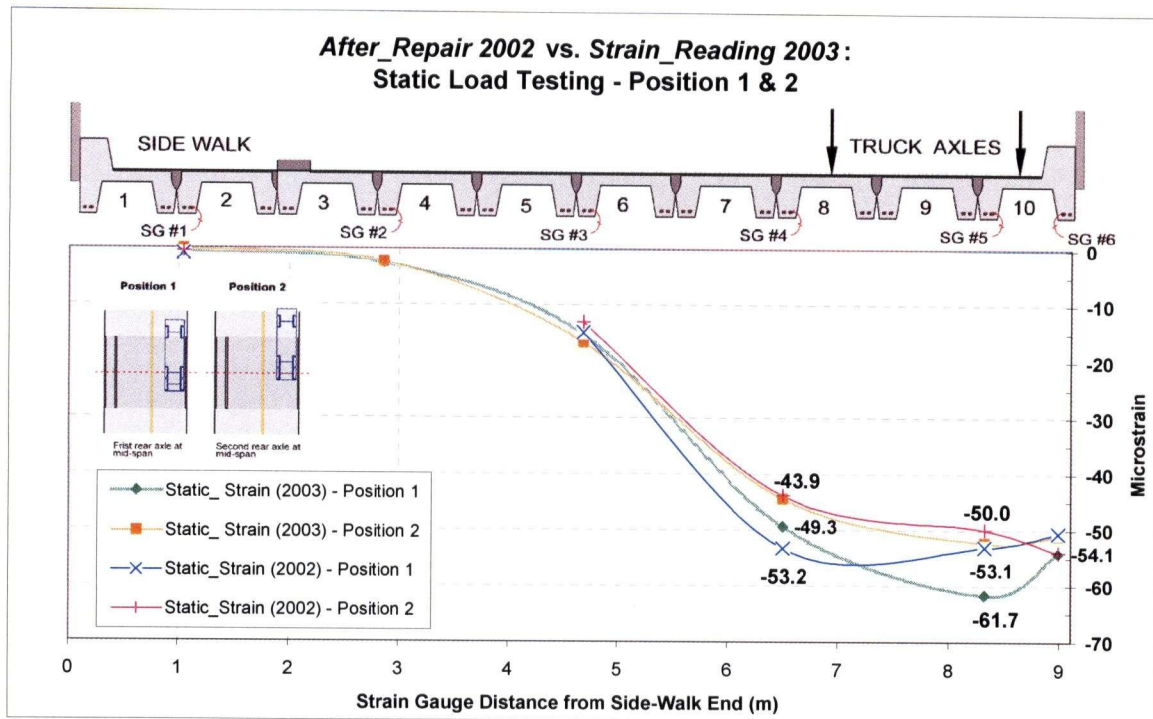


Figure 4-18 Comparison between 2002 and 2003 Field Test Results - Load Position 1 & 2

Higher difference is found on SG#5. Again, for Position 2, the values from the two testing are about the same, but the 2003 strain is  $8.6 \mu\epsilon$  higher than the 2002 value (Figure 4-18). As discussed earlier, 2003\_SG#5-Position 1 gave an unusual high value in its static strain ( $61.7 \mu\epsilon$ ), when compared to its counterpart Position 2 ( $52.3 \mu\epsilon$ ); since the standard deviation for the  $61.7$  value is up to  $4 \mu\epsilon$ , it is reasonable to judge the “actual effect from truck loading” may be lower. At the same time, even though standard deviation for 2002\_SG#5-Position 1 ( $53.1 \mu\epsilon$ ) is not too high ( $\pm 1.8$ ), it was surprising to see the value of SG#5 be lower than SG#4 under Position 1. Therefore it is highly likely that the “actual difference” between the 2002 and 2003 SG#5 under Position 1 be less than  $8.6 \mu\epsilon$ . For now we conclude that there could be slight increase in SG#5.

As for SG#6 (also in critical girder) and SG#3, the 2002 and 2003 values are very close to each other (see Figure 4-18); the difference between the largest and smallest of the four values (two from 2002 and two from 2003) are within  $5 \mu\epsilon$ . Overall, for the total 12 sets of comparisons (6 strain gauges and 2 loading positions), only one set showed noticeable difference; but the two numbers in this set could be problematic itself, as discussed earlier. Therefore, it is conclude that the five girders, especially Girder 8 and 10 are in similar condition during the two field testing.

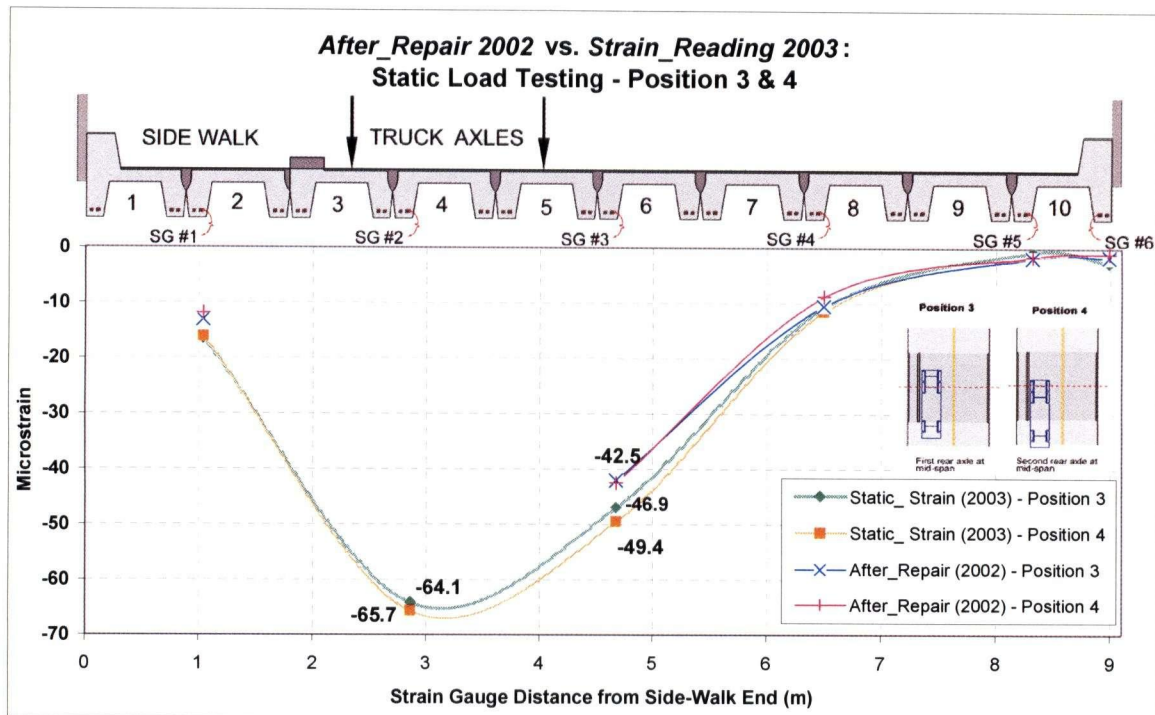


Figure 4-19 Comparisons between 2002 and 2003 Field Test Results - Load Position 3 & 4

For Position 3 and 4 (Figure 4-19), GS#2 (in Girder 4) is the one on the most critical location and should give the highest strain readings. Unfortunately, data from 2002 is missing, so the comparison for GS#2 can not be made. When comparing the SG#3 values (give second large strains ) from the two testing, the 2003 value is about 5  $\mu\epsilon$  higher than 2002 for Position 3, and almost 7  $\mu\epsilon$  higher for Position 4; but the 2003 GS#3 value under Position 4 also gives a high standard deviation ( $\pm 2.3$ ). Similarly, both 2003 GS#1 values are a little higher than their 2002 counterparts, by about 3  $\mu\epsilon$ . As for the less critical girders (GS#4~6), the readings were about the same for both years.

Based on this set of data, the performance of the *sprayed FRP* on Girder 4 could not be evaluated, and on Girder 6 seemed not working as well as on Girder 8 and 10. Nonetheless, keep in mind that the data for Position 4 is questionable. The initial value for 2002 Position 4 was calculated by assuming the strains in Girder 10 would be close to zero. If the actual strains should be higher, all the static strains for 2002 Position 4 would be higher, and the value could be the same as 2003. Therefore, the author believes that the “actual” strain increase in Girder 6 should be less than 7  $\mu\epsilon$ . Before drawing conclusions for the performance of Girder 6 here, the next plot (Figure 4-20) should be evaluated first, because Girder 6 is the most critical girder under Load Position 5&6.

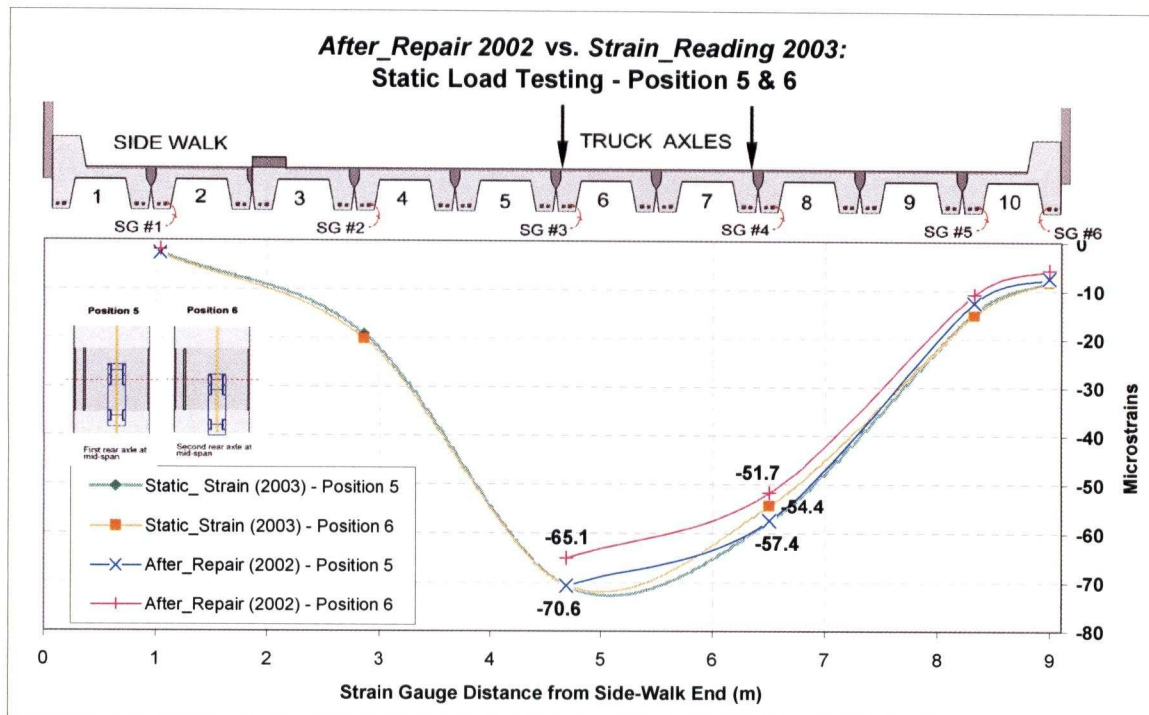


Figure 4-20 Comparisons between 2002 and 2003 Field Test Results - Load Position 5 & 6

Figure 4-20 presents the comparison between 2002 and 2003 static strains under Position 5 & 6. Under this set of loading positions, Girder 6 should experience the greatest loading, and then Girder 8. Indeed, for both years, SG#3 gave the highest strain values, followed by SG#4. For SG#3, the largest strain obtained was 70.6  $\mu\epsilon$  (under Position 5), and the smallest was 65.1  $\mu\epsilon$  (under Position 6); but both values were from the 2002 data. As mentioned earlier, the data for 2002 Position 6 is questionable, and therefore it is less reliable. If the value from Position 5 is taken to represent the strain reading for SG#3, then the 2003 results are the same as 2002's. Similarly for SG#4, both the largest and smallest values were from 2002 data; again Position 6 gave a much lower strain value (almost 6  $\mu\epsilon$  lower than its Position 5 counterpart). Again, if the more reliable Position 5 result is taken, then the 2003 results are about the same as the 2002 values, as can be seen on Figure 4-20. Based on this set of data, the five instrumented girders (more confidence with Girder 6 and 8) should be in similar conditions in both the 2002 and 2003 field testing.






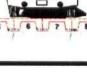
Overall, based on all the three plots (Figure 4-18 ~ 4-20), it is concluded that the static strains obtained from 2003 field testing are about the same as the 2002 field testing, and therefore the GFRP layer is working well under operating environment over the 20 months period.



#### 4.5.1.2 Before\_Repair 2001 vs. Strain\_Reading 2003

Similar comparing procedures will be applied to the *Before\_Repair 2001* and *Strain\_Reading 2003* data as well. As mentioned before, the 2001 testing results given by Nandakumar [79] will be used directly; they are shown in the table below (Table 4-5); standard deviations could not be calculated because the original data were not available. Since the author's 2002 analyzing results were quite similar with Nandakumar's 2002 results, it is assumed that similar analyzing procedures had been taken by both, and therefore using Nandakumar's 2001 results to perform the comparison should still provide valid conclusions regarding the performance of the GFRP repair.

Table 4-5 Static Strains under Six Loading Positions – *Before\_Repair 2001* (Load Factor Applied)

2001 Static Load Testing Results (load factor applied)							
Strain Gauge Locations		Girder 2	Girder 4	Girder 6	Girder 8	Girder 10L	Girder 10R
Truck Position	Load Position	SG #1	SG #2	SG #3	SG #4	SG #5	SG #6
	Position 1	0	-2.7	-18.6	-58.2	-62.8	-53.2
	std. dev.						
	Position 2	0	-1.7	-16.3	-57.6	-62.4	-51.8
	std. dev.						
	Position 3	-17.3	-62.8	-39.7	-11.5	-1.9	-1.9
	std. dev.						
	Position 4	-17.3	-59.9	-42.8	-11.5	-1.0	-1.9
	std. dev.						
	Position 5	-3.8	-18.8	-83.5	-70.1	-15.9	-9.6
	std. dev.						
	Position 6	-2.9	-17.9	-101.8	-64.4	-16.9	-10.6
	std. dev.						

The 2001 results seem quite “reasonable” in terms of: (1) the maximum strain values were given by the same strain gauge from the “load position pairs” (1&2, 3&4, 5&6); (2) the numbers for each strain gauge from the “pairs” matched pretty well with each other (most of them within 10%), except the readings from Girder 6 under Position 5 and 6 (see Table 4-5). SG#3 gave the largest static strain values under Position 5 and 6, which was not surprising since Girder 6 is at the most critical location for that set of loading position. However, the difference between the strain readings from these two positions was 18  $\mu\epsilon$ , equivalent to almost 20% difference. If using the readings from SG#4 as reference, the 101.8  $\mu\epsilon$  from Position 6 seems high. Regardless the “correctness” of the numbers, it was likely that Girder 6 was in more severe deteriorating condition than the other girders.

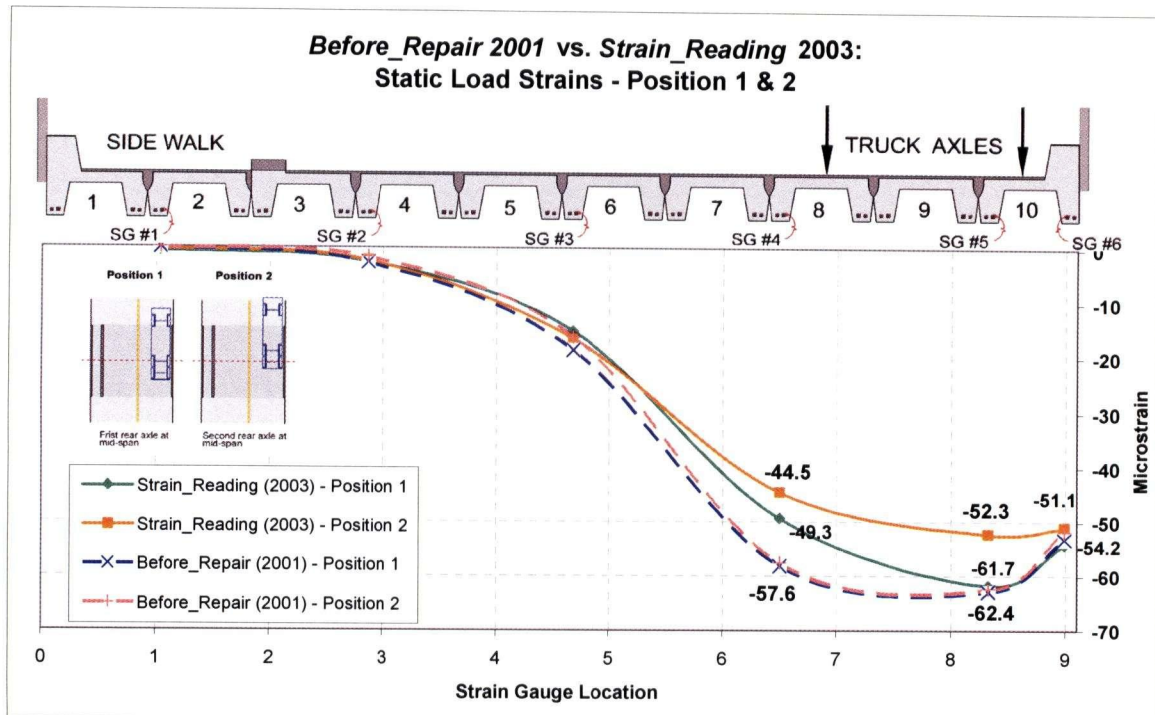


Figure 4-21 Comparison between 2001 and 2003 Field Test (Static Load) - Load Position 1 & 2

Figure 4-21 is the plot of comparisons between the 2001 and 2003 test results for Static Load Position 1 & 2; the critical girders are Girder 10 and 8 (SG#5,6 and SG#4). For SG#4, even the 2003 reading under Position 1 is much bigger than its Position 2 value, both numbers from 2003 are still smaller than the *Before\_Rpair 2001* values. As for SG#4, clear from the graph that both 2003 readings are much smaller 2001s'. For SG#6, the strain values from both field testing are about the same, with the 2003 values slightly lower.

In fact, all strain values obtained from the 2003 testing were either smaller or equal to the 2001 results under Position 1 & 2; and the larger the strain values, the larger the differences. This shows that the new repair method does improve the bridge performance from its original state, at least we can be sure that Girder 8 and 10 are in better health condition than before.

Figure 4-22 (next page) shows the comparison results for Load Position 3 & 4. For this set of loading positions, truck axles are sitting on girder 3 and 5, and therefore SG#2 should give the largest strain reading, and then GS#3 in girder 6. For SG#2 under Position 3, the static strain from the two field tests years are about the same; but under Position 4, the difference is about 6  $\mu\epsilon$ .



For SG#3 in Girder 6, the differences for both Position 3 and 4 are about  $7 \mu\epsilon$ . Taking the fact that the value  $-49.4 \mu\epsilon$  has a higher standard deviation, the differences can still be considered as not significant. However, the graph (Figure 4-22) seems saying the “after repair” condition is not better than “before repair”. When back checking the 2002 data, it is found that the 2002 values were about the same as 2001 values, which shows that even right after the repair, there was no recognizable improvement on girder 4 and 6 (under Position 3 & 4). Therefore, the GFRP material itself is not degrading over this period of time. Two possibilities: (1) when the GFRP mates were applied on Girder 6 and 4, the work was not done properly; de-bonding may have happened right at the beginning, so that the “reinforcing effect” was not shown and there were no changes in strain readings before and after the repair; (2) the data from 2001 testing under Position 3 & 4 contain errors (could be due to various reasons).

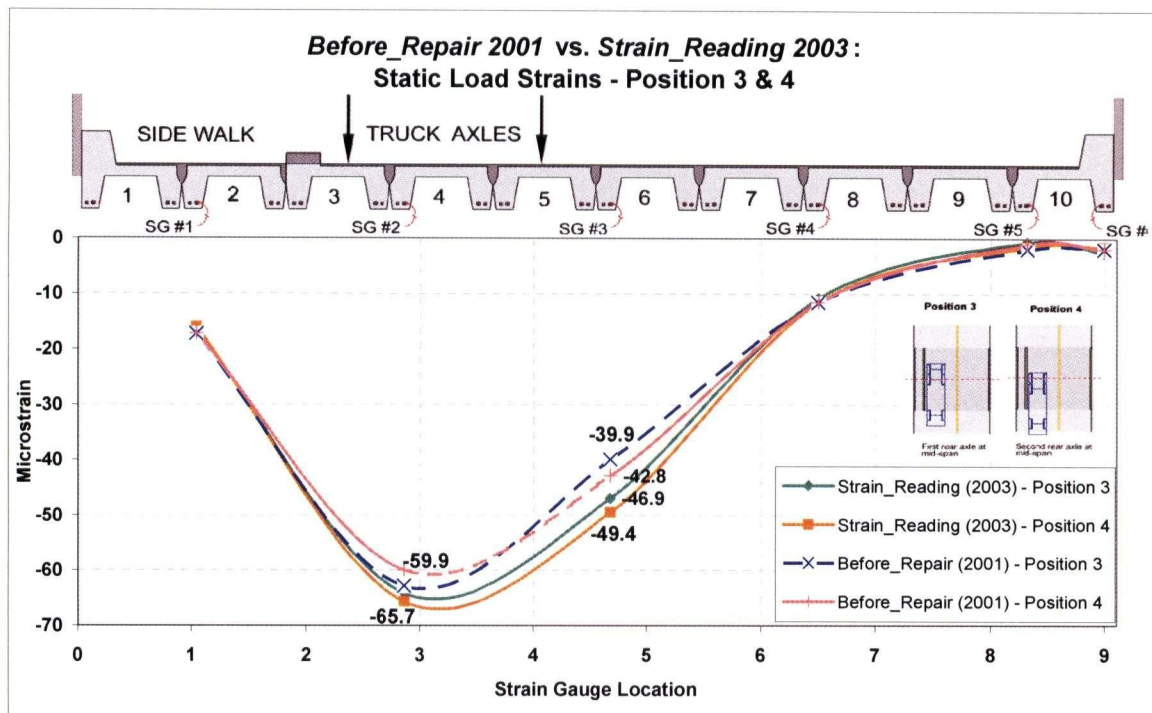


Figure 4-22 Comparison between 2001 and 2003 Field Test (Static Load) - Load Position 3 & 4

As for all other less critical girder locations, the static strains from both field tests were about the same, as shown in Figure 4-22. One other interesting finding from the graph is that, the “relative position to the truck axles” for SG#1 and SG#6 are actually similar, with SG#1 a little bit further. However, when looking at their strain values, SG#1 gave much lower strains, and all four values (two positions for two testing) are about the same. This could be due to the thickening effect of the

concrete curb on Girder 3, which “reinforced” the cross section; or the load transfer between girder 2 and 3 is different from others. Or, the *sprayed GFRP* works better than the GFRP mats. Actually the GFRP were applied to Safe Bridge with two different techniques; Girder 1 and 2 were repaired with the sprayed technique, whereas the rest was using GFRP sheets.

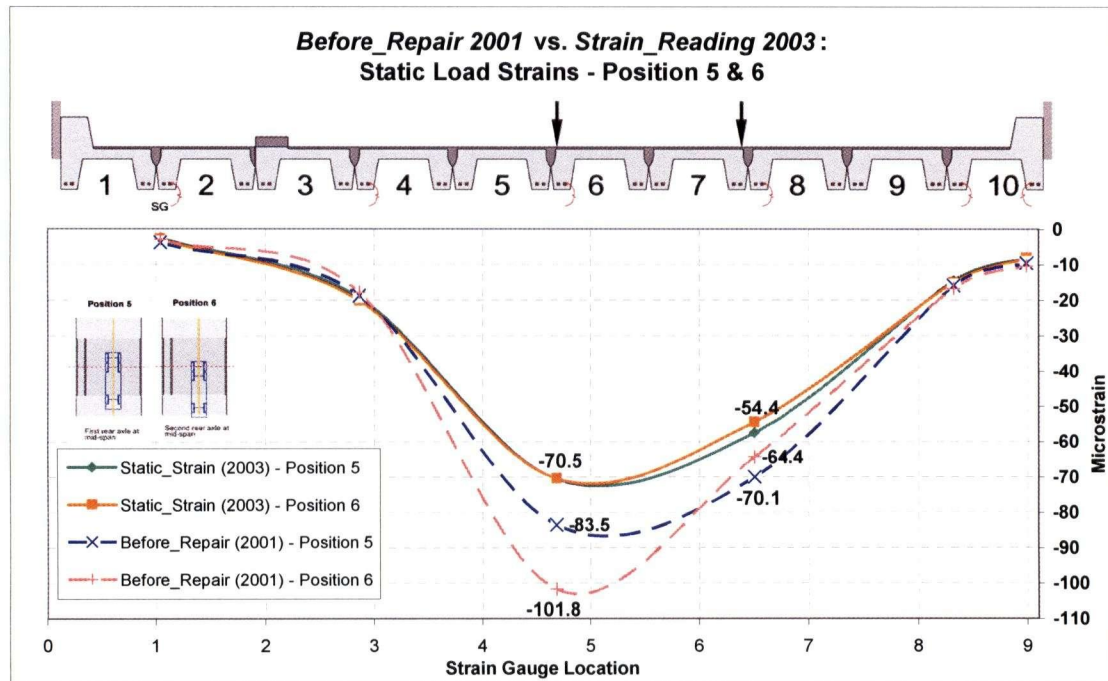


Figure 4-23 Comparison between 2001 and 2003 Field Test (Static Load) - Load Position 5 & 6

Figure 4-23 is the comparison results for Load Position 5 & 6; the truck position is on the middle of the roadway, so SG#3 is expected to give the largest reading. The maximum static strains indeed came from SG#3; but for the 2001 testing, the strain value under Position 5 and 6 were differed by almost 20  $\mu\epsilon$  (83.5  $\mu\epsilon$  for Position 5 vs. 101.8  $\mu\epsilon$  for Position 6). Regardless the abnormal difference between the two 2001 static strains, the SG#3 values from 2003 are still less than the smaller of the two by 13  $\mu\epsilon$ . This shows that the performance of Girder 6 has significantly improved by the GFRP reinforcement. As for the second large SG#4, the 2001 results still showed some difference between the two positions, although not as significant ( $\sim 5 \mu\epsilon$ ); but this time the value for Position 5 became the larger one. Again, both values from 2003 testing were smaller even if the lower Position 6 value was used (see Figure 4-23). In fact, similar to Position 1 & 2, all the static strains from the 2003 testing results were either smaller or equal to the 2001 results. Significant differences were shown on the strain gauges with larger strain readings. The result from this set of loading positions again

concludes that the new retrofit system works very well; girder 6 and 8 showed much better load carrying capacity than the time before they were repaired.

The results from Position 5&6 seems to be in conflict with the conclusions drawn from Position 3&4; the speculation about the early de-bonding could not stand if based on Position 5&6's comparing results. Due to the concerns on the accuracy of the 2001 Position 3&4 data, and the fact that SG#2 was malfunctioning during the 2002 field testing, comparisons made based on Position 3 & 4 data are less reliable. After considering all the factors, it is concluded that besides girder 4, the performance of all other four instrumented girders have improved significantly with the GFRP reinforcement. In terms of the durability of GFRP, all test results showed there were not much changes after 20 months of field service, so it is so far satisfying.

The next section is to present the comparisons made with Rolling Load testing results to see if the results match with the Static Load testing results. If the results match, the evaluation of the *sprayed FRP* repair method and the long term performance of the material GFRP can be further confirmed.

#### **4.5.2 Rolling Load Test Results**

For Rolling Load results, the comparisons will be made by observing the Time-Strain Curves from each field test directly, according to the three loading positions. General observations on the time-strain curves will first be discussed; then the comparisons 2002 vs. 2003 and 2001 vs. 2003 will be presented in the following sub-sections.

As can be observed from all the Rolling Load plots, the time-strain curves from the "critical girders" (i.e. the girders located right beneath the truck axles) all follow a general pattern in shape; using 2003 Roll I as example: there are always two distinct "peaks", with the smaller one ("Peak 1" in Figure 4-24) always appears first, and the magnitude is about  $1/2 \sim 2/3$  of the bigger peak ("Peak 2"); the bigger "peak" almost always has two "horns" at its tip section (see Figure 4-24). The observed pattern actually make sense: the first small peak happened when the front axle passing through the mid-span; the following big peak is caused by the heavier rear axles, and two rear-axles give two "horns". The rear axles are very close to each other so that the elastic strain value did not have enough time to decrease much, and created the horn-like shape at the tip of "Peak 2". Also, the weights of the two rear axles are equal, so if there were no influence from noise or lag, the two "horn

tips” should give similar strain value. As for the curves from the “less critical girders”, because of further distances from the concentrated loads (axle loads) and the load-sharing mechanisms between the girders, their shapes are much more “smoothed out”; nonetheless, the “tips” (if recognizable) still occur at the same time as the critical girders. Therefore, the comparisons will be made only based on the “critical girders” results (also for clarity).

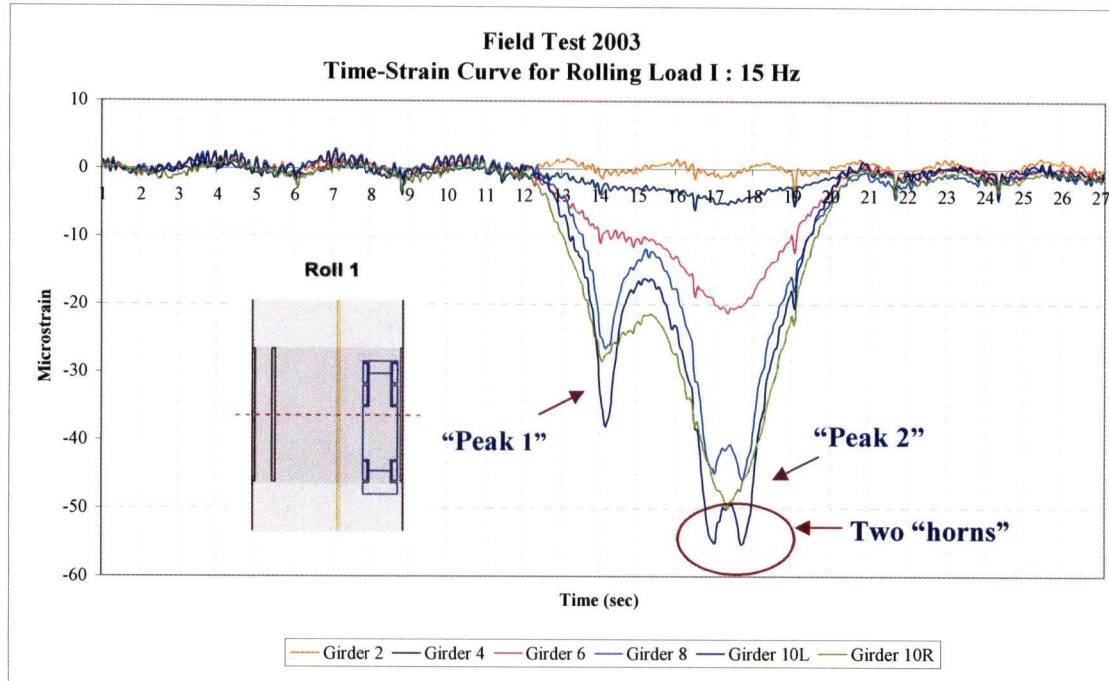


Figure 4-24 Example of Rolling Load Time-Strain Curve Pattern – 2003 Roll I

Another finding from the plots is that, for the time after the truck left the bridge, “residual strains” are often seen in many of the plots, even though theoretically, the strain of the girders before and after the loading of truck should be the same. Either not enough time was given for the bridge to return to its original state, or the bridge girders were not truly elastic. Therefore, the “initial strain” is calculated based on the strains before the truck enters the bridge, unless not enough data during that period of time, then the “after truck” values are used.

As mentioned earlier, original data from 2001 and 2002 testing were gathered and re-analyzed for consistency; but the 2002 Rolling Load data were not original; they had all been modified to have a time-range of 15 seconds. Since the comparisons will be made by visually observing two plots, the time-scale of the 2001 and 2003 plots were also modified to be around 15 seconds for the ease of comparison. “Roll I”, “Roll II”, and “Roll III” will be used to refer to the three loading positions.



#### 4.5.2.1 After\_Repair 2002 vs. Strain\_Reading 2003

Similar to the static load comparison, ideally we would like to see that the time-strain curves for the 2002 and 2003 data and their maximum strains are similar, which means the GFRP reinforcement is working well under field condition.

For Roll I, the truck ran through the bridge along the upstream curb, so girder 8 to 10 are the “critical girders”, and SG# 4, 5, 6 are plotted for comparisons for Position 1 (see Figure 4-25 next page). The two plots appear to be quite different. First, regarding the “order of maximum strains”, 2003 plot shows  $SG\#5 > SG\#6 > SG\#4$ ; but 2002 plot shows  $SG\#4 > SG\#5 > SG\#6$ . If the truck axles were located like what are shown on Figure 4-25, and assuming all girders in similar “health condition”, then SG#5 is expected to give the largest strain readings; SG#4 and SG#6 are in similar “relative positions” to the truck axles, so the two are expected to give similar strain readings. By the way, curve shape for SG#6 is different from all other strain gauges; it does not show the two “horns” at the tip; this could be due to the hardening effect of the concrete curb.

The 2003 results followed what was expected, but the 2002 results did not. 2002 testing had SG#4 showing the largest strain; two possible causes: (1) during the 2002 field test, the truck was not running as close to the concrete curb as possible, so the truck axles were closer to SG#4, and therefore Girder 8 got loaded higher; (2) Girder 8 were in more severe deteriorating condition than Girder 10. Reason 2 is less likely because the 2002 field test was performed right after the completion of the repair, and “theoretically” all girders should be back to their “healthy state”, unless the GFRP layers were not applied properly and de-bonding happened right away. Nonetheless, from the 2003 result, SG#4 gave the smallest maximum strain within the three (SG# 4 to 6), which showed that health condition of Girder 8 should not be worse than Girder 10.

If the three maximum strain values plotted in Figure 4-25 are compared directly, besides SG#4, the 2003 values are much larger than the 2002 values for SG#5 and 6. However, we actually can not conclude anything based on this comparison result, because the two field tests performed the rolling load tests under different speed. As mentioned earlier, the faster the truck running across the bridge, the smaller the strains will be experienced by the girder. Clearly from Figure 4-25, it took less than 5 seconds for the truck to run through the bridge during the 2001 Roll I testing, but the time spent during the 2003 Roll I testing was around 8 seconds. In terms of speed, the truck was moving at



around 11km/hr during 2001 Roll I, and around 6 km/hr during 2003 Roll I. Therefore it is not surprising to see the 2002 testing results gave lower strain values.

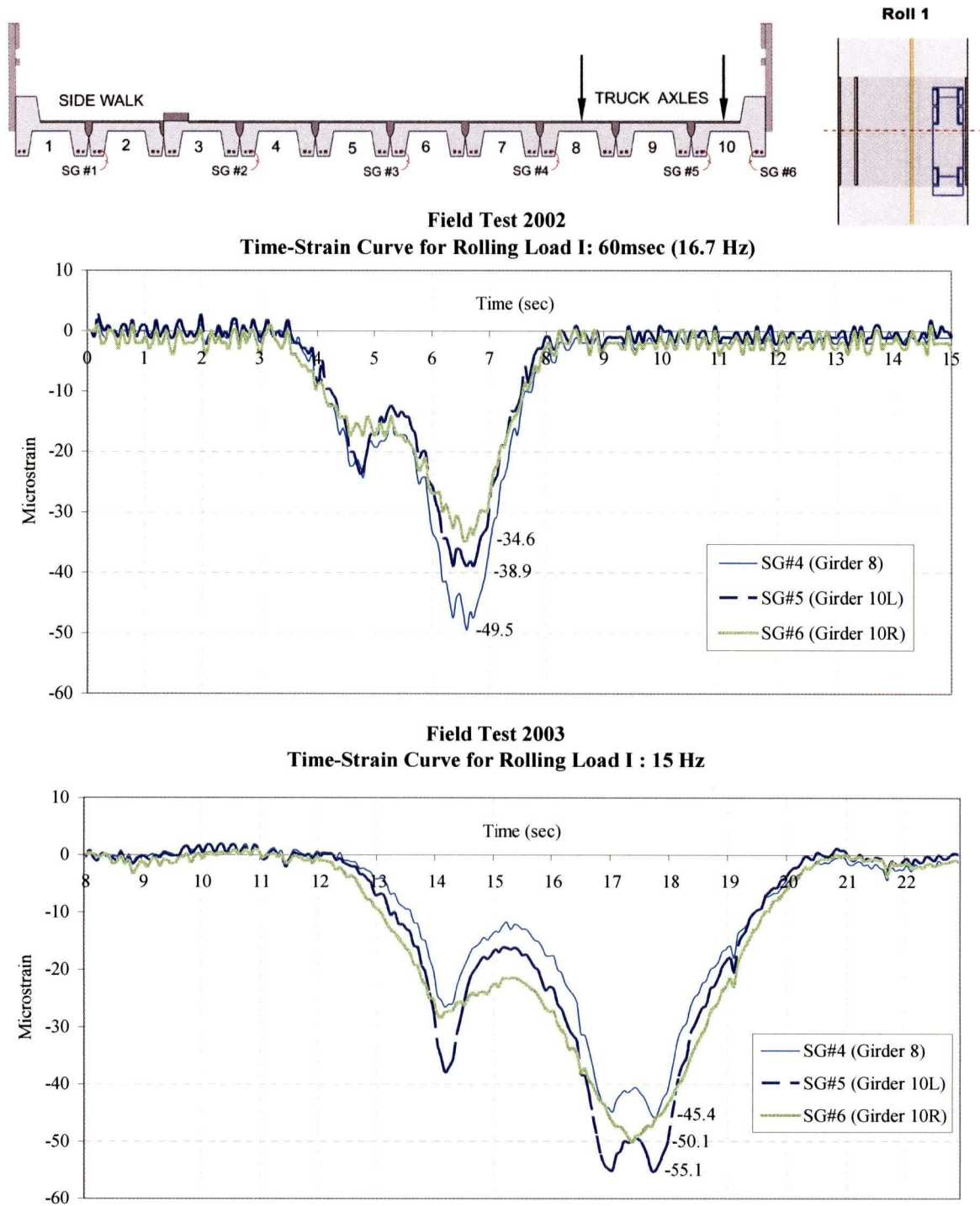


Figure 4-25 Comparisons between 2002 and 2003 Rolling Load Test - Position I

For Roll II, the truck traveled along the curb on the down-stream side, so the readings from strain gauges on girder 4 and 6 (SG#2 and 3) are plotted for comparison, and their maximum strain values are marked on plot (see Figure 4-26). SG#2 was not working properly during 2002 testing, so the time-strain curve was only plotted for SG#3 for 2002 testing.

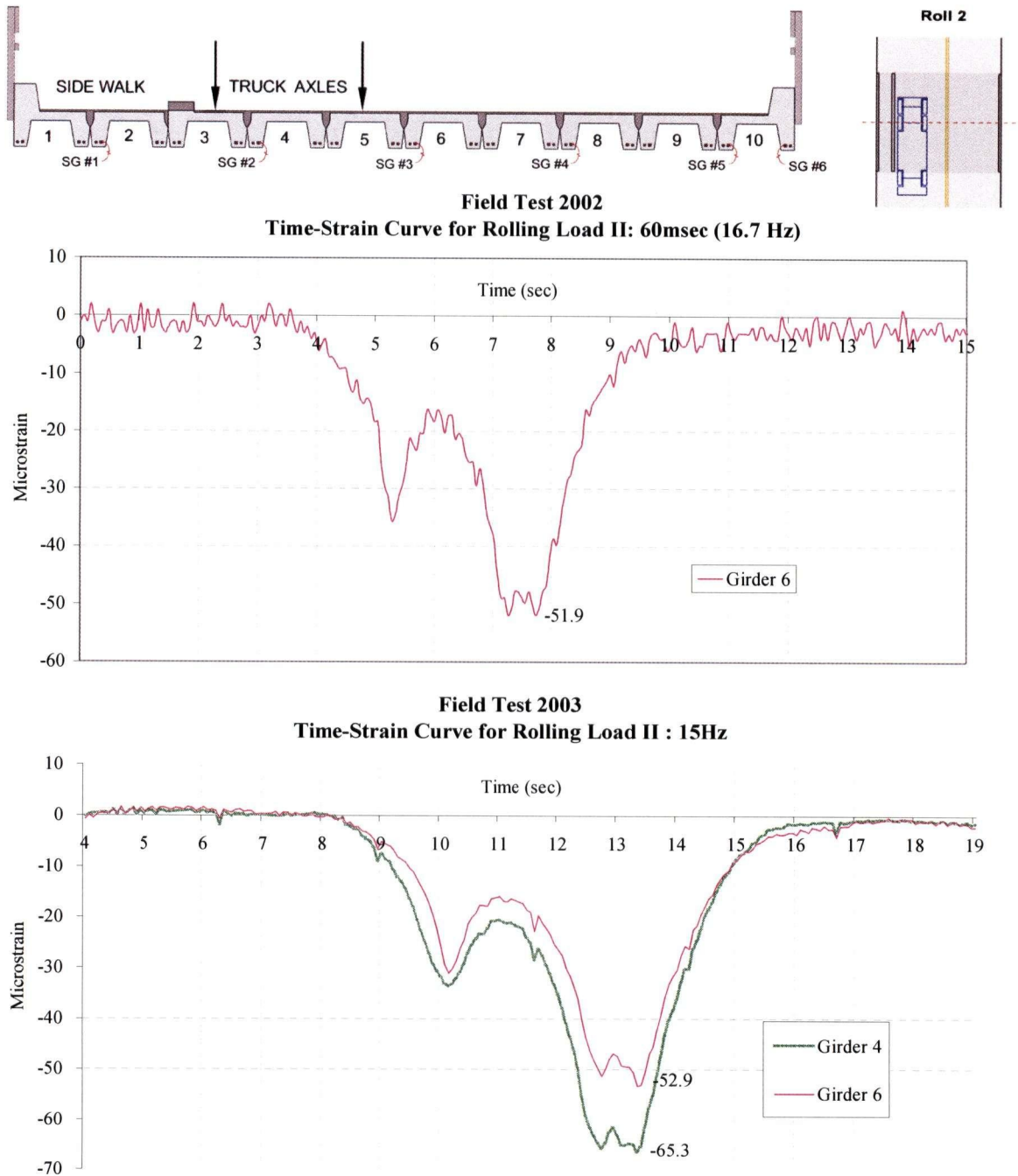


Figure 4-26 Comparisons between 2002 and 2003 Rolling Load Test - Position II

As can be observed from Figure 4-26, the traveling time for 2002 Roll II was about 6.5 seconds, and the traveling time for 2003 Roll II was about 7 seconds. Compared to Roll I, the traveling times for this set of data are much closer, and therefore the comparisons for Roll II is more meaningful. As can be seen from the figure, the shape of the curves for SG#3 from both field tests are similar, and the maximum strain value for 2002 is  $51.9 \mu\epsilon$ , and for 2003 is  $52.9 \mu\epsilon$ ; the strain values are about the same. Consider the traveling speed in 2002 was higher, we can conclude that there is no increase in strains for Safe Bridge (especially Girder 6) under Load Position II.

Other observations from the figure further reinforced this conclusion: (1) regarding the “tip value” of the smaller “peak” (which caused by the front axle), the 2002 value is actually a little greater than the 2003 value; (2) the two “horns” of 2003 peak are not equal; the  $52.9 \mu\epsilon$  value is obtained from the “higher horn”, which could be magnified by lagging, as can be observed from the plot. Roll II results show that the performance of the GFRP reinforcement is the same over 20 months period in field condition.

For Roll III, the truck was running directly above girder 6 and 7, so SG#3 in Girder 6 and SG#4 in Girder 8 are plotted for comparison (see Figure 4-27). Clearly from the 2002 Roll III plot, the data had been reversed (for unknown reason), as the smaller peak induced by the front axle occurs after the maximum peak. It is unlikely that the truck was running backwards. Nonetheless, this should not affect the comparison. In addition, the two curves for SG#3 and SG#4 for 2002 Roll III are very close to each other. It is possible that during the 2002 Roll III testing, the truck was running a bit towards the up-stream side of the bridge, so the two axles were right in between the locations of SG#3 and SG#4; whereas during 2003 Roll III, the axles were closer to SG#3, so that the 2003 SG#3 maximum strain is much larger than its SG#4 value.

Regarding the traveling time, different from the above two sets (Roll I and Roll II), the truck ran slower during the 2002 Roll III test; the traveling time for 2002 was about 9 seconds and about 7 seconds for 2003. If converting the time to speed, the difference between the two-time testing is about 1.5 km/hr (5.5 km/hr to 7 km/hr).

When the two plots are compared, the values for SG#3 (Girder 6) are about the same for the two testing; but for SG#4, the 2003 maximum strain is actually less than the 2002 value by almost  $10 \mu\epsilon$ . Taking the effects from truck position and speed, as mentioned above, the strain values should be about the same for the two field tests.

Overall, regarding the GFRP field performance, no conclusion can be drawn from Roll I; but both Roll II and Roll III showed that no significant changes in strain between the two field testing. Therefore, we can at least conclude that Girder 4, 6, and 8 are in same health condition after 20 months of field usage, so field performance of GFRP repair is satisfying

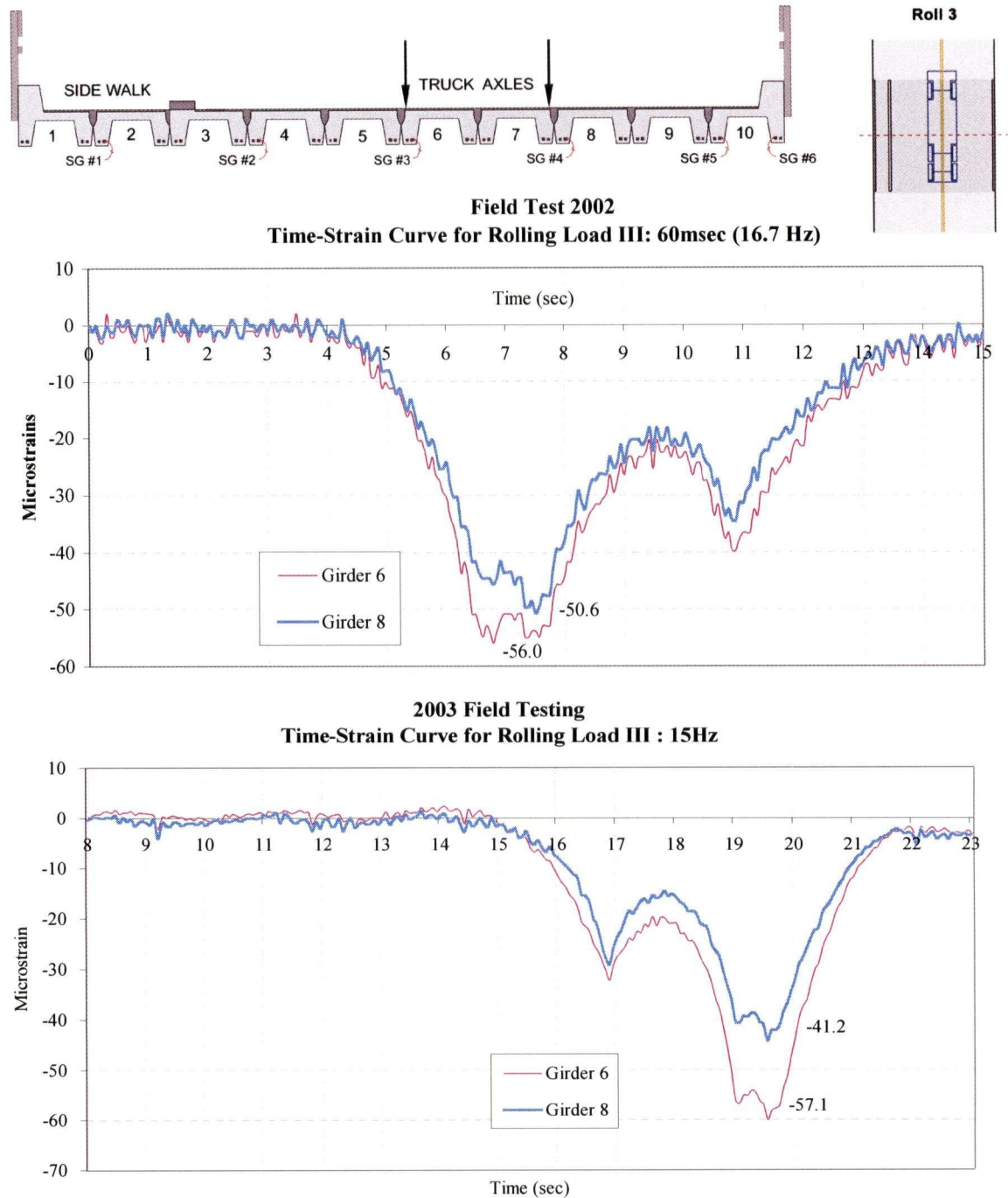


Figure 4-27 Comparisons between 2002 and 2003 Rolling Load Test - Position III

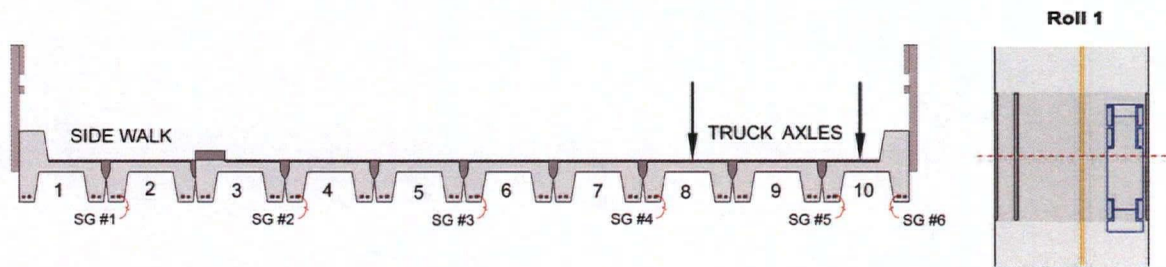
#### **4.5.2.2 Before\_Repair 2001 vs. Strain\_Reading 2003**

When re-analyzing the 2001 data, it was found that the 2001 Rolling Load tests used much longer recording time; the time for the truck to cross the bridge was longer as well. Therefore, the 15-seconds time scale is not suitable (too short) for the 2001 data. As a result, the time-scale is adjusted for both 2001 and 2003 data again for better comparison results. Again, it was aimed to use similar time-scale for the two plots from the two field testing.

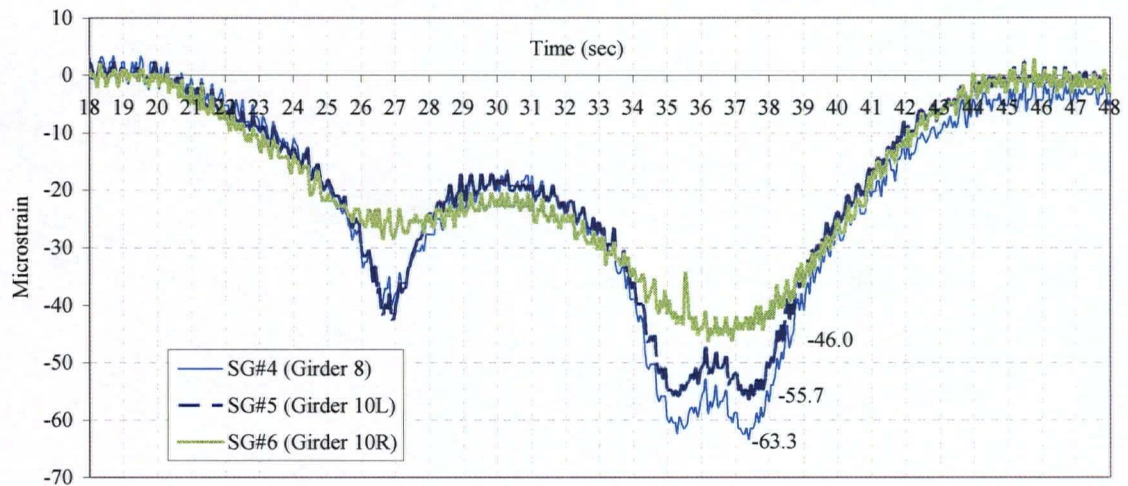
For Roll I (see Figure 4-28 next page), as explained in Section 4.5.2.1, SG#5 supposed to give the largest strain, and SG#4 and #6 show similar maximum strain values, if the truck was running though the bridge as close to the concrete curb as possible. However, just like the 2002 Roll I plot, the 2001 Roll I plot show the order of SG#4>SG#5>SG#6. Therefore, the position of the truck must have been more towards the center of the road, so that Girder 8 became most heavily loaded; or, before the repair, Girder 8 was in worse deteriorating condition.

Besides the possible difference in actual truck position, the bigger problem is again, the running speed. Clearly from the two plots in Figure 4-28, the traveling time spent during the 2001 field testing for Roll I was way longer than the time spent in 2003 testing. It took about 23 seconds (equivalent to 2 km/hr) for the truck to pass Safe Bridge in 2001 testing, compared to the 8 seconds (6 km/hr) in 2003. Since the relationship between truck speed and strain reading is not linearly proportional, there is no way to adjust the strain values for the speed difference. With such significant difference in speed, this set of data (2001 Roll I vs. 2003 Roll I) can not be compared. If we ignore the effects from vehicle speed and position, on surface, the strain values obtained from 2003 testing are way smaller for SG#4, about the same for SG#5, and a little bigger for SG#6. Nonetheless, the comparison itself is problematic that no valid conclusions on the performance of the new repair technique can be drawn here.





**Field Test 2001**  
**Time-Strain Curve for Rolling Load I: 60msec (16.7 Hz)**



**Field Test 2003**  
**Time-Strain Curve for Rolling Load I : 15 Hz**

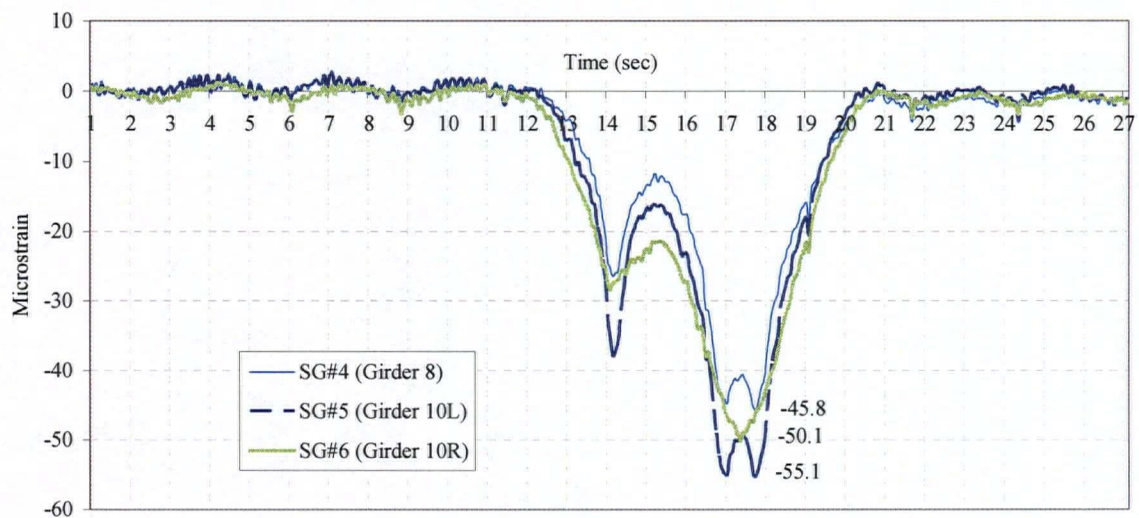
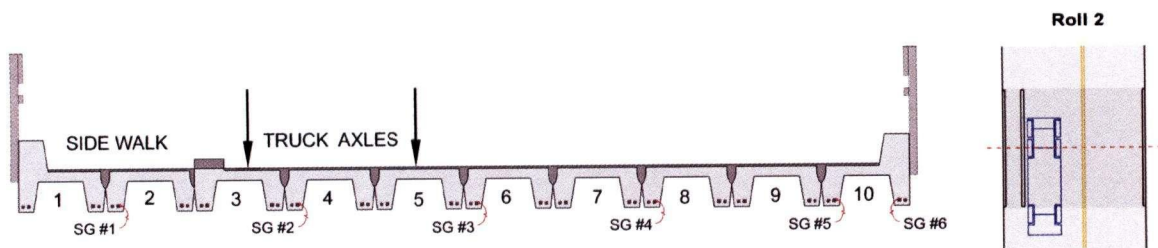


Figure 4-28 Comparisons between 2001 and 2003 Rolling Load Test - Position I

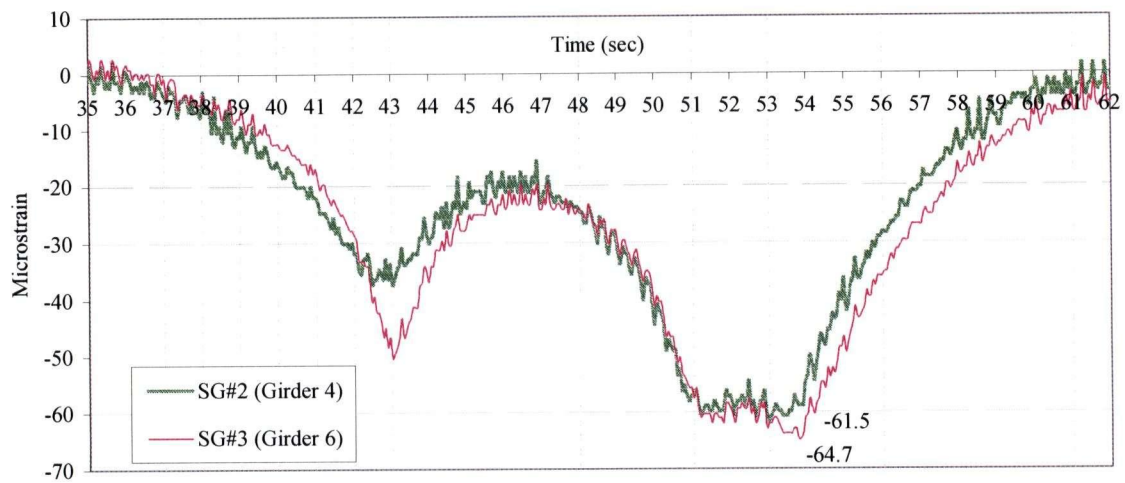
For Roll II (see Figure 4-29), similar problems; the traveling time in 2001 testing was 23 seconds, and the speed was less than half of the 2003 testing speed. Also, for the 2001 plot, it was surprising to see that SG#3 in Girder 6 actually gave a little bit larger strain value than SG#2. Therefore, regarding the exact truck position, it is believed that the truck was not running as close to the downstream curb as possible during the 2001 testing; because if it did, SG#2 should have given larger maximum strain reading than SG#3, according to their relative positions to the truck axles. If the truck was driven more towards the center of the roadway, each of the axle could be located right above SG#2 and 3, and the results would be like what is observed on the 2001 Roll II plot. Nonetheless, since 2001 testing was done before the repair, Girder 6 could be in worse deteriorating condition than Girder 4, and resulted in what is seen here. Again, the Roll II comparison also can not give much information regarding the performance of the new repair method.

For Roll III (see Figure 4-30), the result seems "good"; both testing have the largest strain reading occur at SG#3, and then SG#4, as expected. Also, both readings from 2001 testing are much greater than (over 10  $\mu\epsilon$ ) those from 2003 testing. However, it took only 7 seconds for the truck to run through the bridge during the 2003 testing, but the time spent during the 2001 testing was 13 seconds, almost double the time. Since the truck was moving much slower during the 2001 testing, it is not surprised to see greater strain readings. We can not tell how much the slower traveling speed contributes to the larger strain readings.

To conclude, strictly speaking, the comparison between *Before\_Repair 2001* vs. *Strain\_Reading 2003* Rolling Load results can not prove that the performance of the girders in 2003 is better than before they were reinforced because there were too many variables. Significant difference in truck traveling speed is a sure one; it is also likely that the exact truck positions of Roll I and Roll II were not the same.



**Field Test 2001**  
**Time-Strain Curves for Rolling Load II: 60msec (16.7 Hz)**



**Field Test 2003**  
**Time-Strain Curve for Rolling Load II : 15Hz**

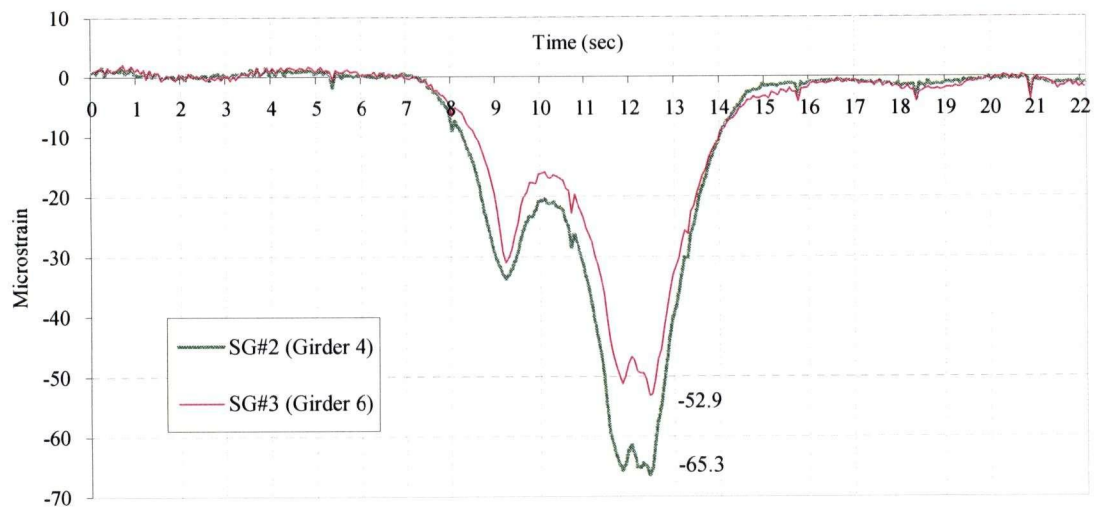
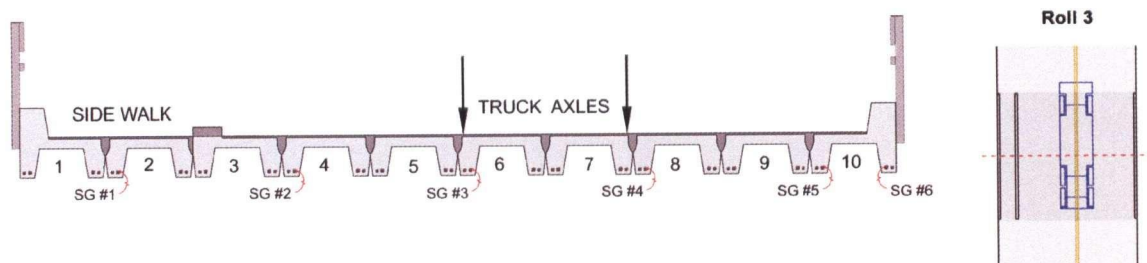
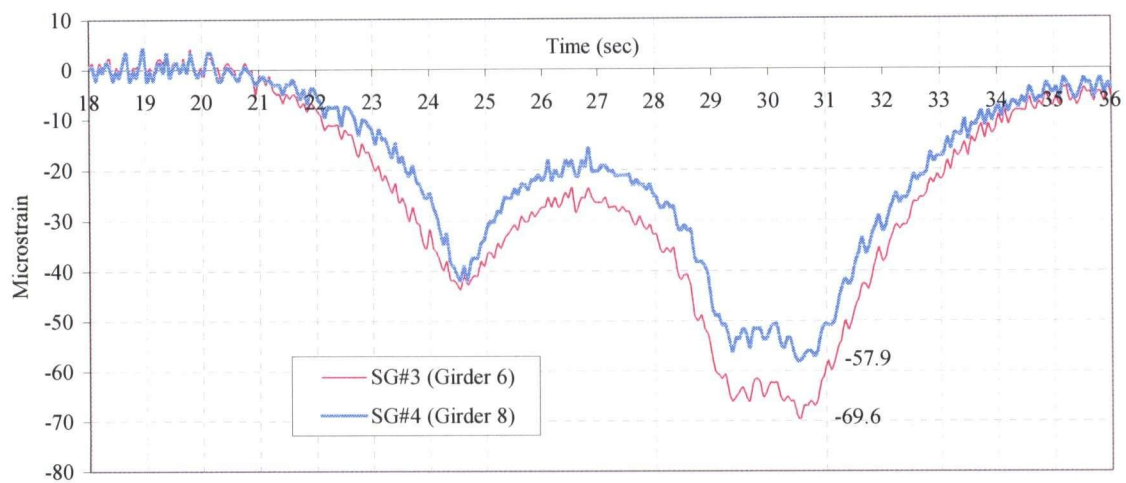


Figure 4-29 Comparisons between 2001 and 2003 Rolling Load Test - Position II



**Field Test 2001**  
**Time-Strain Curves for Rolling Load III: 60msec (16.7 Hz)**



**2003 Field Testing**  
**Time-Strain Curve for Rolling Load III : 15Hz**

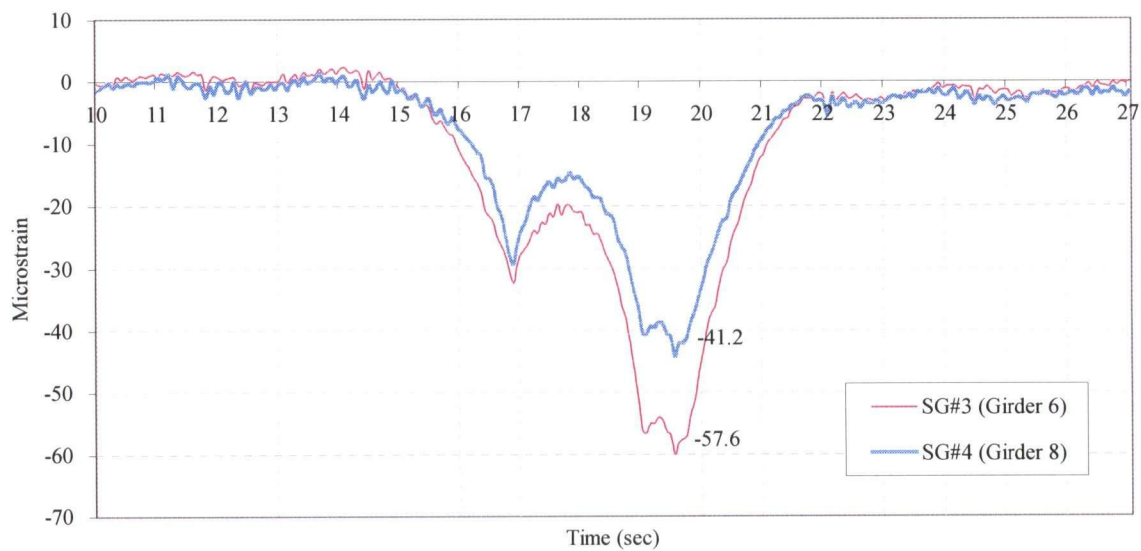


Figure 4-30 Comparisons between 2001 and 2003 Rolling Load Test - Position III

#### 4.6 Data Comparisons between Different DAQ Systems

This section is for the second objective of the 2003 field testing: to test out and gain field experience with *WebDAQ/100*, a data acquisition unit with IP built-in function. *WebDAQ/100* has many functions that are suitable for the use of remote control and monitoring. It will be ideal that eventually Safe Bridge can be monitored remotely from Vancouver. Therefore the study of *WebDAQ/100* is part of the learning process for SHM. This is the first time for the UBC Material team to use *WebDAQ/100* for bridge field testing; the focus this time is on the “correctness” of the measurements, the internet access control, and to test out the automatic e-mailing function. The triggering function was not used so the start/stop of measurement was controlled manually by the technician. *WebDAQ/100* was located purposely in a distance from the bridge and the signal conditioner, and connected with the signal conditioner by wires. The team would like to know if this set-up would affect the strain readings. Therefore, the results gathered from *WebDAQ/100* will be compared with the results from *I/O Tech DaqBook* and presented in this section.

The sampling rate used for the Static load tests was 10 Hz and for Rolling load tests was 30 Hz; same as the *I/O TechDaqBook*. The raw data from *WebDAQ/100* has a similar format as the data from *I/O TechDaqBook*; the first column records the time, and the rest of the columns record the voltages detected from each strain gauge. Therefore, it was planned to apply same processing procedures to the *WebDAQ/100* data and then compared the results from both DAQ systems. However, during the processing of data, it was discovered that base-line-correction could not be applied to some sets of data (Position 2, 4, and 6) because both the beginning and end sections were missing. Even for the other three sets of data, the beginning data got cut-off as well; the zeroing was done based on the readings after the truck left the bridge. All six “half-processed” plots for *WebDAQ/100* data are attached in Appendix V, one can clearly see what just described.

The cause for the incompleteness in data was not clear. Possible reasons were two. Since *WebDAQ/100* and the technician controlling it were located indoor, the technician could not see the testing truck and Safe Bridge; three people were standing in distance to pass the message to tell the technician when to start and stop the collecting of data. Even though the distance was not that far and it should have taken less than a minute to pass the message through, mistakes could have made during the process; this could have contributed to the data error.



Another reason could be related to the system itself. Due to unfamiliarity with the system, maybe there were automatic cut-off set-up as default in *WebDAQ* that we were not aware of. As mentioned earlier, originally the team was also interested in trying the auto-emailing function, which had been tested in lab in UBC and succeeded. Therefore, before the truck load testing started, the technician spent a little time in the set-up for auto-emailing. Unfortunately, due to time-limit, the auto-emailing set-up was not successful. This could have relate to the data error because for auto-emailing, only certain size of data can be sent each time, which means the time period is limited to a certain range, based on the sampling rate used.

Nonetheless, the purpose of the comparison is to see if strain readings collected by *WebDAQ/100* is the same as the other DAQ system. For this field testing, both DAQ systems were connected to the same signal conditioner. Theoretically speaking, if the signals were sent from the same conditioner, the readings recorded by the two systems should be similar. In light of this, the author decided to compare the raw data from both DAQ systems directly (after apply the gauge factor). The comparisons for both the static load tests and rolling load tests are presented in the following two sub-sections.

One thing to be notice is that *WebDAQ/100* only collected data from five strain gauges instead of all the six during the 2003 field testing. This was because, base on the data collected during the 2002 field testing, it seemed that one strain gauge (SG#2) was malfunctioning. It was the first time for the technician in charge with *WebDAQ/100* to join the Safe Bridge field testing, and he was told that one strain gauge was probably broken and only five would work. As a result, only five sets of wire cables were prepared for *WebDAQ/100* for the 2003 testing. Nonetheless, the strain gauge left out from measuring was SG#6, the one in Girder 10 under the concrete curb. Girder 10 has strain gauges installed in both "legs", so it was believed that missing the readings from SG#6 would affect the testing results the least.

#### **4.6.1 Static Load Testing Results**

The raw data from *I/O TechDaqBook* was already in microns, which means the technician in charge of *I/O TechDaqBook* had applied the gauge factor to the data already. The raw data of *WebDAQ/100* was in voltage, so the author applied the gauge factors to the data. The comparisons were done on all six sets of data. In the following, Position 1 and Position 4 results are randomly picked to represent

the comparison between the two DAQ systems. Note that the curve for SG#6 is removed from the *I/O TechDaqBook* plot for clarity. Please see Figure 4-31 for Position 1 data comparisons.

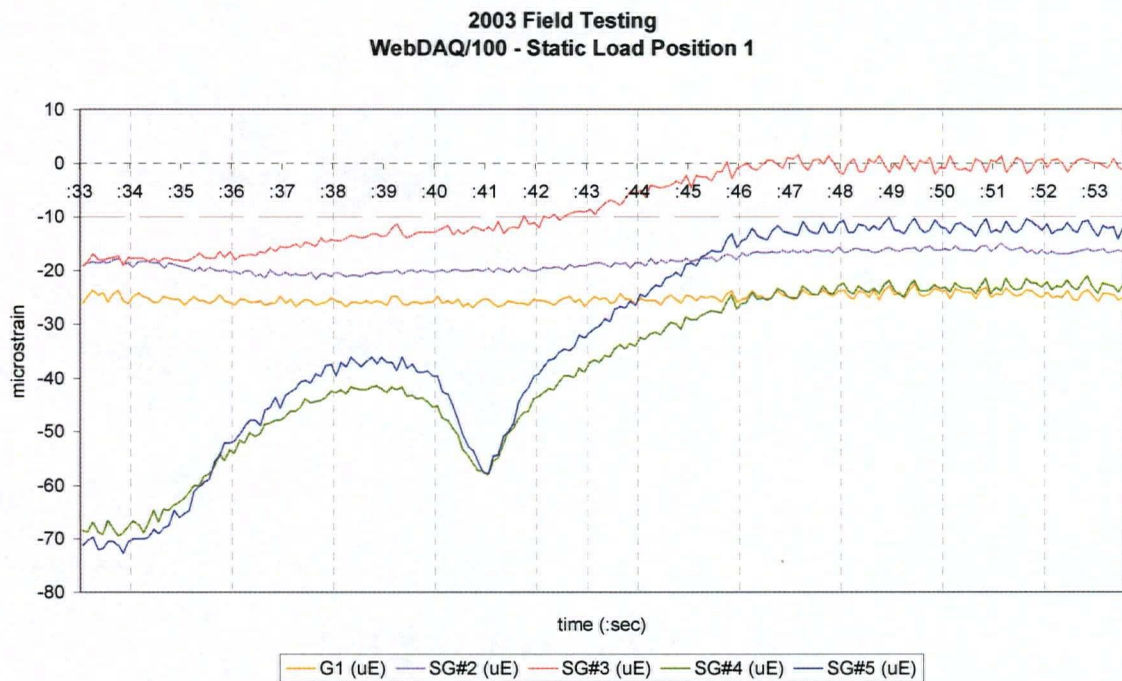
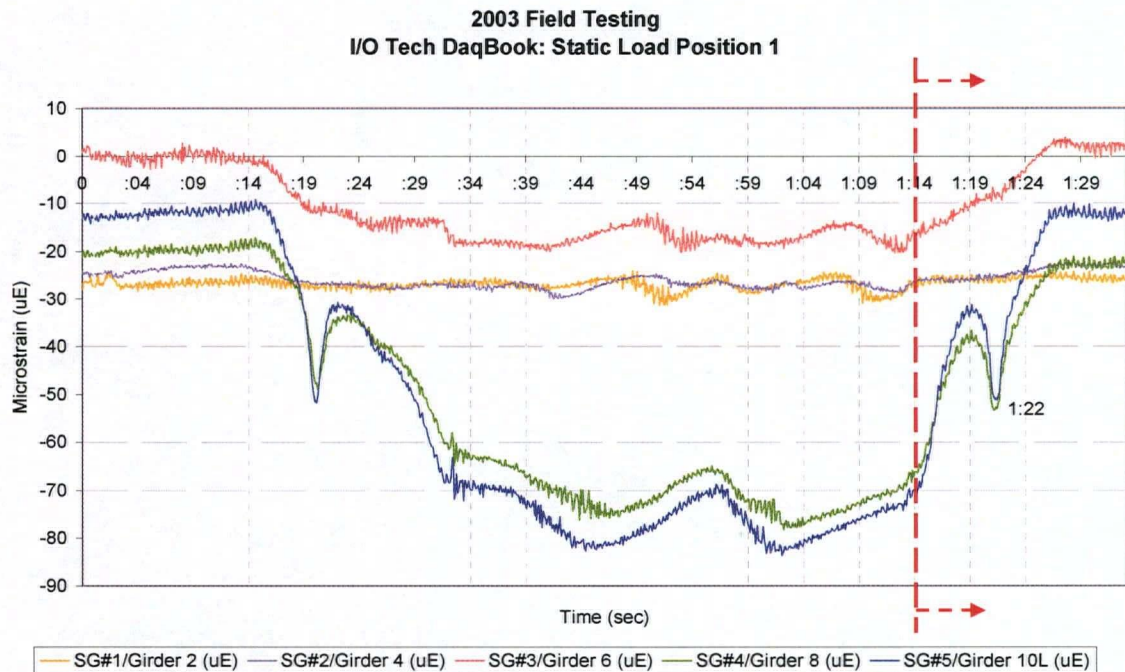


Figure 4-31 *I/O TechDaqBook* Data vs. *WebDAQ/100* Data: 2003 Field Test Static Position 1

Clearly from the plot, the WebDAQ/100 plot missed a significant portion of data. Nonetheless, the rest of the data can still be compared. Using the tip of the blue curve (SG#5) as a reference, one can estimate that the WebDAQ/100 started recording at around “ 1:14 ” of I/O Tech DaqBook’s time scale. When comparing this portion of the data, one can find that the strain readings are very similar for both DAQ systems, except for the SG#2 readings (purple line), the I/O TechDaqBook’s readings were all about 5  $\mu\epsilon$  higher. Following is the results for Position 4.

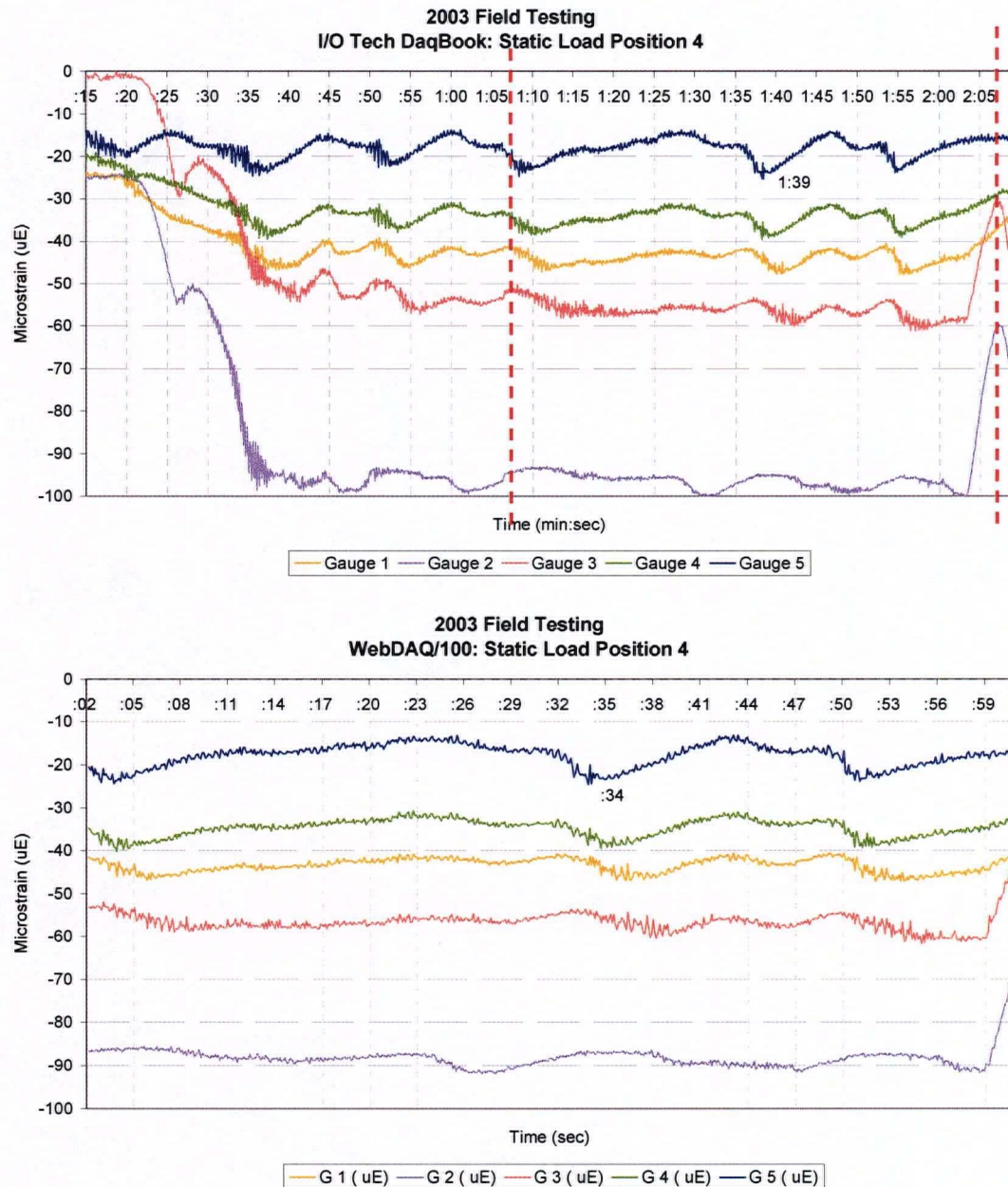


Figure 4-32 I/O TechDaqBook Data vs. WebDAQ/100 Data: 2003 Field Test Static Position 4

As for the Position 4 comparisons (see Figure 4-32), the measuring time period that *WebDAQ/100* recorded was probably from 1:07 ~ 2:05 based on the time scale of *I/O TechDaqBook*. Again, when observing the two plots, the magnitude and the fluctuation of the curves are almost identical for the two DAQ systems, except for SG#2; readings from *I/O TechDaqBook* of SG#2 (purple line) are almost 10 microns higher than that of *WebDAQ/100*. In fact, similar observations were found in all six sets of the static load comparisons: all the time-strain curves from the strain gauges are almost identical for the two DAQ systems, except for SG#2; and it is always that the readings from *I/O TechDaqBook* is about 5 to 10  $\mu\epsilon$  higher than the *WebDAQ/100* SG#2 readings, depending on the magnitude of strain it experienced under the particular load positions; the larger the readings themselves, the larger the difference, but the maximum is about 10 microns. SG#2 also happens to be the malfunctioning strain gauge during the 2002 field testing.

Based on the observation, it is possible that, either a wrong gauge factor was used for SG#2 - that is why the difference between the two DAQ systems is proportional to its own magnitude and it is always the *I/O Tech DaqBook* shows the larger values; or there are indeed some kind of problem with SG#2. Nonetheless, it is clear that *WebDAQ/100* is providing the "correct measurements". Considering all the possible environmental noise effects and the fact that *WebDAQ/100* is using a longer lead wire for data transfer, the comparison results are very satisfying; one can conclude that *WebDAQ/100* is suitable for low-frequency monitoring.

The next section will show the comparisons of the rolling load results, to see if *WebDAQ/100* still performs well when a higher sampling rate is used.

#### **4.6.2 Rolling Load Testing Results**

With the experience with the static load results, the first thing performed with the rolling load results was to check the "completeness" of the *WebDAQ* data for all three sets of rolling load tests. Compared to the static load sets, the rolling load data are much more complete even though Roll I still got the beginning portion cut-off, and Roll III had the ending portion missed. Nonetheless, base-line-correction can still be applied to all three sets of data; the three processed plots for *WebDAQ/100* Rolling test results are attached in Appendix VI. Since Roll II is the only set of data completely show the moving load from entering the bridge until leave, Roll II will be used here as the example for the comparison between the two DAQ systems (see Figure 4-33). As mentioned in earlier section, the



original sampling rate for *I/O Tech DaqBook* was 60Hz; the sampling rate for *WebDAQ/100* was 30 Hz; therefore the 60 Hz data needed to convert to 30 Hz first. The two graphs were modified to have similar time-scale for easier comparison.

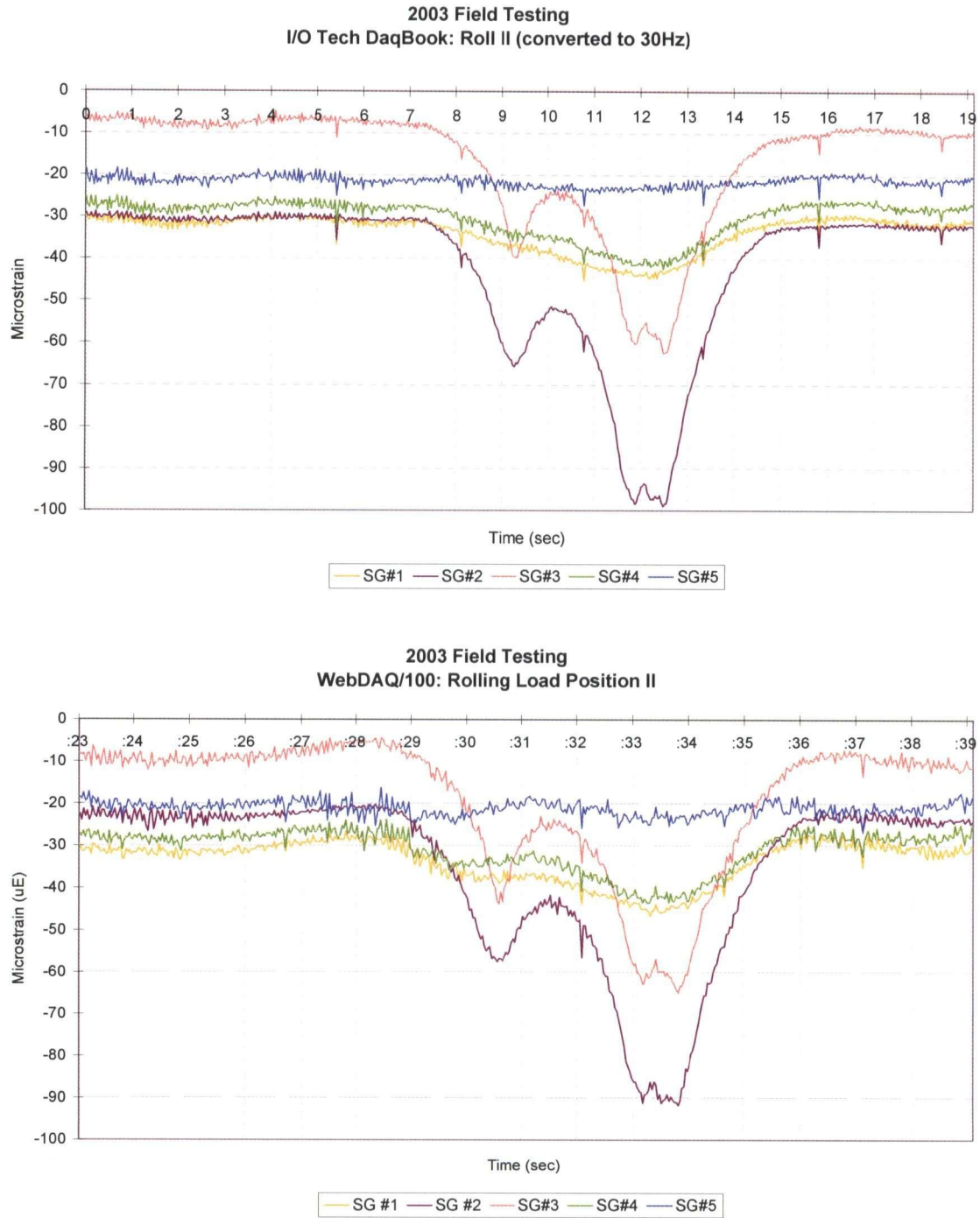


Figure 4-33 *I/O TechDaqBook* vs. *WebDAQ/100*: 2003 Field Test – Rolling Load Position II



As can be observed from Figure 4-33, the two graphs give very similar time-strain curves, even the locations of the “little spikes” (due to lagging) are the same, which show that the strain readings obtained from both DAQ systems are similar. The only time-strain curve that differed more between the two systems is again from SG#2; the *I/O Tech DaqBook* data are about 10  $\mu\epsilon$  higher than that of *WebDAQ/100*. The *WebDAQ/100* data do seem to fluctuate more and the *I/O Tech DaqBook* curves are more “smooth”; this could be due to the fact that the *I/O Tech DaqBook* data were averaged to decrease its frequency from 60Hz to 30 Hz, and the averaging step more or less average out the fluctuation.

The comparisons were applied to all three rolling load test positions and the observations were similar. Possible causes of the greater difference in SG#2 have been discussed in the Static load section.

Overall, for both the static load and rolling load tests, the results obtained from *WebDAQ/100* are close enough with the data from *I/O Tech DaqBook*. The strain measurement function with *WebDAQ/100* for field testing is satisfying; the online interface worked as well (will be covered more in Chapter 6). *WebDAQ/100* can be the potential data acquisition system for Safe Bridge to perform continuous, remote- online monitoring in the future.

---

## **Chapter 5**

### **Second Field Testing (2005)**

---

The second field testing covered in this thesis was performed on May 30, 2005. The main purpose for this field testing was to gain hands-on field experiences with the long-gauge fibre optic sensor (LG FOS), and to continue the checking and study of the long-term performance of the sprayed FRP. This field testing is hereby referred to as "*FOS\_2005*". Specialist was sent from ISIS Canada to instruct the instrumentation and data gathering with the FOSs; testing results were sent to FOX-TEK Inc. for analysis.

Similar to Chapter 4, in this chapter, discussion of sensor choice and locations will first be given, then the information about the loading truck and loading positions used during *FOS\_2005*, and finally the analysis of data and the comparison of testing results. Note that during the 2005 testing, data were collected only from the fibre optic sensors; the strain gauges were not used. Again, details about the instrumentations, including the sensors and the data acquisition system used for *FOS\_2005*, will be given in Chapter 6, when Safe Bridge project is discussed from a SHM point of view.

#### **5.1 Sensor Locations**

There are total six long-gauge fibre optic sensors (LG FOSs) installed in Safe Bridge, and each of them is 5 meters long (i.e. gauge length = 5m). As mentioned in Ch 2, the major difference between the LG FOS and conventional strain gauges is that LG FOS measures the average strain over the gauge length, whereas foil strain gauges measure "point strains".

The reasons for choosing LG FOS to be installed on Safe Bridge are as follows. One major concern for the GFRP reinforcement is the occurrence of debonding (delaminations). When debonding of the composite occurs, the stiffness and strength of the girder will decrease; the stiffness is directly related to strain, and therefore strain was chosen to be the monitoring parameter. Also, debonding can happen at any place along the tension side of the girders; therefore, it was believed that the long gauge FOS will provide better monitoring on delamination of the reinforced girders, and with minimal influence from local stress concentrations. "Point-" type strain sensors are sensitive to local

stress concentration, which easily lead to false interpretation on the occurrence of delamination [166]. In addition, LG FOSs can be easily attached on the surface of the reinforcing FRP composite, which make the installation work fast and convenient.

The monitoring strategy is to have the strains measured on both the tension rebar and the GFRP layer; if the bonding between the GFRP laminate and concrete is perfect, the two materials should show same strain changes at their interface. Therefore, if the strain change measured from each source varies significantly, it may indicate the occurrence of de-bonding. The FOS strain readings will also be compared to its initial readings gathered when the LG FOSs were just installed to see if there will be significant increase on strain. It was decided to place the LG FOSs at two locations on a girder: one is parallel to the tension rebar on the GFRP surface, and the other is along the “mid-depth” of the girder “leg” (see Figure 5-1).

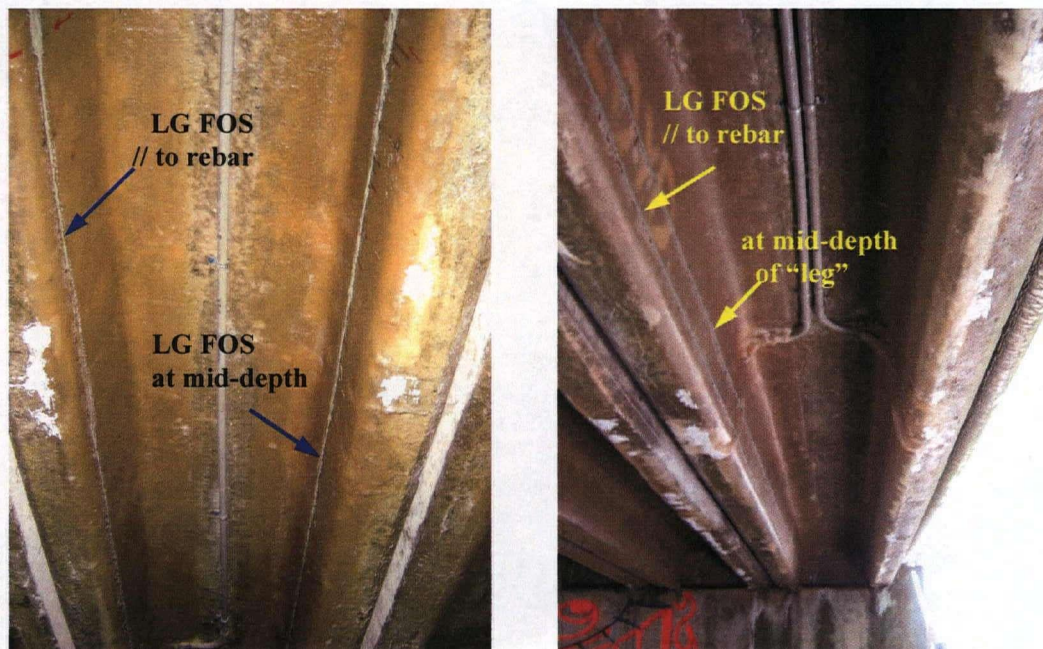


Figure 5-1 Photos of the 5 m-Long Gauge FOS Locations: (a) Girder 2 & 6; (b) Girder 10

Assuming the cross section of the beam remains plane and normal to the longitudinal axis, the LG FOSs located parallel to the steel rebar should experience similar longitudinal strain changes to the rebar. The “center” LG FOSs (the ones attached along the mid-depth of girder leg) are acting more like a reference point for their bottom counterparts; because they are closer to the neutral axis of the

cross section of the girder, the “center” LG FOSs should give smaller strain readings than the “bottom” ones parallel to the tension rebar.

Note that for girder 10, both the “center” and “bottom” LG FOSs were installed on the same leg of the girder. Girder 10 is the exterior girder of Safe Bridge and the right leg is beneath the concrete curb, the strain values from that right leg will be affected by the “hardening effect” from the much deeper cross section, and therefore it was decided to put both the LG FOSs on the inner leg. The LG FOSs were installed on each leg of Girder 2 and 6, and both legs of Girder 10. The sensor numbers and their corresponding locations are shown in Figure 5-2.

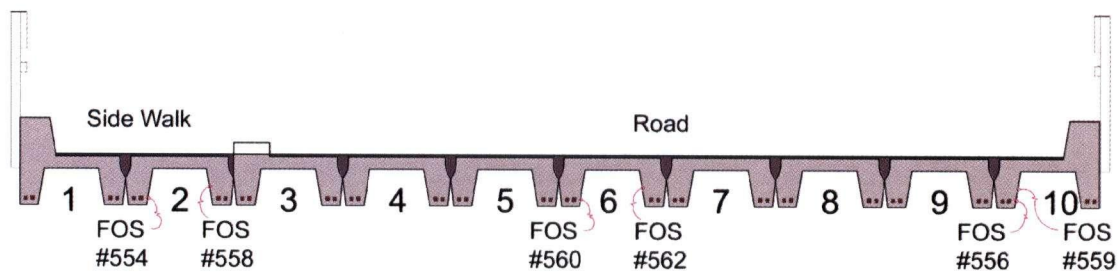


Figure 5-2 Locations of the Long Gauge FOS on Safe Bridge

The LG FOS on Safe Bridge is a commercially available product from FOX-TEK Inc., called the FT sensors, and they come in six standard gauge lengths (ranging from 1 to 30m) or custom lengths. Standard length is preferred because of economic consideration. The gauge length should be selected with the sensing length and required sensitivity in mind. The 5 m standard length was chosen for Safe Bridge for the following reasoning.

For simply supported girder, the moment is approaching zero towards the two ends; if Safe Bridge is simply supported and since the clear span for Safe Bridge is 7.6 m, 5 m-gauge length is sufficiently long to catch most of the strain changes. For a totally fix-ended beam, negative moments are induced at the two ends and the inflection points occur at about 0.2 times the span from the two ends. If the LG FOS were attached end-to-end on the tension side of the beam, tension from the mid-span section and compression from the end-span section would cancel out and show minimum strain. The real support condition for Safe Bridge should be somewhere between the “simply-supported” and “fully-fixed”, and leans toward the simply-supported condition. Assuming the inflection points occur at 0.1 times the span length from the two ends, the section between the inflection points would be around 6



meters; therefore, the 5 m-standard-length of LG FOS is the best choice. For 5m gauge length, the sensitivity is  $\pm 4$  microstrain, which is a reasonable value for Safe Bridge as well.

## 5.2 Testing Vehicle

The loading truck used for Field Test 2005 was also the standard 28-tons-dump-truck that was used in all previous field testing, except that the exact weight differed a little bit. The total weight of the 2005 testing truck was 26,610 kg (29.33 ton), with 8,990 kg went into the front axle (34% of total weight) and 17,620 kg on the two rear axles (66% of total weight). The weight scale ticket of this loading truck is attached in Appendix VII. The photo taken from the testing site and the detailed dimension of this particular loading truck is shown in Figure 5-3.

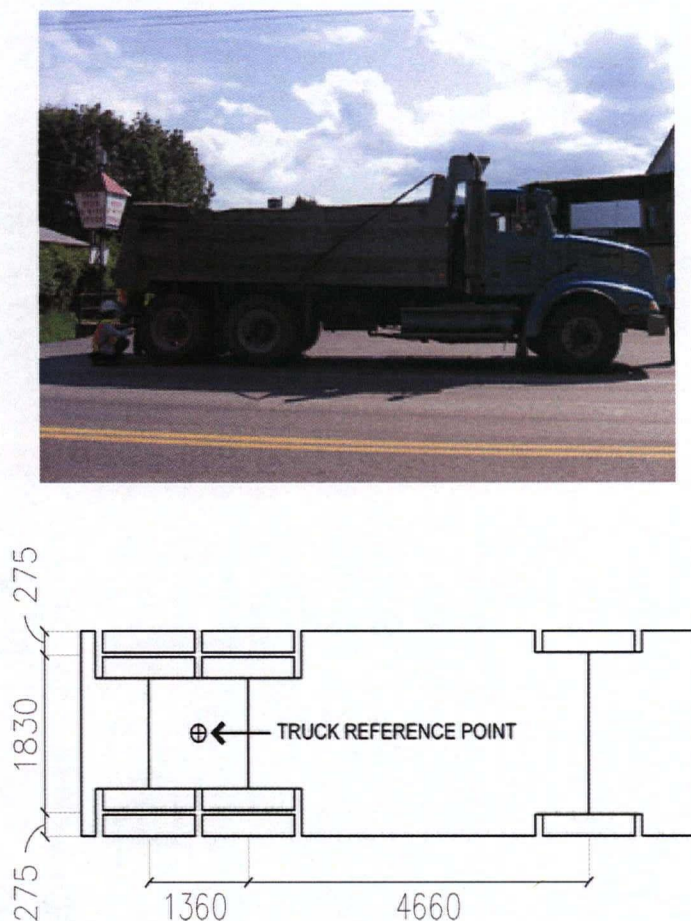


Figure 5-3 The Standard Three-Axle 28 ton Truck used for Field Test 2005



### 5.3 Loading Positions

The static-load positions adopted in *FOS\_2005* were different from the three previous field tests. Since the LG FOSs measure average strain over the span, the original 6-positions-scheme (as shown in Fig. 4-5) which focuses the loading condition only at mid-span is not suitable; more loading positions and to be distributed more evenly over the bridge deck should be used. Therefore, it was decided to have the truck stop at nine loading positions for *FOS\_2005*. The three positions in the transverse direction were not changed (as shown in Fig. 4-6); but longitudinally, instead of stopping the truck twice around mid-span, the truck will pause at every quarter-span-length when it is crossing the bridge. Therefore, there are three longitudinal positions for each transverse direction; three transverse positions times three longitudinal stops equal nine loading positions (see Figure 5-4). The truck stops when its tandem axle arrives at the quarter- and center- of the span. Position 1 to 3 are used as examples to show the exact loading positions corresponding to the truck's tandem axle (see Figure 5-5).

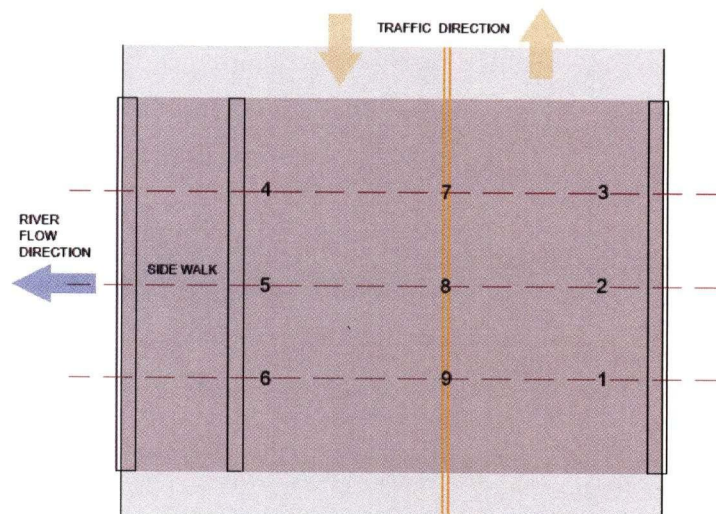


Figure 5-4 Planned Truck Loading Positions for *FOS\_2005*

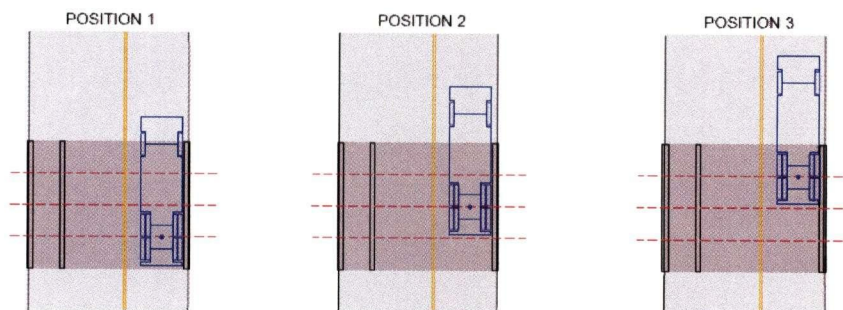


Figure 5-5 Truck Loading Position 1, 2, and 3 for *FOS\_2005*



The bridge roadway surface was measured and marked before the truck load test. Marking of the loading positions is actually an important step for static field testing to make sure the loading positions are as desired. During *FOS\_2005*, first, five yellow marks were made by paint along the concrete curb: one mark at the center of span, and two more on each side of the center mark for every 1.83 meters (clear span divided by 4); please refer to Figure 5-6 [a]. Then, the middle three marks on both side of the curb were connected by chalk to construct the three reference lines for the load testing, showing quarter-span and middle-span positions (see Figure 5-6 [b]). Figure 5-6 [c] shows the truck position in reference to the center of tandem axle and the reference line (in blue). Figure 5-6 [a] was taken during the loading test when the truck was in position 1.

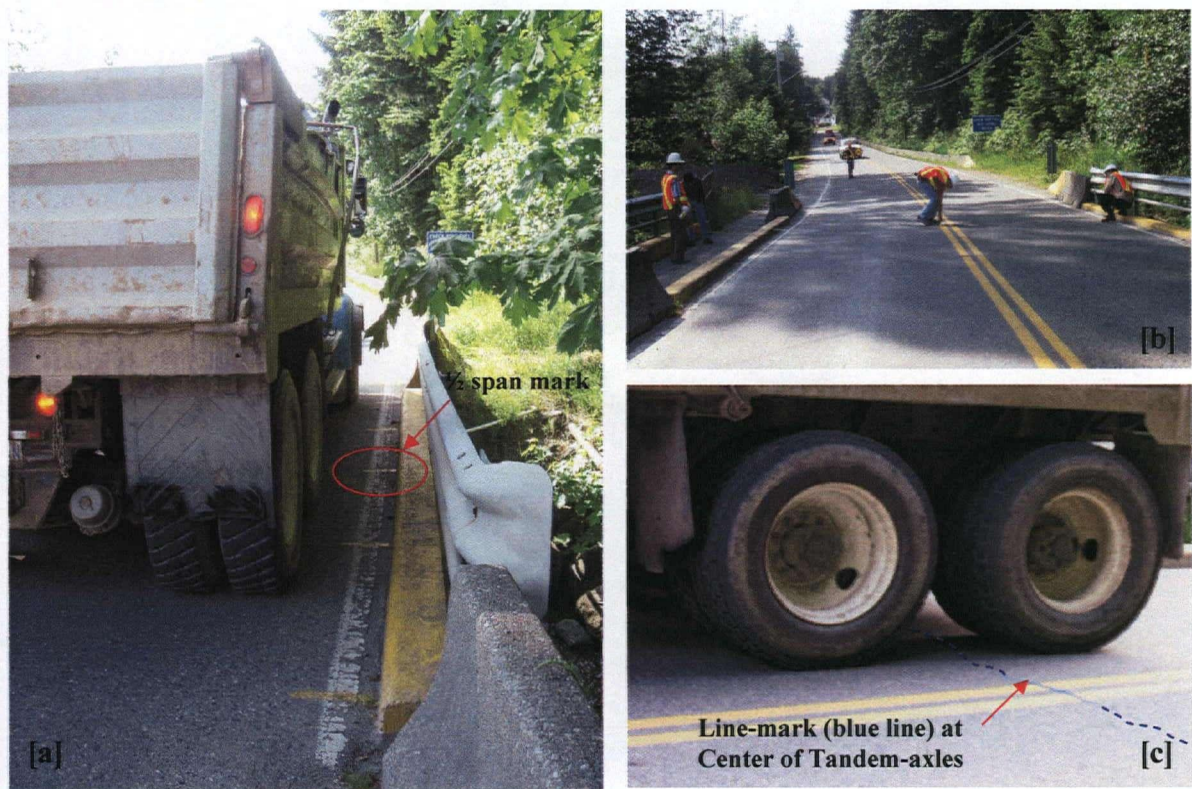


Figure 5-6 (a) Mark-ups along the Concrete Curb; (b) Draw *Quarter-* and *Center-* Reference Lines; (c) Position of the Tandem-axle to the Reference Line

The truck was moving at crawling speed ( $< 1$  km/hr) to minimize dynamic effect on the strain readings. When the truck are on the desired position, it was paused for about 5 minutes. The interrogator used to read the sensor data was FOX-TEK's FTI-3300. The actual loading positions for *FOS\_2005* are shown in Figure 5-7 with measured distances to the edge of the bridge. Note that the center positions (especially Position 7 and 8) were off from the desired locations. This difference



affects the transverse distribution of the truck load to each girder; that is, one can assume that the distribution ratio for each girder will be the same for all 1 to 3 loading positions because they have the “same transverse position”. However, for Position 7 to 9, both of their transverse and longitudinal positions are not the same. This is a “potential source of error” that one should be aware of when using the testing results for comparisons.

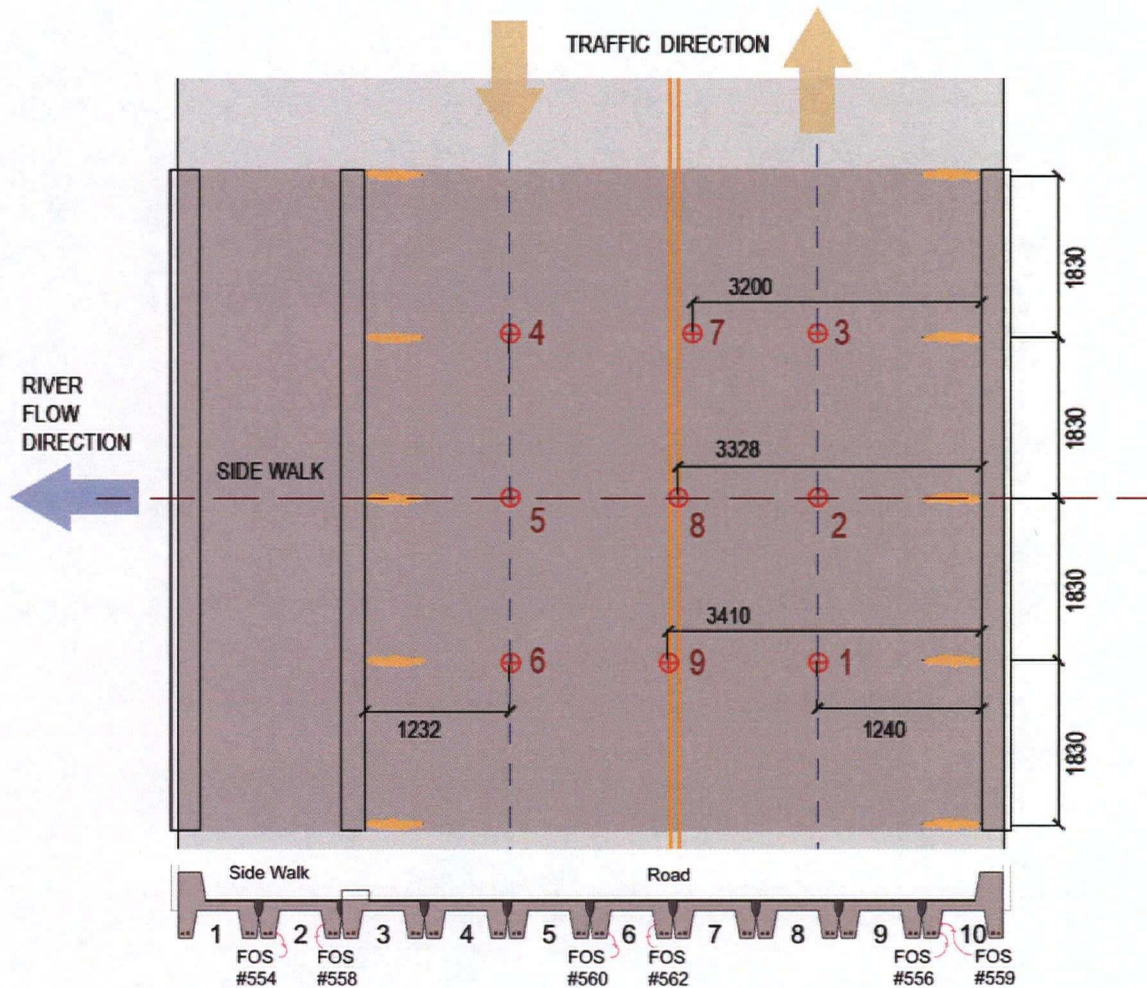


Figure 5-7 Actual Truck Loading Positions for Field Test 2005

## 5.4 Data Processing

The interrogator (the data acquisition system for fiber optic sensors) used for the FT sensors during *FOS\_2005* was FOX-TEK's FTI-3300. The raw data contain four parameters (see a segment of the raw data in Figure 5-8 as example). Column 1 shows the time; Column 2 shows the channel; Column 3 gives the displacement readings in milli-meters; Column 4 gives the temperature readings in °C. For data processing of the *FOS\_2005* testing results, three major steps needed to be performed: (1) convert the raw data to strain readings for each FT sensor; (2) adjust temperature and load effects; (3) convert the average strains to the equivalent maximum strains.

30/05/2005 18:15	5	25.1598	23.254
30/05/2005 18:15	6	28.3858	23.364
30/05/2005 18:15	1	7.9733	23.438
30/05/2005 18:15	2	28.6271	23.248
30/05/2005 18:15	3	8.4327	23.291
30/05/2005 18:16	4	23.187	23.389
30/05/2005 18:16	5	25.741	23.425
30/05/2005 18:16	6	26.2363	23.236
30/05/2005 18:16	1	8.4743	23.413
30/05/2005 18:16	2	26.4721	23.212
30/05/2005 18:17	3	8.473	23.37
30/05/2005 18:17	4	23.5551	23.151
30/05/2005 18:17	5	26.3488	23.212
30/05/2005 18:17	6	27.5444	23.395
30/05/2005 18:18	1	7.7811	23.206
30/05/2005 18:18	2	24.8951	23.285
30/05/2005 18:18	3	8.5035	23.206
30/05/2005 18:19	4	21.6583	23.26
30/05/2005 18:19	5	28.0205	23.175
30/05/2005 18:19	6	27.9365	23.383
30/05/2005 18:20	1	7.8179	23.181
30/05/2005 18:20	2	6.3599	23.273

Figure 5-8 A Segment of Raw Data from *FOS\_2005*

The reason for converting the average strain values to the equivalent maximum strain values is that, the data from the previous field tests were all gathered from the foil strain gauges, which give the maximum strain values. In order to compared this testing results to those performed before, the average strain measured by LG FOSs need to be converted first. These three analysis steps will be discussed in details in the following sections.

### 5.4.1 Conversion: Displacement to Average Strains

Since the FT sensors measure the total displacement along the gauge length, to obtain the average strain, simply divide the displacement by the gauge length. The gauge length in this case is 5 meters. For the “actual” strain change on the sensor since it is installed, it is important to have the “initial baseline reading”. The standard FT sensors typically give an unstrained reading around 14 to 16 mm, to provide measurement capability for both tension and compression [216]. Therefore, during the installation stage, it is important to take the initial reading on the sensor when it is just installed on the structure. This reading is the baseline for the future readings to be compared with to find the total change in the sensor’s length. Note that if the Total Sensor Displacement (see formula below) is a negative value, that means the sensor is under compression; a positive value indicates tension.

$$\text{Total Strain} = \text{Total Sensor Displacement} \div \text{Sensor Gauge Length}$$

$$\text{Total Sensor Displacement} = \text{Current Reading} - \text{Initial Baseline Reading}$$

Referring back to the raw data in Figure 5-8, the channel number 1 to 6 represents the signal inputs from the six FT sensors. The FTI-3300 interrogator reads the signals from the six sensors serially, that is, it scans through all six channels first then goes back to channel 1 and repeats the process; that is why the raw data is like what is shown in Figure 5-8. Therefore, the very first step in processing the raw data is to re-organize the table and categorize the data according to the channel numbers, to obtain the Time-Displacement plots for each FT sensor. After the rearrangement, one can see that the sampling rate is about one to two readings per second for each sensor.

The interrogator ran continuously during the period when the truck was moving around the nine loading positions. The collecting of data started at around 6:25pm and lasted for about an hour. The exact times corresponds to the loading positions are given as follows:

*Position 1 @ 6:37 pm - 6:42 pm (truck facing west)*

*Position 2 @ 6:43 pm - 6:49 pm (truck facing west)*

*Position 3 @ 6:50 pm - 6:55 pm (truck facing west)*

*Position 4 @ 6:58 pm - 7:04 pm (truck facing east)*

*Position 5 @ 7:05 pm - 7:10 pm (truck facing east)*

*Position 6 @ 7:11 pm - 7:16 pm (truck facing east)*

*Position 7 @ 7:18 pm - 7:22 pm (truck facing east)*

*Position 8 @ 7:23 pm - 7:26 pm (truck facing east)*

*Position 9 @ 7:27 pm - 7:30 pm (truck facing east)*



It is important to keep a correct track on the exact loading time for each loading positions, especially when the data is in format like what FTI-3300 gave, in order to get the correct displacement values corresponding to the different loading positions.

For the change in displacement due to the truck load, one can estimate it roughly from the Time-Displacement plot of each sensor. Using Sensor#560 as example, which locates on Girder 6\_bottom, the “original displacement” of the sensor before the truck enters the bridge can be estimated to be around 8.6 mm (please refer to Figure 5-9). According to the loading time for each loading position, one can estimate the new displacement of the sensor due to the truck on the particular position. From the graph one can observe that, the displacement changes are about the same when the truck was on quarter-span (Position 1&3, 4&6, 7&9), and the strains were higher when the tandem axle was on mid-span (Position 2, 5, and 8). This shows that, because the distance of the bridge span and the distance between the front and tandem axles are quite close, the front axle is either off or on the edge of the bridge for the nine loading positions, and therefore it does not give much loading effect.

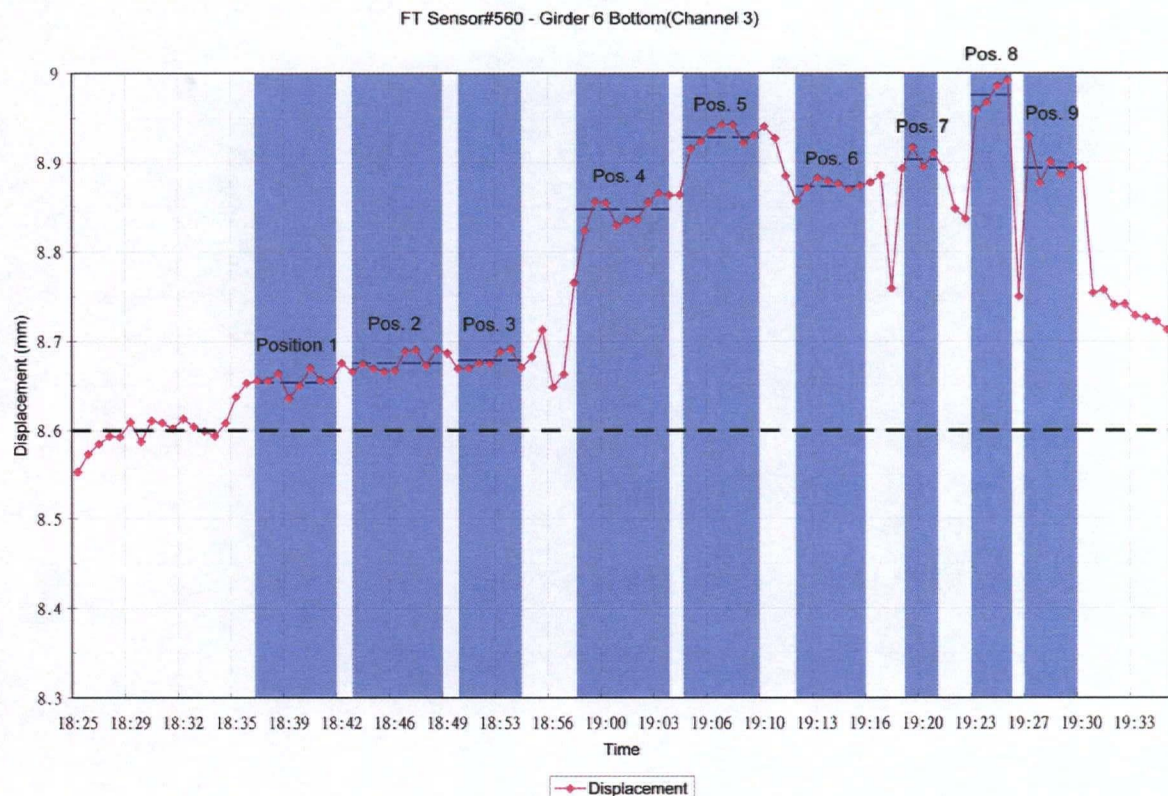


Figure 5-9 Time-Displacement Graph for FT Sensor #560

#### 5.4.2 Temperature and Load Effect Adjustment

The displacement measured by FT sensor is actually due to both the thermal strain and mechanical strain, according to the formula shown below [217]. The temperature of the structure must be known at installation to allow thermal corrections to the sensor data [166]. Therefore, in order to find the true strain value due to load effect, the thermal strain must be calculated and deducted from the strain value calculated from the sensor readings.

$$\epsilon_s = (\alpha + \beta) \Delta T + \left\{ \int_0^{L_s} \epsilon(z) dz \right\} / L_s$$

Where  $\epsilon_s$  = sensor strain

$\alpha$  = thermal coefficient of expansion for the structure/substrate

$\beta$  = thermal optic coefficient for fiber sensor

$\Delta T = T - T_0$ , where  $T$  = temperature at time of measurement,

$T_0$  = temperature at the time of installation

$L_s$  = sensor gauge length

$z$  = axial co-ordinate along sensor, defined by  $0 \leq z \leq L_s$

The thermal strain is equal to  $\epsilon_{\text{thermal}} = (\alpha + \beta) \Delta T$ . The GFRP layer has a longitudinal coefficient of thermal expansion similar to concrete, which is in the range of  $6 \sim 10 \times 10^{-6} / ^\circ\text{C}$  [48]. The thermal optic coefficient for the fiber sensor is about  $8 \times 10^{-6} / ^\circ\text{C}$  [218]. To be conservative with the thermal coefficient of the GFRP layer,  $10 \times 10^{-6} / ^\circ\text{C}$  will be used. Therefore, to sum them up, the thermal strain is  $18 \mu\epsilon$  for every  $^\circ\text{C}$  change in temperature. Based on the experiences with previous loading tests and the readings obtained from strain gauge,  $18 \mu\epsilon$  is actually quite significant because the strains induced by the truck load is also in the tenth-magnitude of microstrain. Therefore, thermal correction is very important for the correct testing result.

Saying so, for the strains due to the nine loading positions, the testing was hold within an hour, which means the change in temperature was not significant. The temperature changes were all around  $0.1^\circ\text{C}$ , which is equivalent to about  $\pm 2 \mu\epsilon$  strain effect. Therefore, the temperature adjustment can be disregard but one should keep the  $\pm 2 \mu\epsilon$  in mind when comparing the data.

If the data from FOS\_2005 is to be compared with the earlier field testing results from Safe Bridge, one more correction needs to be made: the difference in truck weight. The weight of the truck for *After\_Repair\_2002* was 24,940kg; for *Strain\_Gauge\_2003* was 25,450 kg; and for *FOS\_2005* was 26,610 kg. Therefore, when comparing the test results of *FOS\_2005* and *After\_Repair\_2002*, a load factor of 0.937 should be applied to the *FOS\_2005* data. Similarly when compared between *Strain\_Gauge\_2003* and *FOS\_2005* test results, a load factor 0.956 should be applied to *FOS\_2005* strain values.

In fact, the operation variation was not only on the weight of the loading truck, the loading positions were different as well. Since quarter-span- positions were not used in previous field testing, strain values for Position 1, 3, 4, 6, 7, 9 can not be used to do the comparison. As for Position 2, 5, and 8, even though they are not identical to the loading positions before, but they were considered close enough. Using Position 5 as example, please refer to Figure 5-10. The lines on the figure indicates the different “reference line” used for different position during different field tests. For example, load position 5 for the 2003 testing was to have the first tandem axle lined up with the mid-span. Load position 5 for the 2005 testing was to have the center of the two tandem axles to be lined up with the mid-span. The *FOS\_2005* Load Position 2, 5, and 8, were located in between the Position 1&2, Position 3&4 and Position 5&6 respectively of the previous testing. Therefore it is still reasonable to compare the strain values.

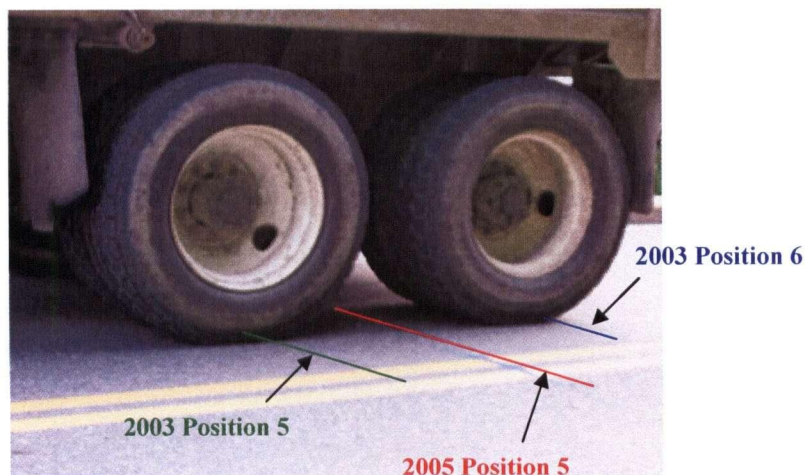


Figure 5-10 The Reference Lines Used to Match the Mid-span Line

### 5.4.3 Data Conversion: Maximum Strain vs. Average Strain

There is one more step required for data processing if the *FOS\_2005* readings are to be compared with the previous three field testing results. Since the readings from all previous field testing were collected from strain gauges at mid-span, the readings represent the maximum strains of the girder. Nonetheless, the testing results for *FOS\_2005* are the average strains of the girder. Therefore, in order to compare them, one value needs to be converted to the other. Under certain assumptions, it is possible to determine the maximum bending strain of the girder based on the known average strain value over the same section of the girder [166]. This section is devoted to the formulation for the conversion.

Assume a simply supported beam with length  $L$ , and  $z$  is the axial coordinate along the beam, so  $z = 0$  at one support and  $z = L$  at the other. First, relate the beam's strain at  $z$  to the moment at  $z$  with the axial bending stresses (Hooke's Law):

$$\sigma_z(z) = M(z) y / I = E \epsilon_z(z) \quad \dots \text{Eq. (1)}$$

where  $M(z)$  = axial bending moment function

$y$  = distance from neutral plane to sensor location

$I$  = second moment of area for cross section of the beam

Assume the maximum bending moment occurs at " $z_m$ ", therefore:

$$\epsilon_z(z_m) = M(z_m) y / EI \quad \dots \text{Eq. (2)}$$

The value of  $z_m$  can be calculated by the following equation because at  $z_m$ , the slope of the maximum moment is zero (assuming there are no discontinuities on the moment curve). Therefore, if the bending moment function  $M(z)$  is known, the value of  $z_m$  can be obtained.

$$dM(z_m) / dz = 0 \quad \text{and} \quad d^2M(z) / dz^2 < 0$$

Next is to relate the maximum bending strain to the sensor average bending strain  $\epsilon_s$ , assuming a long gauge sensor is located at " $y$ " from the neutral plane; this is the formula to determine the maximum bending strain of the beam from a known average strain value [166].

$$\epsilon_z(z_m) / \epsilon_s(y) = L_s M(z_m) / \int_0^{L_s} M(z) dz \quad \dots \text{Eq. (3)}$$



For example, if a simply supported beam is subjected to a UDL (uniformly distributed load) equal to “w”, the moment function is known as:  $M(z) = (w/2) (z^2 - L z)$ ; and since the maximum moment occurs at mid-span,  $z_m = L/2$ . Assuming the sensor length is the same as the beam,  $L_s = L$ , when substitute these values into Eq. (3),  $\epsilon_z(z_m) / \epsilon_s(y) = 1.5 \rightarrow$  at location “y”, the maximum bending strain is 1.5 times the sensor strain. To find the absolute maximum bending strain over the section, one more step is required: factor-up the value by “ $y_{max}/y$ ”. In our case, what we care is the tension strain, so Eq. (3) can be used directly. If it is for compression strains, the bending stress must be compared to the buckling stress and use the smaller [92].

For Safe Bridge case, the loading condition can be represented as shown in Figure 5-11. Assuming the bridge is simply supported, and the truck load can be modeled as two concentrated loads: one represents the heavier tandem axle ( $W_1$ ) and the other represents the lighter front axle ( $W_2$ ).

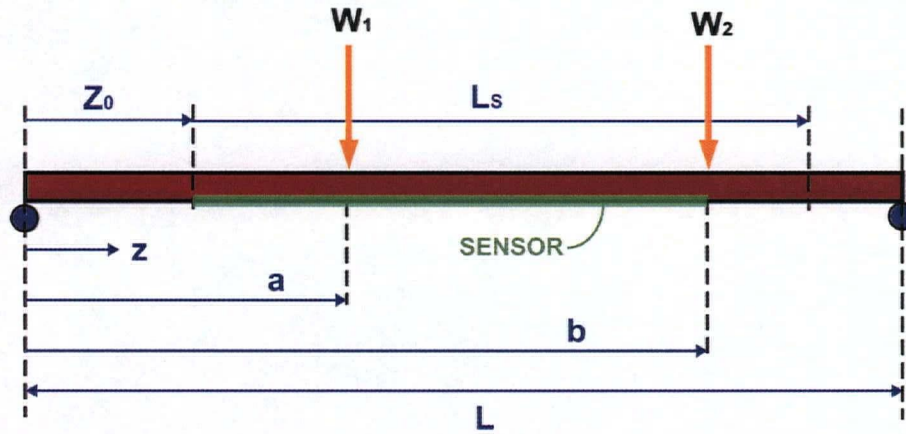


Figure 5-11 Beam Model for Safe Bridge Loading Cases

Source: [166]

Using Eq. (3) and the parameters from Figure 5-11, the following equation is derived for the relationship between the average sensor strain and the maximum bending strain [166]. This long equation can be simplified for special loading cases and sensor length.

$$\epsilon_{max} / \epsilon_s = a \left\{ \left[ \frac{W_1(1 - a/L) + W_2(1 - b/L)}{L_s} \right] \right\} / \left\{ \left[ \frac{W_1(1 - a/L)}{2} + \frac{W_2(1 - b/L)}{2} \right] \left[ L_s^2 + 2 L_s z_0 \right] - \left( \frac{W_1}{2} \right) \left[ a^2 + (L_s + z_0)^2 - 2 a (L_s + z_0) \right] - \left( \frac{W_2}{2} \right) \left[ b^2 + (L_s + z_0)^2 - 2 b (L_s + z_0) \right] \right\} \dots \text{Eq. (4)}$$



As mentioned earlier, the front axle barely has any load effects on the bridge, therefore it is reasonable to assume  $W_2 = 0$  for our case. To further simplify Eq. (4), assume the sensor length is the same as the beam, which is not exactly true but close to Safe Bridge's condition ( 5m sensor on 7m span). Therefore,  $Z_0 = 0$  and  $L_s = L$ . Only load position 2, 5, and 8 will be compared to the previous loading test results, and for these three cases, the tandem axle ( $W_1$ ) is located on mid-span, therefore  $a = L/2$ . Substitute all these values (the bold equations) back to Eq. (4) and the result is:

$$\epsilon_{\max} / \epsilon_s = 2 \dots \text{Eq. (5)}$$

Therefore, this relationship can be used to approximate the maximum strain values based on the *FOS\_2005* testing results, to be compared with the previous testing results. Note that the actual ratio of  $\epsilon_{\max} / \epsilon_s$  should be a little less than 2.

## 5.5 Testing Results and Comparisons

This section will present some of the testing results for *FOS\_2005*. Because the data and the site condition during the initial measurements from the time of installation (FT sensors) are not available to the UBC team, the actual conducting of the average strain values for *FOS\_2005* can not be performed. Nonetheless, if the initial data were available, the raw data would be processed in exactly the same way as described in last section, *Chapter 5.4 - Data Processing*. The testing results shown here are from FOX-TEK [166]. Strain values for three FT sensors according to the nine loading positions will be presented below.

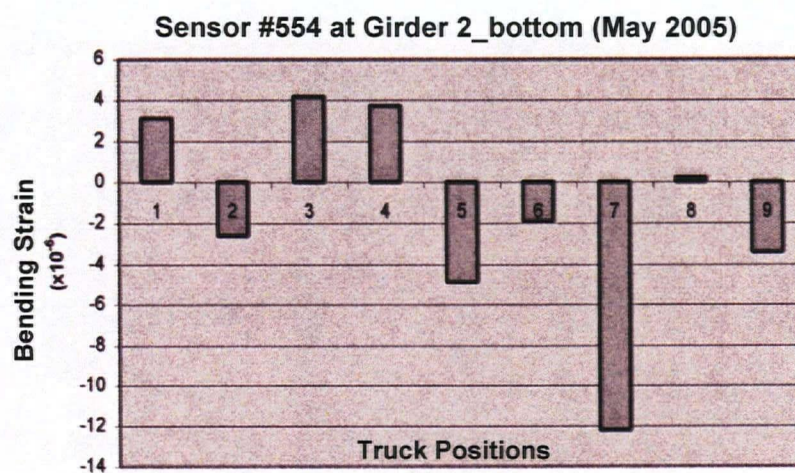


Figure 5-12 Microstrains for Sensor#554 under 9 Loading Positions: *FOS\_2005*



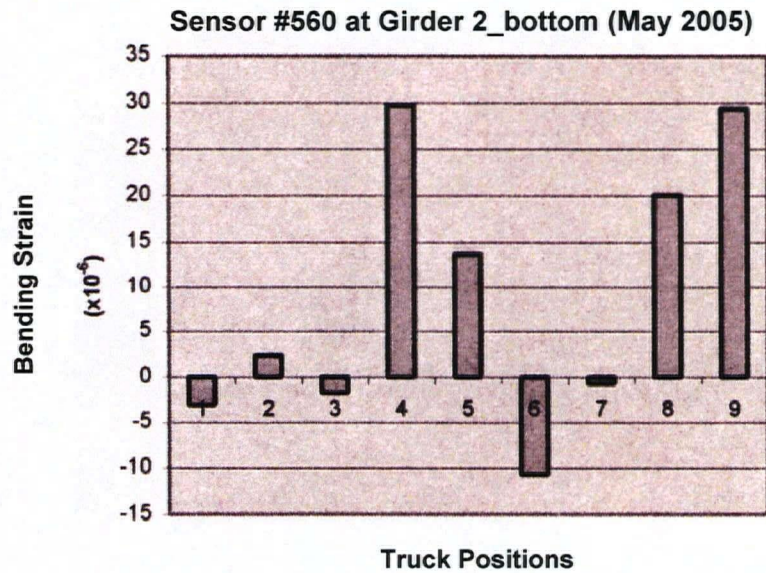


Figure 5-13 Plot of FT Sensor#560 under 9 Loading Positions: *FOS\_2005*

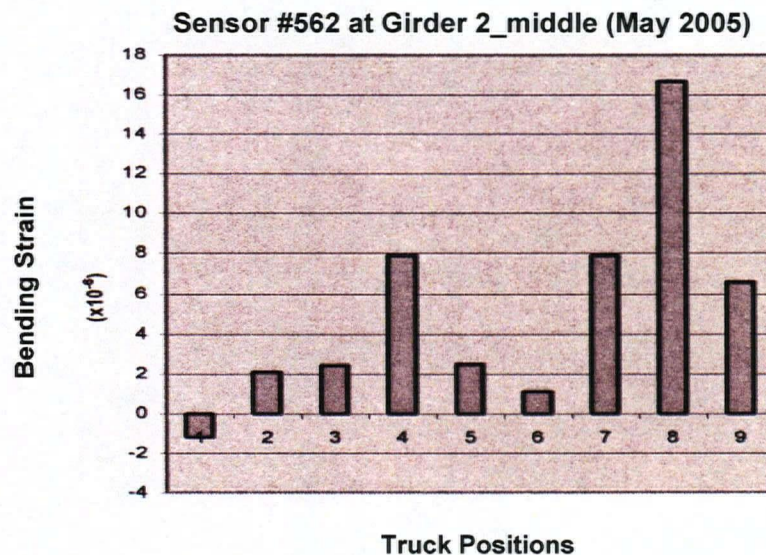


Figure 5-14 Plot of FT Sensor#562 under 9 Loading Positions: *FOS\_2005*

From these plots, it is clear that under certain loading positions, the sensors were under compression; this indicates that the support conditions of the girders are not purely simply-supported; some fixity do exist. Sensor #560 and #562 are the counterparts both installed on Girder 6; it can be observed from the plot that, indeed, the one located closer to the bottom of the beam (#560) is experiencing higher strains than the one closer to the neutral plan (#562).

In the following, the testing results from Sensor #562 will be compared to its initial measurement made on Feb. 2002, and to be compared with the values obtained from strain gauges in the previous field tests.

### 5.5.1 FOS\_2005 Reading vs. Initial FOS Reading

According to FOX-TEK's record, during the initial installation of the FT sensors, data were collected from Sensor #560, the one located at Girder 6 Bottom (parallel to the tension rebar), with respect to the six static loading positions (as shown in Figure 4-4) used for all 2001, 2002, and 2003 field testing; the testing result is shown in Figure 5-15.

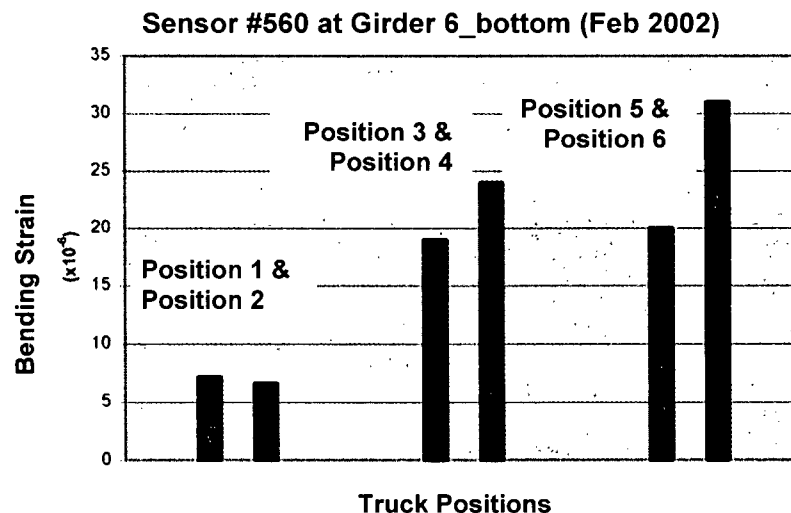


Figure 5-15 Plot of FT Sensor#560 under Six Loading Positions in *After\_Repair 2002*

The loading positions that are comparable from these two testing are Position 2 (2005) to Position 1&2 (2003); Position 5 (2005) to Position 5&6(2002); and Position 8 (2005) to Position 3&4(2002). One can obtain the corresponding strain values from Figure 5-13 and Figure 5-15; it is found that the strain values between the two field testing are very similar (2 $\mu\epsilon$  vs. 6 $\mu\epsilon$  ; 14 $\mu\epsilon$  vs. 20 $\mu\epsilon$ ; 20  $\mu\epsilon$  vs. 25 $\mu\epsilon$ ), and the *FOS\_2005* values actually turned out to be smaller. Microstrain is a very small value and any variations and environmental effect can easily induced a couple of microstrains. It is unknown that is the load factor has been applied to account for the difference in truck weight; nonetheless, with such close results, one can conclude that delaminations on Girder 6 is highly unlikely. Next we compare the FOS results to the strain gauge results.

### 5.5.2 FT Sensor Readings vs. Strain Gauge Readings

The strain gauges are located on the tension rebar, therefore the only FT sensors that can be compared with the previous field testing results are sensor #554, #560 and #556 (see Figure 5-16). Since only Sensor #560 has the initial measurements available, FT Sensor#560 will be used to compare with the strain gauge readings. The conversion factor of 2 for maximum strain to average strain value (from Chapter 5.4.3 Eq.5) will be applied to the FOS readings. From the May 2005 plot (Figure 5-15), one can observe that the largest average strain value from FT#560 was about  $30\ \mu\epsilon$  (occurred under load position 4 and 9), which means the maximum strain experienced by Girder 6 during the 2005 testing was about  $60\ \mu\epsilon$ . It was surprising to see the maximum strain occurred under load position 4 and 9 though. As for the 2002 plot (Figure 5-15), the maximum strain value was also around  $30\ \mu\epsilon$ , which occurred under load position 6 (equivalent to load position 8 in 2005); the location was as expected.

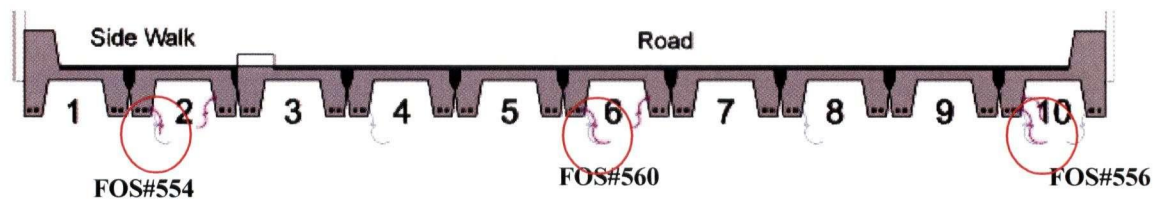


Figure 5-16 Locations of both Strain Gauges and FOSs

As for the strain readings, since it has already been concluded from Chapter 4 that the strain readings from *Strain\_Reading2003* is about the same as *After\_Repair2002*, the results from the 2002 field testing will be used directly to be compared with the FOS readings. The corresponding strain gauge to FT#560 is Strain Gauge#3 (SG#3). The highest strain reading for SG#3 during the 2002 testing was  $70\ \mu\epsilon$ , occurred under Position 5. For Position 6, the strain value was  $65\ \mu\epsilon$ . The load factor and temperature adjustment for the strain gauge readings have not been applied, so the comparable results between *2005\_FOS\_readings* and *2002\_SG\_readings* are less convincing. Nonetheless, both results from 2002 testing also matches well; since the loading truck and loading position were the same during the 2002 testing, and the temperature was very close as well, one can conclude that the bonding condition of the GFRP layer on Girder 6 was perfect when it was just applied. Actually, the truck is heavier for the 2005 testing, and the temperature should have been higher as well (Feb. vs. May), therefore the 2005 FOS strain value is probably less than the 2002 strain gauge value, which shows that the bonding condition of GFRP is still in very good condition after three years in field.



Regarding the results of Sensor #554 (Figure 5-12) which is indicated in FOX-TEK's record that it is located in Girder 2\_bottom, the highest tension strain was found under Position 3 (above Girder 10) with a magnitude of  $\sim 4\mu\epsilon$ . Its largest strain was actually a compressive strain, under Position 7 (above Girder 6), with a magnitude around  $12\mu\epsilon$ . This result seems very weird. If there were no mistake made during the processing of data, and the sensor were not malfunctioning, it is highly likely that the strain number was recorded wrong. In the author's opinion, the FT sensor located at the bottom of Girder 2 should be #558 and the one on "center-leg" should be #554 (please refer to Figure 5-2), based on the observations on the Time-Displacement plots for these two sensors.

---

## Chapter 6

### Structural Health Monitoring on Safe Bridge

---

This chapter will present Safe Bridge project from the aspects of the five components of SHM process: *operational evaluation*, *data acquisition*, *data communication*, *data management*, and *diagnostics*, as discussed in Chapter 2, to cover whatever has not yet discussed in earlier chapters (Ch 3 to 5). In addition, this chapter also serves as a “record” for Safe Bridge project, focusing on the last two field tests. Since the ultimate goal of Safe Bridge project is to investigate the long-term performance of the GFRP reinforcement, more field testing will be performed in the future. It is important to learn from past experiences and to correct mistakes. The value and lessons from the last two field tests should be passed on to people that will work on Safe Bridge project in the future; therefore keeping a detailed record is important. Also, for students without field test experiences, reading this chapter will be helpful for them to understand the project faster. With these purposes in mind, many site photos are presented in this chapter to make the content easier to be understood.

#### 6.1 Operational Evaluation and Set-Up Design

Safe Bridge was found to be shear-deficient according to current standard, and also had severe concrete spalling problem on the bottom side of the girders. Shear reinforcement was done by an innovative repair method, the *sprayed FRP*. Therefore, according to chapter 2.1.1, within the four types of bridges that particular need SHM, Safe Bridge is qualified for two. The life-safety and economic justifications for performing SHM on Safe Bridge have been discussed in chapter 3; to summarize in short: it is essential that delaminations of the strengthening layer (in this case is the GFRP) does not occur, otherwise the benefit of the reinforcement is lost; however, environmental effects, especially moisture ingress and temperature changes, may lead to de-bonding of the reinforcement, and it is important to investigate the field performance of this new repair method. It is worth to mention again that, the potential of the *sprayed FRP* repair method is huge; the structural safety and performance monitoring of Safe Bridge may actually be the “smaller benefit” of this SHM study, the knowledge of the field performance of *sprayed FRP* and the experiences with more advanced set-up for bridge monitoring may ultimately be the real significant benefits of this project.

Most of the considerations for operational evaluation have been covered in earlier chapters (Ch 3-5), such as what to be monitored and how the damage should be defined; what have not been discussed much yet are the operational and environmental conditions for the overall set-up of instruments and equipments on site. An important step for operational evaluation is to investigate the site in advance and to gain a “good understanding” about the site, such as the geographical profile, existence and effect of “physical obstacles” (e.g. river, power tower, etc.), availability of source of power, and potential source of noise. The set-up scheme for a SHM system depends largely on the “characteristics” of the particular site. One should try to make use of the advantages of the site to come up a most safe, economical, and convenient set-up scheme. This section will be devoted to the discussion on major “site characteristics” of Safe Bridge, and the actual set-up schemes for the two field tests covered in this thesis.

Almost all sensors and DAQ systems need power to run, and the availability of power is one of the most common problems for bridge testing/monitoring applications. Fortunately, source of power is not a problem for Safe Bridge. Safe Bridge is located right beside resident (only about 15-20 meters away); this is rare for most bridges and it could be a major advantage for long-term monitoring set-up. For long-term remote monitoring, in most cases the DAQ system will need to be left on the site permanently; many cases set up special storage box(es) and locate them beneath the bridge; if necessary, a small control room may need to be constructed for the equipments. Environmental attack and vandalism are always concerns for permanent set-ups. For Safe Bridge, keeping the DAQ system under the bridge is doable but less preferred, because the clearance between the girder and the water surface is less than 2 meters. Therefore, if the near-by resident can be utilized, many problems can be solved.

Remote, continuous monitoring on Safe Bridge has not been actually done yet, therefore the set-up scheme for the two time field testing were relatively “conventional”. Nonetheless, the idea of utilizing the resident had been tried. In the following, the actual set-up schemes used for the two field testing will be briefly presented. More details for the potential long-term remote control set-up will be given in Chapter 7 as future recommendations.

### 6.1.1 Set-Up for Strain\_Reading 2003

As mentioned in Chapter 4, the two objectives for the 2003 testing were, first to gather strain gauge readings under both static and ambient-static (“rolling”) load tests like the two initial tests to compare the results; second, to test out a new DAQ system with IP-built-in for remote monitoring. Instrument set-up for the first objective basically followed what had been done previously. As for the second objective, the idea was to operate WebDAQ/100 in a place indoor. The final set-up scheme for field test 2003 is shown in Figure 6-1.

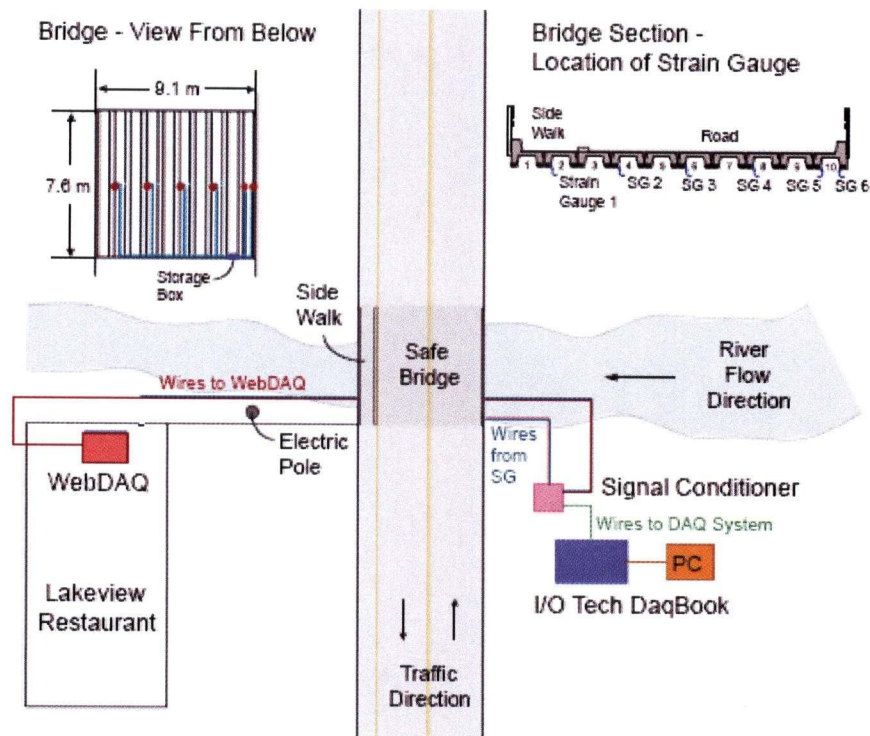


Figure 6-1 Schematic Drawing of System Set-Ups for Field Test 2003

The signal conditioner (SC) (pink box in Figure 6-1) was placed as close to the bridge (sensors) as possible because the longer the wires from the sensors to the SC, the higher the noise effects. The SC was shared by both DAQ systems, to save resource and space, also for the comparison of data between the two DAQ systems. The testing day was a raining day, so all the equipments needed to be set up inside the trunk of the van (see Figure 6-2 [a]); this demonstrated one of the many disadvantages of the conventional bridge testing method. Luckily not many sensors were used on Safe Bridge so that all the equipments required could be fitted inside the trunk. Also, the total time



spent on all the equipment set-up was about the same as the time spent on the truck load testing. The truck was parked to be as close to the bridge as possible (see Figure 6-2 [b]).



Figure 6-2 Field Test 2003 Site Photos: [a] Data Acquisition Equipments on the Trunk of a Van; [b] Position of the Van to Safe Bridge (red circle)

As for the IP-built-in WebDAQ/100, it was chosen for its various functions suitable for remote monitoring and its reasonable price. The house beside Safe Bridge is a restaurant; a visit to the site and a negotiation with the restaurant owner was made before the testing date. The owner was willing to help with the school project so the set-up of WebDAQ/100 was in the basement on the back of the house, where would be the potential location for WebDAQ/100 for long-term remote monitoring.

The blue- and red- line on Figure 6-1 are the wires from the SG to the two DAQ systems; clearly the wires for WebDAQ/100 were much longer. Therefore, another purpose of comparing the data from the two DAQ systems was to see if the longer wiring would affect data much (noise). Nonetheless, comparing to many other bridge projects, the wiring distance for WebDAQ/100 was still relatively short (~50 m).

### 6.1.2 Set-Up for *FOS\_2005*

The set-up scheme for the 2005 field testing is shown in Figure 6-3. Again, sensors were taken out from the storage boxes (three in total; each stores two FOSs) located beneath the bridge and connected by the optical fibers from the interrogator. As mentioned before, the interrogator to fiber optic sensors is equivalent to the data acquisition system to conventional sensors; the interrogator used for the FT sensors is FTI-3300. FTI-3300 works as both the signal conditioner and the data

acquisition system, so it is connected to the FOSs and the computer directly. Interrogator is relatively pricy when compared to the DAQ systems for conventional sensors; therefore, even theoretically FOSs are more suitable for long-term monitoring because they are almost free from many kinds of interference and noise effects, it is currently not a practical idea to do remote monitoring on Safe Bridge through the FOSs.

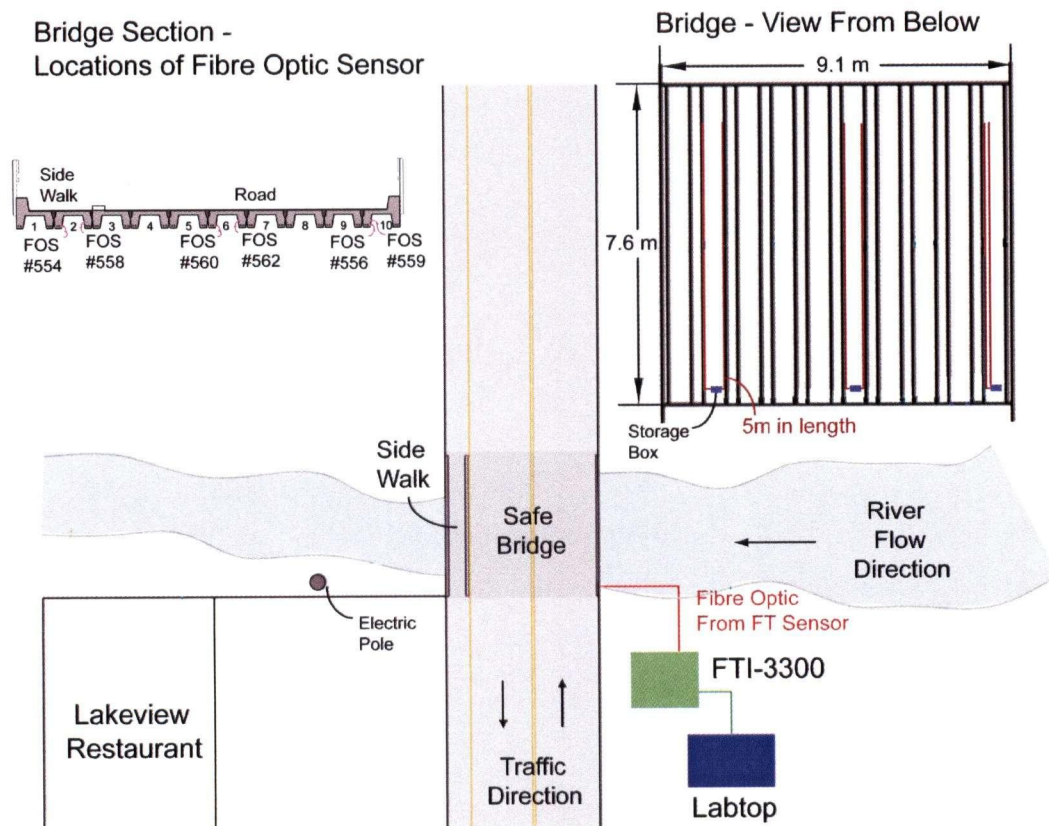


Figure 6-3 Schematic Drawing of System Set-Ups for Field Test 2005

The equipments for the 2005 field testing were also placed on the back of a truck (see Figure 6-4 [a]). Note that the FTI-3300 were not connected to the power directly, but through the grey box shown on Figure 6-4 [b]. The grey box was used to provide surge protection for the expensive interrogator; it can also work as a battery back-up.





Figure 6-4 Field Test 2005 Site Photos: [a] Equipments Set Up on the Back of a Truck;  
[b] Surge Protection Equipment for FTI-3300

## 6.2 Data Acquisition

Data acquisition for Safe Bridge project involves with two types of sensors and three different DAQ systems. Again, most of the main issues to be considered for this subset, such as the monitoring strategy, the sensor types, numbers and locations, and choices of DAQ system, have been discussed in earlier chapters. In this section, each of the five elements (2 types of sensors and 3 DAQ systems) will be introduced in more details about their unique features and specifications.

### 6.2.1 Sensors

This section will focus the discussion on the strain gauge and the long-gauge fiber optic sensor only; even though LVDTs were also used during the first two initial field testing on Safe Bridge, they were not used during the two field testing covered in this thesis, therefore information about the LVDTs will not be covered.

Also note that a temperature sensor of the type RTD (Resistive Temperature Device) actually was also installed on Safe Bridge [219]. No data have ever been collected from the RTD yet, and it is not documented well. According to the technician who were involved in the earlier field work, the RTD was an extra add-in, and it has never been used because all testing performed on Safe Bridge so far are short term field tests and the temperature does not change much during such short period of time; therefore the measurement for temperature had never been necessary [219]. Also according to the

technician, the only information known about the RTD is that, it should also be attached on the steel rebar, like the strain gauges, and with the *cyanoacrylate* type of glue (also referred to as general purpose adhesives), and covered in a similar way as the strain gauges [219]. If long-term monitoring will be carried out on Safe Bridge in the future, the temperature sensor will play an important role to correct the readings from strain gauge.

#### 6.2.1.1 Strain Gauge

The type of strain gauge installed in Safe Bridge is the *Micro-Measurements Foil Strain Gauges* model CEA-06-W235A-350 [219]. The sensing alloy used in the foil grid is *constantan*, the material with best overall combination of properties. This model is specifically designed for temperature compensation when mounted on steel [219]; this feature is important because the steel rebar can get heat up easily and affect the measurement of the strain gauge attached on it.

The grid dimensions for this strain gauge are approximately 0.25 inch (~6 mm) in gauge length and 0.125 inch (~3mm) in grid width [219]; the gauge length falls under the common 3~6 mm gauge length. Since the SG is to be attached on steel but not concrete, longer gauge length is not required. Therefore, a normal gauge length was selected for its lower cost, availability, and ease in installation.

The three most important parameters on the specification for strain gauge are its gauge resistance, thermal expansion coefficient, and its gauge factor. The strain gauge used on Safe Bridge is the 350 ohms type (most common ones are 120 ohms or 350ohms), which generates less heat than the 120ohms (most common ones are 120 ohms or 350ohms) [219,220]. Higher gauge resistance also has the advantages of decreasing lead wire effect and unwanted signal variation caused by temperature fluctuations, and higher signal-to-noise ration [49]. The 120 ohms strain gauge is better only when the application is for long term, because it has longer fatigue life [49]. Since the type of testing on Safe Bridge mostly will be of short duration, fatigue is of less importance than better measurement accuracy. The gauge factor for the strain gauge is  $2.08 \pm 0.5\%$  at 24 °C, and the temperature coefficient of the gauge factor is  $1.2 \pm 0.2 \%$  per 100 °C [219]. It is always good practice to select a strain gauge with a thermal expansion coefficient that matches or is close to the material of the instrumented component.



In terms of the attachment technique, the strain gauge is of weldable type, which the surface preparation requirement is minimal and the gauge is useable immediately after spot welding and lead wire attachment [49]. For efficient welding, the surface for the strain gauge to be attached to must be free of grease, rust, scale, oxides and irregularities. As shown in Figure 6-5 [a], the surface of the rebar was smoothed and cleaned for the strain gauge to be attached. A three-wire connection was used which is the preferred method for a bridge circuit when a quarter configuration is used [49]. Spot welding is accomplished with a portable, rechargeable hand-probe spot welder [49] (see Figure 6-5 [b]).



Figure 6-5 Safe Bridge Site Photos (2002): [a] Installation of Strain Gauge on Steel Rebar; [b] Spot Welding of Strain Gauge

The strain gauges have encapsulation over their grids mainly to protect them from finger smudges and other contamination during the installation stage. The lead wires were connected with “bondable terminals”, which means the lead wires are not attached directly to the solder tabs but to a base material adjacent to the gauge [49] (see Figure 6-6 [a]). This configuration prevents degrading and damaging of the strain gauge by the forces transmitted along the main lead wires. In addition, all the cables have out jackets and shielded in rubber conduits (see Figure 6-6 [b]).

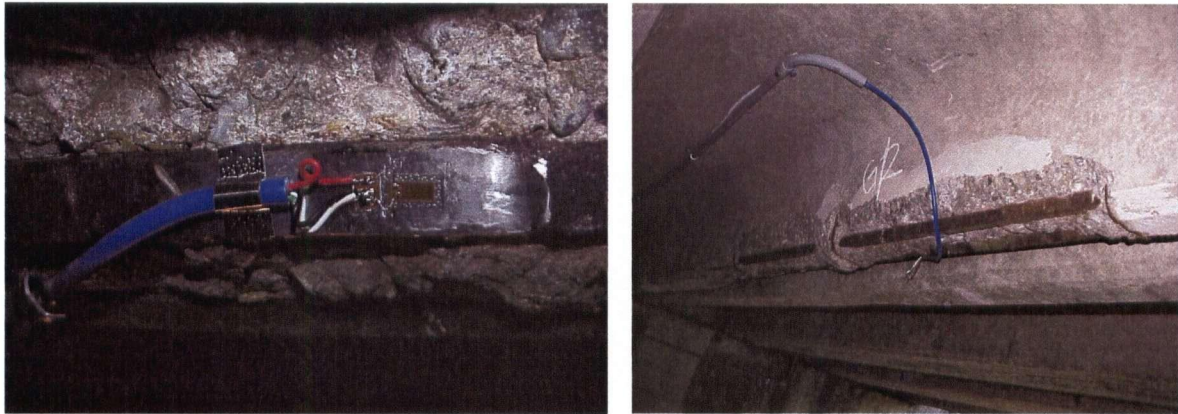


Figure 6-6 Safe Bridge Site Photos (2002): [a] Strain Gauge with 3-wire Bondable Terminals; [b] Shielded Cable for Strain Gauge

For strain gauge installed for bridge applications, it is critical to provide proper protection for the sensors, especially when the location can be easily attacked by moisture; as mentioned in Chapter 2, moisture is the most common cause of field installation failure for foil strain gauges [49]. For Safe Bridge, the good thing about the strain gauge location is that the gauge is not susceptible to rain and snow, but it is close to water surface of the river. ASTM E 1237-93 requires that the lead wires be coated with a minimum distance of 25 mm from the installation [49]. After the strain gauges were welded on steel rebar, they were coated with three coats of Mcoat-A Polyurethane and then the whole gauge/wire area was covered with a 1/8" thick mastic foil coating (HBM 75) to protect them from the environmental effects [79] (Figure 6-7 [a]). Finally the whole thing is covered by a special CFRP mortar as patching (Figure 6-7 [b]).

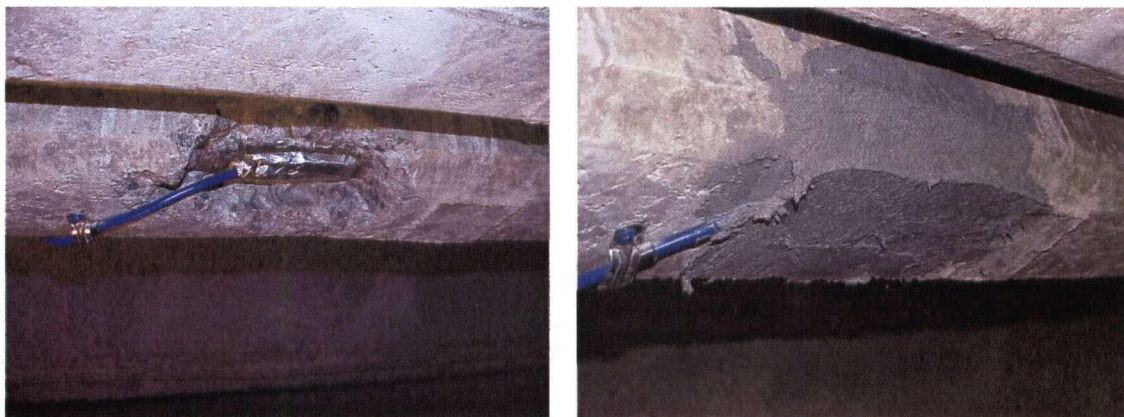


Figure 6-7 Safe Bridge Site Photos (2002): [a] Strain Gauge with Mastic Foil Coating Protection; [b] Strain Gauge Covered with Patching Material

Special attention must be paid to the place where the lead wires exit the protective coating, to ensure that an adequate bond exists between the lead wire insulation and the protective coating, because moisture can be drawn into the gauge area along the lead wires by the capillary action.

#### **6.2.1.2 Long-Gauge Fibre Optic Sensor**

As mentioned in Chapter 5, the long-gauge FOS installed on Safe Bridge is the FT sensor fabricated by FOX-TEK. The FT sensor is the “bare fiber” type which can be attached easily to any kind of structure surface, such as around a column or along a girder. The bare fiber is the conventional single-mode optical fiber with a 0.25 mm diameter [221]. The FT sensor is so thin that it is also suitable to be embedded inside a structural component with minimal intrusive effect. As mentioned in Chapter 2, the FT sensor works based on the principle of interference of light. This type of sensor is quite robust itself toward environmental effects, and additional protection can be easily applied with hermetic coatings. Data from FT sensors can be collected continuously or with periodic site visits (more likely to be used for Safe Bridge case), either is a convenient way to check the bonding condition of the GFRP layer by comparing the data to its initial installation state. Reasons for sensor length and locations of the FT-sensor have been given in Chapter 5.

The specification of FT sensor from FOX-TEK is attached in Appendix VIII. The total displacement range of the sensor is 40mm, regardless the gauge length; this is the maximum elongation/contraction for the fiber, which is limited by the physical properties of the fiber itself and therefore is not bonded by the length of the gauge [221,222]. The accuracy of the sensor is  $\pm 20 \mu\text{m}$ ; the sensor measures displacement with a fixed measurement error. Therefore, the sensitivity of the sensor to strain actually increases with the increase in strain length (sensitivity = change in length / gauge length). For example, for a 1 m FT sensor, the sensitivity is  $\pm 20 \mu\epsilon$ ; for a 20 m gauge length, the accuracy becomes  $\pm 1 \mu\epsilon$ . In this case, the gauge length is 5m, which gives a sensitivity of  $\pm 4 \mu\epsilon$ . Nonetheless, the actual measurement range of the sensor is controlled by the measurement range of the scanning equipment, in this case is the FTI-3300, which gives up to maximum strain at 3% at 22 °C [72,223].

Unfortunately the site photos of the FT sensors during the installation stage are not available. Figure 6-8 shows some site photos taken during the 2005 field testing; the FT sensors are covered with some kind of grey-color epoxy resin for protection. As can be seen from the photo, after more than three



years of installation, the FOSs are still in very good condition. The *Civionic Specifications* [72] by ISIS Canada provides specifications for the installation of FOSs.

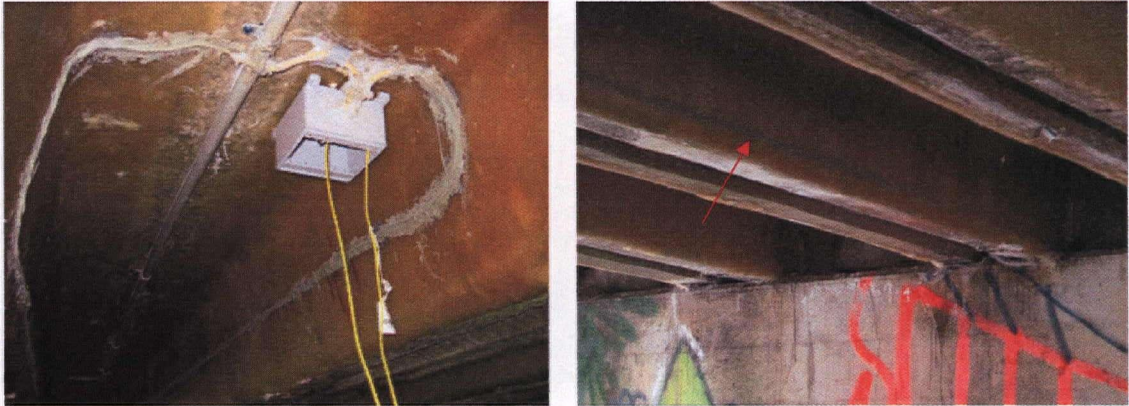


Figure 6-8 Field Test 2005 Site Photos: [a] FT-Sensor on Girder 6 with Storage Box Open; [b] FT-Sensor Covered with Protection Epoxy

### 6.2.2 Data Acquisition Systems

During the two field testing, there were total three types of data acquisition systems used. One system is a conventional type for traditional sensors: adequate for short period testing, one-time, on-site data collection. One system is with IP-built-in and is chosen to test out the idea of remote monitoring, as part of the study and exploration on SHM process. One is the interrogator particularly used for long-gauge fiber optic sensors. The first two DAQ systems were used to collect data from the strain gauges, and they shared the same signal conditioner. This section will introduce each of the DAQ system briefly, focusing more on the latter two systems.

#### 6.2.2.1 Traditional DAQ Systems

The conventional DAQ system used during 2003 field testing was the portable *I/O-Tech DaqBook* system. This system has a 16-bit resolution, which provides extremely accurate digital representation of the analog signals. The range was setup to be  $\pm 10$  volts. Figure 6-9 shows all the instruments used during the 2003 field test as the conventional PC-based DAQ system. The grey box beneath the laptop in Figure 6-9 [a] is the signal conditioner, which provides standard functions as discussed in Chapter 2, such as generating the DC excitation voltage and providing circuitry for bridge completion for the strain gauges. The black box behind the signal conditioner is the *I/O-Tech DaqBook*. Note



that the yellow equipment besides the signal conditioner is *Fluke 87 Multimeter*, which was used for testing the voltage levels of input and output signals; it was used for checking the signal conditioner and DAQ board during the setup stage, and was not involved in the actual data acquisition of strain readings.

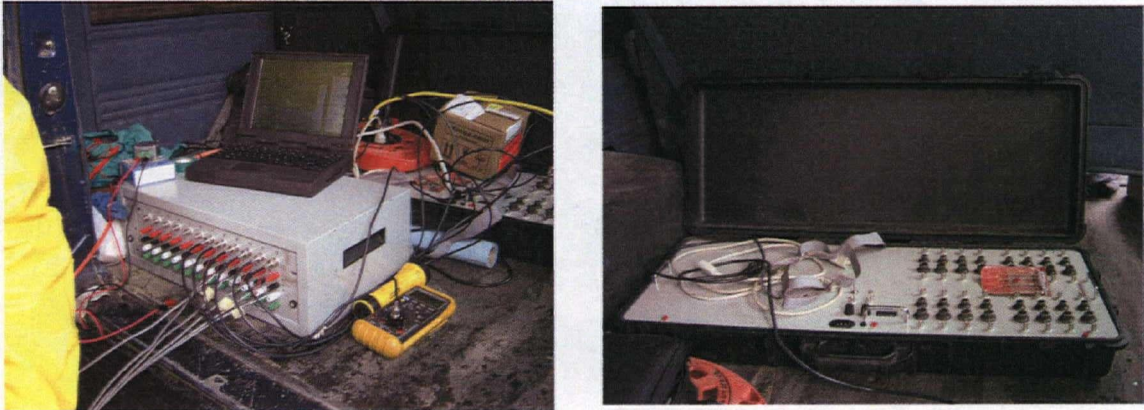


Figure 6-9 Field Test 2003 Site Photos: [a] Data Acquisition Systems for Strain Gauge Readings  
[b] The I/O Tech DaqBook

Regarding the data acquisition software program, *I/O-Tech DaqBook* used commercial-based software called *DaqView* supplied by the manufacturer (see Figure 6-10). The interface is user-friendly and is “sufficient” for typical static field testing usage. Therefore, the software can be configured by users, but no modification or extra programming was required for Safe Bridge testing.

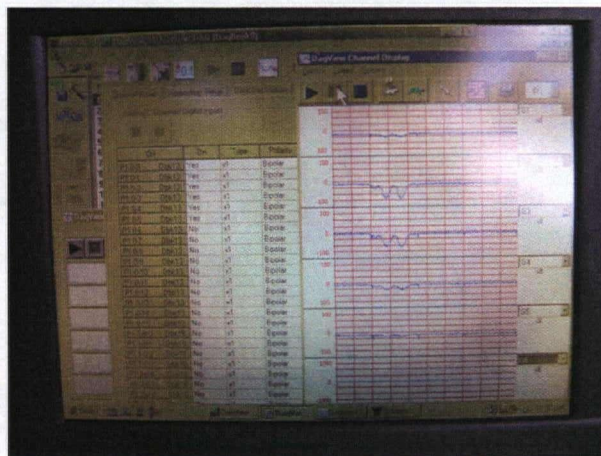


Figure 6-10 Field Test 2003: Example of A Screen Shot of *DaqView*

The most important step was actually that, the technician shunt calibrated all the strain gauges before each test; this ensured that the signals measured were in fact calibrated correctly with the particular data acquisition system used. Taking zero measurements before and after the loading ensured that there were no major drifting of the signals during the load tests.

#### **6.2.2.2 Web-Based DAQ System**

As mentioned earlier, a DAQ-system was required to study the setup for remote monitoring, and possibly performing continuous monitoring in the future. Also, since the system would probably be left on site for a long period of time, the size/weight of the system, the power supply requirement, and its environmental limits (to temperature, humidity, etc.) were important factors for the choice. Finally, as for all projects, economic consideration plays one major role in decision-making: the cost has to be within budget. As a result of all considerations, the DAQ system chosen finally is an IP-built-in system called *WebDAQ/100*, a commercial product from *Capital Equipment Corporation*. The main reasons for choosing WebDAQ/100 were its fair price, compact design, and a fully integrated web server with built-in web interface that provides internet communication, convenient transportation, and easy installation at the site. Users have complete control over channels, rates and other acquisition parameters, a dynamic view of data, and direct download in a desired formats, from any place with access to internet browser.

*WebDAQ/100* itself is a multi-purpose system; it can be used locally, as directly connect to a computer for bench-top use; or forming a network, as multiple WebDAQ/100s placed in different places in structure and connected by standard LAN wiring; or configured to be a standalone data logger, which runs independently without any computer connection, and can store (up to 32 MB of memory) and transfer data according to user needs [224]. The last mode was the one applied in Safe Bridge project during the 2003 load testing. The specifications of *WebDAQ/100* from the manufacture are attached in Appendix IX for readers' reference. The main data acquisition features of *WebDAQ/100* include:

- Take data and download it via a web browser
- 12-bit resolution, 500 KHz max. sampling rate
- 32 channels (16 differential)
- Triggering options

- 8 analog waveform outputs
- Automatic scheduled reports
- Reports via download, e-mail, or FTP
- Local, remote, or stand-alone operation
- Sensor Conversions
- Command-line Interface and Programming

A quick walkthrough of WebDAQ/100's web pages will be presented below. The main purpose for the presentation is not to learn how to use the WebDAQ/100 software, but using it as an example for DAQ software; to see what are some common features for a remote-control setup. The control of the program is usually (and should be) in the hand of an experienced technician with the system; nonetheless, civil engineers should be involved in the design and control of the set-up, especially for decisions like what sampling rate to be used, what is a reasonable triggering value (the magnitude, if used), etc.. Again, good communication between different disciplines is the key for a successful SHM system.

After assigning a network IP address to WebDAQ/100, the home page of WebDAQ/100 can be easily accessed by entering the IP directly on the web browser (see Figure 6-11). In our case, the *Analog Inputs* section is where the strain readings are shown. The wire connections were made differential-ended, so the maximum number of channel input was 16, as shown on the figure; five channels (IN1~5) were used during the 2003 field testing. Note that there is also section for *Analog Outputs*; this is because WebDAQ/100 can also act as a signal conditioner to provide circuit stimulus to sensors. The signal readings can always be viewed directly from the website, but only when the *Status* is in *Run* mode that the data will actually be saved into *WebDAQ/100*'s memory; the "download data" and "view graph" links are only available when the system is in *Run* mode.

The web interface of *webDAQ/100* has four main pages: *Home*, *Acquisition Setup*, *Reports*, and *System* (on the tool bar on top; see Figure 6-11). Each of the pages will be briefly introduced:

- The **Home** page displays updating values of each of the input and output channels and allows control and data download (Figure 6-11).
- The **Acquisition Setup** page allows configuration of the desired channels, rates, gains, and other sampling parameters. It also has "triggering" function which will be beneficial in saving the amount of useful data for long-term monitoring (see Figure 6-12)



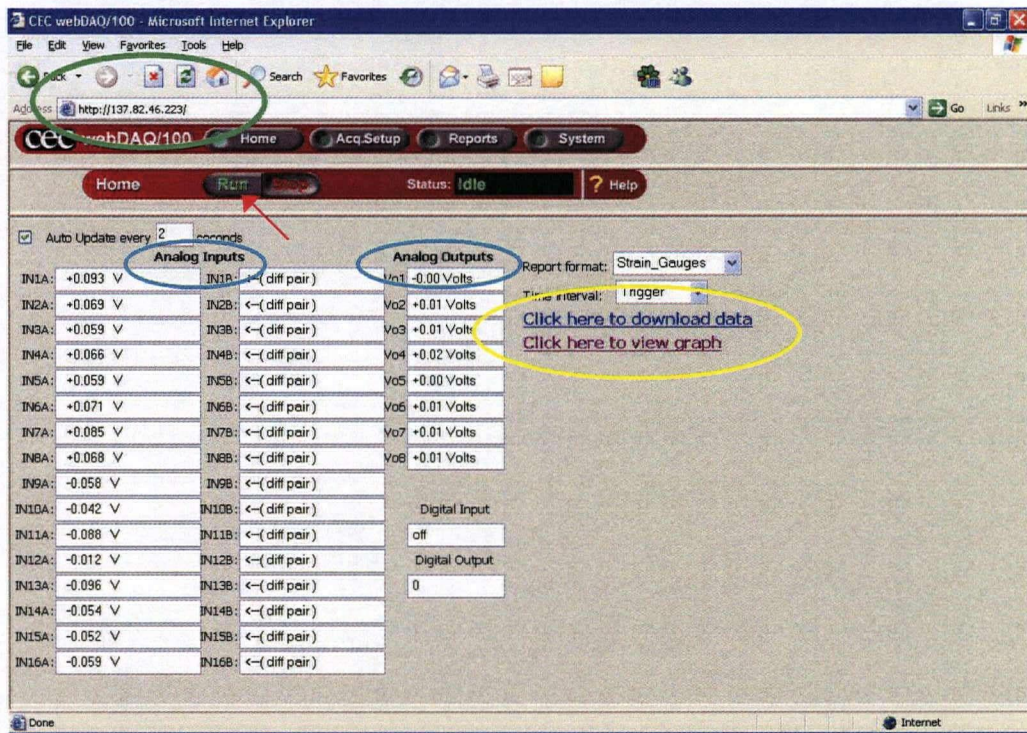


Figure 6-11 Field Test 2003: Web Site for *WebDAQ/100* - Home Page

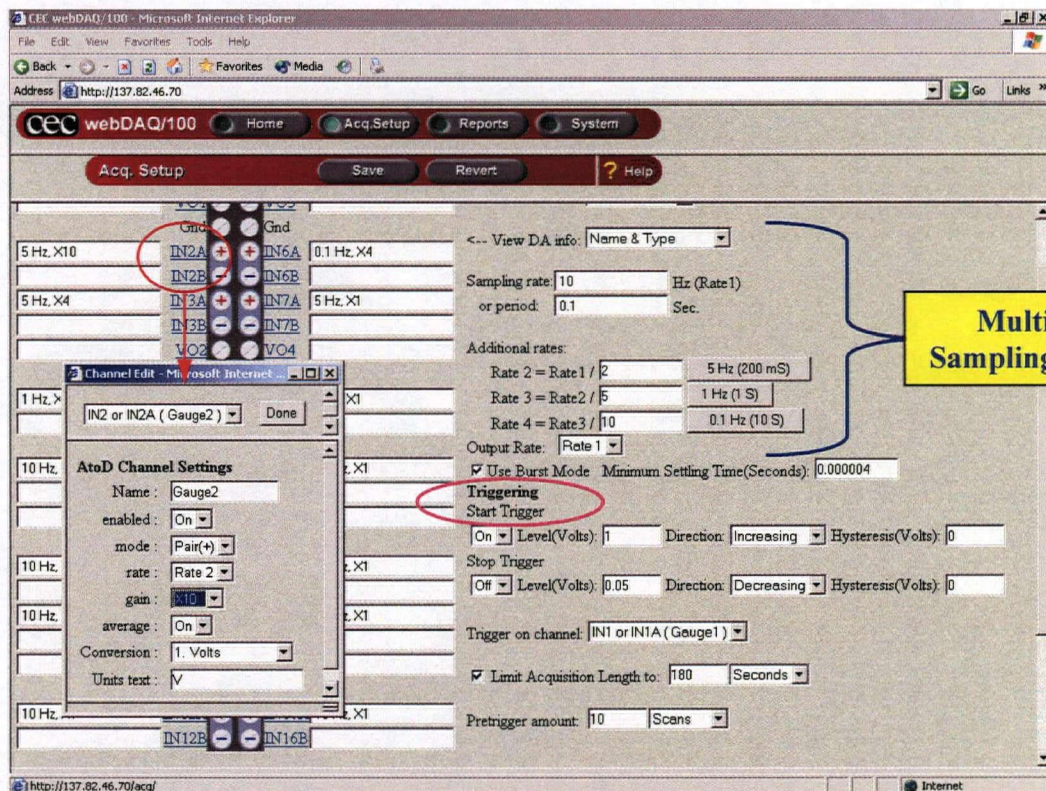


Figure 6-12 Field Test 2003: Web Site for *WebDAQ/100* – Acquisition Setup Page



- The **Reports** page lets users customize data formats, as well as set up automatic scheduled data transmissions; this is also an important function for continuous remotely monitoring (Figure 6-13).

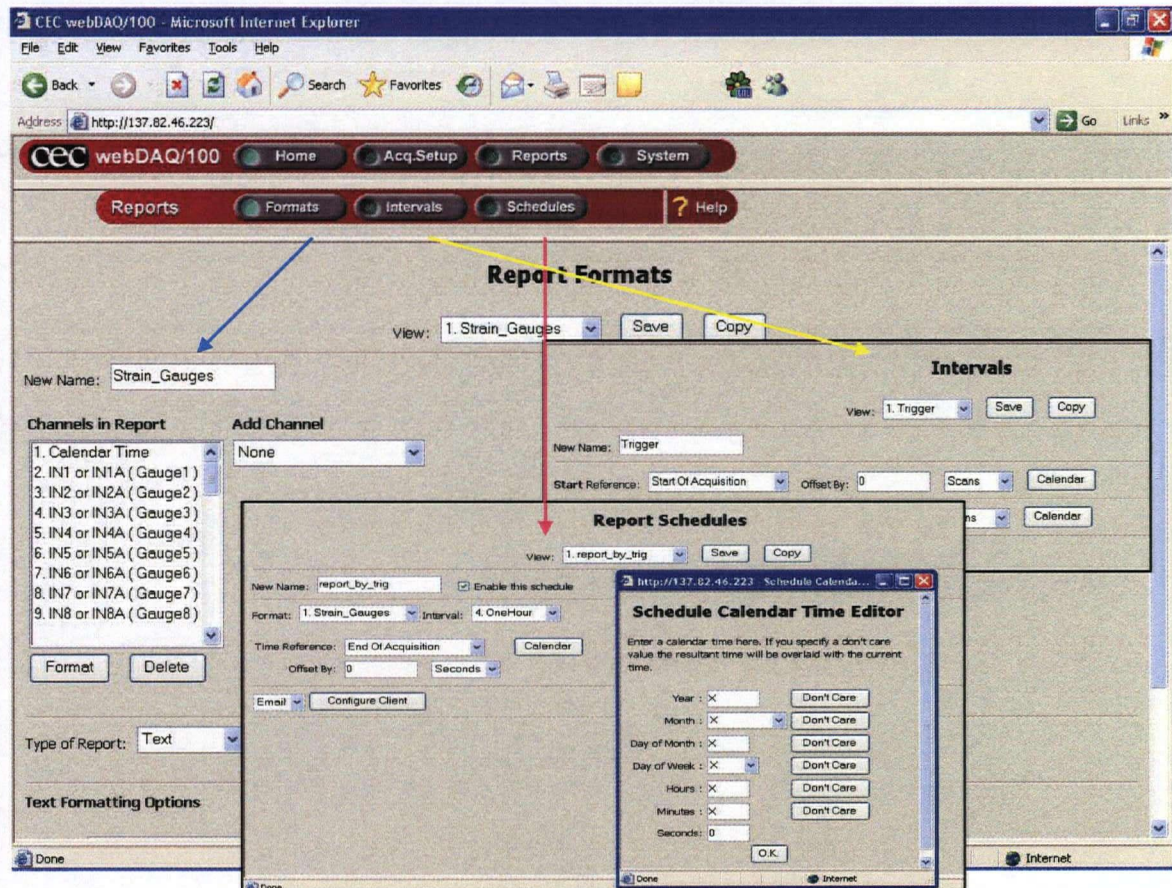


Figure 6-13 Field Test 2003: Web Site for WebDAQ/100 – Report Page

- The **System** page has a variety of maintenance functions such as setting the time/date clock, viewing error information, etc.

In order to set up the automatic e-mailing function, the following networking information should be obtained from the service provider (e.g. Shaw Cable) in advance: two IP addresses, gateway address, DNS address, and Subnet [225]. The testing on the auto-e-mailing function was not achieved during the 2003 field testing due to lack of time for setup; nonetheless, lessons were learnt and the technician is confident with the setup for future testing. In addition, the technician had built a compact system integrating *WebDAQ/100* and the *LINKSYS* system (including wireless access point routers for



wireless communication) all into a storage box (see Figure 6-14). The compact box can be easily stored some where in the restaurant or even under outdoor condition for long-term monitoring purpose.



Figure 6-14 Field Test 2003: [a] Integrated System with WebDAQ/100 & Wireless Communication  
[b] Location of DAQ system with WebDAQ/100 and Operator

Following are some photos taken during the 2003 Field Testing. Photos in Figure 6-15 were taken during the setup stage, showing the wiring and connection for *WebDAQ/100*. Figure 6-16 shows screen shots of the software interface taken during the load test. Figure 6-17 shows the screen shots for the sampling rate set-up. Note that for the setup of sampling rate, if the desired sampling rate is 30 Hz for the strain readings (in this case), on the setup, 300Hz should be used as the input sampling rate, because 10 channels (differential-ended connection) were used for the five strain gauges (see Figure 6-17 [b]), so the rate needs to be ten times.

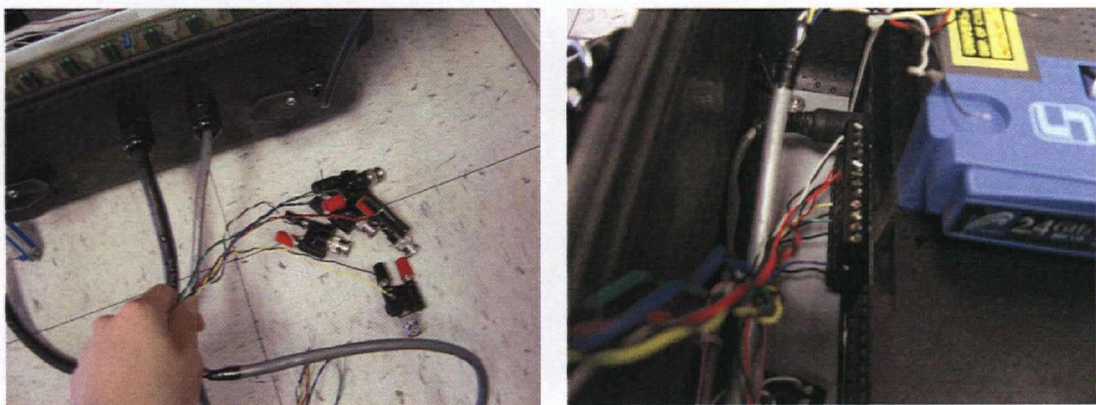


Figure 6-15 Field Test 2003: Connectors of Wires and Connecting to WebDAQ/100



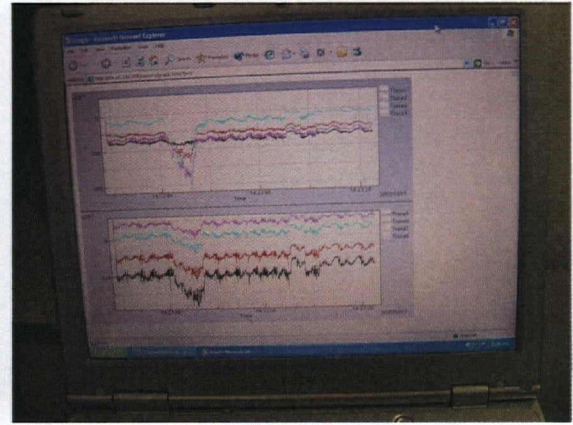
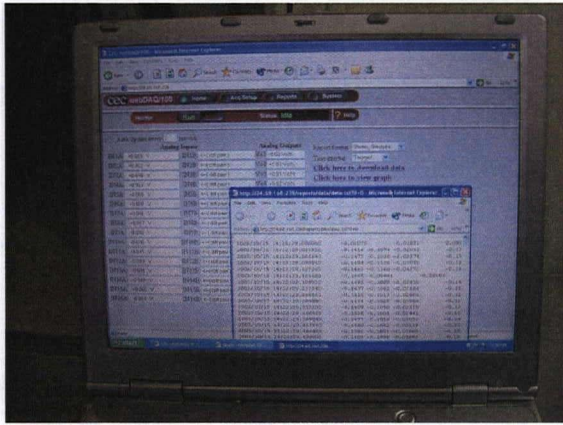


Figure 6-16 Field Test 2003: WebDAQ/100 Screen Shots: [a] Hyperlink: “Download Data”; [b] Hyperlink: “View Graph”

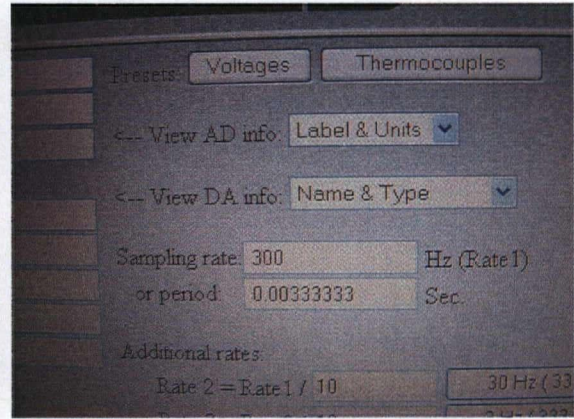
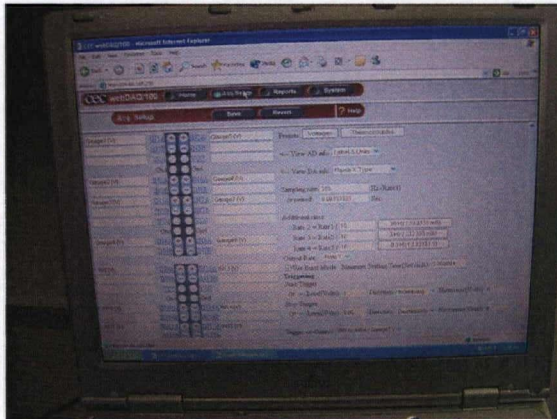


Figure 6-17 Field Test 2003: WebDAQ/100 Screen Shots: [a] Acquisition Setup Page; [b] Sampling Rate Setup

### 6.2.2.3 FOS Interrogator

The interrogator used to read the FT-sensors on Safe Bridge is the FTI-3300, also fabricated by FOX-TEK Inc., which is effectively a fiber optic extensometer. FTI-3300 is the light-grey box shown in Figure 6-18, and its specification is attached in Appendix X. FTI-3300 has 8 input channels, and its dimension is 17”×17”×5.5”. This interrogator can read any three of the seven standard FT lengths provided by FOX-TEK, with the default to read 0.1m, 1m and 5 m length (5 m in our case). This system operates by scanning the attached sensors for changes in the reflected intensity of light, and recording the locations where that signal was detected [226]. Any change in the sensor’s length can be detected by the shift in the signal to a different displacement location, which is detected and



recorded by the instrument. The measurement range is  $\pm 15\text{mm}$  or  $\pm 4000\ \mu\epsilon$ , whichever is less. The accuracy is  $\pm 0.067\%$  of full scale (30mm).



Figure 6-18 Field Test 2005: DAQ System Setup - FTI-3300 and Laptop

As mentioned earlier, interrogators for fiber optic sensors are usually expensive; therefore it is important to use the instrument properly and carefully. Users must read the operating manual thoroughly before actually operating the unit. Care must be exercised to avoid damaging the equipment and the fragile ends of the optical connector. The setup and actual operation of the FTI-3300 were done by a specialist from ISIS Canada during the 2005 field testing.

If the FTI-3300 fails to detect a signal, in most cases is due to a weak signal level from the sensor [226]. This problem usually can be solved after proper cleaning with the connectors (details given later). If repeated scans still fail, one need to determine if the sensor or the channel is broken itself. If the sensor is found to be damaged, but it was previously functional, then both the sensor lead cable and the structure around the sensor need to be inspected carefully. Under normal condition, the strength of the sensor should be much higher than any expected mechanical loading. If the cause of the sensor failure is due to rare loading event (but not physical damage from human/animal, etc.), the structure may have been undergone significant impact/damage. In this case, the failed sensor also acts as an early warning for potential structural problems.

Another common cause for weak signal readings is related to the “bending” of the lead cable. Optical fiber usually needs to maintain a minimum bend radius ( $\geq 6''/15\text{cm}$ ) to transmit light properly [226].



If the lead cable is kinked (e.g. forced over corners or sharp bends) or coiled too tightly, the FTI-3300 will not be able to obtain readings properly. This kind of knowledge should be taught to all people involved on site to minimize human error.

Figure 6-19 are screen shots from the FTI-3300 software during the 2005 field testing. Six channels were used for the six FT-sensors. The scanning interval is set to be 0.05 min (3 sec). The instrument temperature is also given so that thermal effect can be adjusted.

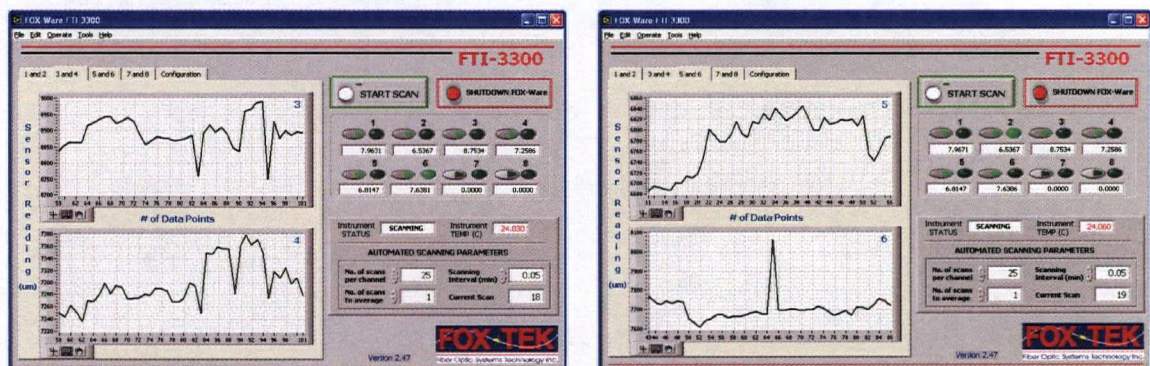
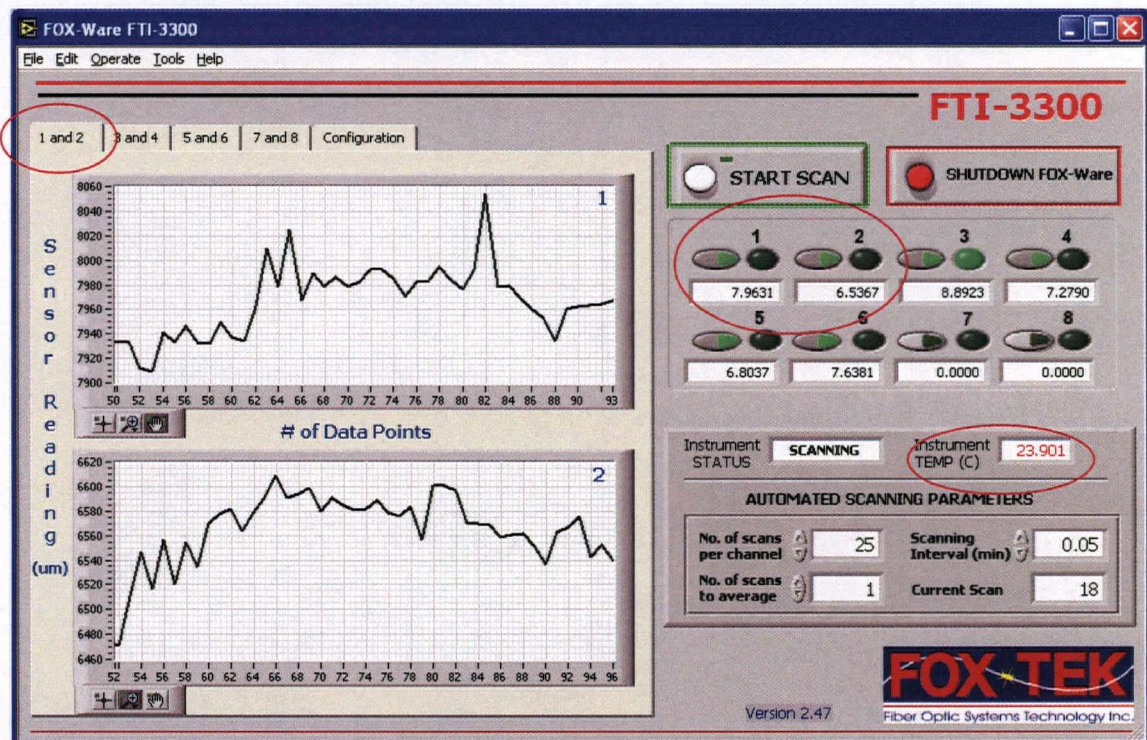


Figure 6-19 Field Test 2005: Screen Shots of FOX-Ware for FTI-3300 (Channel 1~6)



### 6.3 Data Communication

This section discusses the means for transferring the data from the sensors to the DAQ systems, and from the DAQ systems to laptops. The selection of a suitable communication system is essential for a cost-effective SHM system. As mentioned earlier, selecting the optimum communication links require knowledge of the sensors deployed, the surrounding environment, and the specific application objectives. For this project, with the near-by restaurant available, source of power and length of wire are of fewer problems. Also, since the total number of sensors used is not significant, wiring arrangement and storage can still be relatively simple and wireless sensing is not a must. Therefore, during the two field testing, the communication medium for strain gauge data was still the conventional wire cables. As for the FT-sensor, optical fiber is the communication medium. In the following, the setup of the connections between different systems during the two field testing will be presented in detail with site photos.

#### 6.3.1 For Strain Gauge Readings

The strain gauges are connected with lead wires; it is important to protect the wires and have proper design in wiring route and their storage. For Safe Bridge, since the six strain gauges are located at mid-span of five different girders, it was decided to have the storage boxes located on one side of the bridge abutment, and have rigid PVC conduits running down the girders to guide and protect the wires from the strain gauges to the two storage boxes (see Figure 6-21 and Figure 6-21; the storage boxes are the square PVC boxes with black cover on the photos).

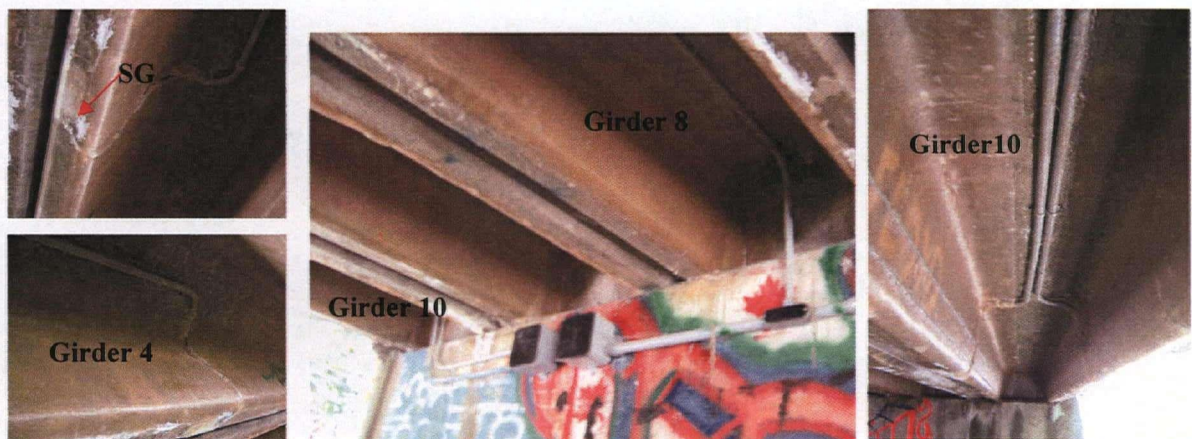


Figure 6-20 Safe Bridge Site Photos: Conduits for Strain Gauge Wires





Figure 6-21 Conduits for SG Wires and Storage Boxes on the East Abutment

During the 2003 field testing, the wires were first took out from the two storage boxes (Figure 6-22), and then connected to the extension cables prepared by the technician to be connected to the signal conditioner (see Figure 6-23 [a]); the testing day was a raining day so that the connectors of the wires needed to be wrapped and protected from moisture (Figure 6-23 [b]).



Figure 6-22 Six SG Wire Cables Taken Out from Storage Box to Connect to Signal Conditioner



Figure 6-23 Field Test 2003 Site Photos: Connect Sensor Cables with Signal Conditioner Cable



The extension cables connected to the signal conditioner were also in three-wire connections (see Figure 6-24); and all the connections between equipments (signal conditioner to DAQ board and DAQ board to laptop) were all by wires. It is not hard to imagine that if the number of sensors were more, the wiring of all equipment could be a mess.



Figure 6-24 Field Test 2003 Site Photos: Wire Connections to Signal Conditioner and DAQ Board

As for the *WebDAQ/100* connection, it was purposely operated inside the house, so the wiring from the signal conditioner to *WebDAQ/100* needed to go all the way to indoor. The wire cable ran across Safe Bridge (beneath) first, through the grass field, and then down the stairs beside the house to enter the basement of the restaurant, where *WebDAQ/100* was located (see Figure 6-25). The photos shown in Figure 6-25 have been modified (cable line has been traced in red) in order to show the location of the wire cable clearly.

Theoretically speaking, longer wire will lead to higher noise in the data. Nonetheless, from Ch 4, one can see that the difference is not significant; the reason could be that length of the wire cable was still relatively short (~50 meters longer) when compared to many other bridge applications; therefore the data collection can be considered as not affected. Also note that the route shown in Figure 6-25 is not “final”. If long-term monitoring will be performed in the future, the exact route of the wire cable will be designed to minimize damage from the environment; e.g. place the cable high along the wall with conduit. “Safety” is the major concern (for both people and the cable itself).



Figure 6-25 Field Test 2003 Site Photos: Wiring between Signal Conditioner and *WebDAQ/100*



### 6.3.2 For Fiber Optic FT Sensor Readings

The communication medium for the FT-sensors is the optical fiber, as expected. Since one of the objectives for the 2005 field testing was to learn the setup and handling of FOSs, the following will present what have been done in detail during the 2005 field testing to connect the FT sensors with FTI-3300 to collect data successfully.

First the FT-sensors were taken out from the storage boxes (two FT sensors in a box, total three boxes located between the two “legs” of Girder 2, 6, and 10; see Figure 6-3). The condition of the connectors determines if the data signals can be collected successfully. The connector is fragile and sensitive, so it is covered with a protective cap, as shown in Figure 6-26 [a]. It is important to record the sensor numbers to indicate which sensor is connected to which channel of FTI-3300 (Figure 6-26).

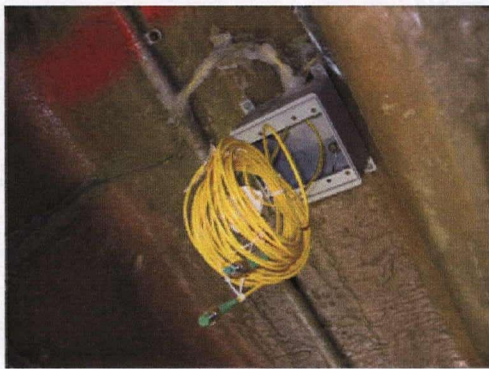


Figure 6-26 Field Test 2005 Site Photos: [a] FT-Sensors Taken Out from Junction Box  
[b] Connector of FT Sensor and Sensor Number

Fibre optic extension cables are required to elongate the FT-sensors to the FTI-3300 interrogator (Figure 6-27). As mentioned earlier, one need to be careful not to kink or coil the optical fiber over the radius limit, which will effect the signal readings.



Figure 6-27 Field Test 2005 Site Photos: Fiber Optic Extension Cables to FT-Sensor and FTI-3300



One important step for the FOS setup is to clean the connectors of the FT-sensors and the optical inputs of the FTI-3300 machine. All connector heads and the optical inputs must be cleaned with link-free foam swabs dabbed in “optical grade” (>99% pure) iso-propyl alcohol (propanol), or “laboratory grade” (>95%) ethyl alcohol (ethanol). During the Safe Bridge field testing, the laboratory graded ethanol was used as the solution to clean the optical connections (see Figure 6-28 and Figure 6-29).



Figure 6-28 Field Test 2005 Site Photos: FT-Sensor Head; Cleaning the Optical; FO Connection

The connector to be inserted into the FTI-3300 Input Port is with the standard FC-APC connector. To connect the sensor, line up the notch on the input connector on the FTI-3300 front panel with the key on the sensor connector, and gently insert the white ceramic ferrule inside the inner ring of the input port. Then screw in the connector until it is finger tight; be very careful not to over-tight the connection [226]. The white ceramic ferrule is very fragile and once it is damaged will result in loss of signals or false signals. All connectors and the input ports of FTI-3300 have protective caps supplied; when not in use, they should always be covered with the protective caps.



Figure 6-29 Field Test 2005 Site Photos: [a] Connecting Optical Fiber to FTI-3300  
[b] Cleaning Optical Head with Laboratory-grade Ethanol

## **6.4 Data Management**

As defined in Chapter 2, Data Management includes the processing of data and the storage & retrieval of data. What have been done in cleaning and normalizing the raw data from the two field testing have been covered in earlier chapters. As for the storage of data, the amount of data is the major factor for deciding what to be and not to be saved. The steps applied to the two field testing results for data management will be briefly summarized in the following.

### **6.4.1 Data Processing**

The data processing procedures for field test 2003 and 2005 have been presented in details in Chapter 4 and 5; therefore they will not be repeated here. In summary, for the raw data from strain gauges, based-line correction (“zeroing”) has been applied to all sets of data. The static load testing data have been averaged as well to obtain the static load strain. Note that temperature adjustment was not applied to strain gauge readings, because when base-line corrections were applied to all data, the “initial values” (i.e. the strain values before the truck entered the bridge) were subtracted from each of the static strains under different loading positions; therefore, most of the thermal effects on strain have been canceled out. The thermal effect “left” to be adjusted was from the slight difference in temperature before this base-line period and the loading periods. Since the load testing were done in a relatively short period of time, the temperature difference was so small (less than 0.5 °C) that the thermal effect can be ignored.

For the data from the FT-sensors, the actual data processing was done by FOX-TEK because the initial measurements of FT-sensors taken when they were just installed in 2002 are not available to the author. How FT-sensor data should be processed was presented in a general way. Base-line correction and the conversion from displacements to average strains should always performed first. Thermal and load effects corrections should always be applied between the initial measurements and the field testing results. For comparisons with strain gauge readings, the FT-sensor results should be converted from average strain values to the equivalent maximum strain values.

#### 6.4.2 Data Storage and Retrieval

Since the amount of data from Safe Bridge field testing is relatively small (because all of them were performed in a short-term base), the storage for both raw data and analyzed data is possible, and actually is preferable. Currently, both the raw data and the analyzed results are saved in computer hard drive, as well as copied to CDs as backups. Therefore, the retrieval of data is straight-forward as well. It is strongly recommended to keep all the raw data for Safe Bridge testing, especially for the static-load testing readings. In fact, for any projects that the diagnostic approach is to compare new data to initial/previous testing results (most periodic monitoring are of this kind), the raw data should be kept, unless variations from different times of testing can be avoided completely, which is highly unlikely. Just like what happened in this thesis, the old data from the initial two field tests were required for data comparison, and because one could not be sure about the analysis method taken before, and if the load factors had been applied, the raw data were needed to be re-analyzed for more accurate comparison results. Even for a small project like Safe Bridge project demonstrates how important proper data storage and data retrieval ability to the success of a SHM system.

#### 6.5 Diagnostics

The interpretations of the cleansed data have also been covered in Chapter 4 for strain gauge readings, and Chapter 5 for long-gauge fiber optic sensor readings; therefore they will not be repeated again here. What have been done to the cleansed data in order to “diagnose” the health condition of Safe Bridge girders will only be briefly summarized in the following.

The *diagnostic* for Safe Bridge’s health conditioning is done by directly comparing the strain measurements taken from different times of field testing. Load factors have been applied to all data to adjust for the weight difference of testing vehicles. The static load testing results (from strain gauge readings) are summarized in Table 6-1 and Figure 6-30. From Table 6-1, one can see that besides Position 1&2 for *After\_Repair 2002*, the locations (the girder experienced the largest strain) were all very consistent. The static strain values between *After\_Repair2002* and *Strain\_Reading2003* are very close, which shows that the GFRP condition in these two times were about the same. When compared with *Before\_Repair2001*, the 2001 strain values are either greater or about the same, with a significant improvement in Girder 6; this can be seen clearly in Figure 6-30. It can be concluded that the GFRP reinforcement works well and de-bonding was unlikely.



Table 6-1 The Magnitude and Location of the Largest Strain for the Six Static Loading Positions

		Magnitude and Location of the Largest Strain Value Obtained					
		Truck Loading Position					
Testing Date		1	2	3	4	5	6
Nov. 2001	Value	62.8	62.4	62.4	59.6	83.5	101.8
	Location	Girder 10L	Girder 10L	Girder 4	Girder 4	Girder 6	Girder 6
Feb. 2002	Value	53.2	54.1	n/a	n/a	70.6	65.1
	Location	Girder 8	Girder 10R			Girder 6	Girder 6
Oct. 2003	Value	61.7	52.3	64.1	65.7	70.5	70.4
	Location	Girder 10L	Girder 10L	Girder 4	Girder 4	Girder 6	Girder 6

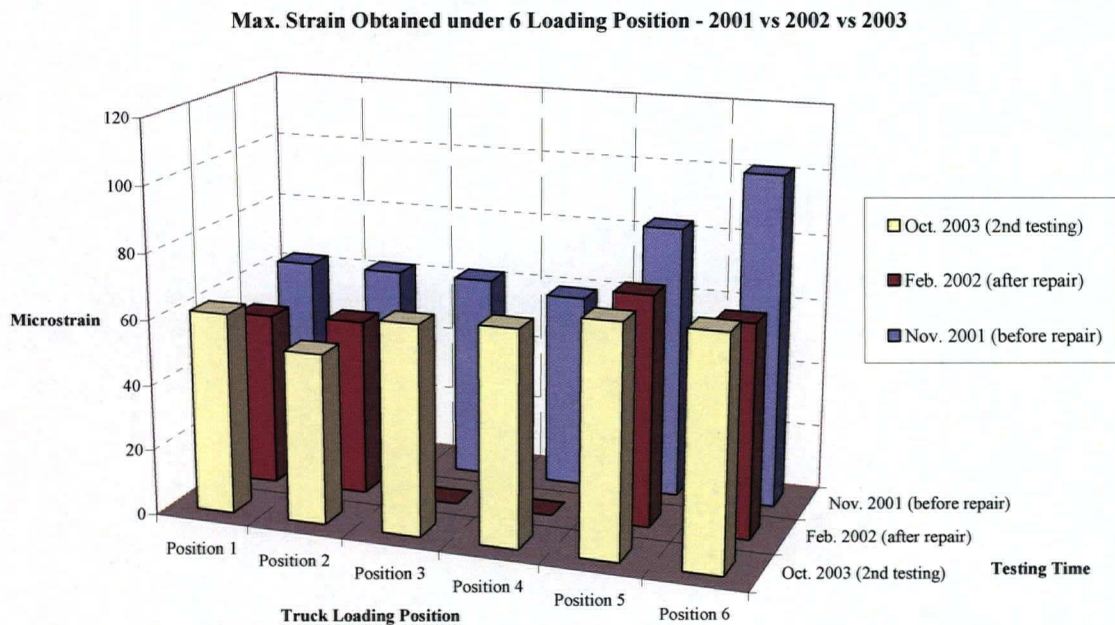


Figure 6-30 Maximum Static Strain Comparisons between Three Field Tests

For the rolling load testing, since the sampling rate used varied during different times of field test, adjustments on the sampling rate have been applied on some of the data, for better comparison. For the FOS readings, conversions from average strain to maximum strain needed to be done in order to compare the FOS strains to the strain gauge readings.

The conclusions drawn from all the comparisons will be given in the next chapter, the last chapter of this thesis, *Chapter 7 Conclusions and Recommendations for Future Projects*.

---

## Chapter 7

### Conclusions and Recommendations for Future Works

---

Besides the field testing of Safe Bridge and the data analysis and comparison, learning about the SHM process in general and to bridge the “gap” between civil engineers and the multidisciplinary SHM field are also objectives for this thesis; therefore, a significant amount of work was devoted to the literature research on SHM process, focusing on its applications on concrete bridges. However, for conclusion and future recommendations, the focus will be on Safe Bridge project only.

It is too early to draw “conclusions” for SHM yet, as this new field is still developing and progressing everyday, and at the same time there are still many practical problems to be solved. The author also do not feel “qualified” to give any recommendations for the new field, as all her understanding about SHM are based on many people’s work and knowledge. Nonetheless, the author strongly agrees that, for true growth and acceptance of SHM, besides the continual research works on all the sub-fields under SHM, “education” plays a critical role. As mentioned in Chapter 1 of the thesis, the construction industry has the longest *lag time* within all industries, and many people in the field are conservative with innovations and changes; *“believe it or not, that is a very difficult, foreign concept for the bridge engineer to grasp and implement,”*; *“... one reason is that the bridge engineer feels he has to put his budget into steel and concrete rather than accepting and implementing newer technologies that would actually improve their return on investment”* [103]. This phenomenon will not change until the people in the field have a different mentality, and “education” is probably the key. If today’s civil engineers are taught since their schooling that aging of infrastructure is a serious problem, that needs in reinforcement/rehabilitation maybe greater than needs for new construction, that SHM is important and beneficial to push civil engineering into next level, then to accept and utilize innovations will become the general attitude. People have to think/believe in a way in order to act in that way. That is how new technologies become wild-spread and affordable. Hopefully “smart bridges” and “smart buildings” will become part of everyone’s daily life in a near future.

In the following, the chapter will first conclude the findings from the two field testing on Safe Bridge, and then recommendations will be given for future work on Safe Bridge.

## 7.1 Conclusions

Compare to most current-running SHM projects, Safe Bridge project is a relatively simple and small-scale bridge application. Nonetheless, this project still demonstrates the following:

- how SHM system is utilized in the study for new repair method and material;
- how conventional strain gauges can be integrated with FOSs to be a monitoring system;
- how static field testing is incorporated into the long-term process of periodic monitoring.

The GFRP reinforcement condition of Safe Bridge was evaluated by the comparisons of different sets of field testing results. Each of the comparisons and the “problems/concerns” discovered from them will be concluded in the following.

### I. *Comparisons between Static Strain (based on SG readings under 6 loading positions):*

Generally speaking, the static strains for *After\_Repair 2002* and *Strain\_Reading 2003* are about the same. Especially when the average of the loading-pairs (Position 1&2, 3&4, 5&6) are used, all the differences between the two testing are within 5  $\mu\epsilon$ . The thermal coefficient of steel rebar is similar to concrete and the GFRP, around 6~10  $\mu\epsilon/^\circ\text{C}$ . In addition, with the effect of noise (standard deviation of the static strains were around  $\pm 2 \mu\epsilon$ ), a variation of 5  $\mu\epsilon$  can be considered as “no changes”. Therefore, these sets of comparison concluded that the condition of the GFRP reinforcement stayed the same after 20 months of field usage.

When compared to *Before\_Repair 2001* results, most of the static strains are smaller; for Position 3&4, the static strains are about the same. In one particular case (Position 6), the static strain drops from 102  $\mu\epsilon$  before repair to 70  $\mu\epsilon$  during the 2003 testing, which is more than 30% of improvement. Even when the average values of the “position-pairs” are used (to minimize “error effect”), the static strain still decreased by almost 25%. The comparisons showed that the *spray GFRP* is a very effective reinforcement method.

### *“Problems”:*

Strain Gauge#2 (the SG installed in Girder 4) was malfunctioning during *After\_Repair 2002*; therefore, comparison for the data under Position 3 and 4 were affected significantly because SG#2 supposed to give the largest static strains. In addition, the raw data for Position 4 and Position 6 for *After\_Repair2002* seemed incomplete/damaged (please refer to Figure 4-16 and 4-17).

Another “possible problem” identified, based on the observation of the strain plots, was that the exact truck positions during the three times of field testing might have varied slightly, in terms of the relative positions to the concrete curb. Also, a few static values seemed to be affected by higher noise because they have larger standard deviation values.

## **II. *Comparisons between Time-Strain Histories (SG readings under 3 rolling load positions):***

Generally speaking, the rolling load results also show relatively small strain changes between the 2002 and 2003 field test results, and decrease in strain readings when compared to the *Before\_Repair 2001* data. However, the comparison results from this set are less convincing because more “variables” were identified; see below.

### ***“Problems”:***

The biggest problem was that different vehicle speed was used during the three times of field testing. Generally speaking, the higher the testing vehicle’s speed, the lower strain the bridge girder will experience. The time spent for the testing vehicle to cross the bridge varied from as little as 4 or 5 seconds to as much as 24 seconds. With such significant difference in “rolling speed”, the comparisons between the strain readings can not be made. Nonetheless, there was one set of data used similar traveling speed (2002 vs. 2003 Position Roll II), and their strain results were about the same, which matched the results from the static-load comparisons.

Other “smaller” variations include the difference in sampling rate (which had been adjusted, but still not exactly the same) and the possibility of different truck positions in relation to the concrete curb (i.e. in one field testing, the truck was “rolling” against the curb, but in another, the truck was moving in a distance to the curb).

## **III. *Comparisons between FOS\_2005 and Its Initial Measurement at 2002 (based on FT readings):***

The raw data of the long-gauge fiber optic sensors (FT-sensors) on Safe Bridge provide both displacement and temperature measurement. Instead of getting the “point strain” like what strain gauges provide, the FT-sensors measure the average strain over the gauge length. The FT sensors are typically made to give an unstrained initial reading, for example, 15mm, to provide both tension and compression measurement capability. Therefore, it is important to take the initial reading when the FT-sensor is just installed, to obtain the true strain changes. It is also important to make thermal adjustment for temperature changes.



One of the long-gauge fiber optic sensor (FT#560, located on Girder 6 parallel to the tension rebar) was tested during its initial installation for the six-static-load positions during the 2002 field test. That testing results were compared to the strain values from three “comparable positions” of *FOS\_2005*, and the comparison showed that the strain values were about the same (differences around or less than 5  $\mu\epsilon$ ). The comparison result proves that the condition of the GFRP reinforcing layer has not changed much since its installation.

*“Problems”:*

The major problem for this set of comparison is the difference in loading positions; *FOS\_2005* used the 9-static-load positions (please refer to Figure 5-5) whereas the 2002 field testing used the 6-static-load positions. None of the loading positions were identical; only three of the *FOS\_2005* positions were “in between” the 2002 6-positions. Therefore the comparisons were made based on those three loading positions. In addition, the weight of the loading truck for these two field tests were slightly different, which should have been adjusted as well, even though the effect is small. All the initial readings for the FS-sensors should be obtained from FOX-TEK.

**IV. Comparisons between SG Readings and FT-Sensor Readings:**

In order to be compared with the strain gauge readings, the average strains measured by FT-sensors were need to be converted to maximum strain values first. The formulation of the conversion is given in Chapter 5.4.3. Under certain assumptions (assume the girder is simply supported, the gauge length is equal to the span length, the front axle load can be ignored and the tandem axle load is on mid-span), the relationship between the average strain and the maximum strain caused by the point load can be simplified into  $\epsilon_{\max} / \epsilon_s = 2$ . Even though the assumptions did not represent the real conditions fully, they are reasonably close to the actual condition; and therefore the factor “2” was applied to the average strains to approximate the equivalent maximum strain values.

The readings from the sensors installed on Girder 6 (SG#3 and FT#560) were used for this set of comparison. For *FOS\_2005*, the largest average strain obtained under the 9 loading positions was about 30  $\mu\epsilon$ , so it is estimated that the maximum strain experienced by Girder 6 should be around  $30 \mu\epsilon \times 2 = 60 \mu\epsilon$ . For strain gauge readings, the *After\_Repair 2002* data was used and the maximum strain given by SG#3 was 70  $\mu\epsilon$ . Since the value 60  $\mu\epsilon$  itself was an approximate itself, the two numbers were considered close enough to conclude that, after three years of field service, the

condition of the GFRP reinforcing layer stays about the same as when it was just installed, and the occurrence of debonding on Girder 6 was highly unlikely.

*“Problems”:*

This set of comparison should be seen as “reference” only because the result was based on many too many assumptions. The gauge length is actually a little shorter than the span length (5 m gauge on 7.3m span); the support condition is not purely simply supported; the front axle indeed does not cause much effect but it is still not outside the span completely. In addition, thermal effect was not adjusted for the strain gauge readings and load factor (for different truck weight) was not applied.

Overall, based on all four sets of comparison results mentioned above, one can conclude that the GFRP reinforcement works well under the operating environment so far, and debonding has not yet occurred. The GFRP reinforcement conditions were checked visually as well during the 2003 and 2005 field testing, and the reinforcing layer appeared intact.

*WebDAQ/100 Testing:*

As for the testing of the web-based DAQ system (*WebDAQ/100*), comparisons were made between the *WebDAQ/100* data and the *I/O Tech DaqBook* data. The *I/O Tech DaqBook* is a conventional DAQ system that the technician is familiar with, and during the load testing, the system was placed right beside the sensors (bridge) to minimize noises (such as the lead wire effect). By comparing the data from the two different DAQ systems, one can double-check the strain measurements and to see if *WebDAQ/100* is suitable for bridge field testing.

The comparisons showed that, except for Strain Gauge #2 (located on Girder 4), the readings for all other five SGs were almost identical. This shows that the longer wiring (details see Ch 6) did not increase the noises much, and *WebDAQ/100* can provide accurate strain measurements under both static and rolling loads. The reading differences in SG#2 were consistently in a certain ratio to the magnitude of the measurements; the readings from *WebDAQ/100* were all about 90% of that from the *I/O Tech DaqBook*. The reason for the difference was unknown, but SG#2 also happened to be the malfunctioning sensor during the 2002 field testing. The functionality of SG#2 needs further examination. This could also be the reason why for the comparisons of strain readings between 2001 (before repair) and 2003 testing, the 2003 readings were actually a bit greater ( $\sim 5 \mu\epsilon$ ) than the strain readings before the reinforcement.

The problem found with the *WebDAQ/100* measurements was that the data was not complete; that is, for the six static load positions, three sets of data got both the beginning and the end cut-off; three sets of the data have the beginning sections missing. This could have been due to some set-up error of the software, so that only a portion of the data were actually saved (all the data were available on site during the field testing when directly reading them from screen).

In addition, it was intended to test the auto-e-mailing function, but due to time constraint, the testing was not realized. According to the technician, if more time were given, the system could have been setup to work perfectly as intended. Actually, *WebDAQ/100* was integrated with another system for wireless networking, and the whole unit was used in another site monitoring project in UBC. The system was used to continuously monitor the repaired overpass of the UBC aquatic center for two weeks with auto-e-mailing, and the monitoring process was very successful.

## **7.2 Recommendations for Future Work**

The recommendations for future work will focus on two aspects of Safe Bridge project: (1) what should and should not be done for the truck load testing in the future; (2) what is a potential set-up for a remote, long-term monitoring system for Safe Bridge in the future?

With all the problems identified above, the major lesson learnt was that, better control in “variables” should be applied for field testing. Difference in truck weight can be easily fixed by applying a load factor, but loading positions and sampling rate, and in particular, truck traveling speed, should be kept consistent. For future testing, when time is allowed, data should be collected from both the strain gauges and the FT-sensors, under both the six- and nine- static loading positions, with consistent sampling rate. For the rolling load test, the traveling speed used during 2001 field testing should be applied again; and then another set of rolling load testing can be based on either the 2002 or 2003 field testing speed (2002 is preferred). Data comparison with that of *Before\_Repair 2001* shows the effectiveness of the reinforcement, and the comparison with that of *After\_Repair 2002* data shows the field performance of the reinforcement. The comparison between the strain gauge and FT-sensor readings shows the bonding condition of the reinforcement.

For remote monitoring on Safe Bridge, the suitability of *WebDAQ/100* has been tested, and further steps can be taken for future work. For long-term monitoring, the first issue to consider is to find a

“safe place” or think of a way, to leave the equipment on site. The remote monitoring will require about 50 watts of AC 120 V power, a cable internet connection, and consume a space about 3 square feet (signal conditioner is also required) [219]. The best scenario is to make arrangements with the restaurant owner to allow the placement of the storage box with *WebDAQ/100* some place indoor (like the basement location where we operated *WebDAQ/100* during the 2005 field testing). This is the most ideal because weather and humidity will be out of concern. Also, internet hookup and AC power will be easy to arrange. A low voltage (15 volts) polyurethane cable can take the strain gauge signals from the bridge to the *WebDAQ/100* system inside the restaurant [219]. The length required for the cable should be less than 60 meters unless extra routing is required for safety and damage concerns. The cable should be protected and conduit should run underneath the grass field, and then along the wall of the restaurant. Detailed routing can be designed later, the idea is to minimize people/animal interactions. If storing the unit in the restaurant is not an option, what can be done is to place the equipment in a steel weather resistant enclosure and mounted it either somewhere under the bridge or to the power pole right beside Safe Bridge. The choice of location is mainly for security concern (vandalism). The main disadvantage of this scenario is that extra power (probably 30 watts) and a temperature control system are required to protect the equipment from getting to cold/damp, especially during winter.

As for the fiber optic FT-sensors, more issues need to be considered, and the main reason is the high cost associate with the interrogator, and the high sensitivity and fragility of the sensor connectors. Temperature limit need to be maintained. Again, renting an indoor space from the restaurant besides Safe Bridge to store the interrogator is the most ideal scenario. Power will not be a problem, but a laptop will be required. Both equipments can be stored in a NEMA box to protect them. An air card will be required to monitor Safe Bridge remotely via internet and a cellular network for data transfer. For example, a Sierra aircard that fits into computer slot can be used for communicating the measured data through a cellular network, as long as there is cell coverage in the area [218]. Another possibility is to use *WebDAQ/100* to transmit the data through internet; this part has not been tested yet (to connect *WebDAQ/100* to FTI-3300) and further testing is required before the actual set-up for remote monitoring. FOX-TEK has the people and knowledge to assist in the set-up for remote monitoring. The FTI-3300 used during the 2005 field testing was borrowed from ISIS Canada. If the system needs to be left on site of Safe Bridge for a period of time, it is not economical to purchase one; renting the equipment from FOX-TEK is a better option.



Future work on Safe Bridge includes the continue truck load testing and a possibility for a period of continuous monitoring. The benefit of the continuous monitoring is to be able to collect “stress cycle counting” information. Stress counting produces a snapshot of the size and associated number of stress cycles that a bridge has been exposed to [227]. The stress range frequency data (stress spectrum) can then be used for fatigue analysis and study [227], which is also an area for *spray GFRP* that requires further investigation. For a good representative stress ranges and their respective frequencies, the data acquisition should be left running continuously to capture the true traffic condition during different period of time in a day, in a week, or even a month; the most ideal is to obtain seasonal changes in the traffic pattern, which will require continuous monitoring for a year. For continuous monitoring, making the data acquisition to be fully automatic web-based system (remote monitoring) will be required, and for Safe Bridge, the process can be done as discussed earlier.

Clearly, the technology is available. Experiences with Safe Bridge so far have been very beneficial in the study of SHM process. The performance of the *GFRP reinforcement* so far has been very satisfying. To obtain the long-term performance of the new repair method under field condition still has a long way to go. Nonetheless, SHM technology will make this “long way” smoother and shorter. The *spray GFRP* technique should and will be applied to more field projects in the future, and with more knowledge about SHM techniques, more advanced set-up can be installed on these future projects, for even better and effective monitoring results.

## REFERENCES

---

- [1] McNeil, Sue. "*The Infrastructure Crisis: Are we there yet?*" Institute of Civil Infrastructure System (ICIS), Oct. 27, 2001.
- [2] Sanders, Heywood T. "*What Infrastructure Crisis?*" **The Public Interest**, No. 110, p.3(16), 1993.
- [3] Tatom, John A. "*Is an Infrastructure Crisis Lowering the Nation's Productivity?*" **Review**, The Federal Reserve Bank of St. Louis, Vol. 75, No. 6, Nov./Dec. 1993, pp. 3-22.
- [4] East Asia Analytical Unit (EAAU). **Asia's Infrastructure in the Crisis**. Harnessing Private Enterprise, Oct. 1998.
- [5] Infrastructure Canada, *Assessing Canada's Infrastructure Needs: A Review of Key Studies*, Sept. 2004.
- [6] "Government Acutely Aware of Infrastructure Crisis", Engineering News.  
<[http://www.l2b.co.za/Construction\\_News/Article/Article~ID~1171.asp](http://www.l2b.co.za/Construction_News/Article/Article~ID~1171.asp)>
- [7] The World Bank, "*Averting an Infrastructure Crisis*," Indonesia Policy Briefs – Ideas for the Future. Jan. 2005.
- [8] Business Council of Australia. "*Urgent National Plan Needed for Infrastructure says BCA*", Mar. 26, 2005. <<http://www.bca.com.au/content.asp?newsID=97872>>
- [9] Aktan, A.E., A.J. Helmicki, and V.J. Hunt. "*Issues in Health Monitoring for Intelligent Infrastructure*," **Smart Materials and Structures**, Vol. 7, No. 5, (Oct. 1998): 674 –692.
- [10] "2005 Report Card for America's Infrastructure," American Society of Civil Engineering.  
<<http://www.asce.org/reportcard/2005/index.cfm>>
- [11] **Civil Infrastructure Systems Technology Road Map 2003 – 2013: A National Consensus on Preserving Canadian Community Lifelines**. The Canadian Society of Civil Engineering, June 2003.  
<[http://www.csce.ca/TRM/TRM-Report\\_english\\_01.pdf](http://www.csce.ca/TRM/TRM-Report_english_01.pdf)>
- [12] Zuker, Richard C. "*Closing the Municipal Infrastructure Gap in Canada*." Prepared for The Federation of Canadian Municipalities (FCA), Sept. 8, 2004.
- [13] Chapin, Tim, "*Infrastructure Crisis*," Power Point Slides for Course: The Planning of Community Infrastructure. Department of Urban and Regional Planning, Florida State University. <<http://garnet.acns.fsu.edu/~tchapin/urp5731/lectures/InfraCrisis.ppt>>
- [14] Mirza, M. Saeed, and Murtaza Haider. "*The State of Infrastructure in Canada: Implications for Infrastructure Planning and Policy*," **Infrastructure Canada**, Mar. 2003.
- [15] Pritchard, Brian. **Bridge Design for Economy and Durability – Concepts for New, Strengthened, and Replacement Bridges**. Thomas Telford, London, Great Britain, 1992.

- 
- [16] "Civil Infrastructure Systems Technology Road Map," **DIALOGUE for Engineers and Geoscientists**, Association of Professional Engineers and Geoscientists of Newfoundland, Issue Sept. 2003. <[http://www.pegnl.ca/dialogue/issues/2003/september\\_2003/article\\_5.htm](http://www.pegnl.ca/dialogue/issues/2003/september_2003/article_5.htm)>
- [17] Vanier, D. J. "Why Industry Needs Asset Management Tools," **Journal of Computing in Civil Engineering**, Vol.15, No.1, Jan. 2001, pp. 35-43.
- [18] Hameed, A., G.F. Fernando, D. Winter, etc.. "Structural Integrity Monitoring of Concrete Structures via Optical Fiber Sensors: Sensor Protection Systems," **Structural Health Monitoring**, Vol. 2(2), June 2003, pp. 123-135.
- [19] Maalej, Mohamed, Anestis Karasaridis, Stavroula Pantazopoulou, and Dimitrios Hatzinakos, "Structural Health Monitoring of Smart Structures", **Smart Materials and Structures**, Vol. 11, 2002, pp 581-589.
- [20] Chopra, A.K. **Dynamics of Structures – Theory and Applications to Earthquake Engineering**. Prentice-Hall, 2<sup>nd</sup> Ed., 2001.
- [21] Heidebrecht, A.C. "Overview of Seismic Provisions of the Proposed 2005 Edition of the National Building Code of Canada," **Canadian Journal of Civil Engineering**, Vol. 30, 2003, pp.241- 254.
- [22] Scott, Richard. **In the Wake of Tacoma: Suspension Bridge and the Quest for Aerodynamic Stability**. ASCE Publications. Jan. 1, 2001. pp. 22,41,55.
- [23] McBean, Gordon, and Dan Henstra. "Disaster Resilient Cities – A Goal for the Future", **Opinion Canada**, Vol. 6, No. 18, May 13, 2004.
- [24] "1995 Kobe Earthquake, Japan." University of Washington, College of Engineering. <<http://www.ce.washington.edu/~liquefaction/html/quakes/kobe/kobe.html>>
- [25] Kishore, Kamal. "Disasters in Asia and the Pacific: An Overview." **Proceeding of FAO Asia-Pacific Conference on Early Warning, Prevention, Preparedness and Management of Disasters in Food and Agriculture**, Chiangmai, Thailand, June 12-15, 2001.
- [26] "Is the World Shaking More Now than Before?" **U.S. Geological Survey**. Oct. 1999. <[http://hvo.wr.usgs.gov/volcanowatch/1999/99\\_10\\_21.html](http://hvo.wr.usgs.gov/volcanowatch/1999/99_10_21.html)>
- [27] "Earthquake in India January 26, 2001, Magnitude 7.7." **U.S. Geological Survey**, Earthquake Hazards Program. <[http://earthquake.usgs.gov/activity/latest/eq\\_01\\_01\\_26/](http://earthquake.usgs.gov/activity/latest/eq_01_01_26/)>
- [28] "Earthquakes with 1,000 or More Deaths since 1900." **U.S. Geological Survey**, Earthquake Hazards Program. <<http://neic.usgs.gov/neis/eqlists/eqsmajr.html>>
- [29] Harzy, Joe. **Historical Tornado Events**. 8 May 2003. <<http://www.ezl.com/~fireball/Disaster15.htm>>

- 
- [30] “*Billion Dollar Disasters: A Chronology of U.S. Events*” **Live Science**.  
<[http://www.livescience.com/forcesofnature/disaster\\_chronology\\_1980\\_2004.html](http://www.livescience.com/forcesofnature/disaster_chronology_1980_2004.html)>
- [31] “*Katrina's official death toll tops 1,000*”, **CNN**.  
<<http://www.cnn.com/2005/US/09/22/katrina.impact/index.html> >
- [32] “*Katrina damage estimate hits \$125B*”, **USA Today**.  
<[http://www.usatoday.com/money/economy/2005-09-09-katrina-damage\\_x.htm](http://www.usatoday.com/money/economy/2005-09-09-katrina-damage_x.htm)>
- [33] **Floods**. Emergency and Disaster Management, Inc. 2005.  
<<http://www.disaster-management.net/flood.htm>>
- [34] “*2001 Global Register of Extreme Flood Events*”, Dartmouth Flood Observatory,  
<<http://www.dartmouth.edu/~floods/Archives/2001sum.htm>>
- [35] “*2005 Global Register of Extreme Flood Events*”, Dartmouth Flood Observatory,  
<<http://www.dartmouth.edu/~floods/Archives/2005sum.htm>>
- [36] “*2003 North America blackout*”, Wikipedia Encyclopedia.  
<[http://en.wikipedia.org/wiki/2003\\_North\\_America\\_blackout](http://en.wikipedia.org/wiki/2003_North_America_blackout)>
- [37] “*September 11, 2001 attacks*”, Wikipedia Encyclopedia.  
<[http://en.wikipedia.org/wiki/September\\_11,\\_2001\\_attacks](http://en.wikipedia.org/wiki/September_11,_2001_attacks)>
- [38] “*Sept. 11 didn't bankrupt any insurance companies, study says*”, Ball State University  
<<http://www.bsu.edu/update/article/0,1384,38104-5107-24536,00.html>>
- [39] Fujino, Yozo, and Masato Abe. “*Structural Health Monitoring in Civil Infrastructures and Research on SHM of Bridges at University of Tokyo*”, **International Forum on Infrastructure Maintenance**, Tokyo, Japan, Nov. 12, 2003.
- [40] Harchaoui, Tarek M., Faouzi Tarkhani, and Paul Warren. “*Public Infrastructure in Canada: Where do We Stand?*” **Statistics Canada**, Nov. 2003.
- [41] “*Integrity of Infrastructure Renewal Imperative*,” Ontario Concrete Pipe Association: News and Information, Posted Date: Apr. 7, 2004.  
<<http://www.ocpa.com/db/db/db2file.asp?fileid=64>>
- [42] “*Mind the Gap: Finding the Money to Upgrade Canada's Aging Public Infrastructure*.” TD Bank Financial Group, May 2004.
- [43] U.S. Department of Transportation Federal Highway Administration. “*Bridge Study Analyzes Accuracy of Visual Inspections*”. **FOCUS – Reporting on Innovative Products and Strategies for Building Better, Safer Roads**. Jan. 2001.
- [44] Virmani, Paul, and J.M. Hooks. “*Mitigation of Corrosion in Concrete Bridges*.” **19th US-Japan Bridge Engineering Workshop**, Tsukuba, Japan. Oct. 27-29, 2003.



- 
- [45] Pritchard, Brian. **Bridge Design for Economy and Durability – Concepts for New, Strengthened, and Replacement Bridges**. Thomas Telford, London, Great Britain, 1992.
- [46] Mufti, A.A., R.C. Tennyson, and J.R. Cheng. “*Integrated Sensing of Civil and Innovative FRP Structures*”, **Progress in Structural Engineering and Materials**, (5) 2003, pp. 115-126.
- [47] Banthia, N, “*Fiber Reinforced Polymers in Concrete Construction and Advanced Repair Technologies*,” Geosynthetica website – Technical Documents.  
<[http://www.geosynthetica.net/tech\\_docs/NBanthia15Dec.pdf](http://www.geosynthetica.net/tech_docs/NBanthia15Dec.pdf)>
- [48] Rizkalla, Sami, and Aftab Mufti. **Design Manual No. 3: Reinforcing Concrete Structures with Fibre Reinforced Polymers**. ISIS Canada, September 2001.
- [49] Mufti, Aftab. **Design Manual No. 2: Guidelines for Structural Health Monitoring**. ISIS Canada, September 2001.
- [50] Kiyosaki, R.T. and Lechter, S.L.. **Rich Dad’s Guide to Becoming Rich without Cutting Up Your Credit Cards**, Warner Business Books, New York, 2003.
- [51] **Moore’s Law**.  
<[www.archivebuilders.com/pdf/22017v005.pdf](http://www.archivebuilders.com/pdf/22017v005.pdf)>
- [52] Chang, Peter C., Alison Flatau, and S.C. Liu. “*Review Paper: Health monitoring of Civil Infrastructure*”, **Structural Health Monitoring**, Vol. 2, No. 3, Sept. 2003, pp.257-267.
- [53] Worden, K. and J.M. duLieu-Barton. “*An Overview of Intelligent Fault Detection in Systems and Structures*.” **Structural Health Monitoring**, Vol. 3, No. 1, March 2004, pp.85 –98.
- [54] Inman, Daniel J. “*General Overview of Advanced Technologies*.” Center for Intelligent Material Systems and Structures, Department of Mechanical Engineering Virginia Tech., Nov. 2, 2000.  
<[http://mceer.buffalo.edu/publications/sp\\_pubs/01-0002/presentations/InmanOverview.pdf](http://mceer.buffalo.edu/publications/sp_pubs/01-0002/presentations/InmanOverview.pdf)>
- [55] Van der Auweraer, H., and Bart Peeters. “*International Research Projects on Structural Health Monitoring: An Overview*”, **Structural Health Monitoring**, Vol. 2, No. 4, Dec. 2003, pp. 341–358.
- [56] Adams, Beverley, Charles Huyck, Babak Mansouri, Ron Eguchi, and Masanobu Shinozuka. “*Post-Disaster Bridge Damage Assessment*,” **Proceedings of the Joint ISPRS and TRM Conference**, Denver, US, Nov. 2002.
- [57] David, Prine. “*Remote-Controlled Bridge Monitoring*.” **Roads & Bridges**, Vol. 34, Issue 11, Nov. 1996.
- [58] Hoesly, Nathan, and Catherine Whyte. “*Optimal Sensor Placement and Damage Detection for Structural Health Monitoring*.” REUJAT 2004.  
<<http://wusceel.cive.wustl.edu/reujat/2004/hoeslywhyte.ppt>>

- 
- [59] Xu, Fanli. *"Health Assessment and Monitoring of A Post-Tensioned Segmental Concrete Bridge."* University of Illinois at Chicago, 2002.
- [60] Elgamal, A., Joel P. Conte, Sami Masri, etc.. *"Health Monitoring Framework for Bridges and Civil Infrastructure"*.
- [61] Sohn, Hoon, Charles R. Farrar, Francois M. Hemez, etc.. *"A Review of Structural Health Monitoring Literature: 1996 -2001"*, **Los Alamos National Laboratory Report**, 2003.
- [62] Uomoto, Taketo. *"Importance of Non Destructive Inspection."* **Proceedings of Construction Materials 2005 and Mindess Symposium**, Vancouver, Canada, Aug. 2005.
- [63] Gassman, S.L. and Waleed F. Tawhed. *"Nondestructive Assessment of Damage in Concrete Bridge Decks."* **Journal of Performance of Constructed Facilities**, Vol. 18, No. 4, Nov. 2004.
- [64] Nondestructive Testing. TISEC Inc.  
<http://www.tisec.com/PDFs/ServicesLit.pdf>
- [65] Brownjohn, J.M.W., *"Lessons from Monitoring the Performance of Highway Bridges,"* **Proceedings of International Workshop on Advanced Sensors, Structural Health Monitoring, and Smart Structures**, Keio University, Japan, 10-11, Nov. 2003.
- [66] Mufti, Aftab A. *"An Introduction to Structural Health Monitoring, and ISIS Technologies for Civil Engineering Smart Infrastructure,"* Presented at Civil engineering Materials Seminar at University of British Columbia, March 3, 2005.
- [67] Aktan, A. Emin. *"Justification for ISHMII: a US Perspective."* International Society for Structural Health Monitoring of Intelligent Infrastructure (ISHMII), July, 2004.  
<<http://www.ishmii.org/News/USperspective>>
- [68] Farrar, C.R., Doebling, S.W., Duffey, T.A., etc. *"A Statistical Pattern Recognition Paradigm for Vibration-Based Structural Health Monitoring."* **Proceedings of the 2<sup>nd</sup> International Workshop on Structural Health Monitoring**, Technomic Publishing, Lancaster, PA, pp.764-773.
- [69] ISIS Canada Website.  
<<http://www.isiscanada.com/about/main.htm?about.htm>>
- [70] Tennyson, Roderick. **Design Manual No. 1: Installation, Use and Repair of Fibre Optic Sensors.** ISIS Canada, Sept. 2001.
- [71] Neale, Kenneth. **Design Manual No. 4: Strengthening Reinforced Concrete Structures with Externally-Bonded Fibre Reinforced Polymers.** ISIS Canada, 2001.
- [72] Rivera, E., Mufti, A. and Thomson, D. **Design Manual No. 6: Civionics Specifications.** ISIS Canada, Oct. 2004.

- 
- [73] Banthia, N, Natarajan Nandakumar, and Andrew Boyd. "*Sprayed Fiber-Reinforced Polymers: from Laboratory to a Real Bridge*," **Concrete International**, pp. 49-54, Nov. 2002.
- [74] Banthia, N. and A.J. Boyd. "*Sprayed Fiber-Reinforced Polymers for Repair*." **Canadian Journal of Civil Engineering**, Vol. 27, pp. 907-915, 2000.
- [75] ISIS Canada, Demonstration Project.  
[http://www.isiscanada.com/field/main.htm?field\\_projects.htm](http://www.isiscanada.com/field/main.htm?field_projects.htm)
- [76] Banthia, Nemkumar, "*Monitoring World's First Bridge with Sprayed Fibre Reinforced Polymer Repair*," **Structural Health Monitoring Workshop 2002 Proceedings**, Proceedings of the First International Workshop on Structural Health Monitoring of Innovative Civil Engineering Structures, ISIS Canada, Winnipeg, Canada, 2002, pp 135- 144.
- [77] "*UBC Develops Low-Cost Bridge Repair Technique*," Sept. 7, 2001. From University of British Columbia - Public Affairs Web site:  
<http://www.publicaffairs.ubc.ca/media/releases/2001/mr-01-59.html>
- [78] Mortazavi, Ali R.. **Experimental And Finite Element Analysis of A Damaged Reinforced Concrete Bridge Strengthened with Sprayed Glass Fiber Reinforced Polymers**, M.A.Sc. Thesis, The University of British Columbia, Canada, 2004.
- [79] Nandakumar, N. "*Strengthening of Safe Bridge, Duncan, British Columbia: Use of Hybrid Fiber Reinforced Mortar and Sprayed Glass Fiber Reinforced Polymer*." Department of Civil Engineering, University of British Columbia, Canada, 2001.
- [80] Cook, Michelle. "*Spray Strengthens Structures*," **UBC Reports**, Vol 47, No. 16, Oct. 8, 2001.
- [81] **Status of the Nation's Highways, Bridges, and Transit: 2002 Conditions and Performance Report**. U.S. Department of Transportation Federal Highway Administration.
- [82] **2004 Status of the Nation's Highways, Bridges, and Transit: Conditions & Performance Report**. U.S. Department of Transportation Federal Highway Administration.
- [83] Park, S.H.. **Bridge Inspection and Structural Analysis** (Handbook of Bridge Inspection). 2nd Edition. 2000.
- [84] Chase, Steven B. "*The Role of Smart Structures in Managing an Aging Highway Infrastructure*," NDE for Health Monitoring and Diagnostics, SPIE, CA, March 7, 2001.
- [85] "*Report Card for American's Infrastructure 2005 – Bridges*." ASCE website.  
<<http://www.asce.org/reportcard/2005/page.cfm?id=22>>
- [86] National Bridge Inventory website.  
<[http://www.nationalbridgeinventory.com/structurally\\_deficient.htm](http://www.nationalbridgeinventory.com/structurally_deficient.htm)>

- 
- [87] Chajes, Michael. "Experimental Load Rating of a Posted Bridge," ASCE, **Journal of Bridge Engineering**, Vol. 2, No. 1, Feb. 1997.
- [88] FHWA website.  
<<http://www.fhwa.dot.gov/bridge/deficient.htm>>
- [89] Chase, Steven B and Laman, Jeffrey A.. "Dynamics and Field Testing of Bridges," TRB (Transportation Research Board of the National Academies – *Transportation in the New Millennium*).
- [90] Cooper, James D. and Munley, Eric. "Bridge Research: Leading the Way to the Future," U.S. Department of Transportation, FHWA, Vol. 59, No. 1, Summer 1995.
- [91] Merkle, W.J. and Myers, J.J. "Load Testing and Load Distribution Response of Missouri Bridge Retrofitted with Various FRP Systems Using a Non-Contact Optical Measurement System." Transportation Research Board 85<sup>th</sup> Annual Meeting, Washington, D.C., Jan. 22-26, 2006.
- [92] Wardhana, K. and F.C. Hadipriono, "Analysis of Recent Bridge Failures in the United States," ASCE, **Journal of Performance of Constructed Facilities**, Vol.17, No. 3, Aug. 2003, pp.144-151.
- [93] Emerging Construction Technologies – Precast Inverted T Beams  
<<http://www.new-technologies.org/ECT/Civil/itbeam.htm>>
- [94] Frangopol, D.M. Ed. **Bridge Safety and Reliability**. Reston, VA: Structural Engineering Institute of the American Society of Civil Engineers, c1999.
- [95] **CAN/CSA-S6-00 Canadian Highway Bridge Design Code**, National Standard of Canada, CSA International, Canada, Dec. 2000, Section 14-Evaluation.
- [96] Moore, M., Phares, B., Rolander, D., Graybeal, B., Washer, G., **Reliability of Visual Inspection for Highway Bridges, Volume I: Final Report**, U.S. Department of Transportation (FHWA-RD-01-020), Washington, DC, June 2001.
- [97] Livingston, Richard A., "FHWA Fiber-Optics Research Program: Critical Knowledge for Infrastructure Improvement", U.S. Department of Transportation FHWA, Public Roads, Vol. 63, No. 1, July/August 1999.
- [98] Digital Projects - Collections, Library of Syracuse University  
<<http://library.syr.edu/digital/collections/c/Ceraldi/images/D-3%204e.jpg>>
- [99] *Concrete Repair Terminology*, International Concrete Repair Institute.  
<<http://www.icri.org/onlineresources/ConcreteRepairTerminology.pdf>>
- [100] **Manual for Condition Evaluation of Bridges, 1994**. American Association of State Highway and Transportation Officials, Washington, DC, 1994.



- 
- [101] Phares, B.M., G.A. Washer, D.D. Rolander, etc., "Routine Highway Bridge Inspection Condition Documentation Accuracy and Reliability," **Journal of Bridge Engineering**, July/August 2004, pp.403-413.
- [102] Chase, Steven B. "Long Term Bridge Monitoring to Support Bridge Technology Innovations," **Proceedings of the 19<sup>th</sup> US-Japan Engineering Workshop**, Tsukuba, Japan, Oct. 27-29, 2003.
- [103] "Bridge - The Road to Repair, Renovation or Replacement." **Engineering News-Record (ENR)**, Issue Sept. 26, 2005.  
<<http://enr.construction.com/resources/special/archives/2005/Bridges.asp>>
- [104] Raina, V.K.. **Concrete Bridges: Inspection, Repair, Strengthening, Testing and Load Capacity Evaluation**. McGraw-Hill Professional, 1996.
- [105] Klaiber, F.W., T.J. Wipt, M.J. Nahra, etc., "Field and Laboratory Evaluation of Precast Concrete Bridges," Iowa DOT Project TR-440, Iowa State University, Nov. 2001.
- [106] Jáuregui, David V. and Barr, Paul J. "Nondestructive Evaluation of the I-40 Bridge over the Rio Grande River," **Journal of Performance of Constructed Facilities**, ASCE, Vol. 18:4, Nov. 2004, pp. 195-204.
- [107] Bakht, B., and Jaeger, L.G., "Bridge Testing – a Surprise Every Time," ASCE, **Journal of Structural Engineering**, Vol. 116 (5), 1990.
- [108] **Associated Press**, "Police: Five Dead in Overpass Collapse Near Montreal," Oct. 1, 2006.  
<<http://www.foxnews.com/story/0,2933,216926,00.html>>
- [109] Lunau, Kate, Alana Coates, Sidhartha Banerjee, and Brenda Branswell. "Dust Settles, Questions Arise," **The Gazette**, Sept. 30, 2006.
- [110] Keller, James. "Laval Overpass Collapse Likely Linked to Steel Bars Inside, Engineer Says," **Canadian Press**, Oct. 1, 2006.
- [111] Mehrkar-Asi, S., "Supplementary Load Testing in Assessment of Bridges," Gifford and Partners, UK, 1998.
- [112] Pinjarkar, S.G., O.C. Guedelhoefer, S.B. Smith, etc. "Nondestructive Load Testing for Bridge Evaluation and Rating." **NCHRP Project Rep. No. 12-28**, Transportation Research Board, Washington, D.C., 1990.
- [113] Salawu, O.S.. "Assessment of Bridges: Use of Dynamic Testing," **Canadian Journal of Civil Engineering**, Vol. 24, 1997, pp. 218-228.
- [114] Farrar, C.R., Duffey, T.A., Cornwell, P.J., and Doebling S.W.. "Excitation Methods for Bridge Structures", **Proceedings of the 17th International Modal Analysis Conference**, Kissimmee, FL, Feb. 1999.

- 
- [115] Farrar, C.R., Sohn, H., Hemez, F.M., etc., "*A Review of Structural Health Monitoring Literature: 1996 ~ 2001*", **Los Alamos National Laboratory Report**, LA-13976-MS, 2003.
- [116] Bakht, Baidar, Leslie G. Jaeger, and A.A. Mufti, "*Assessment of Bridges: Use of Dynamic Testing: Discussion*," **Canadian Journal of Civil Engineering**, Vol. 25, 1998, p. 188.
- [117] Rizkalla, S., Benmokrane, B., and Tadros, G. (2000) "*Structural Health Monitoring Bridges with Fibre Optic Sensors*," **European COST F3 Conference on System Identification and Structural Health Monitoring**, Madrid, Spain, pp. 501-510.
- [118] Wang, Xiaoyi, Scott Kangas, Divyachapan Padur, etc., "*Overview of a Modal-Based Condition Assessment Procedure*," **Journal of Bridge Engineering**, ASCE, Vol. 10 (4), 2005, pp.460-467.
- [119] Ventura, C.E., Onur, T. and Tsai, P.C., "*Dynamic Characteristics of the Crowchild Trail Bridge*," **Canadian Journal of Civil Engineering**, Vol. 27, 2000, pp. 1046-1056.
- [120] Carder D.S., *Observed Vibrations of Bridges*, **Bulletin**, Seismological Society of America, Vol. 27, pp. 267-303, 1937.
- [121] **CAN/CSA-S6-00 Canadian Highway Bridge Design Code**, National Standard of Canada, CSA International, Canada, Dec. 2000, Section 3, p. 48.
- [122] Harris, Harry G. and Sabnis, Gajanan M. **Structural Modeling and Experimental Techniques**, Ch 7 *Instrumentation – Principles and Applications*. 2<sup>nd</sup> Ed., CRC Press, 1999.
- [123] Brunner, F.K., "*Bridge Monitoring: External and Internal Sensing Issues*," in Ou J.P., Li H. and Duan Z.D. (Eds.), **Structural Health Monitoring and Intelligent Infrastructure**, Balkema (2006), pp. 693-698.
- [124] Lynch, J.P., "*Overview of Wireless Sensors for Real-Time Health Monitoring of Civil Structures*," **Proceedings of the 4<sup>th</sup> International Workshop on Structural Control and Monitoring**, New York City, NY, USA, June 10-11, 2004.
- [125] Lynch, J.P., Kincho H. Law, Erik G. Straser, etc., "*The Development of a Wireless Modular Health Monitoring System for Civil Structures*," **Proceedings of the MCEER Mitigation of Earthquake Disaster by Advanced Technologies (MEDAT-2) Workshop**, Las Vegas, NV, USA, Nov. 30-31, 2000.
- [126] Arms, S.W. and C.P. Townsend. "*Wireless Strain Measurement Systems – Applications & Solutions*," **Proceedings of NSF-ESF Joint Conference on Structural Health Monitoring**, Strasbourg, France, Oct. 3-5, 2003.
- [127] Brownjohn, J.M.W., Pilate Moyo, Chris Rizos, etc., "*Practical Issues in Using Novel Sensors in SHM of Civil Infrastructure: Problems and Solutions in Implementation of GPS and Fibre Optics*", **4<sup>th</sup> International Workshop on SHM**, pp. 499-506, Palo Alto, September 2003.

- 
- [128] Slowik, Volker, Evelyn Schlattner, and Thomas Klink, "*Fibre Bragg Grating Sensors in Concrete Technology*," **Leipzig Annual Civil Engineering Report**: No. 3, 1998.
  - [129] Thompson, L.D., B.D. Westermo, D.B. Crum, etc., "*Passive and Active Structural Monitoring Experience: Civil Engineering Applications*," **AIP Conference Proceedings**, Vol. 509, May 23, 2000, pp. 2131-2138.
  - [130] Graver, Thomas, Daniele Inaudi, and Justin Doornink. "*Growing Market Acceptance for Fiber-Optic Solutions in Civil Structures*," **Proceedings of SPIE – The International Society for Optical Engineering**, Philadelphia PA, USA, Oct. 25-28, 2004.
  - [131] Land, Richard, Ganapathy Muruges, and Madhwesh Raghavendrachar. "*Assessing Bridge Performance – When, What, How*." **19<sup>th</sup> US-Japan Bridge Engineering Workshop**, Tsukuba, Japan, Oct. 27-29, 2003.
  - [132] Los Alamos National Laboratory Website.  
<<http://www.lanl.gov/projects/ei/shm/sprp.shtml>>
  - [133] Hipley, P., "*Caltran's Current State-of-Practice*," **Proceedings of the Invited Workshop of the Consortium of Organization for Strong-Motion Observation Systems**, Richmond, CA, pp. 11-12, 2000.
  - [134] Sridhar, S., K. Ravisankar, S. Parivallal, etc., "*Remote Health Monitoring of Civil Engineering Structures – An Overview*," **Proceedings of ISSS International Conference on Smart Materials Structures and Systems**, Bangalore, India, July 20-30, 2005.
  - [135] Büyükoztürk, Oral and Tzu-Yang Yu, "*Structural Health Monitoring and Seismic Impact Assessment*," **Proceedings of the 5<sup>th</sup> National Conference of Earthquake Engineering**, Istanbul, Turkey, May 26-30, 2003.
  - [136] Iyengar, S.S., L. Prasad, and H. Min. **Advances in Distributed Sensor Integration**, Prentice Hall, NJ, USA, 1995.
  - [137] Website of **ISHMII** (International Society for Structural Health Monitoring of Intelligent Infrastructure). <<http://www.ishmii.org/SHM%20Glossary/Definitionsfolder/>>
  - [138] Wipf, Terry J., Brent M. Phares, Lowell F. Greimann, etc., **Remote Continuous Evaluation of a Bridge Constructed Using High-Performance Steel – Final Report**, Center for Transportation Research and Education, Iowa State University and Iowa Department of Transportation, May 2006.
  - [139] Wang, Winston and Brandon Muramtasu, "*Lab Room-Apparatus Map-Strain Gauges*," Berkeley University On-line Materials, 2000.  
<[http://bits.me.berkeley.edu/beam/sg\\_2.html](http://bits.me.berkeley.edu/beam/sg_2.html)>
  - [140] "*Strain Gauge: Selection*," efunda Engineering Fundamentals Website.  
<[http://www.efunda.com/designstandards/sensors/strain\\_gages/strain\\_gage\\_selection.cfm](http://www.efunda.com/designstandards/sensors/strain_gages/strain_gage_selection.cfm)>

- 
- [141] "Strain Gage: Sensitivity," efunda Engineering Fundamentals Website.  
<[http://www.efunda.com/designstandards/sensors/strain\\_gages/strain\\_gage\\_sensitivity.cfm](http://www.efunda.com/designstandards/sensors/strain_gages/strain_gage_sensitivity.cfm)>
- [142] "Noise Control in Strain Measurements", Davidson Measurement Website, 2000.  
<<http://www.davidson.com.au/products/strain/mg/technology/technotes/tn501.pdf>>
- [143] "Precision Strain Measurements," VISHAY Website.  
<[http://www.vishay.com/brands/measurements\\_group/guide/indexes/tn\\_index.htm](http://www.vishay.com/brands/measurements_group/guide/indexes/tn_index.htm)>
- [144] "LVDT Basics". Macro Sensors, Division of Howard A. Schaevitz Technologies, Inc, 2003  
<[http://www.macrosensors.com/lvdt\\_macro\\_sensors/lvdt\\_tutorial/lvdt\\_primer.pdf](http://www.macrosensors.com/lvdt_macro_sensors/lvdt_tutorial/lvdt_primer.pdf)>
- [145] "Linear Variable Differential Transformer," Wikipedia Website, last modified March 2006.  
<<http://en.wikipedia.org/wiki/LVDT>>
- [146] "About Linear Position Sensor, LVDT," GlobalSpec Website.  
<http://sensors-transducers.globalspec.com/LearnMore>
- [147] "About Acceleration Instruments." GlobalSpec Website.
- [148] "Types of Accelerometers." Courseware of Mechanical Engineering 107A at the University of California at Berkeley.  
[http://bits.me.berkeley.edu/beam/acc\\_2.html](http://bits.me.berkeley.edu/beam/acc_2.html)
- [149] Rust, Kevin J, "Introduction to Accelerometers and Calibration Techniques," MTS System Corporation, Oct. 29, 1997.
- [150] Johnson, Curtis D., "Types of Accelerometers," Process Control Instrumentation Technology, Prentice Hall PTR, National Instruments Website.
- [151] "Types of Accelerometers." Courseware of Mechanical Engineering 107A at the University of California at Berkeley.  
[http://bits.me.berkeley.edu/beam/acc\\_2.html](http://bits.me.berkeley.edu/beam/acc_2.html)
- [152] "Resistance Temperature Device." Wikipedia Website.
- [153] Hardin, R. Winn, "Fiber Optic Sensors Seek to Prove Their Utility," **SPIE OE Reports** 178, Oct. 1998.
- [154] Lee, Byoung-ho. "Review of the Present Status of Optical Fiber Sensors," **Optical Fiber Technology**, Vol. 9, Issue 2, April 2003, pp. 57-79.
- [155] Merzbacher, C.I., A.D. Kersey and E.J. Friebele. "Fibre Optic Sensors in Concrete Structures: A Review". **Smart Materials and Structures**, Vol.5, 1996, pp.196 -208.
- [156] Tennyson, R.C., T. Coroy, A.A. Mufti, etc.. "Fibre Optic Sensors in Civil Engineering Structures," **Canadian Journal of Civil Engineering**, Vol. 27, 2000, pp. 880-889.



- 
- [157] The Networks Reference Pages. "Fibre Optic Cable".  
[http://www.acerimmeronline.com/networks/fibre\\_optic.html](http://www.acerimmeronline.com/networks/fibre_optic.html)
- [158] "Fibre Optics," Course note of Bell College, School of Science and Technology, 2004.  
<http://floti.bell.ac.uk/MathsPhysics/introduction.htm>
- [159] CORNING – *Fiber 101 Selected Concepts*  
[http://www.corning.com/opticalfiber/discovery\\_center/fiber101](http://www.corning.com/opticalfiber/discovery_center/fiber101)
- [160] Freudenrich, Craig C., "How Fiber Optic Work", HowStuffWorks Website.  
<http://electronics.howstuffworks.com/fiber-optic.htm>
- [161] Sumitomo Osaka Cement Co., Ltd. Website.  
[http://www.socnb.com/techbox/hproduct\\_e/opto.html](http://www.socnb.com/techbox/hproduct_e/opto.html)
- [162] Biala, Nazario, "An Introduction to Fiber-Optic Sensors," SensorsOnline Website, Dec.2001.  
<http://www.sensorsmag.com>
- [163] Schneider, Kenneth S., "Fiber Optic Communications for the Premises Environment," Telebyte Inc. Website. (Courtesy of AMP Incorporated)  
<http://www.telebyteusa.com/foprimer/foch2.htm>
- [164] Strangio, Christopher E., "Data Communications Basics – a Brief Introduction to Digital Data Transfer," CAMI Research Inc., Massachusetts, US, 2003.
- [165] Welch, John C., "Topologies, Signals, and Wires, Oh My!," **Networks 201 – Part 2**, Vol. 16, Issue 6.  
<http://www.mactech.com/articles/mactech/Vol.16/16.06/Jun00GettingStarted/index.html#liber-Optic>
- [166] Tennyson, R.C., N. Banthia, E. Rivera, S. Huffman, and I. Sturrock, "Monitoring Structures Using Long Gage-Length Fiber Optic Sensors," **Caltrans Bridge Research Conference 2005**, Sacramento, CA, Oct. 31<sup>st</sup> – Nov. 1<sup>st</sup>, 2005.
- [167] Schmidt-Hattenberger, Cornelia, "Optical Fiber-Bragg-Grating-Sensors for Statical Strain Measurements in Geoengineering."  
[http://www.gfz-potsdam.de/pb5/pb51/html/conny3\\_en.htm](http://www.gfz-potsdam.de/pb5/pb51/html/conny3_en.htm)
- [168] Davis, M.A., Bellemore, D.G., and Kersey, A.D., "Distributed Fiber Bragg Grating Strain Sensing in Reinforced Concrete Structural Components", **Journal of Cement and Concrete Composites**, Vol. 19, No. 1, 1997.
- [169] Inaudi, D., and B. Glisic, "Combining Static and Dynamic Deformation Monitoring with Long-gauge Fiber-Septic Sensors," **Proceedings of the Second International Conference on Bridge Maintenance, Safety, Management and Cost**. Kyoto, Japan: International Association for Bridge Maintenance and Safety. 543–544, 2004.
- [170] GlobalSpec Website.  
[http://data-acquisition.globalspec.com/LearnMore/Electrical\\_Electronic\\_Components/Wires\\_Cables/Data\\_Acquisition](http://data-acquisition.globalspec.com/LearnMore/Electrical_Electronic_Components/Wires_Cables/Data_Acquisition)

- 
- [171] Shenton, H.T., "Sensors, Instrumentation and Data Acquisition – An Overview," Presentation slides, Center for Innovative Bridge Engineering, University of Delaware
- [172] National Instruments Corporation Website: *DAQ and Instrument Fundamentals – Introduction to Data Acquisition*, Version 29, 2006.  
<http://zone.ni.com/devzone/cda/tut/p/id/3536>
- [173] Bishop, Robert H. (Ed). **Handbook of Mechatronics** – Section VI: Software and Data Acquisition (Ch 44 ~ 50), CRC Press LLC, 2002.
- [174] Proakis, J.G., and D.G. Manolakis, **Digital Speed Processing: Principles, Algorithms and Applications**, 3<sup>rd</sup> Ed., Prentice-Hall, Upper Saddle River, N.J., 1996.
- [175] "Signal Conditioning Fundamental for Computer-Based Data Acquisition Systems," National Instruments Corporation Website Tutorial Material.  
<http://zone.ni.com/devzone/cda/tut/p/id/4084>
- [176] Fuller, Cris, *Chapter 48: Computer-Based Instrumentation Systems*, National Instruments, Inc., **Handbook of Mechatronics** (Bishop, Robert H. Ed.), CRC Press LLC, 2002.
- [177] WebDAQ/100 User Manual, 2001.
- [178] Elsea, Peter, "Basics of Digital Recording," Electronic Music Studios, University of California, US.  
<http://www.sfu.ca/sca/Manuals/Elsa/DigitalRecording.html>
- [179] "Coaxial Cable," Wikipedia Website.  
[http://en.wikipedia.org/wiki/Coaxial\\_cable](http://en.wikipedia.org/wiki/Coaxial_cable)
- [180] *Introduction to Ethernet – Technical Tutorial*, Dec. 2002. SENA Technologies, Inc. website.  
[http://www.sena.com/download/tutorial/tech\\_Ethernet\\_v1r0c0.pdf](http://www.sena.com/download/tutorial/tech_Ethernet_v1r0c0.pdf)
- [181] Todoroki, A., Shimamura, Y., and Inada, T. "Plug and Monitor System via Ethernet with Distributed Sensors and CCD Cameras," **Structural Health Monitoring 2000**, Stanford University, Palo Alto, California, 1999, pp. 571–580.
- [182] Taha, Mahmoud Reda, Husam Kinawi, and Naser El-Sheimy, "The Realization of Commercial Structural Health Monitoring Using Information Technology Based Techniques," **Proceedings of Structural Health Monitoring Workshop**, ISIS Canada 2002.
- [183] *Construction of Bridges – Introduction*. The Hong Kong Polytechnic University.  
<http://www.cse.polyu.edu.hk/~ctbridge/intro/intro.htm>
- [184] Morrissey, Michael. *How Bridges Work*. From howstuffworks web site:  
<http://travel.howstuffworks.com/bridge.htm>
- [185] "Beam Bridge," Tong-Ji University, China.  
<http://bridge.tongji.edu.cn/chinabridge/29.htm>

- 
- [186] Durham, S.A., Heymsfield, E., and Schemmel, J.J., "*Structural Evaluation of Precast Concrete Channel Beams in Bridge Superstructures*," National Academy of Science, TRB Annual Meeting, January 14, 2003.
- [187] "*Old and Ugly, Troubled Bridges Can Be Safe*," University of Arkansas, June 20, 2002. <http://www.wciencedaily.com/releases/2002/06/020620075737.htm>
- [188] Sexsmith, R., Nemy Banthia, Andrew Boyd, etc., "*Potential Retrofit Methods for Concrete Channel Beam Bridges Using Glass Fiber Reinforced Polymer*," ASCE, **Journal of Bridge Engineering**, Vol.19, Issue 1, Jan./Feb. 2004, pp. 67-74.
- [189] Kuennen, Tom. "*Precast Channel Bridge Inspection*." Concrete Product, Apr. 1, 2006. [http://concreteproducts.com/mag/concrete\\_standards\\_questions\\_arise/](http://concreteproducts.com/mag/concrete_standards_questions_arise/)
- [190] Conversation with Dr. N. Banthia, University of British Columbia, Sept. 13, 2004.
- [191] Kuennen, Tom, "*Corrosion Mars Flexural Reinforcement in Precast Beams*," Apr. 1, 2003. [http://concreteproducts.com/mag/concrete\\_scc\\_momentum\\_spreads/](http://concreteproducts.com/mag/concrete_scc_momentum_spreads/)
- [192] Kennedy, G.D., F.M. Bartlett, and D.M. Rogowsky, "*Concrete Strength in Alberta Type G Stringer Bridges*," Report for Bridge Engineering Branch Alberta Transportation and Utilities, Jan. 1996.
- [193] Jones, J.X., Ernest Heymsfield, and Stephan A. Durham. "*Fiber Reinforced Polymer Shear Strengthening of Short Span Precast Channel Beams in Bridge Superstructures*," **Transportation Research Board of the National Academies' 83<sup>rd</sup> Annual Meeting**, Jan. 11-15, 2004.
- [194] **AASHTO LRFD Bridge Design Specifications**, 2<sup>nd</sup> Ed., 1998.
- [195] Pleimann, L.G. and G.R. Riley, "*Pre-Designed Timber Bridges of Three Types for Arkansas County Roads*," University of Arkansas, June 2000.
- [196] **Bridge Design Manual**, Department of Transportation of Texas, Dec. 2001.
- [197] Boyd, Andrew J., **Rehabilitation of Reinforced Concrete Beams with Sprayed Glass Fiber Reinforced Polymers**, PhD Thesis, The University of British Columbia, Dec. 2000.
- [198] Drimoussis, E.H., **Shear Strengthening of Concrete Girders Using Carbon Fibre Reinforced Plastic Sheets**, M.A.S. Thesis, The University of Alberta.
- [199] Mao, S, S.D.B. Alexander, and D.M. Rogowsky, "*Tests of Alberta HC Type Stringers*," Report for Bridge Engineering Branch, Alberta Transportation and Utilities, Feb. 1997.
- [200] Nanni, A, "*Relevant Field Applications of FRP Composites in Concrete Structures*," **Proc., CCC 2001, Composites in Construction**, Porto, Portugal, Oct. 10-12, 2001, pp. 661-670.

- 
- [201] Hag-Dlsafi, Osman, Jonathan Kunin, and Streenivas Alampalli, "*In-Service Evaluation of a Concrete Bridge FRP Strengthening System*," **Special Report 139 of Transportation Research and Development Bureau**, New York State DoT, March 2003.
- [202] Mayo, R., A. Nanni, W. Gold, and M. Barker, "*Strengthening of Bridge G270 with Externally-Bonded CFRP Reinforcement*," SP-188, American Concrete Institute, **Proceedings of 4<sup>th</sup> International Symposium of FRP for Reinforcement of Concrete Structures**, Baltimore, MD, Nov. 1999, pp. 429-440.
- [203] Kachlaken, D.I. and David D. McCurry, "*Testing of Full-Size Reinforced Concrete Beams Strengthened with FRP Composites: Experimental Results and Design Methods Verification*," Final Report 387 of Oregon DoT Research Group, June, 2000.
- [204] Papakonstantinou, C.G., Michael F. Petrou, and Kent A. Harries, "*Fatigue Behavior of RC Beams Strengthened with GFRP Sheets*," **Journal of Composites for Construction**, Nov. 2001.
- [205] Banthia, N., "*Sprayed Fiber Reinforced Polymers: Coming to a Structure near You*," **Canadian Civil Engineer**, Winter 2005-2006, pp. 8-11.
- [206] Banthia, N., **Civil 527: Specialized Concretes**, Course Note, Oct. 2001.
- [207] Banthia, N., N.Nandakumar and A.J. Boyd, "*Sprayed Fiber Reinforced Polymers: from Laboratory to a Real Bridge*," **Proceedings from the 6<sup>th</sup> International Conference on Short and Medium Span Bridges**, Vancouver, Canada, CSCE, 2002, pp. 337-346.
- [208] Banthia, N., "*Fiber Reinforced Polymers in Strengthening and Blast Resistant Design*," **Proceedings of 4<sup>th</sup> International Conference on Concrete under Severe Conditions**, CONSEC04, Korean Concrete Institute, Seoul, South Korea, 2004, pp. 56-73.
- [209] Martazavi, R. *Seismic Response of Columns with Sprayed FRPs*, Project Report, The University of British Columbia, 2004.
- [210] From BC Ministry of Transportation database, as of May 27, 2005. From Ian Sturrock, Bridge Evaluation and Inspection Standards, Victoria, BC MoT.
- [211] American Association of State Highway and Transportation Officials (AASHTO), **Standard Specifications for Highway Bridges**, 16<sup>th</sup> Edition, Washington D.C., 1996.
- [212] Field Inspection Record by Mike Penner, June 6, 2001. Record copy provided by Ian Sturrock, Vancouver Island Region, Ministry of Transportation and Highways, BC.
- [213] **CAN/CSA-S6-00 Canadian Highway Bridge Design Code**, National Standard of Canada, CSA International, Canada, Dec. 2000.
- [214] Copy of written memorandum from Mike Penner, provided by Ian Sturrock, Bridge Engineer of BC Ministry of Transportation and Highways, Victoria.



- 
- [215] Nandakumar, N. *A Novel Repair Technique Using Glass Fibre Reinforced Plastics and Fiber Reinforced Mortar to Strengthen Concrete Girders of Safe Bridge*, Duncan, BC, Canada, Department of Civil Engineering, University of British Columbia, 2001.
- [216] **FTI-3300 Operating Manual**. Fiber Optic Systems Technology Inc. Revision 1.1, 2002.
- [217] Tennyson, R.C., and Tom Miesner, "Fiber-Optic Monitoring Focuses on Bending, Corrosion," **Oil & Gas Journal**, Vol. 104, Issue 7, Feb. 20, 2006.
- [218] Tennyson, Rod C., FOX-TEK Inc., e-mail communications.
- [219] Jackson, Scott, Engineering Technician, University of British Columbia, Personal/e-mail communications, 2003 ~ 2004.
- [220] *Practical Strain Gage Measurements*, Omega Engineering Inc. Stamford, CT.
- [221] "Primer on FOX-TEK FT Sensor System," website of Fiber Optic System Technology (FOX-TEK) Inc., 2003.
- [222] Rivera, Evangeline, ISIS Canada, E-mail communications, June 2005.
- [223] Rivera, E., Aftab Mufti, and Douglas Thomson, **Design Manual No. 6: Civionics Specifications**, ISIS Canada, October, 2004.
- [224] CEC Capital Equipment Inc. website.  
<http://www.cec488.com/wbapp.htm>
- [225] Wong, John, Engineering Technician, University of British Columbia, Personal communications, October 2003.
- [226] **FTI-3300 Operating Manual**. Fiber Optic Systems Technology Inc., Revision 1.1, 2002.
- [227] Mohammadi, Jamshid, Sidney A. Guralnick, Ramakrishna Polepeddi, "Bridge Fatigue Life Estimation from Field Data," **Practice Periodical on Structural Design and Construction**, Aug. 1998.

---

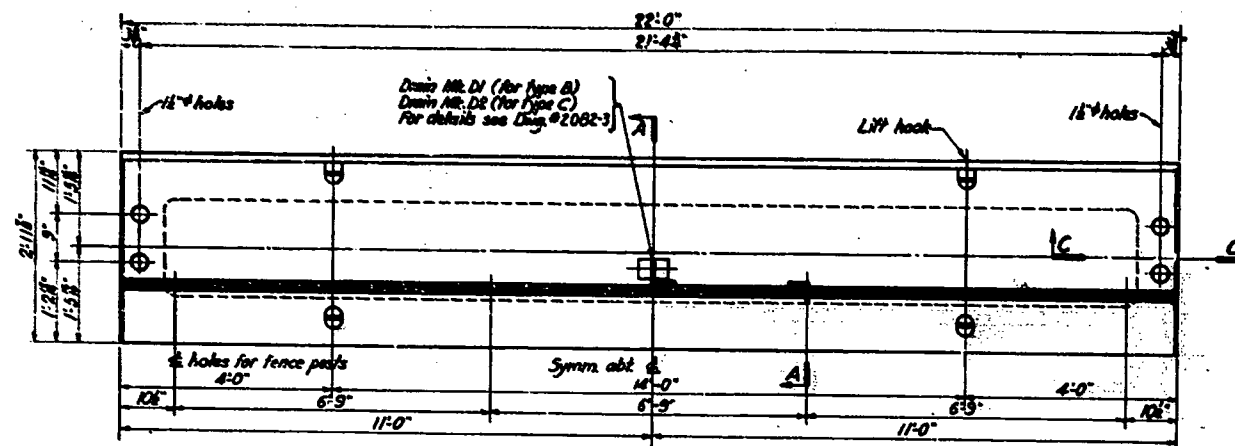
## **APPENDICES**

---

### **Appendix I**

#### **Standard Drawings of PCCB Girder (1950s-60s)**

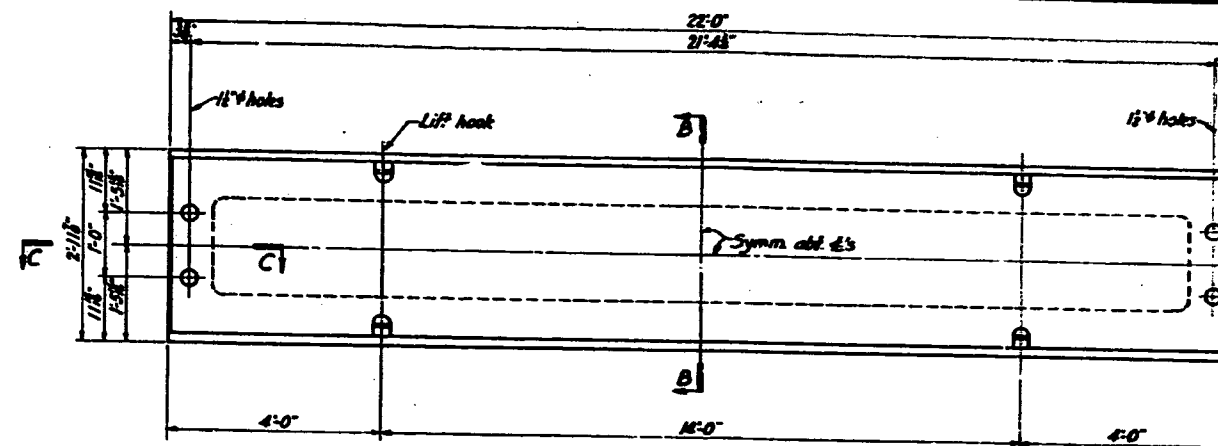
- B.C Ministry of Transportation
- Alberta Ministry of Transportationo



**CURB STRINGER UNIT - TYPE B (FOR ROADWAY)**  
**CURB STRINGER UNIT - TYPE C (FOR SIDEWALK)**

Wt./Unit:-  
 ORD. CONC. - 5.5 TONS  
 LT. WT. do. - 3.65 do.

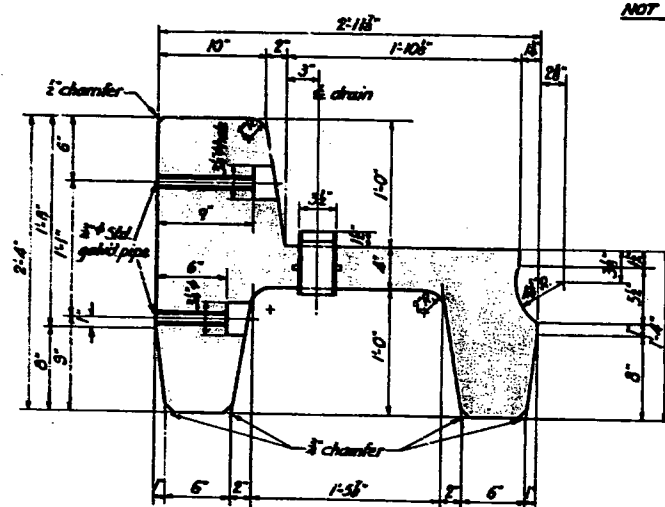
NOT TO SCALE



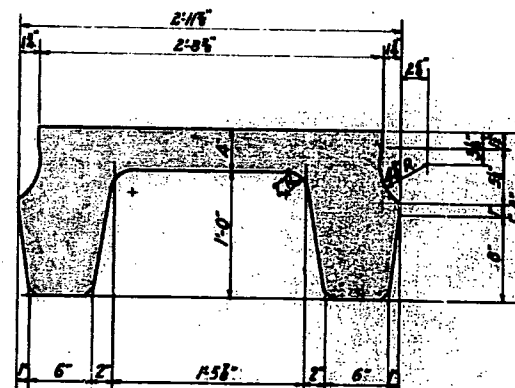
**INNER STRINGER UNIT - TYPE A**

Wt./Unit:-  
 ORD. CONC. - 3.82 TONS  
 LT. WT. do. - 2.67 do.

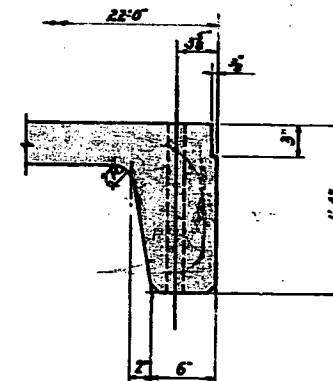
NOT TO SCALE



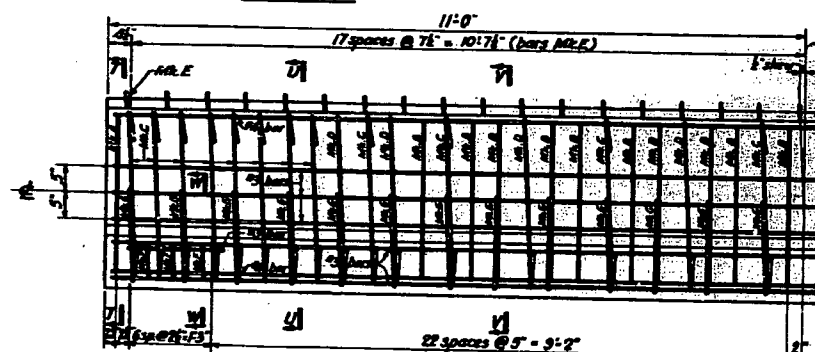
**SECTION A-A**  
 SCALE: 1/8"=1'-0"



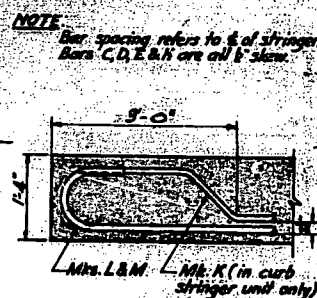
**SECTION B-B**  
 SCALE: 1/8"=1'-0"



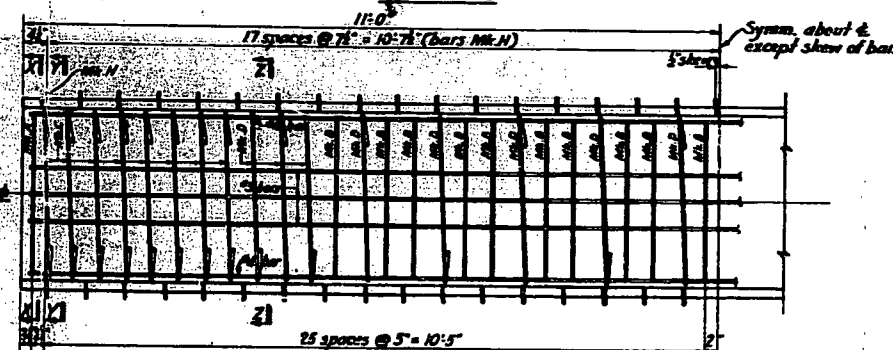
**SECTION C-C**  
 SCALE: 1/8"=1'-0"



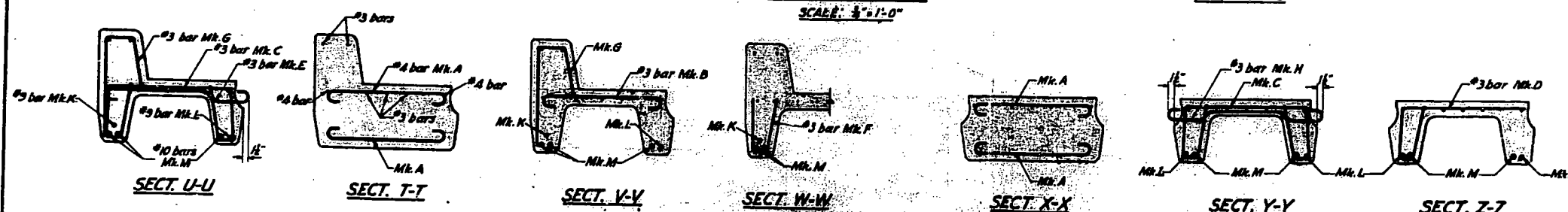
**CURB STRINGER UNIT REINFORCING**  
 SCALE: 3/8"=1'-0"



**PART ELEVATION OF LONGER BARS**  
 SCALE: 3/8"=1'-0"



**INNER STRINGER UNIT REINFORCING**  
 SCALE: 3/8"=1'-0"



QUANTITIES REQUIRED					
CONTRACT		TYPE OF CONTRACT	STRINGER UNIT		
DWG. NO.	NAME		A	B	C
1304	Gartham Bridge #217	Ord.	24	6	-
1352	Quilchena Reserve Bridge #200	do.	40	10	-
1353	Night Street Bridge	do.	40	8	6
1400	Reserve #21 Bridge	do.	24	6	-
1400	Reserve #23 Bridge	do.	24	6	-
1372	Mohagan Slough Bridge	do.	60	12	12
1170	Pingo Bridge	do.	16	4	-
Revisions	A and B				
227	Silver Creek Bridge	LMF	50	10	10
1473	Kanaka Creek Bridge	do.	50	10	10
1397	Chiluckethen Slough Bridge	do.	10	2	2
---	Stock (Cleveland Yard)	do.	30	6	6
892	Bleton Creek Bridge	LT. WT.	63	14	7
	</				

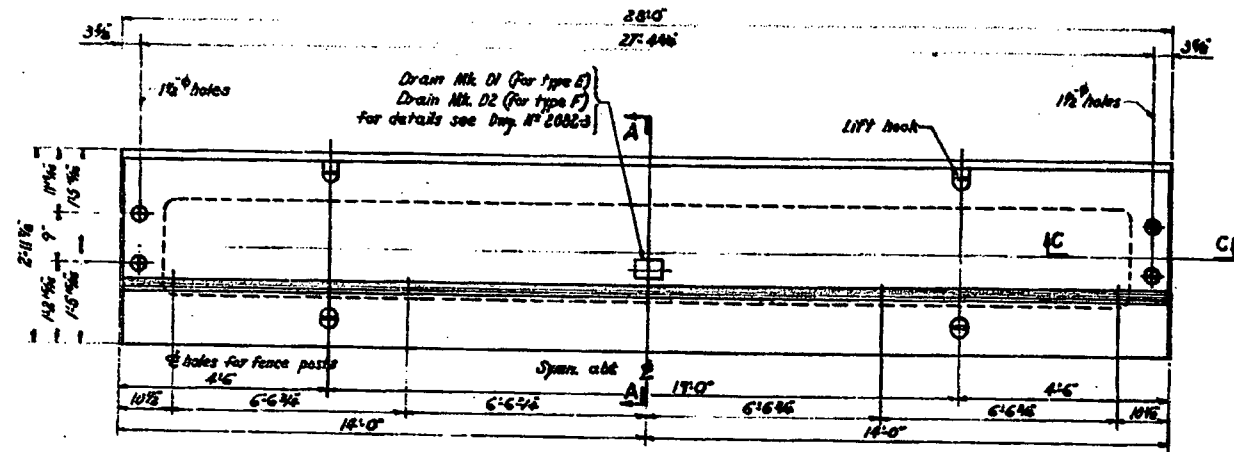
- NOTES:
- Concrete to be Class A.
  - All reinforcing steel to be of structural grade conforming to C.S.A. Specifications G30-1938 or G31-1938.
  - All bars to be deformed.
  - Reinforcing to have 1 1/2" minimum cover.
  - Drains furnished by Dept. Hays, cast in place by precast fabricator.

## PRECAST CONCRETE BRIDGES DETAILS OF 22' STRINGER UNITS

SCALE: AS NOTED

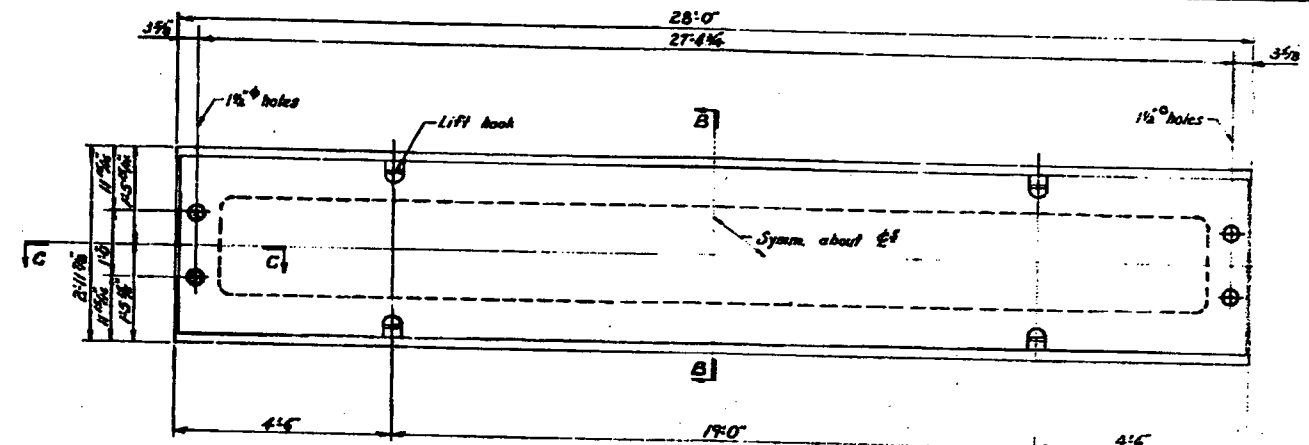
REVISIONS				GOVT. OF BRITISH COLUMBIA DEPT. OF HIGHWAYS BRIDGE ENGINEERS' OFFICE			
No.	Particulars	Init.	Date	Init.	Date	Init.	Date
A	End Discharge and Ht. added	K.W.	July 20/38				
B	Concrete types added	J.D.	Aug 2/38				
	Checked by	R.H.	July 23/38				
	Approved						

Formerly Std. Bridges 225 A-1 B



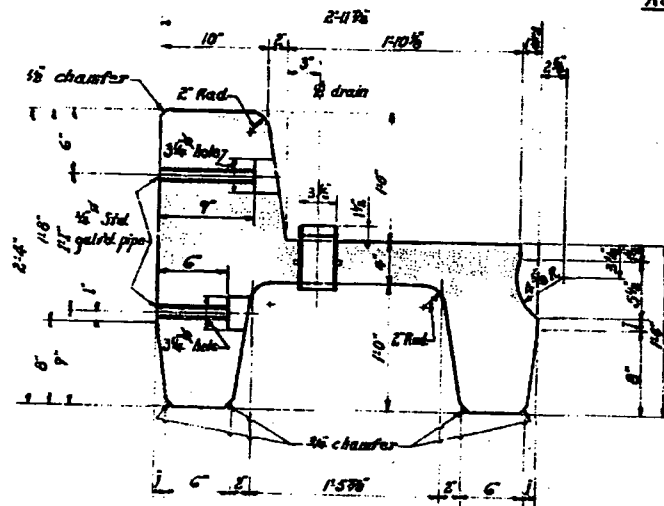
**CURB STRINGER UNIT — TYPE E (FOR ROADWAY)**  
**CURB STRINGER UNIT — TYPE F (FOR SIDEWALK)**  
 Not to Scale

WT./UNIT:—  
 ORD. CONC.—6.83 TONS  
 LT. WT. CONC.—4.77 TONS

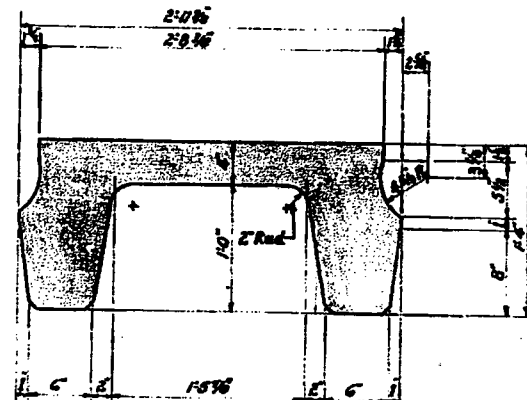


**INNER STRINGER UNIT — TYPE D**  
 Not to Scale

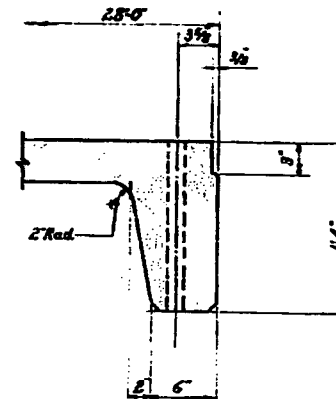
WT./UNIT:—  
 ORD. CONC.—4.75 TONS  
 LT. WT. CONC.—3.33 TONS



**SECTION A-A**  
 Scale: 1/8" = 1'-0"

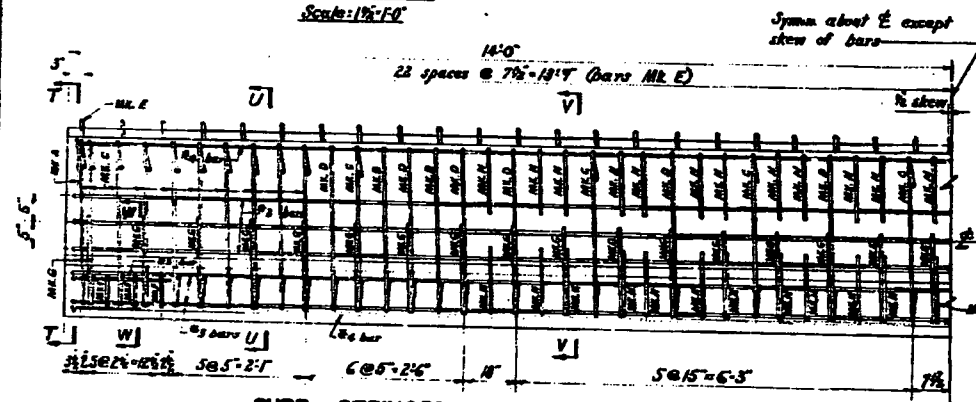


**SECTION B-B**  
 Scale: 1/8" = 1'-0"

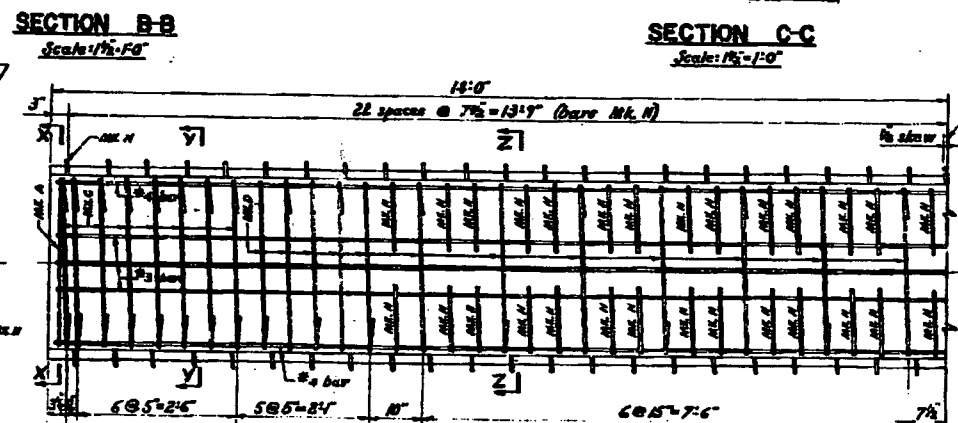


**SECTION C-C**  
 Scale: 1/8" = 1'-0"

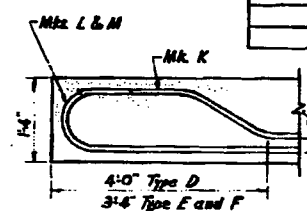
QUANTITIES REQUIRED					
DWG. NO.	CONTRACT NAME	TYPE OF CONCRETE	STRINGER UNIT	D	E F
232	Derby Bridge	LT. WT.	63	14	7
576	Deane Bridge	do	153	34	17
850	Fort Langley Bridge	do	126	36	18
1672	Pump House Bridge	do	58	12	6
1897	Chickadee Slough Bridge	do	20	4	4
2222	Stock (Claydon) Yard	do	30	6	6
2222	Marshall Creek Bridge	do	4	4	12



**CURB STRINGER UNIT REINFORCING**

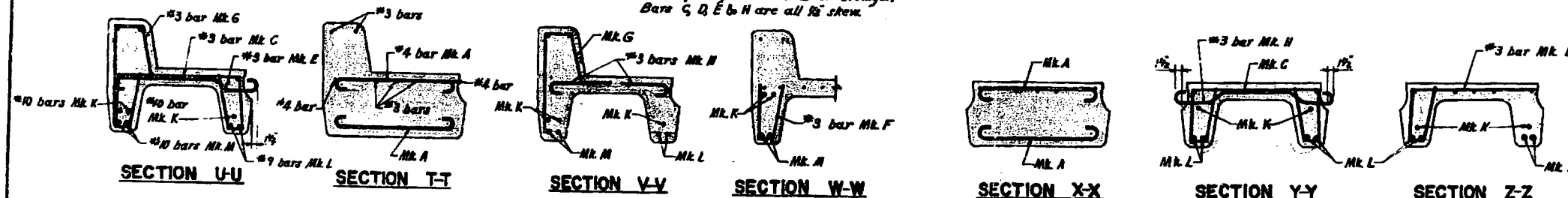


**INNER STRINGER UNIT REINFORCING**



**PART ELEVATION OF LONG'L. BARS**

- NOTES:**
- Concrete to be class "A".
  - All reinforcing steel to be of structural grade conforming to C.S.A. Specifications G30-1938 or G31-1938.
  - All bars to be deformed.
  - Reinforcing to have 1/2" minimum cover.
  - Drains furnished by Dept. of Highways; cast in place by precast fabricators.



**SECTION U-U**

**SECTION T-T**

**SECTION V-V**

**SECTION W-W**

**SECTION X-X**

**SECTION Y-Y**

**SECTION Z-Z**

**PRECAST CONCRETE BRIDGES**  
**DETAILS OF 28' STRINGER UNITS**

SCALE: 3/8" = 1'-0" & AS NOTED

REVISIONS			GOVT. OF BRITISH COLUMBIA	
No.	Particulars	Date	DEPT. OF HIGHWAYS	
A	Concrete types added.	1/24/40	BRIDGE ENGINEER'S OFFICE	
B	Drawing revised & redrawn	1/26/40	MADE BY: R. J. D. Jones	
			CHECKED BY: J. M. Y. Jones	
			APPROVED:	
			DRAWING NO.	
			2082-4	

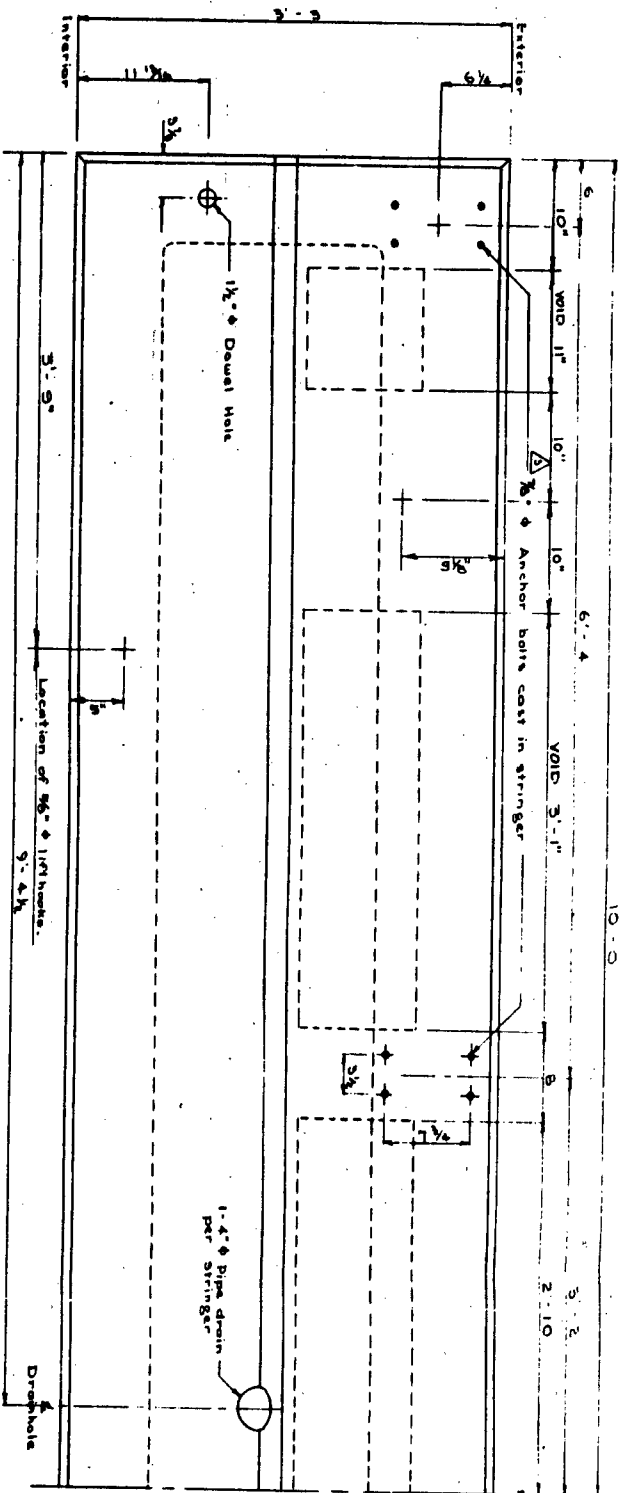
Formerly Std. Bridges 226A-4A



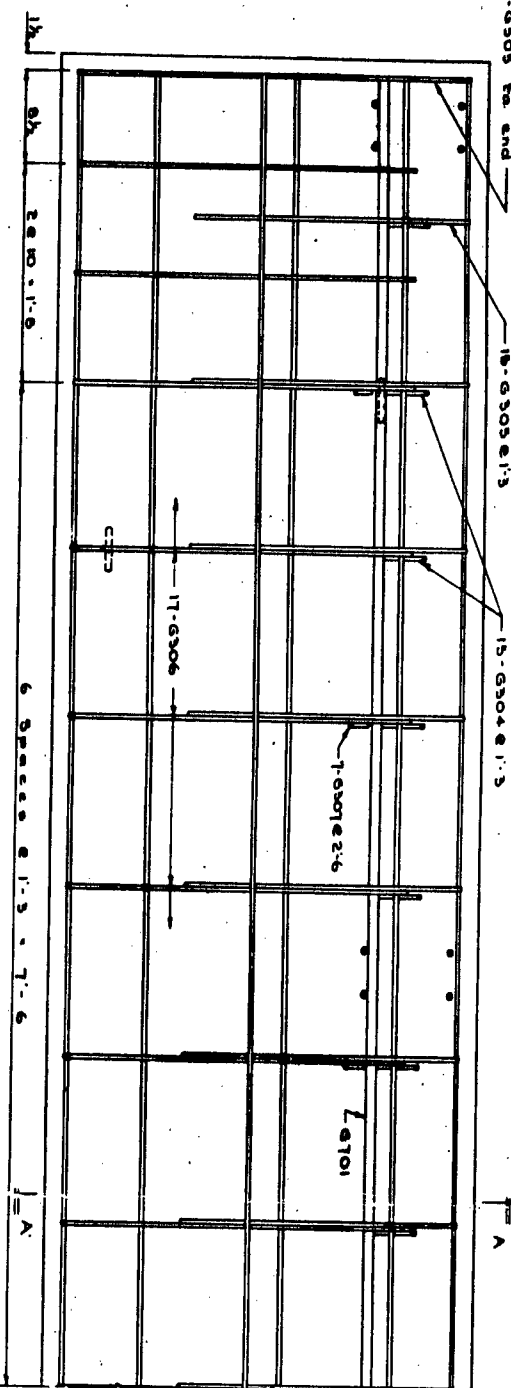
DESIGNED BY: DATE: 10  
DRAWN BY: S.G.W. DATE: MAY 7 1955  
CHECKED BY: DATE: 10

Note:

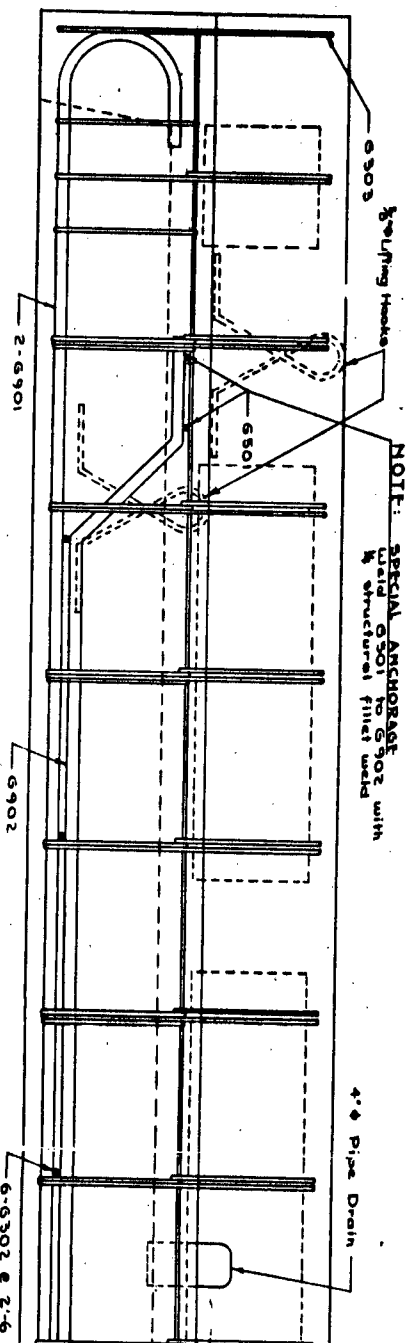
The information and details shown on this document are intended for use and interpretation by the Department. It is the responsibility of others using the information to ensure its integrity and suitability for their use. The Department assumes no responsibility for errors of omissions, and will not accept liability of any nature whatsoever that may be suffered by others using this information.



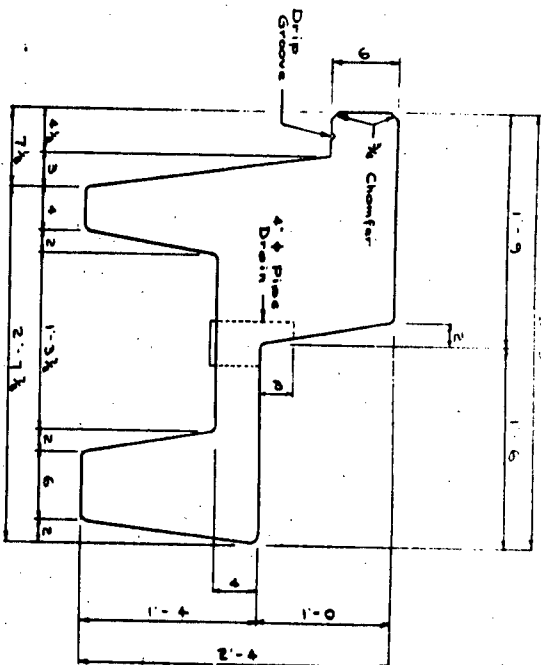
PLAN VIEW



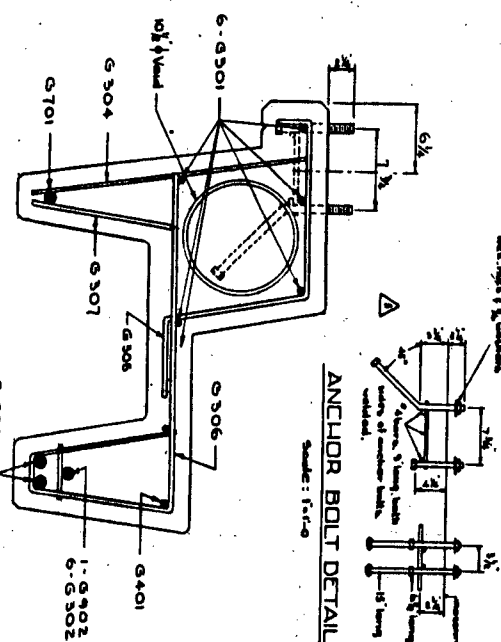
REINFORCEMENT PLAN



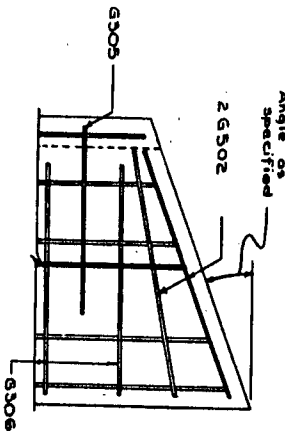
REINFORCEMENT ELEVATION



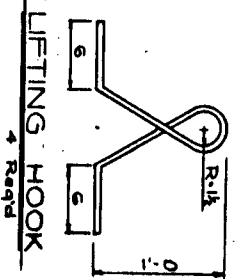
SECTION A-A



ANCHOR BOLT DETAIL



SKEW STRINGER



LIFTING HOOK

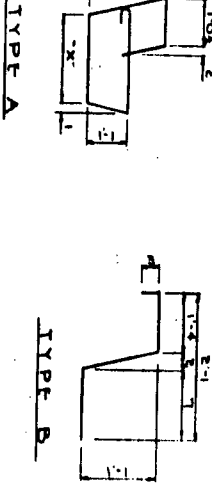
MARK	SIZE	NUMBER	TYPE	LENGTH	WEIGHT
G301	3	6	3R	19'-8"	42
G302	3	6	3R	19'-8"	42
G303	3	2	A	10'-6"	5
G304	3	15	3R	2'-1"	12
G305	3	15	B	3'-5"	18
G306	3	17	C	5'-0"	35
G307	3	7	3R	1'-1"	3
G308	3	7	3R	1'-1"	3
G309	3	7	3R	1'-1"	3
G310	3	7	3R	1'-1"	3
G311	3	7	3R	1'-1"	3
G312	3	7	3R	1'-1"	3
G313	3	7	3R	1'-1"	3
G314	3	7	3R	1'-1"	3
G315	3	7	3R	1'-1"	3
G316	3	7	3R	1'-1"	3
G317	3	7	3R	1'-1"	3
G318	3	7	3R	1'-1"	3
G319	3	7	3R	1'-1"	3
G320	3	7	3R	1'-1"	3

BAR LIST

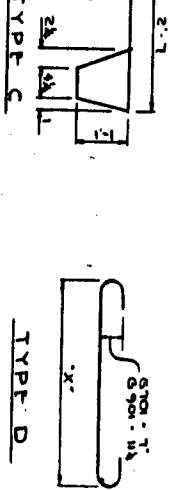
\* For Skewed Stringer only

BAR TYPES

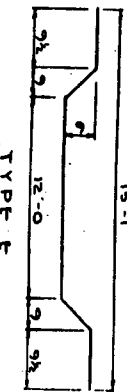
All Bar Dimensions Are Out to Out



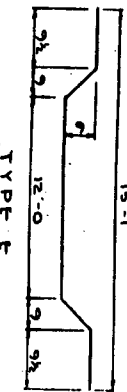
TYPE A



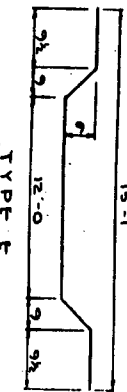
TYPE B



TYPE C



TYPE D



TYPE E

GENERAL NOTES

All concrete materials used shall conform to the current specifications of the Department of Highways. Concrete shall be of 4000 psi strength. Reinforcing steel shall be intermediate grade conforming to the C.A.A. specifications of G301-1954 or G302-1954, and shall be tested in accordance with the requirements of G303-1954. Test cylinders shall be placed 7' 5" from the end of the unit (6'-3" on top of curb). Tests shall be of the rate of 1 cylinder per 2 stringers with not less than 2 cylinders for each day pouring.

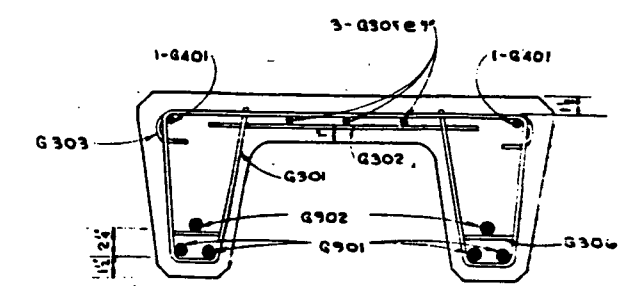
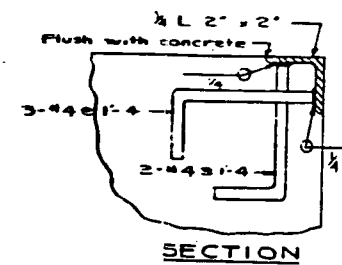
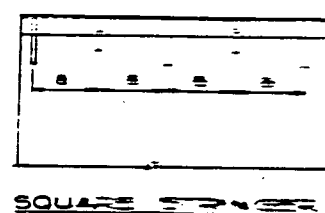
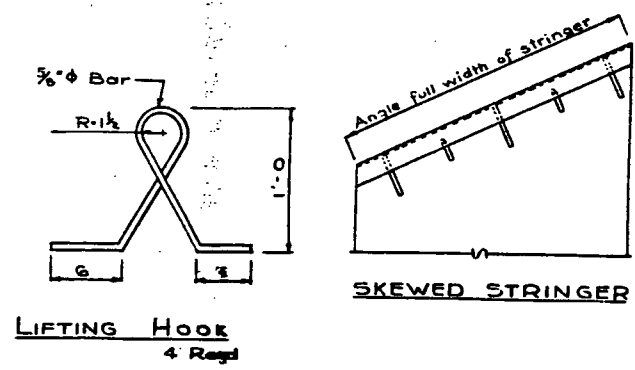
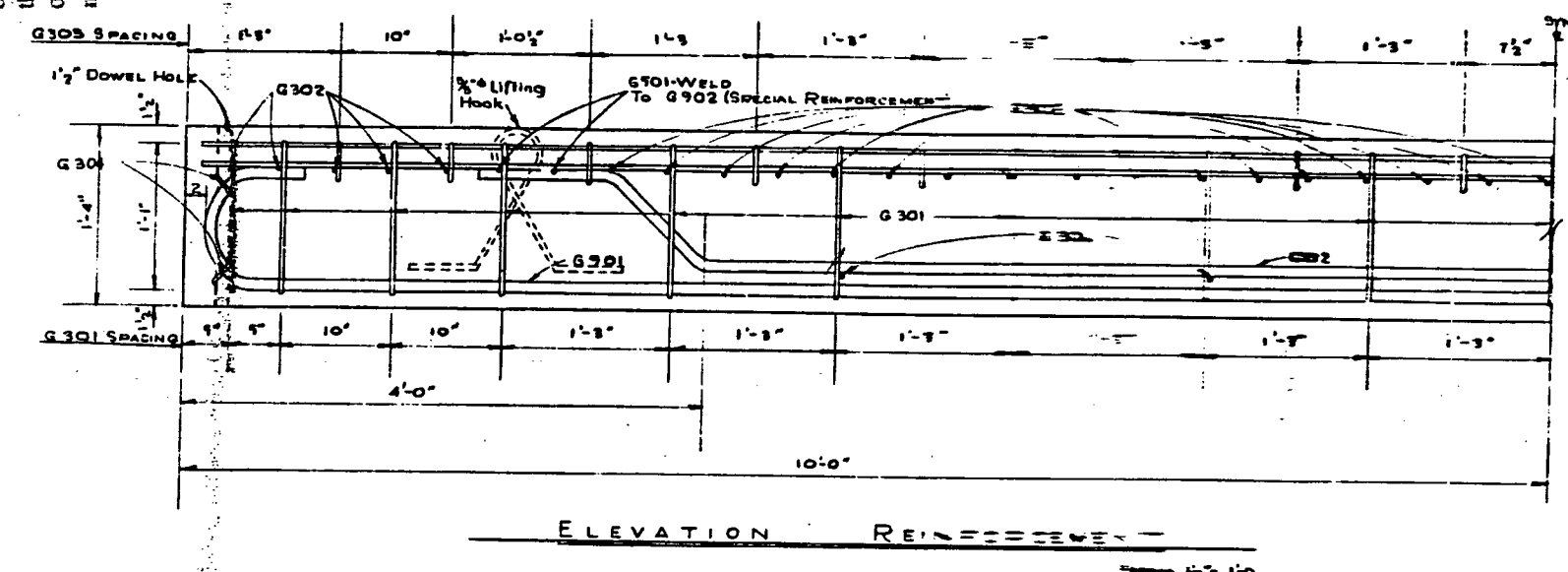
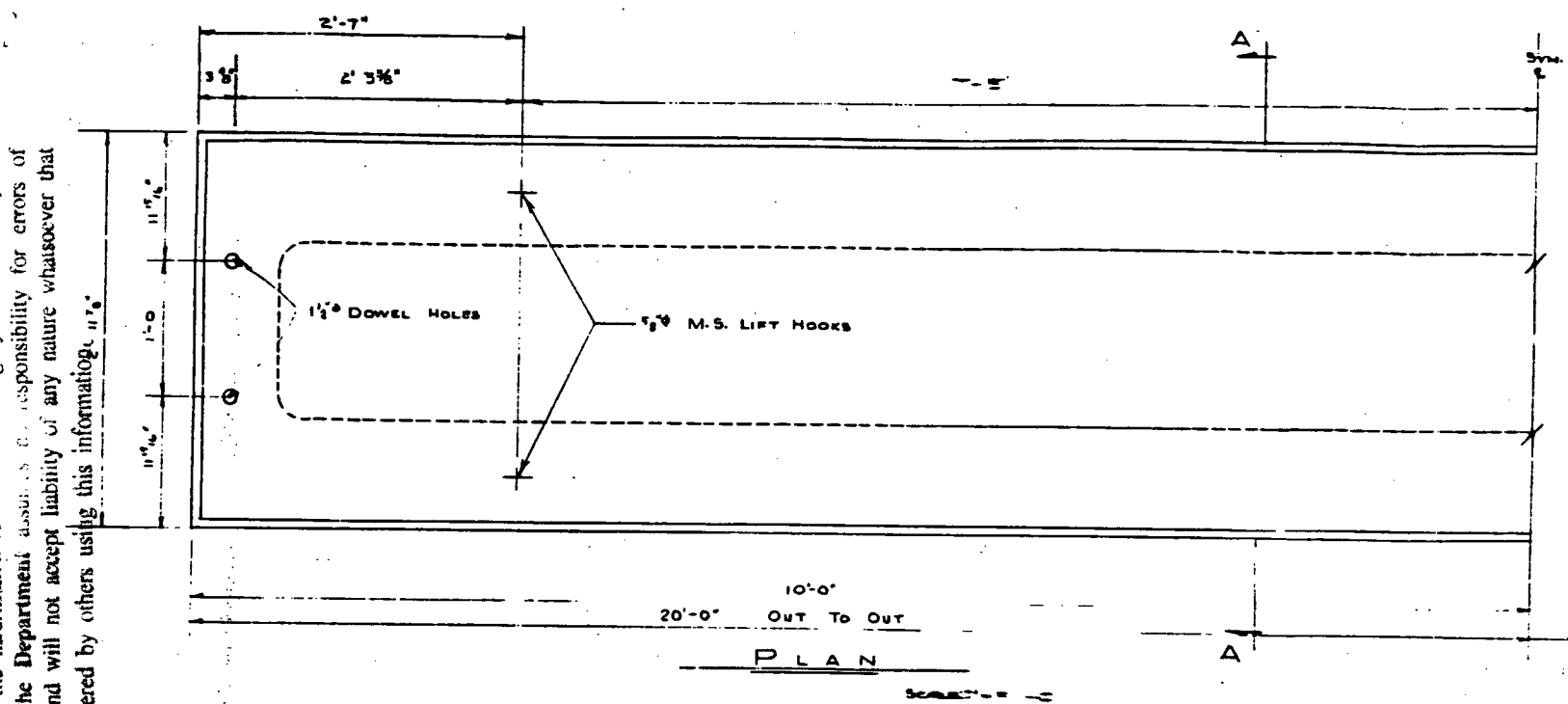
STANDARD CONCRETE

20 FT TYPE G CURB STRINGER

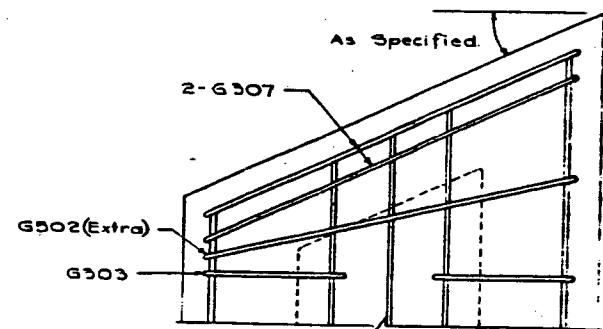
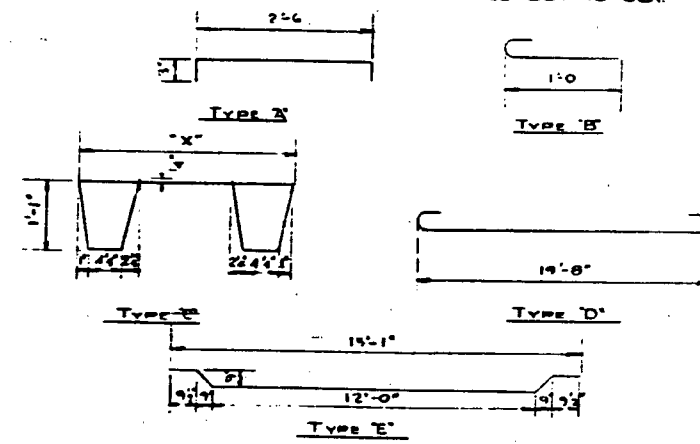
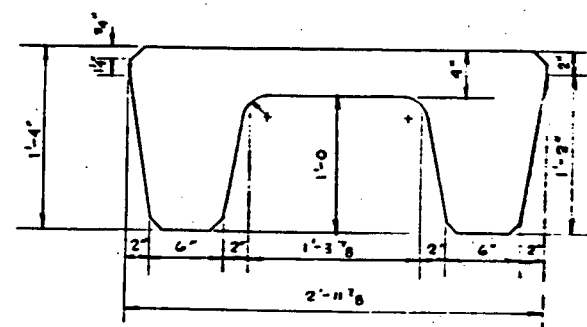
G.C.-20

GOVERNMENT OF THE PROVINCE OF ALBERTA	BRIDGE BRANCH, EDMONTON
FILE NO.	BRIDGE NO.
LOCATION	SCALE 1" = 1'-0"
DATE	5666

DESIGNED BY \_\_\_\_\_ DATE \_\_\_\_\_ 18 \_\_\_\_\_  
 DETAILED BY \_\_\_\_\_ J.D.J.S. DATE MAY 8 18 52  
 CHECKED BY \_\_\_\_\_ DATE \_\_\_\_\_ 18 \_\_\_\_\_



BAR LIST						
MARK	SIZE	NO.	TYPE	X"	LENGTH	WEIGHT
G301	3	19	C	2'-8"	7'-6"	93
G302	3	43	Sec.		2'-0"	32
G303	9	32	B		1'-5"	17
G304	3	4	A		3'-0"	5
G305	1	3	Sec.		19'-8"	22
G306	9	10	Sec.		5"	2
G401	4	2	Sec.		9'-8"	26
G501	5	4	Sec.		2'-4"	10
G901	9	4	D		22'-2"	302
FC902	9	2	E		19'-8"	107
G502	5	2	C			
G307	3	4	C			




- GENERAL NOTES:
- All concrete materials used shall conform to the current applicable ASTM specifications.
  - Concrete shall attain a minimum Compressive strength of 4000 p.s.i. at 28 days.
  - Entrained air shall fall within the limit 3% to 6%.
  - Reinforcing steel shall be Intermediate grade conforming to the specifications Q301-1954 or Q302-1954 and deformed to the requirements of Q306-1954. of the C.S.A.
  - Loading  
AASHTO - I - H20 - S16 wheel line per stringer.
  - Concrete Test Cylinders.  
Test cylinders shall be tested by an independent testing laboratory. Copies of all test results shall be forwarded to the Bridge Branch. Tests shall be taken at the rate of 1 cylinder for each 2 stringers with not less than 2 cylinders for each day's pouring.

4			
5	May 14/59	Lifting Hooks moved	De
6		and Lifting Hooks	Se
7	Jan 30/59	Protection Against Shock Details	
NO.	DATE	DESCRIPTION	
<b>REVISIONS</b>			

STANDARD CONCRETE

20FT. TYPE "G" STRINGER

G 20



GOVERNMENT OF THE PROVINCE OF ALBERTA  
DEPARTMENT OF HIGHWAYS  
BRIDGE BRANCH, EDMONTON

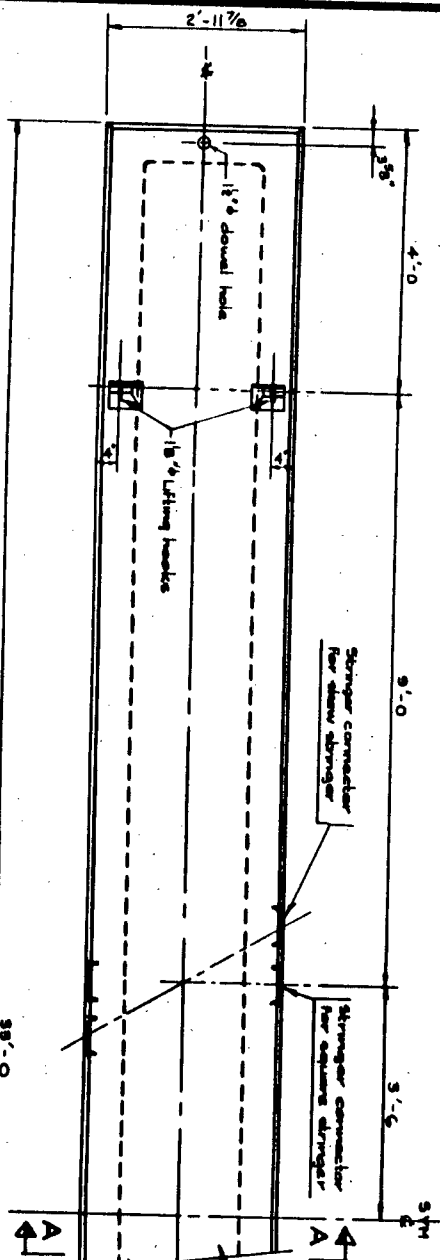
FILE NO. \_\_\_\_\_ HWY. NO. \_\_\_\_\_ DATE NO. \_\_\_\_\_  
LOCATION \_\_\_\_\_ SCALE AS SHOWN \_\_\_\_\_  
STREAM \_\_\_\_\_ STREET OF \_\_\_\_\_

220

Note:

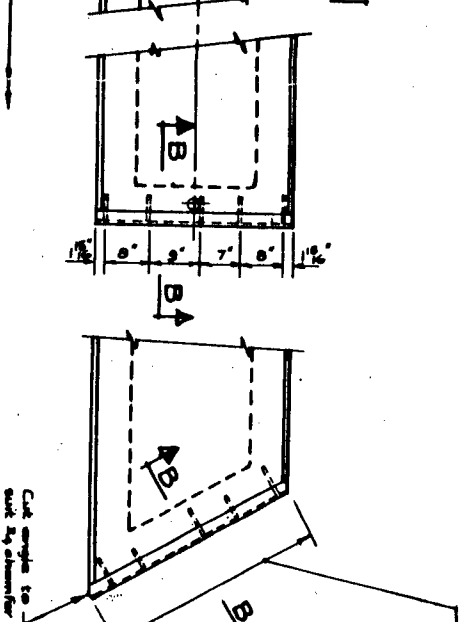
The information and details shown on this document are intended for use and interpretation by the Department. It is the responsibility of others using the information to ensure its integrity and suitability for their use. The Department assumes no responsibility for errors of omissions, and will not accept liability of any nature whatsoever that may be suffered by others using this information.

DESIGNED BY: R.E.B. DATE: May 1962  
DETAILED BY: R.E.B. DATE: May 1962  
CHECKED BY: P.H. [Signature] DATE: May 1962



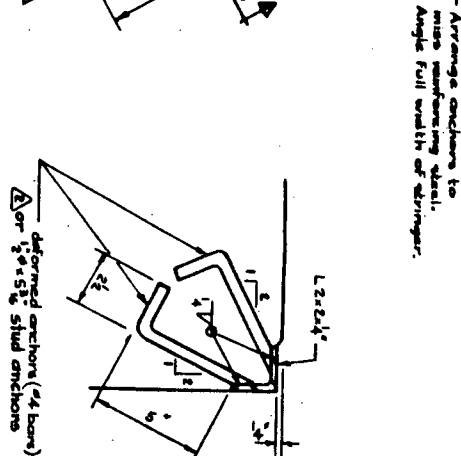
PLAN VIEW

Scale: 3/4" = 1'-0"



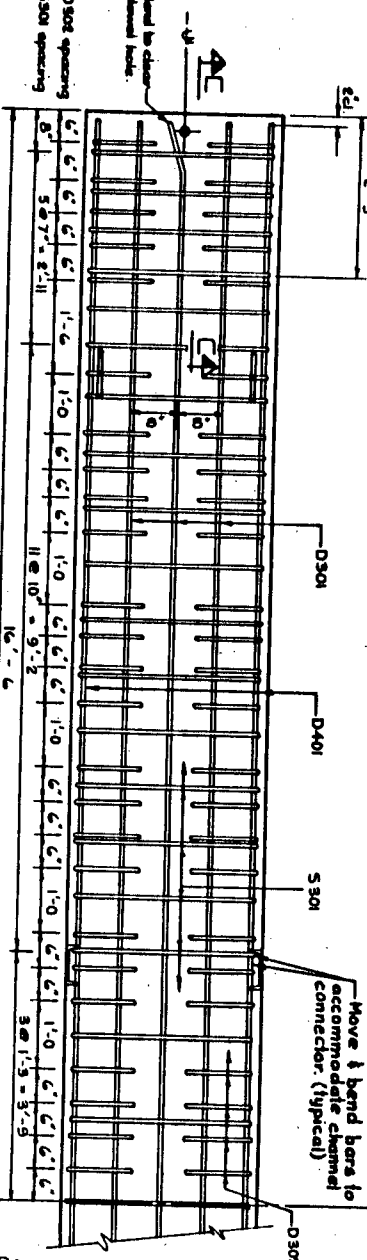
PROTECTION ANGLES

Scale: 3/4" = 1'-0"



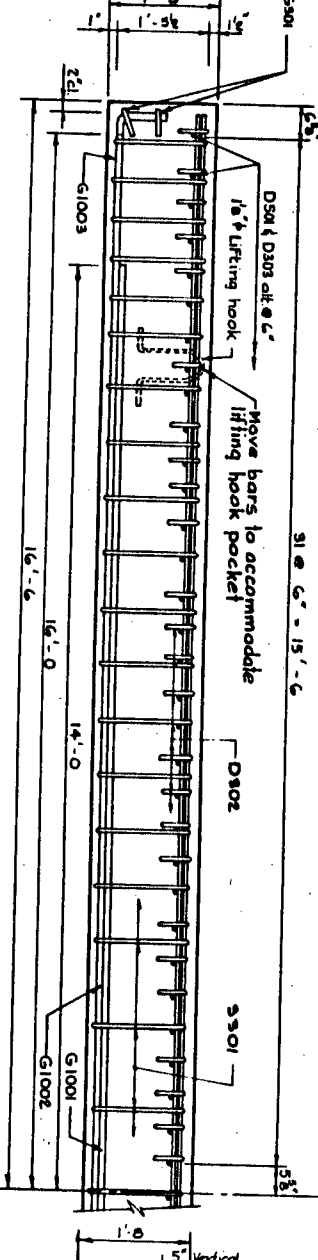
SECTION B-B

Scale: 3/4" = 1'-0"



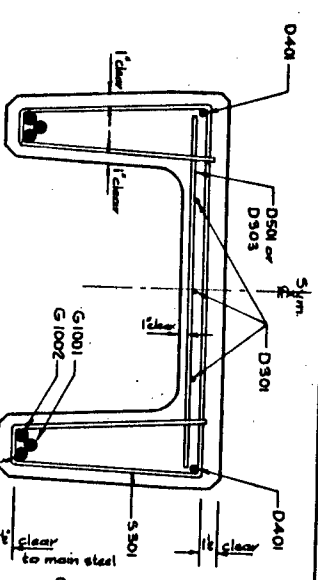
REINFORCEMENT PLAN

Scale: 3/4" = 1'-0"



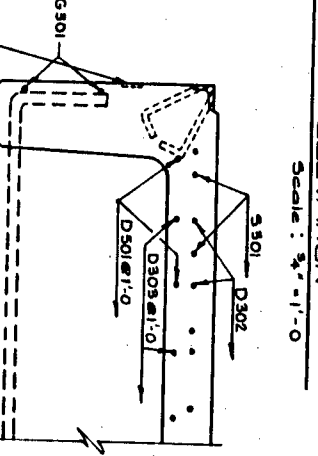
REINFORCEMENT ELEVATION

Scale: 3/4" = 1'-0"



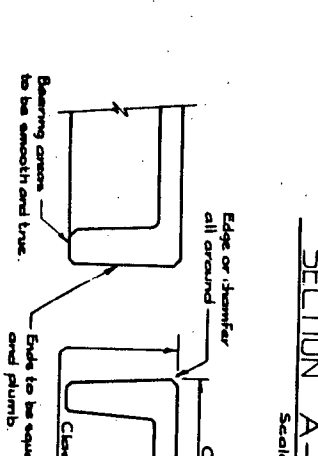
SECTION A-A

Scale: 1/4" = 1'-0"



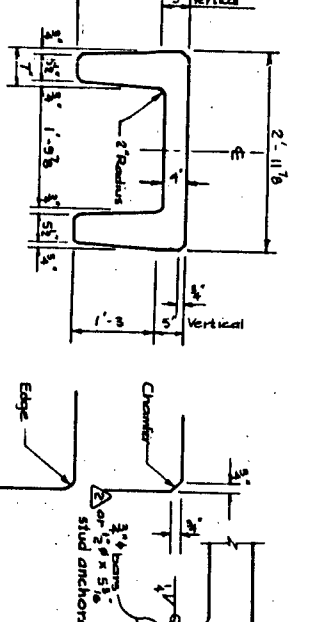
SECTION C-C

Scale: 1/4" = 1'-0"



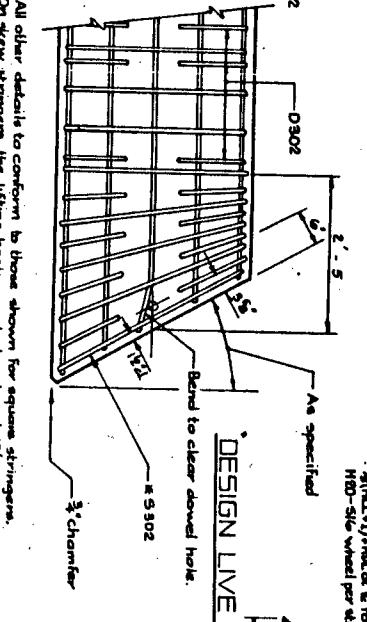
STRINGER FINISHES

Scale: 3/4" = 1'-0"



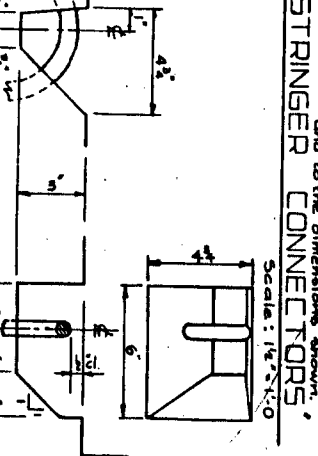
SKEW STRINGER

Scale: 3/4" = 1'-0"



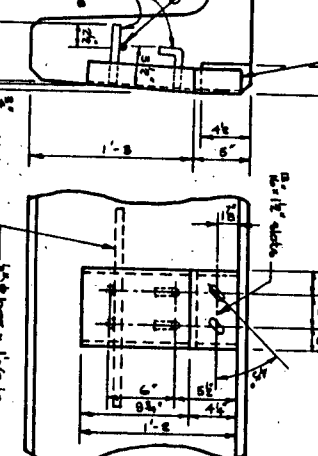
DESIGN LINE & DEAD LOAD MOMENT ENVELOPE

Scale: 3/4" = 1'-0"



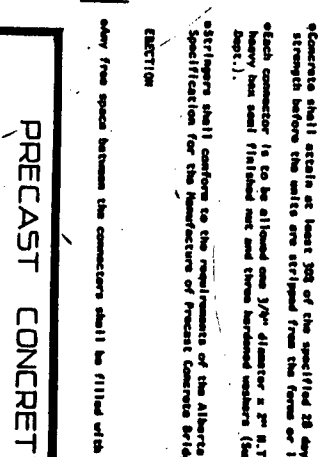
LIFTING HOOK POCKET

Scale: 3/4" = 1'-0"



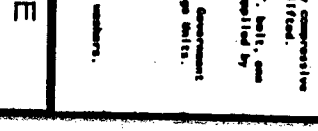
STRINGER CONNECTORS

Scale: 1/4" = 1'-0"



GENERAL NOTES

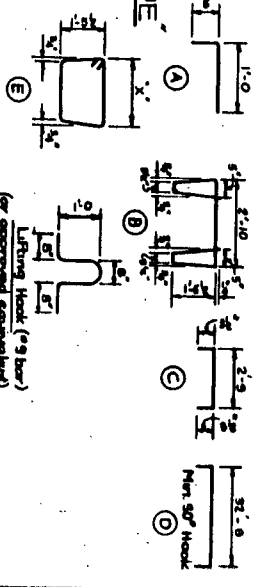
Scale: 3/4" = 1'-0"



BAR LIST

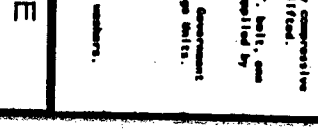
MARK	SIZE	NO.	TYPE	X'	LENGTH	WEIGHT
D 301	3	5	3/4"	A	3'-0"	37
D 502	3	100	A	A	1'-5"	53
S 501	3	58	B	B	5'-4"	137
D 401	4	2	5/8"	D	3'-0"	44
D 501	5	35	5/8"	D	2'-8"	92
G 1001	10	2	5/8"	D	2'-8"	241
G 1002	10	2	5/8"	D	2'-8"	241
G 1003	10	2	5/8"	D	2'-8"	241
S 302	3	2	E	E	5'-4"	5
D 503	3	32	5/8"	D	2'-8"	32

BAR TYPES (All bar dimensions are out to out)	Total weight: 1209
For skewed stringer only	



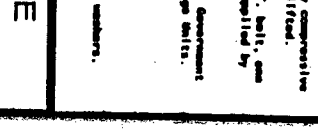
DESIGN

Scale: 3/4" = 1'-0"



GENERAL NOTES

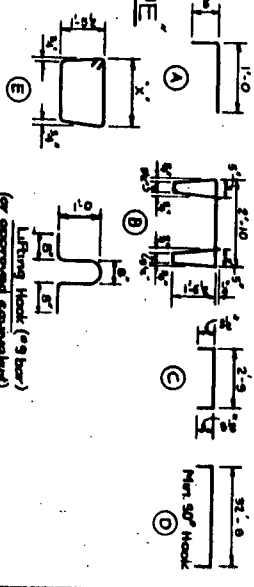
Scale: 3/4" = 1'-0"



BAR LIST

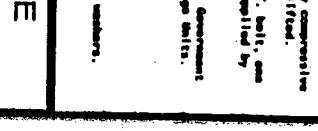
MARK	SIZE	NO.	TYPE	X'	LENGTH	WEIGHT
D 301	3	5	3/4"	A	3'-0"	37
D 502	3	100	A	A	1'-5"	53
S 501	3	58	B	B	5'-4"	137
D 401	4	2	5/8"	D	3'-0"	44
D 501	5	35	5/8"	D	2'-8"	92
G 1001	10	2	5/8"	D	2'-8"	241
G 1002	10	2	5/8"	D	2'-8"	241
G 1003	10	2	5/8"	D	2'-8"	241
S 302	3	2	E	E	5'-4"	5
D 503	3	32	5/8"	D	2'-8"	32

BAR TYPES (All bar dimensions are out to out)	Total weight: 1209
For skewed stringer only	



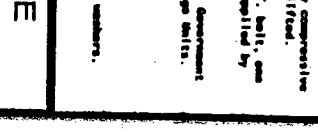
DESIGN

Scale: 3/4" = 1'-0"



GENERAL NOTES

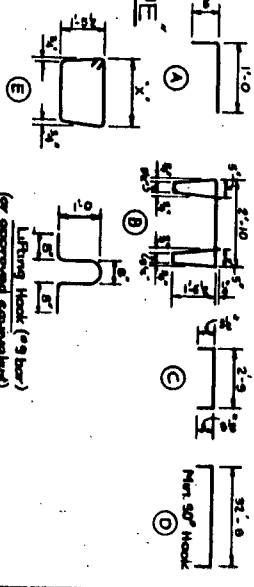
Scale: 3/4" = 1'-0"



BAR LIST

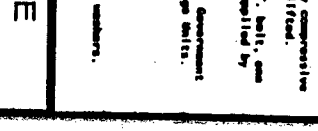
MARK	SIZE	NO.	TYPE	X'	LENGTH	WEIGHT
D 301	3	5	3/4"	A	3'-0"	37
D 502	3	100	A	A	1'-5"	53
S 501	3	58	B	B	5'-4"	137
D 401	4	2	5/8"	D	3'-0"	44
D 501	5	35	5/8"	D	2'-8"	92
G 1001	10	2	5/8"	D	2'-8"	241
G 1002	10	2	5/8"	D	2'-8"	241
G 1003	10	2	5/8"	D	2'-8"	241
S 302	3	2	E	E	5'-4"	5
D 503	3	32	5/8"	D	2'-8"	32

BAR TYPES (All bar dimensions are out to out)	Total weight: 1209
For skewed stringer only	



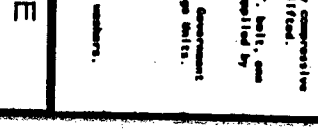
DESIGN

Scale: 3/4" = 1'-0"



GENERAL NOTES

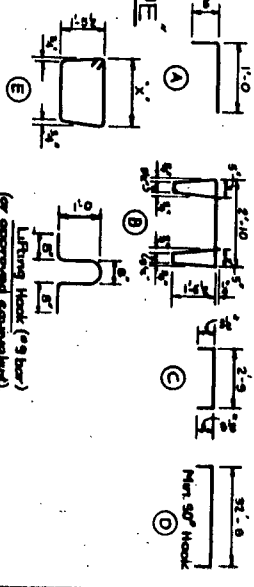
Scale: 3/4" = 1'-0"



BAR LIST

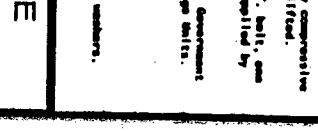
MARK	SIZE	NO.	TYPE	X'	LENGTH	WEIGHT
D 301	3	5	3/4"	A	3'-0"	37
D 502	3	100	A	A	1'-5"	53
S 501	3	58	B	B	5'-4"	137
D 401	4	2	5/8"	D	3'-0"	44
D 501	5	35	5/8"	D	2'-8"	92
G 1001	10	2	5/8"	D	2'-8"	241
G 1002	10	2	5/8"	D	2'-8"	241
G 1003	10	2	5/8"	D	2'-8"	241
S 302	3	2	E	E	5'-4"	5
D 503	3	32	5/8"	D	2'-8"	32

BAR TYPES (All bar dimensions are out to out)	Total weight: 1209
For skewed stringer only	



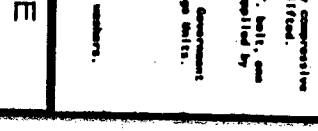
DESIGN

Scale: 3/4" = 1'-0"



GENERAL NOTES

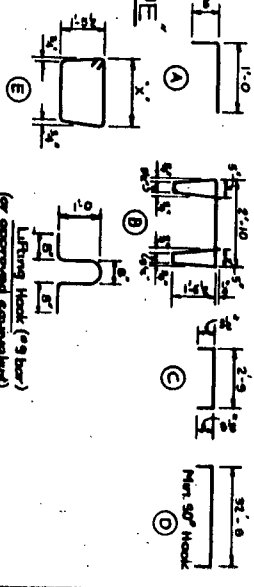
Scale: 3/4" = 1'-0"



BAR LIST

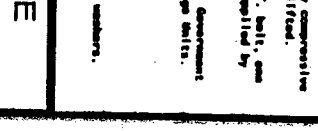
MARK	SIZE	NO.	TYPE	X'	LENGTH	WEIGHT
D 301	3	5	3/4"	A	3'-0"	37
D 502	3	100	A	A	1'-5"	53
S 501	3	58	B	B	5'-4"	137
D 401	4	2	5/8"	D	3'-0"	44
D 501	5	35	5/8"	D	2'-8"	92
G 1001	10	2	5/8"	D	2'-8"	241
G 1002	10	2	5/8"	D	2'-8"	241
G 1003	10	2	5/8"	D	2'-8"	241
S 302	3	2	E	E	5'-4"	5
D 503	3	32	5/8"	D	2'-8"	32

BAR TYPES (All bar dimensions are out to out)	Total weight: 1209
For skewed stringer only	



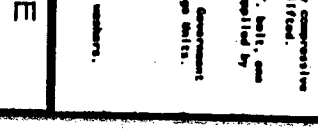
DESIGN

Scale: 3/4" = 1'-0"



GENERAL NOTES

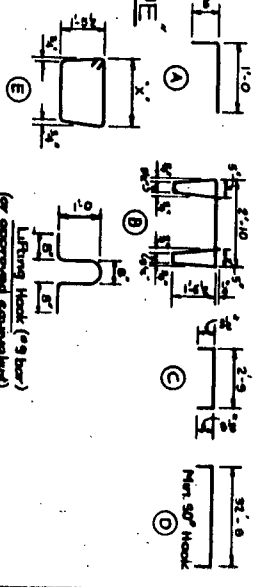
Scale: 3/4" = 1'-0"



BAR LIST

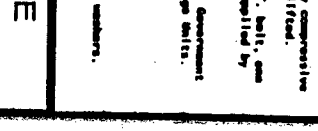
MARK	SIZE	NO.	TYPE	X'	LENGTH	WEIGHT
D 301	3	5	3/4"	A	3'-0"	37
D 502	3	100	A	A	1'-5"	53
S 501	3	58	B	B	5'-4"	137
D 401	4	2	5/8"	D	3'-0"	44
D 501	5	35	5/8"	D	2'-8"	92
G 1001	10	2	5/8"	D	2'-8"	241
G 1002	10	2	5/8"	D	2'-8"	241
G 1003	10	2	5/8"	D	2'-8"	241
S 302	3	2	E	E	5'-4"	5
D 503	3	32	5/8"	D	2'-8"	32

BAR TYPES (All bar dimensions are out to out)	Total weight: 1209
For skewed stringer only	



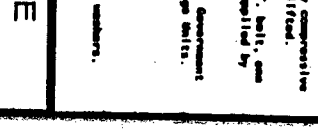
DESIGN

Scale: 3/4" = 1'-0"



GENERAL NOTES

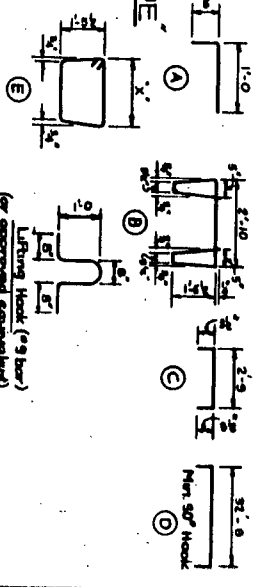
Scale: 3/4" = 1'-0"



BAR LIST

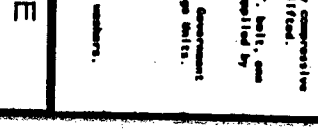
MARK	SIZE	NO.	TYPE	X'	LENGTH	WEIGHT
D 301	3	5	3/4"	A	3'-0"	37
D 502	3	100	A	A	1'-5"	53
S 501	3	58	B	B	5'-4"	137
D 401	4	2	5/8"	D	3'-0"	44
D 501	5	35	5/8"	D	2'-8"	92
G 1001	10	2	5/8"	D	2'-8"	241
G 1002	10	2	5/8"	D	2'-8"	241
G 1003	10	2	5/8"	D	2'-8"	241
S 302	3	2	E	E	5'-4"	5
D 503	3	32	5/8"	D	2'-8"	32

BAR TYPES (All bar dimensions are out to out)	Total weight: 1209
For skewed stringer only	



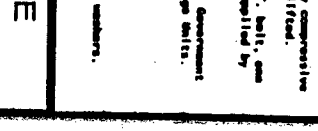
DESIGN

Scale: 3/4" = 1'-0"



GENERAL NOTES

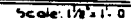
Scale: 3/4" = 1'-0"



BAR LIST

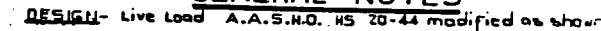
MARK	SIZE	NO.	TYPE	X'	LENGTH	WEIGHT
D 301	3	5	3/4"	A	3'-0"	37
D 502	3	100	A	A	1'-5"	53
S 501	3	58	B	B	5'-4	131
S 502	3	58	B	B	4'-4	44
S 503	3	58	B	B	9'-2	92
S 504	3	0	0	0	2'-4	24
S 505	3	0	0	0	2'-9	27
S 506	3	1	1	1	2'-3	23

The information and details shown on this document are intended for use and interpretation by the **Department**. It is the responsibility of others using the information to ensure its integrity and suitability for their use. The **Department** assumes no responsibility for errors of omissions, and will not accept liability of any nature whatsoever that may be suffered by others using this information.



NOTE  
Slate are to be machine made,  
smooth and to the dimensions shown

Total weight (lbs) 1036



- Dead Load - includes allowance for 2" wearing surface.
- Concrete - to be standard weight aggregates with maximum aggregate size of 3/4 inch. Minimum 28 day compressive strength to be 4000 p.s.i.

## CONSTRUCTION

• Entrained Air shall be not less than 5

• Bladders of all heads shall conform to the recommended minimums and all hooks, unless otherwise noted shall conform to the recommended sizes detailed in the A.C.I. Manual of Standard Practice for Detailing Reinforced Concrete Structures.

• Each stringer shall have a cast camber of 3/4 inch.

• All acute angles on skewed stringers shall have 3/4 inch chamfer.

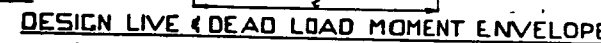
• Concrete shall attain at least 30% of the specified 28 day compressive strength before the units are stripped from the forms or lifted.

\*Each connector is to be allowed one 3/4" diameter x 2" U.T. bolt, one heavy hex semi finished nut and three hardened washers (Supplied by Dept.).

\* Stringers shall conform to the requirements of the Alberta Government Specification for the Manufacture of Precast Concrete Bridge Units.

## ERECTION

\* Any free space between the components shall be filled with foam.



PRECAST CONCRETE  
33 FT. SPAN TYPE "HC"  
CURB STRINGER

**GOVERNMENT OF THE PROVINCE OF ALBERTA**  
**DEPARTMENT OF HIGHWAYS**  
**BRIDGE BRANCH, EDMONTON**

▲	Jan. 27/71	Stud anchors - alternate added	AW
▲	Apr. 16/70	B" dimension removed	J.C.
▲	Jan. 1969	Anchor bolt location (at shear)	P.S.
▲	<b>Redrawn</b>		
NO.	DATE	DESCRIPTION	B"
<b>REVISIONS</b>			

FILE NO. \_\_\_\_\_ HWY. NO. \_\_\_\_\_ DWG. NO. \_\_\_\_\_  
LOCATION \_\_\_\_\_ SCALE as shown U 332



## **Appendix II**

### **Summary Table: Existing PCCB Bridges in Vancouver Island, B.C. Canada**

*[Ref.]: BC MoT, Canada*

## Summary of Channel Beam Bridges

Bridge Number	Name	District	Hwy	Beam Length	Conc. Type	Comments	# Spans	Total Length
232	Deroche	7	7	28	Lt. Wt.		7	59.3
596	Dewdney	7	7	28	Lt. Wt.			136
1472	Pump House	7	7	28	Lt. Wt.		6	51
1537	Waterloo	3	19	28			2	17.1
1523	Sullivan	13	97A	28		35 degree skew		9
1565	Bertrand	6	13	28			1	9
7329	Stowe	4	228	28	Ord.		1	9
1426	Safe	1	N. Shore Road	26			1	8
1304	Guichan	14		22	Ord.		3	20.1
1352	Quilchene Reserve	14		22	Ord.		5	33.5
1400	Reserve No. 1	7	7	22	Ord.		3	20.1
6043	Reserve No. 3	7	7	22	Ord.		3	20.1
997	Silver Creek	7	7	22	Lt. Wt.		5	33.5
7144	Tupper	21	2	22	Lt. Wt.		3	20.1
6082	Windrem	21	97	22	Lt. Wt.		1	6.7
830	Hallhead	1	Renfrew Rd. (68	22		<i>Replaced</i>	3	20.1
1094	Serpentine River	6	1A	17		widened portion only	6	31.2

## **Appendix III**

### **Condition Inspection Reports for Safe Bridge**

- Date: July 30<sup>th</sup>, 2001
- Date: May 26<sup>th</sup>, 2005

*[Ref.]: BC MoT, Canada*

**BRITISH COLUMBIA MINISTRY OF TRANSPORTATION  
BRIDGE MANAGEMENT INFORMATION SYSTEM**

**Condition Inspection Report**  
Criteria: Structure No = 1426

Region: 1 - South Coast      District: 2 - Vancouver Island      Contract Area: 1 - South Island  
Structure No: 1426 - SAFE      Status: Open/In Use      Inspection Type: Detailed Con

RFI: 01-D-L-00098 - YOUNG ROAD

Features Crossed: youbou rd COON CREEK

Component Group/Component	E	G	F	P	V	X	N/A
<b>CHANNEL :</b>							
1. Debris Risk		100					N
2. Bank/Bed Scour/Bulldup		100					N
3. Dolphins/Fenders							Y
<b>SUBSTRUCTURE :</b>							
4. Foundation Movement		100					N
5. Abutments		100					N
6. Wing/Retaining Walls		100					N
7. Footings/Piling		100					N
8. Pier Columns/Walls/Cribs							Y
9. Bearings							Y
10. Caps							Y
11. Corbels							Y
<b>SUPERSTRUCTURE :</b>							
12. Floor Beams/Transoms							Y
13. Stringers		100					N
14. Girders							Y
15. Portals							Y
16. Bracing Diaphragms							Y
17. Truss Chords/Arch Ribs							Y
18. Arch Tiles							Y
19. Truss Diagonals							Y
20. Truss Rods/Verticals							Y
21. Cables							Y
22. Panels							Y
23. Pins/Bolts/Rivets							Y
24. Camber/Sag		100					N
25. Live Load Vibration		100					N
26. Coating (Structure)		100					N
<b>DECK :</b>							
27. Sub Deck/Cross Ties		100					N
28. Wearing Surface		100					N
29. Deck Joints							Y
30. Curbs/Wheelguards		100					N
31. Sidewalk(S)		100					N
32. Railings/Parapets			100				N
33. Median Barrier							Y
34. Drains/Pipes							Y
35. Coating (Railings)			100				N
<b>APPROACHES :</b>							
36. Signing/Lighting		100					N
37. Roadway Approaches		100					N
38. Roadway Flares		100					N

Built: 1955  
Main Span Length: 7.200  
Urgency: 2  
Inspector/Inspected By: Brent Scott

Length (m): 7.900  
Main Span Type: STRINGER  
BCI Rating:  
On 2005/05/26 Amended By:  
Spans: 1  
Adjusted BCI Rating:  
On

**Item Notes:**

- 7 . Footings/Piling      prior 2003: Buried
- 13 . Stringers      prior 2001: One concrete girder has rusting rebar and cracking  
2001: Rusting of reinforcing causing cracks, spalls  
2002: Stringers repaired in 2001 with fibreglass and performance is monitored by Ian Sturrock & UBC.  
2003: Reinforced with fibreglass in 2001.  
2004: Repaired with fibreglass - repair still good.



**BRITISH COLUMBIA MINISTRY OF TRANSPORTATION  
BRIDGE MANAGEMENT INFORMATION SYSTEM**PAGE 2 OF 2  
27 May 2005  
IFS**Condition Inspection Report**

Criteria: Structure No = 1426

Region: 1 - South Coast

District: 2 - Vancouver Island

Contract Area: 1 - South Island

Structure No: 1426 - SAFE

Status: Open/In Use

Inspection Type: Detailed Con

2005: stringer repair stil looks good

**Inspection Notes:****Drainage Area Description**2004: (and prior) Small creek; no problems.  
2005 same**Maintenance Work Notes**prior 2000: -Monitor stringers  
2000: -Investigate repair proceedure for concrete stringer  
2001: -Patch girders  
2004: Monitor fibreglass stringer repair.  
2005: reposition one object marker se corner**Rehab Work Notes**2001: New fibre glass reinforcing repair to be conducted next month system developed by U.B.C. and managed by Ian Sturrock.  
2003: Stringer repair is being monitored by U.B.C. Contact is Ian Sturrock at H.Q.

**BRITISH COLUMBIA MINISTRY OF TRANSPORTATION  
BRIDGE MANAGEMENT INFORMATION SYSTEM**

**Condition Inspection Report**

Criteria: Structure No = 1426

Region: 1 - South Coast

District: 2 - Vancouver Island

Contract Area: 1 - South Island

Structure No: 1426 - SAFE

Status: Open/In Use

Inspection Type: Detailed Con

RFI: 01-D-L-00098 - YIOUBOU ROAD

Features Crossed: youbou rd COON CREEK

Component Group/Component	E	G	F	P	V	X	N/A
<b>CHANNEL :</b>							
1. Debris Risk		100					N
2. Bank/Bed Scour/Buildup		100					N
3. Dolphins/Fenders							Y
<b>SUBSTRUCTURE :</b>							
4. Foundation Movement		100					N
5. Abutments		100					N
6. Wing/Retaining Walls		100					N
7. Footings/Piling						100	N
8. Pier Columns/Walls/Cribs							Y
9. Bearings							Y
10. Caps							Y
11. Corbels							Y
<b>SUPERSTRUCTURE :</b>							
12. Floor Beams/Transoms							Y
13. Stringers		60	30	10			N
14. Girders							Y
15. Portals							Y
16. Bracing Diaphragms							Y
17. Truss Chords/Arch Ribs							Y
18. Arch Tiles							Y
19. Truss Diagonals							Y
20. Truss Rods/Verticals							Y
21. Cables							Y
22. Panels							Y
23. Pins/Bolts/Rivets							Y
24. Camber/Sag		100					N
25. Live Load Vibration		100					N
26. Coating (Structure)							Y
<b>DECK :</b>							
27. Sub Deck/Cross Tiles		100					N
28. Wearing Surface		100					N
29. Deck Joints							Y
30. Curbs/Wheelguards		100					N
31. Sidewalk(S)							Y
32. Railings/Parapets		100					N
33. Median Barrier							Y
34. Drains/Pipes							Y
35. Coating (Railings)			100				N
<b>APPROACHES :</b>							
36. Signing/Lighting		100					N
37. Roadway Approaches		100					N
38. Roadway Flares		100					N

Built: 1955

Length (m): 7.900

Main Span Length: 7.200

Main Span Type: STRINGER

Spans: 1

Urgency: 3

BCI Rating: 1.96

Adjusted BCI Rating: 2.14

Inspector/Inspected By: BRENT SCOTT

On 2001/07/30 Amended By:

On

**Item Notes:**

- 7 . Footings/Piling Buried
- 13 . Stringers 2001 - RUSTING OF REINFORCING CAUSING CRACKS, SPALLS
- One concrete girder has rusting rebar and cracking

**BRITISH COLUMBIA MINISTRY OF TRANSPORTATION  
BRIDGE MANAGEMENT INFORMATION SYSTEM**

27 May 2005

IFS

**Condition Inspection Report**

Criteria: Structure No = 1426

**Region:** 1 - South Coast**District:** 2 - Vancouver Island**Contract Area:** 1 - South Island**Structure No:** 1426 - SAFE**Status:** Open/In Use**Inspection Type:** Detailed Con**Inspection Notes:****Drainage Area Description**

2001 - SMALL CREEK, NO PROBLEMS

Small creek; no problems.

**Maintenance Work Notes**

2001 - PATCH GIRDERS

2000 - investigate repair procedure for concrete stringer

MONITER STRINGERS

**Pre-Conversion Component Notes**

SOME SPALLING OF CONCRETE STRINGERS ON BOTTOM FLANGES.

**Rehab Work Notes**2001 - NEW FIBRE GLASS REINFORCING REPAIR TO BE CONDUCTED NEXT MONTH SYSTEM DEVELOPED BY U.B.C. AND  
MANAGED BY IAN STURROCK.

## **Appendix IV**

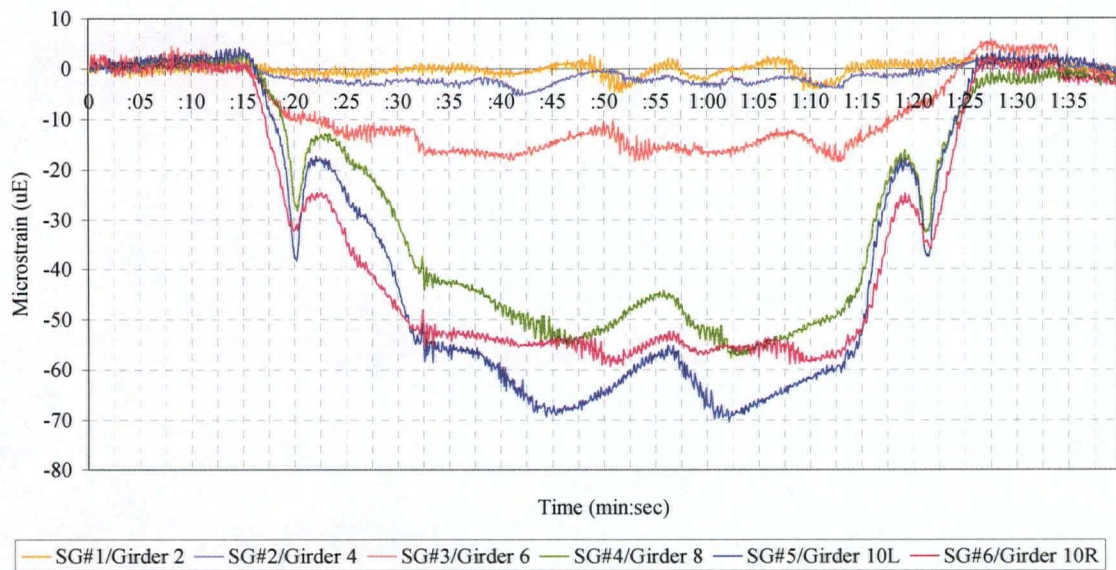
### **Field Test 2003:**

#### **Time-Strain History of the Six Static Load Positions**

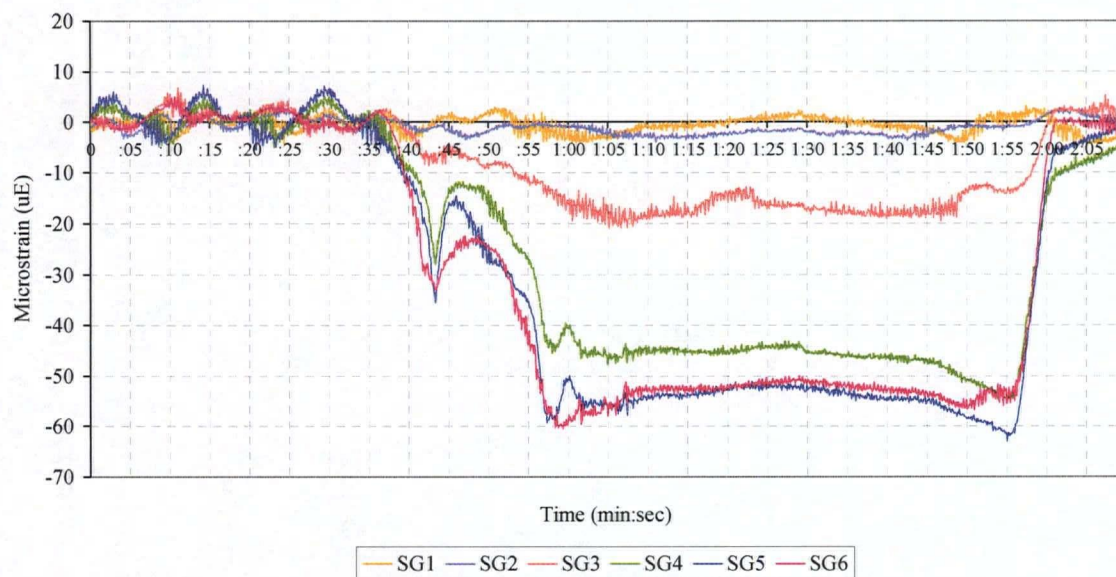
***- I/O Tech DaqBook Results -***



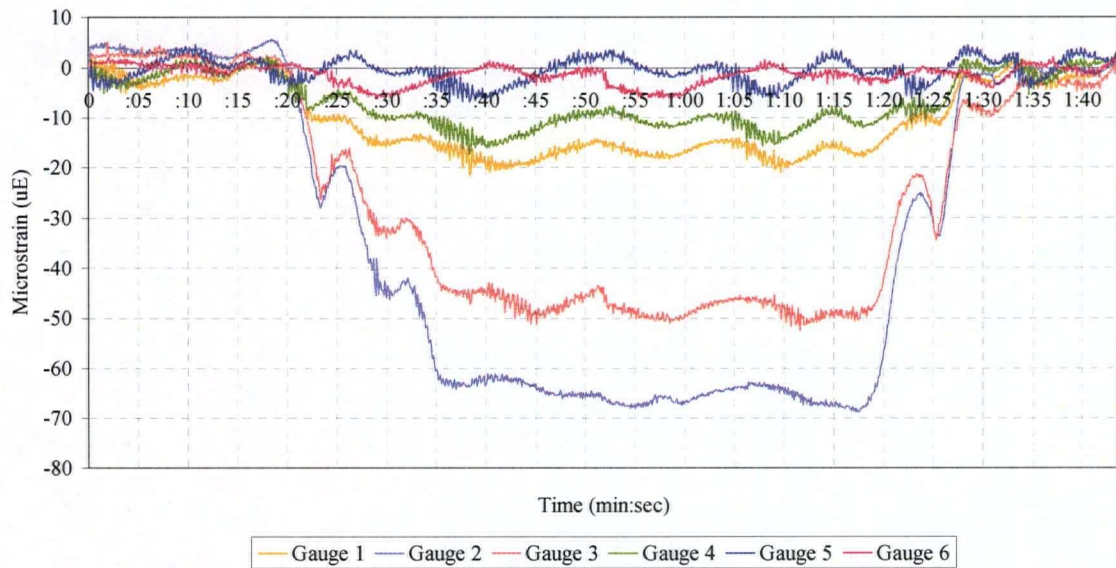
**2003 Field Testing  
I/O Tech DaqBook: Static Load Position 1**



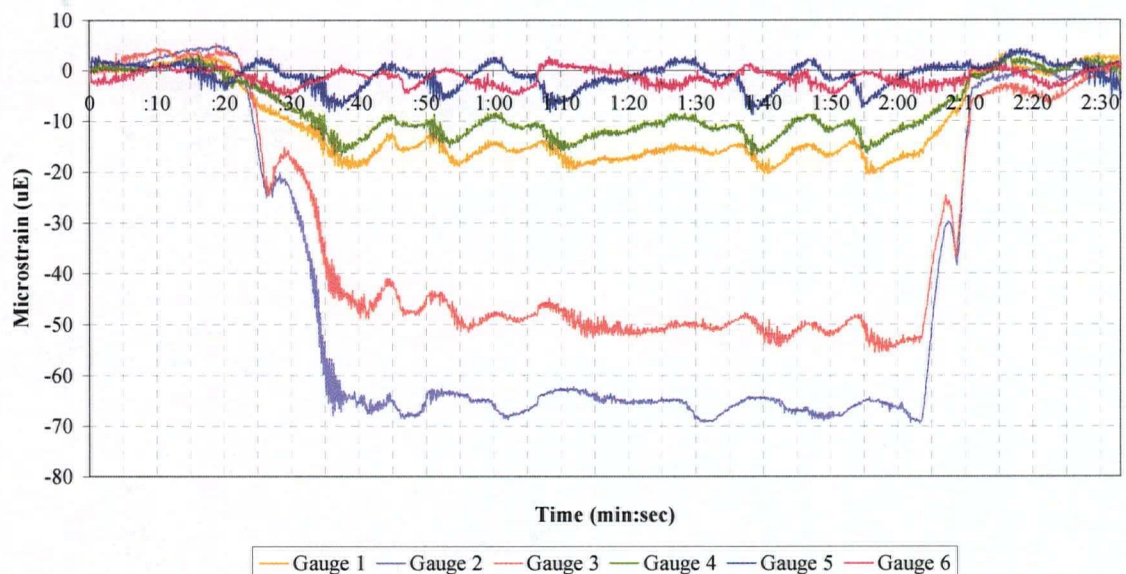
**2003 Field Testing  
I/O Tech DaqBook: Static Load Position 2**



**2003 Field Testing**  
**I/O Tech DaqBook: Static Load Position 3**

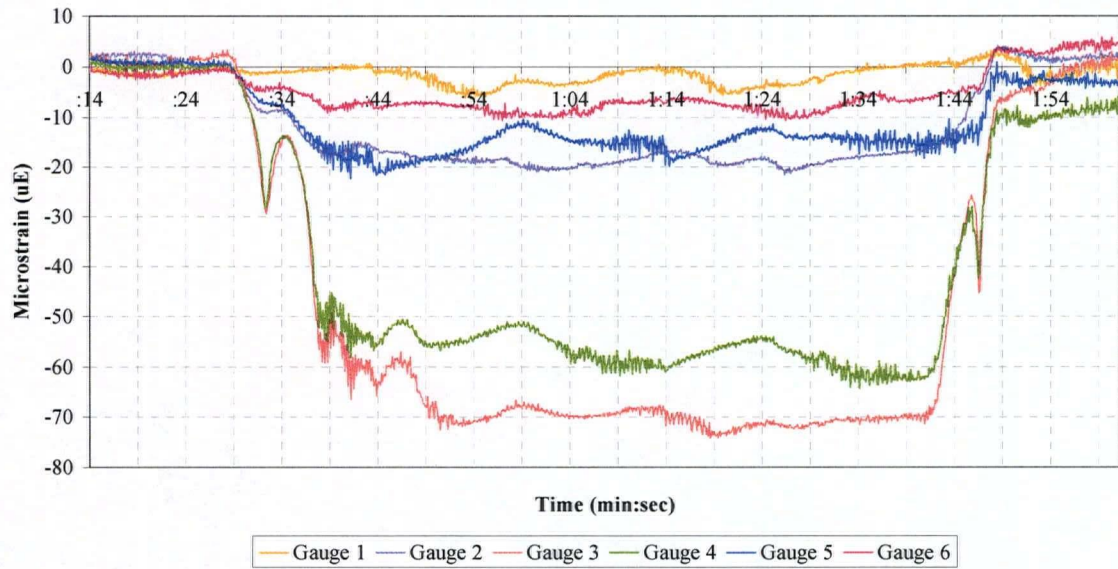


**2003 Field Testing**  
**I/O Tech DaqBook: Static Load Position 4**

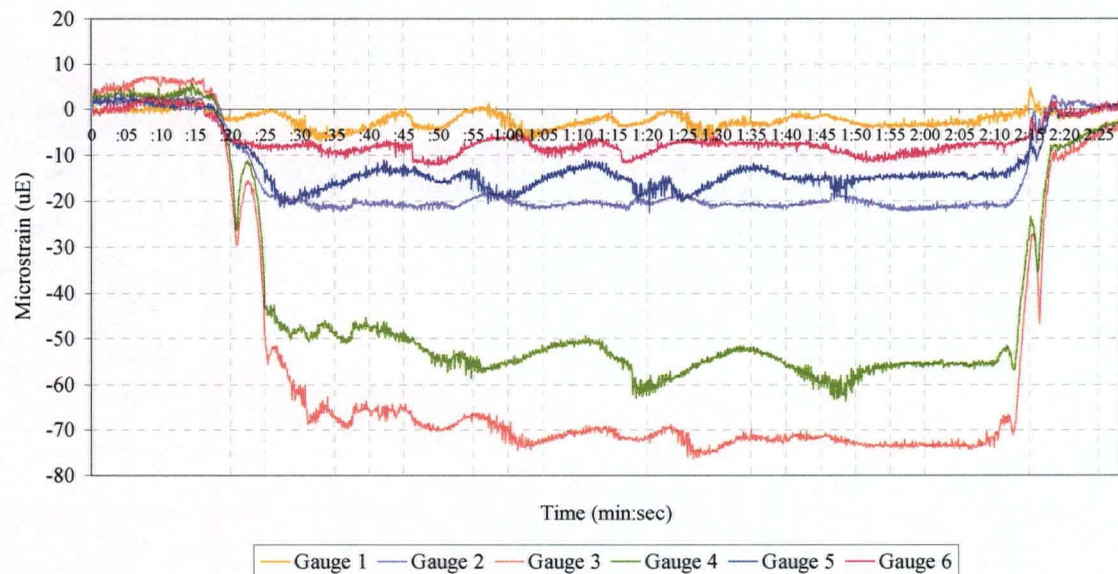




**2003 Field Testing  
I/O Tech DaqBook: Static Load Position 5**



**2003 Field Testing  
I/O Tech DaqBook: Static Load Position 6**



## **Appendix V**

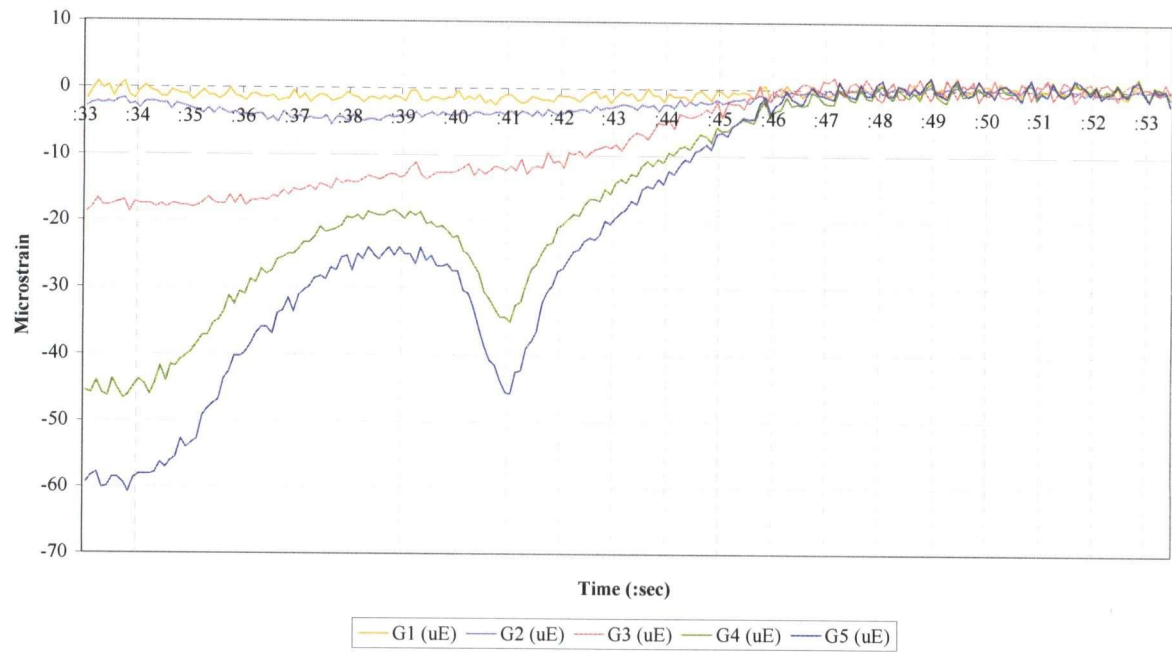
### **Field Test 2003:**

#### **Time-Strain History of the Six Static Load Positions**

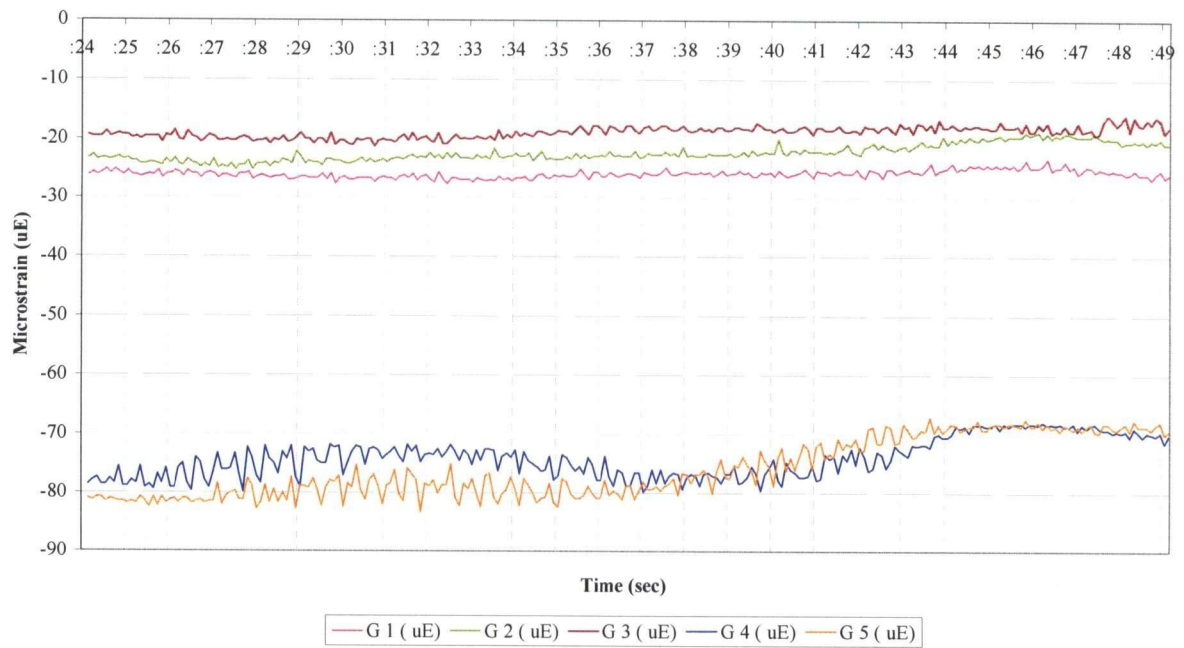
**- *WebDAQ/100 Results* -**



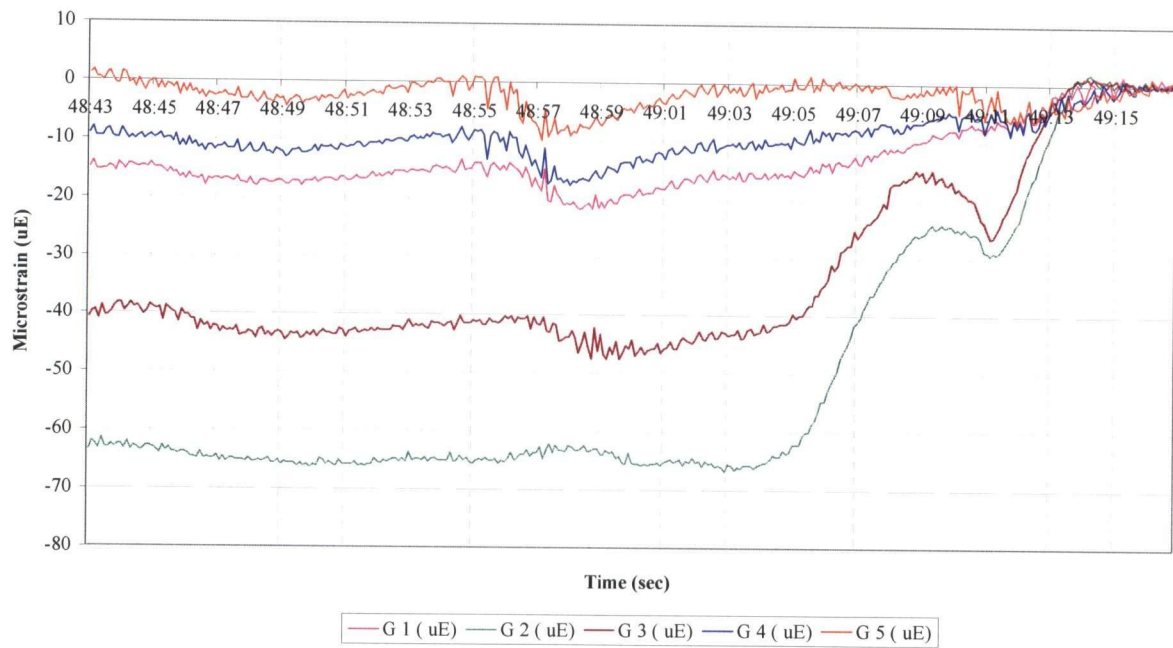
WebDAQ - Static Load Position 1



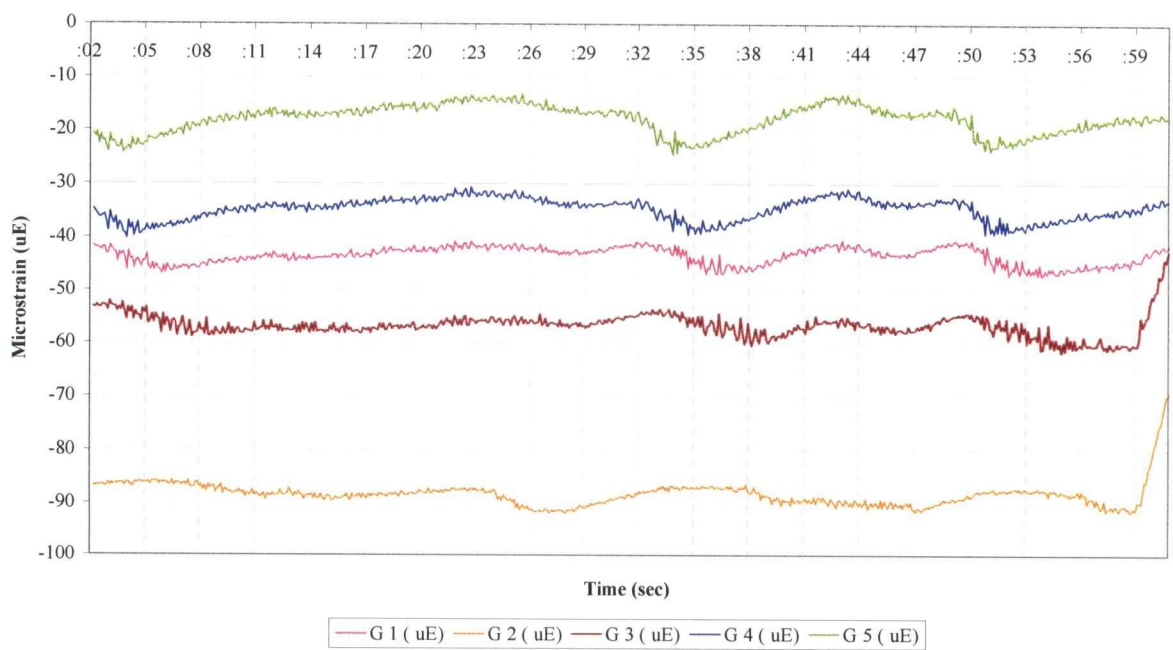
WebDAQ - Static Load Position 2



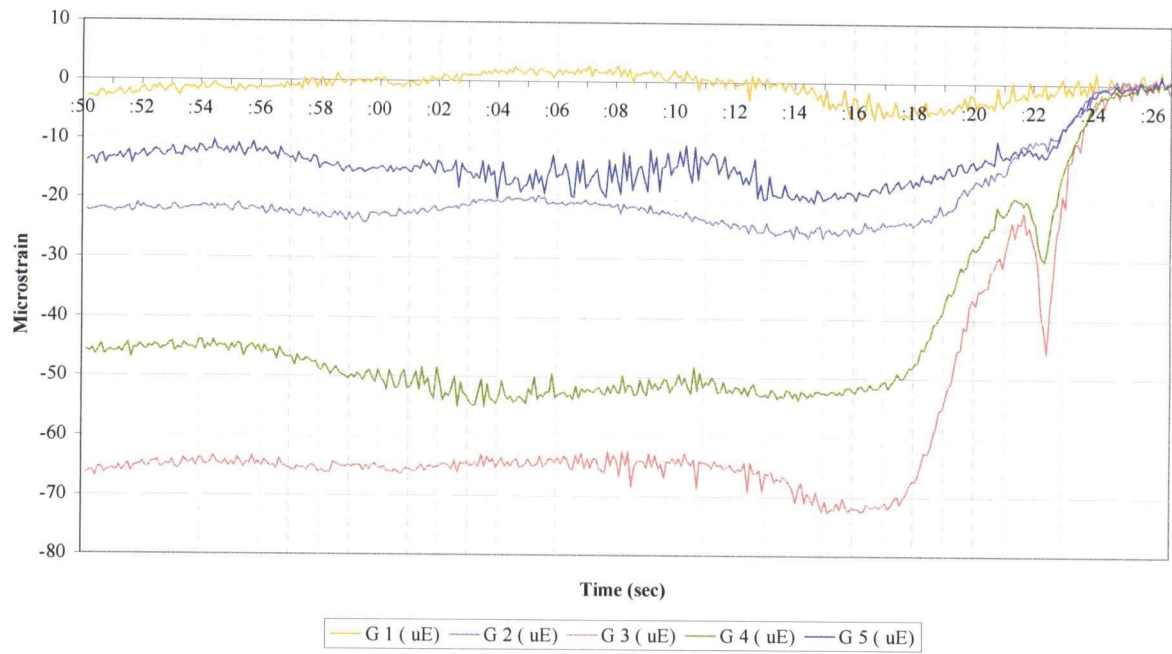
### WebDAQ - Static Load Position 3



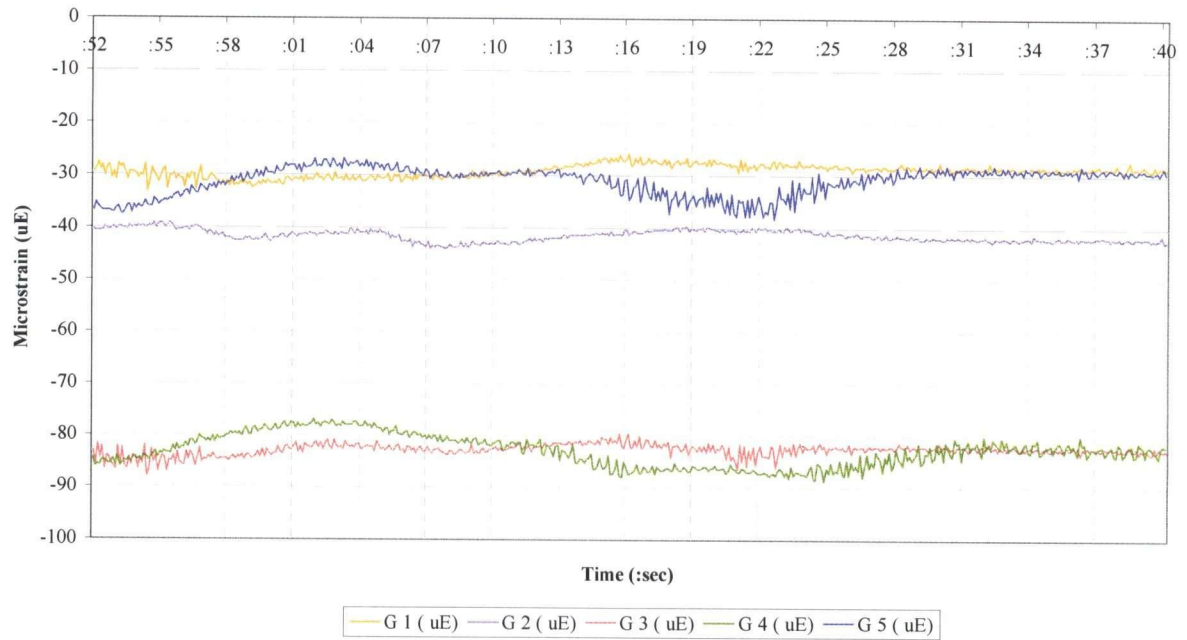
### WebDAQ - Static Load Position 4



WebDAQ - Static Load Position 5



WebDAQ - Static Load Position 6



## **Appendix VI**

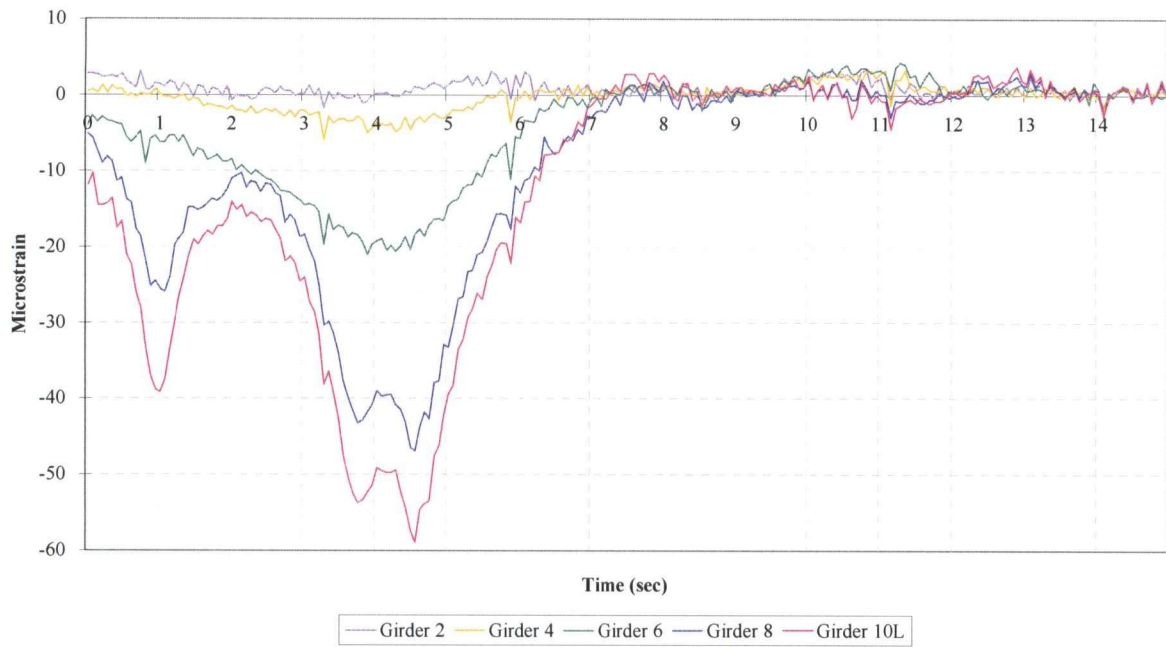
### **Field Test 2003:**

#### **Time-Strain History of the Three Rolling Load Positions**

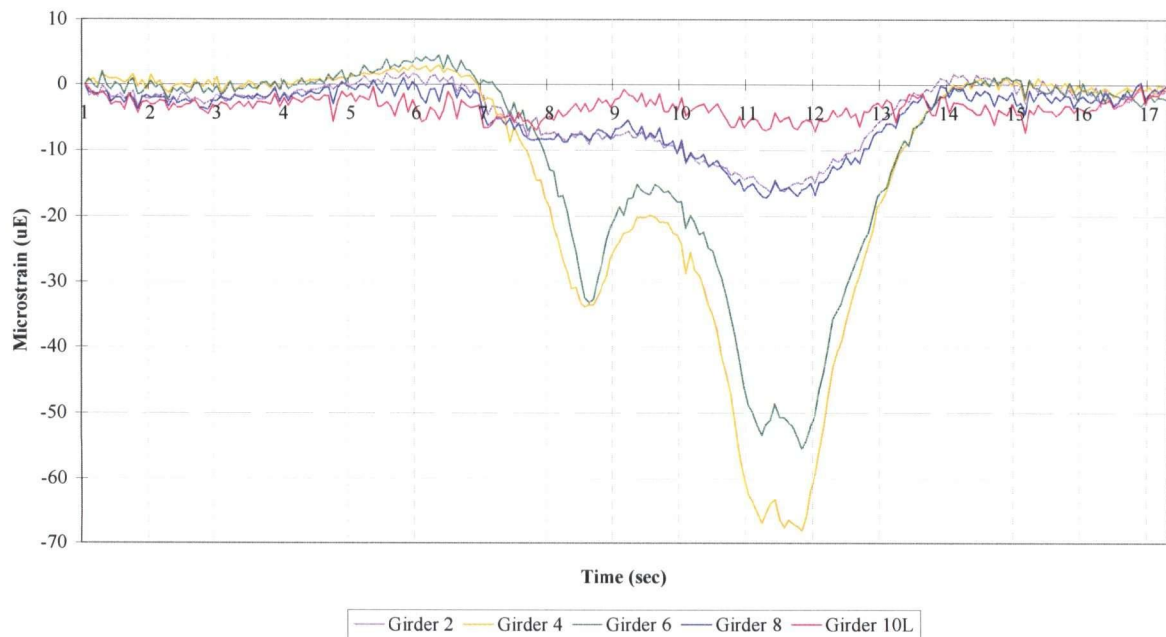
***- WebDAQ/100 Results -***



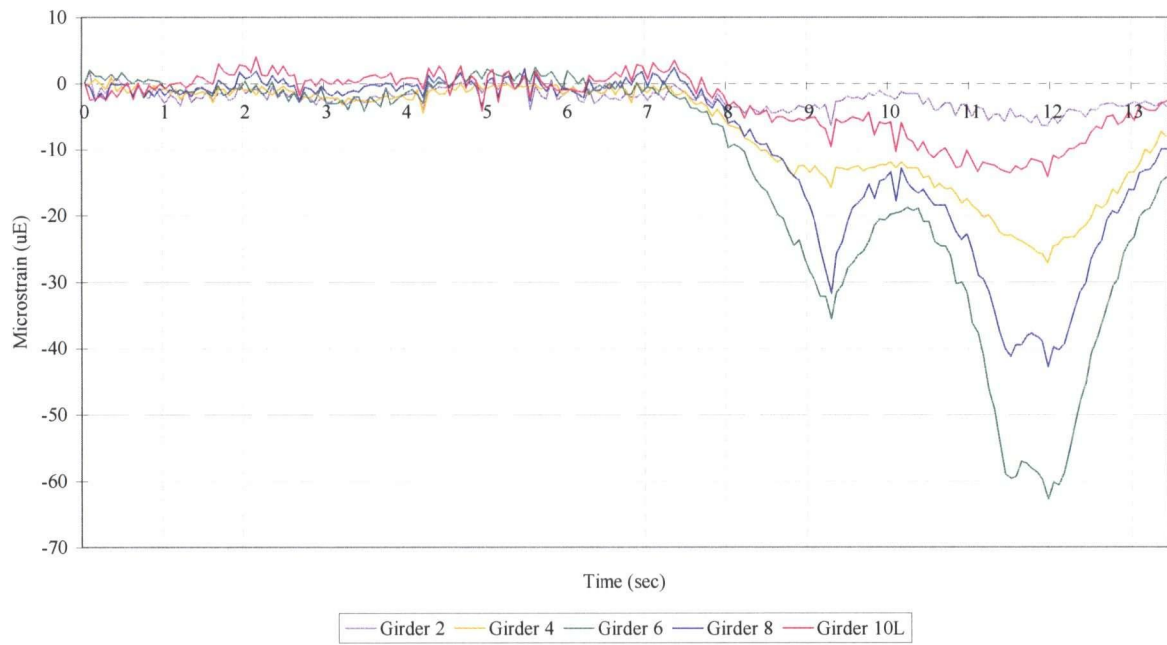
### WebDAQ Result: Rolling Load Position 1



### WebDAQ Result - Rolling Test, Position 2



WebDAQ - Strain Time History of Rolling Load Position 3



## **Appendix VII**

### **Field Test 2005:**

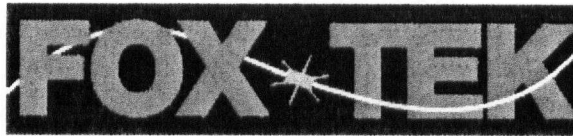
#### **Weight Scale Ticket of the Standard Load Testing Truck**

## **Appendix VIII**

### **Field Test 2005:**

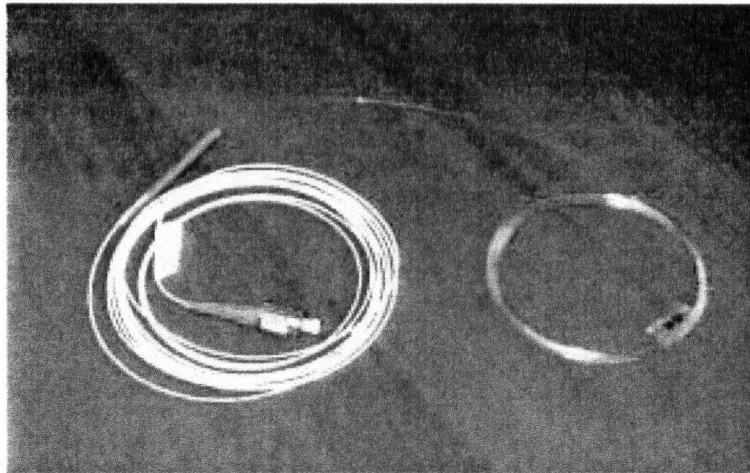
#### **Specifications of the Long-Gauge FT Sensors**





Fiber Optic Systems Technology Inc.

## FT Bare Fiber Optic Sensor



- Measures total displacement along gage length
- Available in gage lengths up to 30 m
- Sub-micron resolution and 15  $\mu\text{m}$  accuracy
- All fiber optic – no EM emissions, immune to EMI/RF – safe for use in explosive or other hazardous environments
- Able to fit complex contours with flexible optical fiber
- Small fiber diameter (250  $\mu\text{m}$ ) for non-intrusive embedding
- Fiber optic lead cable can be run several hundred metres back to instrumentation without signal loss
- Available with rugged fiberglass mesh backing

For more information please contact FOX-TEK @ (416) 665-2288  
[www.fox-tek.com](http://www.fox-tek.com)

### Specifications

Instrumentation	FOX-TEK FTI-3300 or higher
Sensor Length	1m, 2m, 5m, 10m, 20m, 30m standard, custom lengths available
Measurement Range	Up to 3% strain (limited by measurement range of scanning instrument)
Mounting fixtures	Bonds directly to structural surface using appropriate adhesive
Operating Temperature	-25° to +55°C (limited by operating range demodulation instrument)

Specifications subject to change without notice  
©2004 Fiber Optic Systems Technology Inc. All rights reserved.

## **Appendix IX**

### **Field Test 2003:**

#### **Specifications of the IP-built-in *WebDAQ/100* System**

# Specifications

## Power supply

webDAQ/100 is supplied with an AC power adapter module, and has been certified, calibrated, and tested only with this power supply. The power adapter module can operate on:

- 90 - 264 VAC
- 47 to 63 Hz
- Approx. 18 watts power consumption

For direct DC input requirements at the webDAQ/100 power connector, please contact the factory to discuss your needs.

## Size and Weight

Dimensions	7.5" x 10.375" x 2.675"	19cm x 26.5cm x 7cm
Weight	34 oz.	965 gm
Shipping box	12.375" x 14.5" x 5" 4.6 lb.	31.5cm x 37cm x 13cm 2.1 kg
Power supply	2.125" x 4.5" x 1.75" 20 oz with line cord	5.5cm x 11.5cm x 4.5cm 570 gm

## RAM memory:

- 72-pin SIMM module
- Page-mode memory
- 70 nsec or less access time
- size: 4MB, 8MB, 16MB, 32MB, 64MB or 128MB

## Environmental

operating: 0 degrees C to +40 degrees C.  
non-operating: -10 degrees C to +70 degrees C.  
0% to 90% relative humidity (non-condensing)

## A/D

12-bit resolution, 500 KHz, 32 channels (16 differential) *total sampling rate (#ch \* rate)*  
Maximum input range +/- 10 Volts  
Gains: 1, 4, 10, 40, 100, 400

## Overvoltage protection:

Protected for transients (electrostatic discharge).

**Do not apply more than +/-10 Volts continuously to the inputs**

**D/A**

Output range +/- 10 Volts

Factory and self-calibration adjust the D/A range and offset to provide accurate output. In the process, the D/A bit resolution may be adjusted slightly, so the minimum D/A step size can vary from approx. 21.5 mV to 23.5 mV.

**Standard TTL logic voltage levels (low is < 0.8 volts, high is > 2.0 volts)**

## 4 bits

10/100-baseT with RJ45 connector

Default set to 38400 baud, 8 bits, no parity, 1 stop bit

**Conducted Emissions: - Para. 15.107(b)**

This Class A digital apparatus meets all requirements of the Canadian Interference-Causing Equipment Regulations.

### Class A, Conducted Emissions, 150 kHz to 30 MHz



Class A, Conducted Emissions, 30 MHz to 1 GHz  
Immunity requirements of EN 61326:1998  
IEC 1000-4-2:1995 Electrostatic discharge, 8 KV Direct Air, 4 KV Direct and Indirect Contact.  
IEC 1000-4-3:1995 Radiated RF Immunity, 80 MHz - 1000 MHz, 10V/m, 80% AM 1 KHz.  
IEC 1000-4-4:1995 EFT, 2KV Direct to Power Leads, 1KV to I/O Leads through Coupling Clamp.  
IEC 1000-4-5:1995 Surge Immunity, 2KV Common Mode, 1 KV Differential Mode.  
IEC 1000-4-6:1995 Conducted RF Immunity, 150 KHz - 80 MHz, 3 Vrms, 80% AM 1KHz.  
IEC 1000-4-8:1995 Magnetic Immunity, 50 Hz, 30 A/m  
IEC 1000-4-11:1994 Voltage Dips and Short Interruptions

**Australia:**

Conforms to the requirements of: AS/NZS 3548

**Japan:**

Conforms to the requirements of: VCCI V-3/99:05 AMD June 1999, for Class A, ITE, Conducted and Radiated Disturbance.

**Disclaimers**

The information contained in this documentation is believed to be accurate and reliable. However, Capital Equipment Corporation assumes no responsibility for its use or for any infringements of patents or other rights of third parties that may result from its use. No license is granted by implication or otherwise under any patent rights of Capital Equipment Corporation.

This documentation is copyrighted by Capital Equipment Corporation. Copyright 2000 CEC.

Please see printed materials for a statement of warranties. Except as specified in written materials accompanying the product, Capital Equipment Corporation makes no warranties, express or implied of merchantability or fitness for a particular purpose. Customer's right to recover damages shall be limited to recovery of the purchase price. Capital Equipment Corporation shall not be liable for damages resulting from loss of data, profits, use of products, or incidental or consequential damages, even if advised of the possibility thereof. **This product is not designed with components of a level of reliability suitable for use in treatment or diagnosis of humans, life support or clinical applications.**

webDAQ and webDAQ/100 are trademarks of Capital Equipment Corporation. All rights reserved.

**RAM - installation**

webDAQ/100 accepts a single SIMM memory module, of the same type that is commonly installed into PCs.

RAM specs:

- 72-pin SIMM module
- Page-mode memory
- 70 nsec or less access time
- size: 4MB, 8MB, 16MB, 32MB, 64MB or 128MB

To install a new memory module:

1. Take all precautions against static discharge. It is best to work with an anti-static surface and wrist strap - if that is not available, make sure to touch a grounded object such as a water pipe before handling sensitive components. Handle all components by the edges whenever possible.
2. **Unplug the unit!**
3. Remove the four screws from the webDAQ/100 case.
4. Gently pull the top half of the case upwards and set it aside.
5. The memory module stands up vertically near the center of the circuit board. Remove the existing memory module by gently squeezing the retaining clips outward until the module pops loose.
6. Install the new memory module at a slight angle until it is fully seated down into the connector, then tilt it upward until it locks into place.
7. Replace the cover and screws.
8. Apply power - the green LED should light. A yellow light means memory is not correctly installed.

## **Appendix X**

### **Field Test 200:**

#### **Specifications of the FTI-3300 System for the Long-Gauge FT Sensors**

## 1.0 Introduction

The FOX-TEK FTI-3300 instrument is designed to measure changes in displacement of the FT sensor, which is effectively a fiber optic extensometer. The instrument is equipped with 8 input channels, in a 19" rackmount configuration. The instrument will read any three of FOX-TEK's suite of seven standard FT sensor lengths – 0.1m, 1m, 2m, 5m, 10m, 20m and 30m - as specified by the customer. The default configuration will read the 0.1m, 1m and 5m sensor lengths. A custom option is available to incorporate other sensor lengths (5cm to 100m) into the instrument if required.

The system operates by scanning the attached sensor for a change in the reflected intensity of light, and recording the location at which that signal was detected. Any changes in the sensor's length can be detected by the shift in the signal to a different displacement location, which is detected and recorded by the instrument.

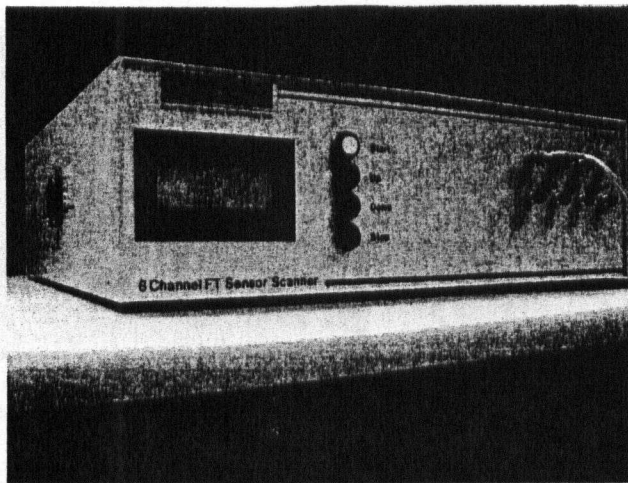


Fig. 1.1 FTI-3300 Instrument

## 1.1 Specifications

Number of Channels	8 standard
Sensor Length	0.1m, 1m, 2m, 5m, 10m, 20m, 30m standard, custom lengths (5cm – 100m) available
Scan Time	5s in Fast Scan Mode, <12s (typical) or 25s (max) in full scan mode (per channel)
Dimensions	17" x 17" x 5.5" (excluding mounting brackets) – 19" rackmount, 3U height
Weight	10kg
Measurement Range	±15mm or ±4000 microstrain, whichever is less
Accuracy	± 0.067% of full scale (30mm)
Operating Temperature	5° – 40°C (41° - 104°F)
Storage Temperature	-10° - +65°C (14° - 149°F)
Power	110V/2A or 220V/1A, 50-60Hz
Fuse	250V, 2.5A (5x20mm – IEC type 60127-2 or UL248-14)
Computer Interface	RS232 or RS485 (RS232 default)